Mass Spectrometric Comparison of the Lipid Residues from Ancient Brain Remains

Emma Jane Thimbleby

MSc (by research)

University of York

Chemistry

May 2018

ABSTRACT

High resolution matrix-assisted laser desorption/ionisation Fourier transform ion-cyclotron resonance mass spectrometric (MALDI FT-ICR-MS) analyses have been carried out on lipidic extracts of preserved brain remains from 14 contexts, obtained from four archaeological sites ranging from 200 to 2,500 years old. The aim of the study was to determine whether the high molecular weight organic material reported in a similar fraction of the well-preserved York brain is a common feature of such unusually preserved brain specimens. Examination of the predominant signals in the resulting spectra in terms of signal-to-noise ratio and intensity, generated a list of peaks for comparison and interpretation. On the basis of the accurate mass measurements afforded by FT-ICR-MS, 37 empirical formulae were assigned. The components identified across almost all the sample extracts analysed fell into the same general class of organic molecules, that were generally functionalised with low numbers of heteroatoms (generally oxygen and nitrogen, or both). These components did not correspond to those identified in adipocere, but were similar in composition to subunits of kerogen-like structures reported in the literature. These results pave the way for further analyses aimed at understanding the processes that take place when brain material is, unusually, preserved in the archaeological record.

TABLE OF CONTENTS

ABSTRACT 3

TABLE OF CONTENTS 5

LIST OF TABLES 9

LIST OF FIGURES 13

ACKNOWLEDGEMENTS 17

DECLARATION 21

1 INTRODUCTION 23

1.1 Chemical Composition of the Brain 23

1.1.1 LIPIDS 25

1.1.2 AMINO ACIDS, PEPTIDES, NUCLEIC ACIDS AND PROTEINS 28

1.1.3 CARBOHYDRATES 29

1.2 Soft Tissue Degradation and Preservation 31

1.2.1 NORMAL TISSUE DECOMPOSITION 31

1.2.1.1 Autolysis 31

1.2.1.2 Bacteria: the effects of normal or enteric flora and environmental microbes 32

1.2.1.3 Burial environment 34

1.2.2 SOFT TISSUE PRESERVATION MECHANISMS 34

1.2.2.1 Moisture 35

1.2.2.2 pH 36

1.2.2.3 Temperature 36

1.2.2.4 Oxygen 37
1.2.2.5 Chemical inhibitors 37
1.2.3 SPECIFIC EXAMPLES OF PRESERVATION 38
1.2.3.1 Desiccation 38
1.2.3.2 Freezing 40
1.2.3.3 Freeze-drying 40
1.2.3.4 Bog bodies 41
1.2.3.5 Heavy metals 43
1.2.3.6 Adipocere 44
1.2.3.7 Fossil fuels 51
1.3 Brain Preservation 53
1.4 Mass Spectrometry 62
1.4.1 OVERVIEW/HISTORY 62
1.4.2 IONISATION: MATRIX-ASSISTED LASER DESORPTION/IONISATION (MALDI) ... 64
1.4.3 MASS ANALYSERS 66
1.4.3.1 Fourier-transform ion cyclotron resonance 66
1.4.3.2 Ion cyclotron motion 67
1.4.3.3 Observations from these equations 69
1.4.3.4 Ion cyclotron resonance 70
1.4.3.5 Ion cyclotron cell geometry 72
1.4.3.6 Broadband resonance 73
1.4.3.7 Image current detection 75
1.4.3.8 Accuracy and resolution 76

1.4.4 PROTEOMICS 77
1.4.4.1 Introduction 77
1.4.4.2 Fractionation 78
1.4.4.3 Digestion 79
1.4.4.4 Mass spectrometry and fragmentation 80
1.4.4.5 Database searching 81
1.5 Aims of the Thesis 83
2 EXPERIMENTAL 85
2.1 Samples 85
2.1.1 YORK 86
2.1.2 HULL MAGISTRATES COURT 91
2.1.3 BLACKPOOL 93
2.1.4 VILLIERS STREET CRYPT 96
2.2 Proteomic Analysis of Villiers Street Sample 100
2.3 Organic Extraction of Samples (mouse brain, modern human brain, archaeological brains, soil, solvent blank) 103
2.4 Recording Spectra 106
2.4.1 PEAK SELECTION 107
2.4.2 PEAK IDENTIFICATION 107
3 RESULTS 109
3.1 Standards, Mouse Brain and Modern Human Brain Lipid Extracts 109
3.2 Protein ID From Villiers Street Sample 113
3.3 Comparison of Spectra of Ancient Brain Lipid Extracts 115

3.3.1 KEY SIGNALS IDENTIFIED AS A RESULT OF MASS SPECTRAL COMPARISONS..... 117

4 DISCUSSION 203

5 CONCLUSION AND FURTHER WORK..... 219

APPENDICES 223

Appendix I: Photos of Ancient Brain Remains..... 223

Appendix II: Unidentified Compound Tables 229

ABBREVIATIONS 261

REFERENCES..... 263

LIST OF TABLES

Table 1. Biochemical composition of grey and white matter (approximate %).[2] 25

Table 2. Percentage composition of 'Hard Clean Adipocere Wax' determined by a variety of chemical methods.[75] 49

Table 3. Chemicals found in adipocere 50

Table 4. Summary of scientific analyses that have occurred on selected surviving brain masses 56

Table 5. Sample summary table, in descending date order 97

Table 6. MassList selection parameters 107

Table 7. Chemistry Smartformula parameters 108

Table 8. Summary of signal at *m/z* 371. C_xH_y 119

Table 9. Summary of signal at *m/z* 518. C_xH_yN 121

Table 10. Summary of signal at *m/z* 490. C_xH_yN 123

Table 11. Summary of signal at *m/z* 487. $C_xH_yN_2$ 125

Table 12. Summary of signal at *m/z* 411. $C_xH_yN_2$ 127

Table 13. Summary of signal at *m/z* 405. $C_xH_yN_4$ 129

Table 14. Summary of signal at *m/z* 498. C_xH_yNO 131

Table 15. Summary of signal at *m/z* 500. C_xH_yNO 133

Table 16. Summary of signal at *m/z* 530. C_xH_yNO 135

Table 17. Summary of signal at *m/z* 544. C_xH_yNO 137

Table 18. Summary of signal at *m/z* 556. C_xH_yNO 139

Table 19. Summary of signal at *m/z* 558. C_xH_yNO 141

Table 20. Summary of signal at *m/z* 586. C_xH_yNO 143

Table 21. Summary of signal at *m/z* 726. C_xH_yNO 145

Table 22. Summary of signal at *m/z* 752. C_xH_yNO 147

Table 23. Summary of signal at *m/z* 754. C_xH_yNO 149

Table 24. Summary of signal at *m/z* 778. C_xH_yNO 151

Table 25. Summary of signal at *m/z* 780. C_xH_yNO 153

Table 26. Summary of signal at *m/z* 782. C_xH_yNO 155

Table 27. Summary of signal at *m/z* 806. C_xH_yNO 157

Table 28. Summary of signal at *m/z* 810. C_xH_yNO 159

Table 29. Summary of signal at *m/z* 501. $C_xH_yN_2O$ 161

Table 30. Summary of signal at *m/z* 511. $C_xH_yN_2O$ 163

Table 31. Summary of signal at *m/z* 513. $C_xH_yN_2O$ 165

Table 32. Summary of signal at *m/z* 463. $C_xH_yN_4O$ 167

Table 33. Summary of signal at *m/z* 502. $C_xH_yNO_2$ 169

Table 34. Summary of signal at *m/z* 514. $C_xH_yNO_2$ 171

Table 35. Summary of signal at *m/z* 464. $C_xH_yNO_3$ 173

Table 36. Summary of signal at *m/z* 518. $C_xH_yNO_3$ 175

Table 37. Summary of signal at *m/z* 564. $C_xH_yNO_3$ 177

Table 38. Summary of signal at *m/z* 648. $C_xH_yNO_3$ 179

Table 39. Summary of signal at *m/z* 584. $C_xH_yNO_4$ 181

Table 40. Summary of signal at *m/z* 527. $C_xH_yN_2O_2$ 183

Table 41. Summary of signal at *m/z* 731. $C_xH_yN_2O_3$ 185

Table 42. Summary of signal at *m/z* 759. $C_xH_yN_2O_3$ 187

Table 43. Summary of signal at *m/z* 321. $C_xH_yO_7$ 189

Table 44. Summary of signal at *m/z* 365. $C_xH_yO_8$ 191

Table 45. Summary of signal at *m/z* 393. $C_xH_yO_9$ 193

Table 46. Summary of signal at *m/z* 549. $C_{32}H_{42}N_6$ or $C_{36}H_{40}N_2O_3$ 196

Table 47. Summary of signal at *m/z* 629. $C_{44}H_{46}O_2$, $C_{41}H_{50}O_3$ or $C_{42}H_{40}N_6$ 198

Table 48. Summary of signal at *m/z* 688. $C_{42}H_{83}NO_4$ or $C_{40}H_{77}N_7O_2$ 200

Table 49. Summary of the chemical identities of the brain lipid residues and their occurrence 209

Table 50. Significant peaks from the initial replicate mass spectra: the top five S:N peaks, plus top five intense peaks 230

Table 51. Summary of signal at *m/z* 437 232

Table 52. Summary of signal at *m/z* 475 233

Table 53. Summary of signal at *m/z* 485 234

Table 54. Summary of signal at *m/z* 497 235

Table 55. Summary of signal at *m/z* 529 236

Table 56. Summary of signal at *m/z* 541.2 237

Table 57. Summary of signal at *m/z* 541.9 238

Table 58. Summary of signal at *m/z* 544 239

Table 59. Summary of signal at *m/z* 547 240

Table 60. Summary of signal at *m/z* 563 241

Table 61. Summary of signal at *m/z* 564 242

Table 62. Summary of signal at *m/z* 569 243

Table 63. Summary of signal at *m/z* 591 244

Table 64. Summary of signal at *m/z* 622 245

Table 65. Summary of signal at *m/z* 629 246

Table 66. Summary of signal at *m/z* 640 247

Table 67. Summary of signal at *m/z* 753 248

Table 68. Summary of signal at *m/z* 769 249

Table 69. Summary of signal at *m/z* 815 250

Table 70. Summary of signal at *m/z* 835 251

Table 71. Summary of signal at *m/z* 836 252

Table 72. Summary of signal at *m/z* 848 253

Table 73. Summary of signal at *m/z* 850 254

Table 74. Summary of signal at *m/z* 852 255

Table 75. Summary of signal at *m/z* 853 256

Table 76. Summary of signal at *m/z* 857 257

Table 77. Summary of signal at *m/z* 866 258

Table 78. Summary of signal at *m/z* 968 259

LIST OF FIGURES

Figure 1. Approximate chemical composition of the mammalian brain.[3] 24

Figure 2. Structure of a glycerophospholipid; insert a representationof a phospholipid bilayer 26

Figure 3. Structures of sphingomyelin and cerebroside related lipids 27

Figure 4. Structure of cholesterol 28

Figure 5. Stearate chemical structures: (above) sodium stearate, (below) calcium stearate 46

Figure 6. Preserved brain soft tissue from the Cova des Pas site (Minorca, Bronze Age) [39] 54

Figure 7. Schematic representation of the elements of a mass spectrometer ... 63

Figure 8. Ion cyclotron motion. The magnetic field (B_0) provides a perpendicular force (F) to the ions' motion (v), creating a circular motion. 67

Figure 9. Resonant excitation. If the oscillating electric field has the same frequency as the ion's cyclotron frequency then the ion is excited, leading to an increase in orbital radius 71

Figure 10. Resonant excitation of ions travelling in phase 72

Figure 11. Geometry of a simple ion cyclotron resonance 'cell' 73

Figure 12. Signal processing (L-R): the varying cyclotron frequencies are detected as changes in voltage over time, a complex image current is built up, this transient signal undergoes Fourier transformation from time to the frequency domain – which then provides *m/z* information..... 76

Figure 13. Peptide showing main backbone fragmentation patterns and standard nomenclature labelling, which indicates the charged species produced 81

Figure 14. (Clockwise, top to bottom): The skull as found (York Archaeological Trust), brain mass viewed using endoscope (Sonia O'Conner), brain fragment in storage at BARC, brain fragment after removal from skull and cleaning (Sonia O'Conner) 87

Figure 15. Above: the location of the Heslington East development and the major archaeological excavation sites, below: the location of the excavated skull.[1] 88

Figure 16. Above: Map showing distribution of burials within the Hull Friary precinct. Below: Plan with burials from which surviving brain remains were used in this study are highlighted; green = juvenile, blue = male, pink = female, yellow = adult (unsexed) 94

Figure 17. Fishtail coffin 116 *in situ*, containing skeleton 117, looking north-west.[143] 95

Figure 18. (a) $[PC + Na]^+$ and (b) $[PC]^+$ ions 109

Figure 19. Above: MALDI mass spectrum of phosphatidylcholine (PC) standard 110

Figure 20. Above: MALDI mass spectrum of sphingomyelin (SM) standard..... 110

Figure 21. Example of a SM ion 111

Figure 22. Above: MALDI mass spectrum of galactocerebrosides (GalC) standard. Below: An example galactocerebroside 111

Figure 23. Human and mouse brain mass spectra 112

Figure 24. Mascot report showing myelin proteolipid protein peptide match found in sample V1 (this same sequence was also found in the proteomic analysis of the York brain)[1] 114

Figure 25. Mascot report showing SLIT and NTRK-like protein 4 peptide match 114

Figure 26. Above: Ethylene glycol Below: Hexaethyleneglycol (3,6,9,12,15-Pentaoxaheptadecane-1,17-diol), a possible structure for $C_{12}H_{26}O_7$ 207

Figure 27. Structural model of Green River oil shale kerogen.[158] 214

Figure 28. Schematic pathway of successive transformations of OM (taken from [159]) 215

Figure 29. Left: Van Krevelen plot of ancient brain lipid residues shown in Table 49 (except the highly oxygenated $C_{12}H_{26}O_7$, $C_{14}H_{30}O_8$, $C_{16}H_{34}O_9$). Right: Van Krevelen plot of kerogen (types I, II and III)[87] 216

Figure 30. Photograph of brain mass HMC SK1709, from which sample H1 had been removed for potential DNA analysis. 223

Figure 31. Photograph of brain mass labelled HMC SK1913, from which H7 was sampled. 223

Figure 32. Photograph of HMC94 SK2039, from which H11 was sampled. 224

Figure 33. Photograph of brain mass labelled HMC SK2123, from which samples H12 and H13 had been sampled. 224

Figure 34. Photograph of brain mass HMC SK2123 which had been stored separately with the additional label 'Red sample', from which H14 was sampled. 224

Figure 35. Photograph of the brain mass labelled SJB09 SK117, after sample B1 was removed. 225

Figure 36. Photograph of the brain mass labelled VSS-A SK2463, from which V1 was sampled..... 225

Figure 37. Photographs of ancient preserved brain matter. From (L-R) Top row: H1, B1, V1, H1. Second row: H2, H3, H4, H5. Third row: H6, H7, H8, H9. Bottom row: H10, H11, H12, H13. 226

Figure 38: (Figure 37 continued) H14..... 227

ACKNOWLEDGEMENTS

My initial thanks goes to Dr Sonia O'Conner who has proved her expertise and access to the majority of brain samples, without which this project would have been impossible. My thanks also go to the Biological Anthropological Research Centre, University of Bradford, for the opportunity to sample these rare remains and to Dr Jo Buckberry, Dr Andrew Wilson, Rob Janaway and Louise Brown who provided access to the Villiers Street sample.

I would also like to thank Dr Martin Rumsby who made the initial lipid extract of the York brain and provided help and advice as well as modern human extracts for comparison. Thanks goes to the Bioscience Technology Facility Proteomics laboratory, Department of Biology, University of York, especially Rachel Bates and Dr Adam Dowle, Dr Jerry Thomas for their assistance with the proteomics analysis. And thanks to Dr Megan Cosgrove who provided the mouse brain, along with her support and friendship.

My gratitude goes to The Department of Chemistry who have supported me throughout my undergraduate and graduate work, especially the Chemistry Graduate Office: Rachel Crooks, Alice Duckett and Sharon Stewart. The many members of the JTO group who have provided help, support, friendship and guidance including: Karl, Ed, Rachel Smith, Kirsty High, Helen, Kirsty Skeene, Lance, Emily, Elena, Bella, Kyle, Lefkothea, Rachel, Carwyn and Anne. I would also like to thank Dr Adrian Whitwood for his advice and guidance.

Last but not least, I am deeply indebted to my supervisor Professor Jane Thomas-Oates, who has been an outstanding support, help and inspiration. Her encouragement has kept me going and her assistance has been invaluable.

In loving memory of my brother, John William Thimbleby, MSc.

DECLARATION

I declare that this thesis is a presentation of original work and I am the sole author. This work has not previously been presented for an award at this, or any other, University. All sources are acknowledged as References.

The proteomic analysis was carried out at the Bioscience Technology Facility Proteomics Laboratory, Department of Biology, University of York, by Rachel Bates and Dr Adam Dowle.

Emma Jane Thimbleby

1 INTRODUCTION

This research project investigates organic compounds found in ancient brain remains. The rare natural survival of soft tissue within burials, let alone survival of brain tissue, provides few opportunities to study such material and hence there is limited scientific literature. However, the fascinating find of a prehistoric human brain in Heslington, York, Yorkshire in 2008 initiated a range of scientific investigations,[1] of which this is a continuation. This is intriguing as it appears that in some cases, the brain tissue is the only soft tissue preserved, prompting the idea of a novel tissue preservation mechanism.

This introduction provides a brief overview of the chemical composition of 'fresh' brain tissue as well as surveying what is known about how soft tissue decomposes. The factors that affect soft tissue preservation and the main non-anthropogenic mechanisms are discussed with examples. The main investigative tool/critical technique of mass spectrometry is presented and the aims and objectives of the investigation are outlined.

1.1 Chemical Composition of the Brain

The human brain is a particularly specialised and complex organ within the human body. It is a well-protected organ enclosed within the bones of the skull and three membranes: the outer dura mater, the arachnoid and the inner patia mater.[2] These membranes form the blood-brain barrier, a highly selective shield that moderates chemical access to and from the blood and isolates the brain from the body. Within these membranes, the tissue consists of two types of cells, neurons and glia, surrounded by interstitial fluid. Neurons are cells along which chemical and electronic signals are passed and are found in a variety of shapes. They generally consist of a cell body containing the nucleus, dendrites

and an axon surrounded by a myelin sheath, which ends in synapses. Three types of glia exist in the brain: oligodendrocytes wrap around the axons of neurons to form the myelin sheath, microglia are specialist immune cells that destroy bacteria and damaged neurons, and astrocytes have multiple functions including supplying nutrients to neurons and physically supporting them in place. The cells found within the brain and central nervous system (CNS) differ in chemical composition from those in the rest of the body and the brain as an organ reflects this. The general macromolecular composition of brain tissue is shown in Figure 1, with water being by far the major constituent. In comparison with other bodily tissues (such as skeletal muscles) the brain has a high lipid content which has a structural function rather than, as in other organs, acting as energy storage.

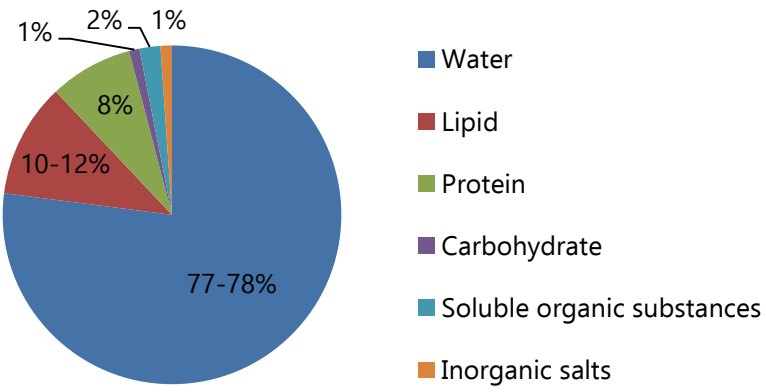

Figure 1. Approximate chemical composition of the mammalian brain.[3]

Within the brain tissue, a distinction is made between white and grey matter: white matter is mainly composed of the myelinated nervous fibres (axons) whilst grey matter consists of the nerve cell bodies, dendrites, and non-myelinated fibres and is the larger proportion at 85%.[4] The macromolecular proportions of white and grey matter vary slightly (see Table 1). The general molecular composition also varies between individuals due to age, sex, diet and health.

Table 1. Biochemical composition of grey and white matter (approximate %).[2]

	Grey matter	White matter
Water	83	70
Lipid	6	15
Protein	7.5	8.5
Inorganic Salts	1.0	1.3
Other	2.5	13.2

There are thousands of chemicals involved in brain chemistry; some of the more robust to degradation, larger and prevalent classes are outlined below as these are most relevant to this study.

1.1.1 LIPIDS

There are several classes of lipids that are found in brain tissue, where they have several roles, including in membrane structure (and function), in metabolism, and in signalling. The major component of the myelin sheath that surrounds nerve axons is lipidic.

Glycerophospholipids are constituents of cell membranes and consist of two fatty acid chains attached to glycerol, which is also attached to a head group (see Figure 2). The glycerol linkages may be ester or ether linkages. The head group may vary (e.g. ethanolamine, serine, choline or inositol) but is polar, compared to the hydrophobic, non-polar hydrocarbon chains of the fatty acids. A bilayer of glycerophospholipids with polar head groups on the exterior and hydrophobic chains on the interior is the backbone of cell membranes, providing stability, permeability and fluidity. Phosphatidates have a phosphate ester attaching to the glycerol and can have functional and structural roles within cells depending on the type of phosphate group. Phosphatidylcholines (PC) are phosphatidates that have a choline head group and are found in cell membranes.

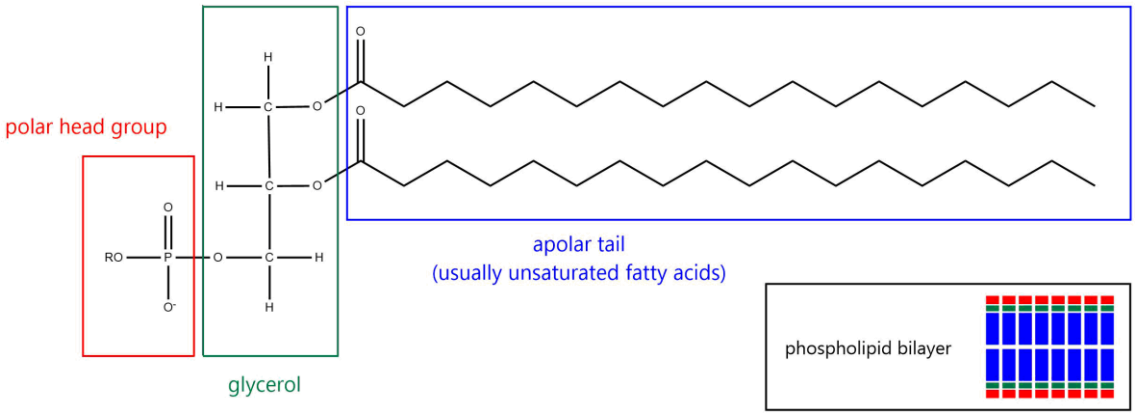

Figure 2. Structure of a glycerophospholipid; insert a representationof a phospholipid bilayer

Sphingomyelins (SM) are phospholipids that are components of the myelin sheath, insulating nerve cells. The basic building block for these molecules are sphingosine, an unsaturated hydrocarbon chain attached to an amino alcohol functional group. Once bound with a fatty acid to form a ceramide, the hydrocarbon chains form the apolar tail and usually have phosphocholine or phosphoethanolamine attached as the polar head group (Figure 3). As well as playing a structural role in the cell membrane, SMs also have a role in signalling.[5]

Cerebrosides consist of a ceramide molecule (sphingosine plus a fatty acid) plus a six carbon carbohydrate ring; in nerve cells this is generally galactose, forming galactocerebrosides (GalC), (Figure 3). GalC is a major component of oligodendrocytes, a type of non-neural cell found in the central nervous system, which insulates and supports axons by creating the myelin sheath.[6, 7] Cerebrosides that occur in myelin sheaths can also contain a sulfate group, in which case they are known as sulfatides.

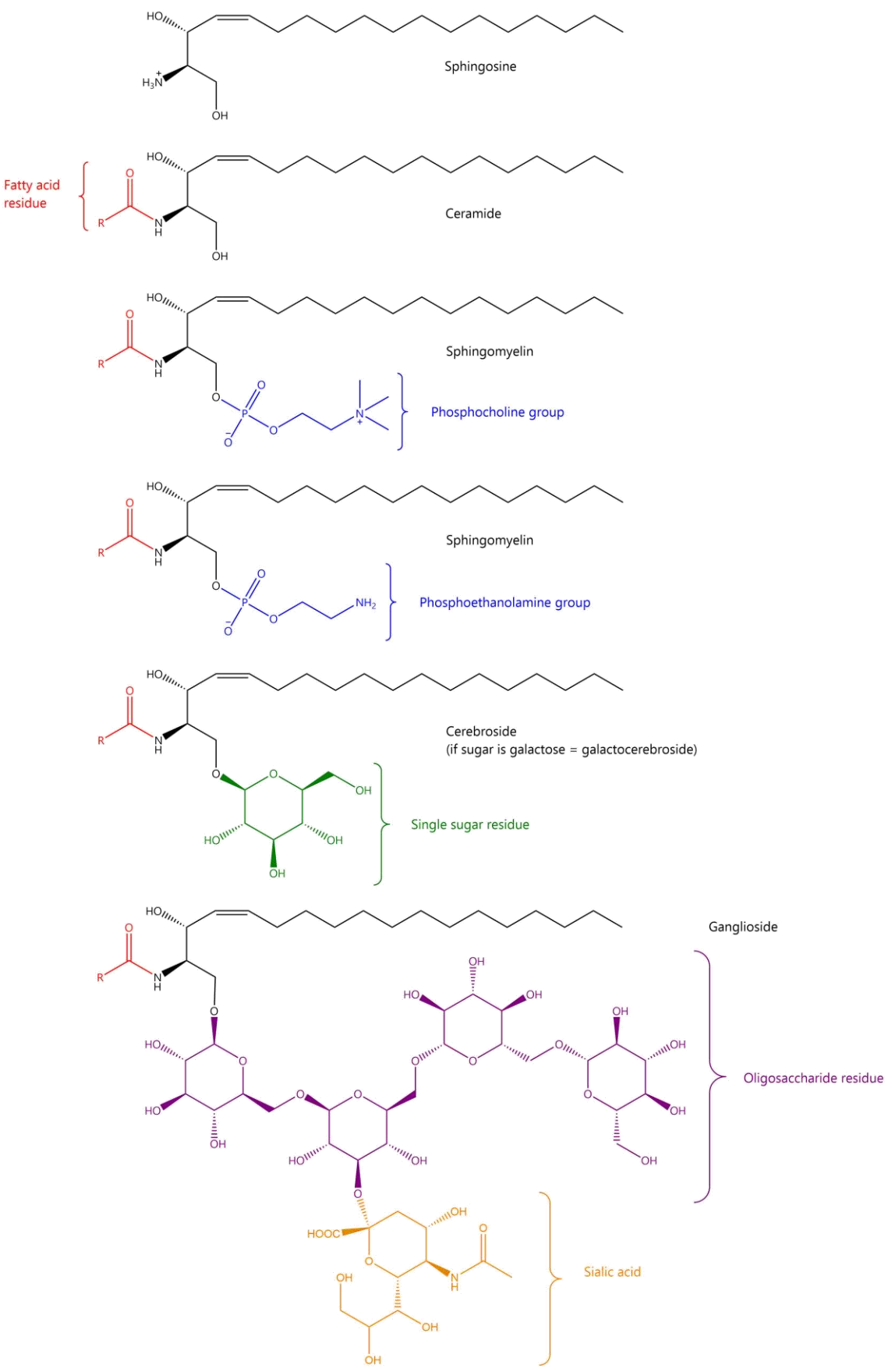

Figure 3. Structures of sphingomyelin and cerebroside related lipids

Gangliosides comprise a ceramide molecule attached to an oligosaccharide (a polymer of a small number of monosaccharides) with one or more sialic acids connected to the oligosaccharide chain. They are found within cell membranes, predominantly those of the nervous system.[8] With most of these lipids, enzyme-mediated hydrolysis releases the head groups, leaving the fatty acid chains attached as ceramides/glycerol esters.

Cholesterol, a sterol, is another lipidic molecule that is very important in cell membranes (Figure 4).

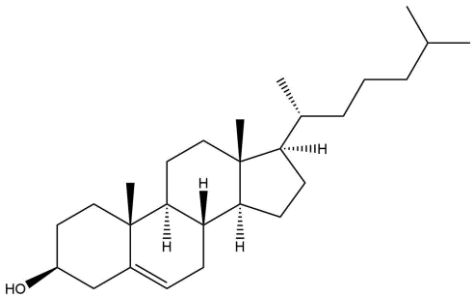

Figure 4. Structure of cholesterol

1.1.2 AMINO ACIDS, PEPTIDES, NUCLEIC ACIDS AND PROTEINS

The brain contains more free amino acids than are found in the plasma and other organs, with concentrations up to 6-8 times higher than elsewhere, partly because some amino acids are used as neurotransmitters[2]. Distribution of amino acids are affected by changes such as fasting, exercise, and anoxia. High concentrations of γ-aminobutyrate and *N*-acetylaspartate are characteristic of brain tissue.[3] A range of peptides can be found widely distributed within the CNS. Some, such as glutathione, are ubiquitous in other tissues; due to rapid oxidation it is reduced in quantity by 50% within three minutes after death.[9] Others such as γ-glutamyl dipeptides, homocarnosine (γ-amino-*n*-butyryl histidine) and *N*-acetyl-α-aspartylglutamate, may be more specific to the brain.[9]

Higher concentrations of some nucleotides, such as cytidine and uridine diphosphate derivatives and cyclic guanosine monophosphate, are found in the

brain than elsewhere in the body, but these rapidly degrade on death or anoxia due to the tissue's high metabolic rate and so are not expected to be found in postmortem brain samples.[2] Adenine, cytidine, guanine and uridine nucleotides and their mono-, di-, triphosphates are found in the brain. Deoxyribonucleic acid (DNA) is mainly found in the nuclei of the brain cells as a component of chromosomes but also in the mitochondria. The combination of a large number of cytoplasmic and endoplasmic ribosomes (sites of protein synthesis), the high metabolic rate (with expectations of high enzyme turnover), high ribonucleic acid (RNA), essential for protein synthesis, and turnover all indicate high protein formation within the brain.[3]

Free proteins comprise 40% of the dry weight of the brain, and have structural and enzymatic functions. They fall into four main classes:

- Phospho-proteins
- Neurokeratin
- Collagen and elastin
- Proteins in association with lipids 'proteolipids'

Some proteins are specific to the brain and its particular functions.

1.1.3 CARBOHYDRATES

Glucose and glycogen are the main sources of energy for brain metabolism. The content of these in brain rapidly decreases on death due to post-mortem anaerobic glycolysis.[10] Other small carbohydrate molecules are present in the brain tissue; however, larger carbohydrate-containing structures

such as glycoproteins, gangliosides and mucopolysaccharides are also present, and would be degraded by endogenous, microbial and insect enzymes on death.

1.2 Soft Tissue Degradation and Preservation

1.2.1 Normal Tissue Decomposition

For the most part the body consists of water, carbohydrates, proteins, lipids, DNA and RNA, which can be broken down into a variety of smaller molecules. Only 15% of the body (the bones and teeth) are durable biominerals.

1.2.1.1 Autolysis

Human death is a process in which the lack of oxygen transported to the tissues by blood from a pumping heart initiates a breakdown in the highly ordered metabolism of cells and their repair mechanisms, leading to irreversible cell death (autolysis) and decomposition.[11] Within cells, energy is transmitted as adenosine triphosphate (ATP) which is predominantly created by a metabolic pathway involving the oxidation and reduction of a series of membrane proteins and cofactors by electrons removed from hydrogen. The final electron acceptor is oxygen and so its absence disrupts ATP production. Although in hypoxic environments respiration is supplanted by fermentation (i.e. anaerobic conversion of pyruvic acid to lactic acid), the energy this produces is insufficient to maintain cell biosynthesis and ATP manufacture.[11] Without the production of ATP, proteins that require energy to transport molecules and ions across membranes fail, leading to extreme concentration gradients across membranes and an increasingly acidic intracellular environment[10] resulting in swelling of the cytoplasmic and mitochondrial matrices.[11]

The release of endogenous enzymes from membrane bound organelles called lysosomes, occurs both intra- and extra-cellularly.[12, 13] The enzymes, many of which are powerful hydrolases, break up large molecules - proteins,

fats, carbohydrates, nucleic acids and complex biomolecules - by insertion of hydrogen or hydroxyl ions from water.[13] This resulting disruption of molecules and membranes is a destructive process within the cell and also affects molecules supporting cell junctions. As cells detach from the tissues in which they were assembled, the macroscopic effects of necrosis are observable and liquefaction of tissues occurs.[11] Successive enzyme-mediated reactions break down the proteins, fats and carbohydrates further into small molecules soluble in water, or into gases.

The most metabolically active cells are affected first by enzymatic self-digestion as these are the cells that are most sensitive to anoxia.[11] An order of tissue decomposition based on autolysis alone proposes that tissues where ATP production is highest and cells with high concentrations of hydrolytic enzymes such as macrophages would decompose first.[11] In this model, brain cells, being the most energy-demanding cells in the body, would decompose first.

1.2.1.2 Bacteria: the effects of normal or enteric flora and environmental microbes

Alongside autolysis, the activity of endogenous microbiota and bacteria from the surrounding environment also cause tissue decomposition. A range of commensal/mutualistic/parasitic[a] bacteria that colonise the digestive and respiratory tracts as well as the skin are present in life and thus at the time of death.[14] Molecules released from cells due to autolysis are taken up as nutrients

[a] Bacteria can have symbiotic relationships with the human body acting as host. Commensalism is defined as the bacteria coexisting with the host, benefiting from it but without causing harm. Mutualistic bacteria have a cooperative and jointly beneficial relationship with the host, whilst parasitic bacteria benefit by harming the host.

by bacteria.[10] Since the immune system (which prevents damage) is no longer operating, the homeostatic mechanisms that control the presence of normal flora fail and bacteria can multiply and invade body tissues quickly. As the body becomes hypoxic, aerobic bacterial activity within the body declines but the environment stimulates growth of anaerobic bacteria that are prevalent throughout the body, and occur in large numbers in the gastrointestinal tract. The bacteria decompose the immediately surrounding host cells and spread throughout the body. Large molecules are degraded into smaller soluble molecules (including organic acids such as propionic and lactic acid) or gases (e.g. methane, ammonia, hydrogen sulfide). This liquefaction and gasification causes bloating, colour changes, purging and odours, processes collectively known as putrefaction. As the soft tissues decompose, the variety of chemical reactions that occur to break down the protein, carbohydrate and lipid components of the body (and products they produce) can influence the body's rate of decay and potential preservation.[12]

Microscopic fungi and animals that specialise in eating decaying matter (saprophages) such as flies, beetles and worms as well as larger fauna such as scavenging mammals may also be involved.[14] The decomposition of the soft tissues leaves the hard tissues (skeleton) which also undergo deterioration, although more slowly. Diagenesis[b] of bone, the replacement of ions within the bone mineral with ions from groundwater occurs and weathering erosion can also take place. Non-enzymatic chemical reactions including hydrolysis, oxidation and esterification also cause tissue breakdown.[15] As the rate of

[b] Diagenesis is the modification of the physical and chemical properties of the bone's organic matter when exposed to the environment. This leads to chemical exchange including adsorption to bone surfaces, leaching into the surroundings and deposition of minerals within pore spaces.

autolysis and bacterial degradation is based on enzyme activity, factors which affect this activity, such as temperature, pH, presence of water and inhibitors such as heavy metal ions, affect the rate of the body's decomposition.

1.2.1.3 Burial environment

The nature of the burial and the environmental circumstances can affect the decay rate with four factors (temperature, moisture, pH, and the partial pressure of oxygen) being widely recognised as important in determining the extent of preservation.[16, 17] The method of disposal also affects the access of flora and fauna to the body, and the environment affects microbial activity and the chemical exchanges that can occur.[11]

Soft tissue in the open is unlikely to be preserved beyond days/months, but depending on the depth, burial of corpses can help to decelerate the rate of decomposition as it can prevent access to scavengers and reduce insect colonization.[18] It also reduces temperature variation.

1.2.2 Soft Tissue Preservation Mechanisms

A wide range of mechanisms for soft tissue preservation are known, some of which are well described and understood, while others are a good deal less easy to explain.

Mummification has been defined as the arrested decay of a body or tissue.[15] There are multiple mechanisms by which this can occur naturally (or spontaneously) and a variety of anthropogenic interventions that may enhance these, whether deliberately or accidentally. There are also intentional methods that humans use to alter decay patterns (such as the Ancient Egyptian forms of embalming) but deliberate 'artificial' techniques will not be surveyed here.

Interactions between the environment and the body occur after death; consequently, how a corpse is disposed of can have a huge effect on the decomposition process. In certain environments, the process of decomposition of a cadaver can be retarded or even stopped. In order to persist, the chemical products of decomposition processes have to be thermodynamically stable and/or kinetically inert in the environment in which the body has been left.

As some processes for soft tissue decomposition rely on enzymes, whether they originate from the body itself or from microbes, factors that decrease their reaction rate or prevent them from working can delay/halt decomposition. The placement of a body has a significant effect on the rate of decomposition as this influences factors such as moisture level, pH, temperature, oxygen and other gas exposure, chemical environment and access of microbiota, flora and fauna.[11] The four main factors are affecting enzyme activity and bacterial growth are discussed in more detail below.

1.2.2.1 Moisture

The presence of water is vital to the decomposition process for a variety of reasons. It acts as the solvent for numerous enzymes, biochemical and non-biochemical molecules and it is the medium in which many metabolic reactions take place (including autolytic and bacterial). The presence of water can dilute reactants and produce an environment in which buffering can occur. It can also be a reactant providing hydrogen and hydroxyl ions, hydrolysis of large biomolecules being an essential reaction in the decomposition process. Water has a high specific heat capacity, requiring absorption or loss of a large quantity of energy before rising or falling in temperature, reducing fluctuations in temperature and providing thermal stability for enzymes. If a body is submerged in water decomposition varies: density and pressure effect oxygen

availability, the microbiome is different from soil, insect activity is prevented (but alternative scavengers are present) and movement of remains including disarticulation is more likely. Whether it is fresh, salt, still or flowing water and depth also has an effect. Water may be present in the soil but even in arid regions, the body itself is a source of water.

1.2.2.2 pH

The acidity or alkalinity of the extracellular and intracellular environments affect enzyme activity. Changes in pH can alter the intermolecular bonds that hold proteins in their specific secondary and tertiary structures, and so lead to changes in how effective the enzymes are. Most enzymes operate within a small 'optimum' pH range. At pH extremes enzymes denature and/or coagulate and activity ceases. The initial stages of decomposition lead to the release of organic acids, and fermentation that occurs in the anoxic body also produces acids resulting in an initial decrease in pH.[19] This acidic environment can increase the growth of fungi[20] and of acidophiles, bacteria that grow at low pH. In later stages of putrefaction, proteolysis products alter the overall pH to the alkaline range, in which alkaliphilic microorganisms may thrive.[21]

1.2.2.3 Temperature

Most enzymes are temperature sensitive. Raising temperatures increases the rate of decomposition reactions. If temperatures rise too high they can lead to denaturation of enzymatic proteins, whilst reducing the temperature reduces the rate of the reaction that the enzymes mediate. In terms of bacterial growth, the optimum temperature range for decomposition is 15-37°C.[22] Low temperatures can inhibit the growth of most microorganisms that cause putrefaction. At temperatures below 4°C proliferation of most commensal bacteria is significantly reduced, and this stops under 0°C.[22] However, there are

psychrophiles (bacteria that thrive near 0°C) and thermophiles (bacteria that thrive at temperatures over 50°C) that can be active at temperature extremes.

1.2.2.4 Oxygen

The partial pressure of oxygen is important in the decomposition process. It is the reduction of the levels of oxygen in the human body that triggers the initial comprehensive autolysis processes. Oxygen-deficient environments (e.g. waterlogged soils, high altitudes, deep burials, those submerged in water) have low redox potential, therefore oxidative decay processes occur more slowly. However, acidic and reducing environments can also occur in soils and water, especially if there is already decaying matter present. Well-aerated soils can have a high redox.[23]

Oxygen availability affects the types of microbiota that can thrive within the body but anaerobiosis alone does not prevent putrefaction, as there are plenty of bacteria that flourish in anaerobic environments.[24]

1.2.2.5 Chemical inhibitors

Activity of enzymes can be affected by inhibitors, molecules that interact with the protein to stop it working in a variety of ways, including irreversible and reversible (both competitive and non-competitive). Inhibitor molecules may compete with the normal substrate preventing a reaction from taking place at the active site, or can bind and alter the structure of the protein at an alternative site so it can no longer react with the original substrate. To prevent decomposition from occurring, irreversible inhibition of enzymes is more effective than reversible inhibition.

1.2.3 SPECIFIC EXAMPLES OF PRESERVATION

1.2.3.1 Desiccation

The process of desiccation, dehydration of tissue, produces the most common form of mummification.[25] It is often called spontaneous or natural mummification but can potentially be intentional, if a body is deliberately placed in a particular location in order to promote mummification. Hot, dry conditions are optimal. Mummification commonly occurs in arid/hyper-arid areas such as deserts[14] and although rare in temperate climates[26] it can occur occasionally in more humid environments if an appropriate microclimate has been formed,[15] e.g. in a cave system.[27]

Hot, dry conditions inhibit bacterial growth due to water loss. In dry conditions water can be lost through evaporation due to heat, capillary action, low pressure (1.2.3.3 Freeze-drying) and possibly by osmosis. The absence of water severely retards enzymatic reactions and prevents decomposition by bacteria and autolytic mechanisms. High temperatures increase the rate of dehydration but can also reduce the rate of decay by retarding the activity of enzymes. At higher temperatures the structural bonds holding the enzymes in their precise conformations are more likely to break, and this denaturation leads to a loss of function. As enzymes increase the rate of reaction, losing this functionality slows down the rate of decomposition.

Provided the soft tissues are dehydrated quickly and water is not reintroduced, remains can be preserved for many years.[12, 28] One of the oldest known examples is over 9000 years old (Chile's Chinchorro mummies).[15] The first areas to dry are those that contain little fluid such as the ear lobes, fingers, toes and scrotum.[13] Provided water is rapidly removed from the skin surface the concentration difference between the water content of the internal organs and

that at the skin provides a high water concentration gradient that increases the rate of water loss. Rapid dehydration of internal soft tissues can occur quickly enough that the complete decay of organs does not have time to occur.[15] In these situations the skin surface is the last to dry, after water has been lost from the internal organs. Instances of mummification have occurred where other soft-tissue has been preserved but the brain has decomposed.[14, 29] In rare cases dehydration of the outer surface occurs due to excessive heat, without the underlying organs dehydrating. Decomposition of the internal tissues can then still occur whilst the leathery skin surface acts as a barrier to further dehydration.[28]

As well as hot, dry conditions, the porosity of the surrounding burial environment can affect the rate of dehydration. Clothing can have a wicking effect, drawing water from the body. In the case of desert burials it is argued that wicking away of water by capillary action due to the sand's porosity is the major factor in dessication.[15, 27] Desiccation can be assisted by the surrounding chemical environment – the hygroscopic effect of limestone has been suggested to lead to tissue preservation.[30]

In anecdotal evidence osmosis (the movement of water from a dilute to a more concentrated solution across a semi-permeable membrane) due to bodies being buried in honey can lead to desiccation.[15] Ventilation may also be a cause of desiccation but would be dependent on the rate of air flow, humidity, access of microorganisms, flora and fauna etc.[15] Spontaneous mummification has occurred when bodies have been exposed to constant air flow[15, 31] and has been demonstrated experimentally.[27] Desiccation has been shown to occur within the same burial as adipocere formation (see 1.2.3.6 Adipocere).[26] The hypothesis suggested in that water within the body is used up in the hydrolysis of fatty acids leading to dehydration of the tissue, so that both desiccation and

adipocere formation processes can occur when exogenous water is unavailable.[26, 32]

1.2.3.2 Freezing

Cooling a body slows decomposition as most enzyme activity occurs within a specific temperature range. For most endogenous enzymes and bacteria this is around normal body temperature, so lowering the temperature inhibits activity and can stop it altogether. At temperatures below 12°C reproduction of bacteria falls as cell division is retarded and between 5-0°C it tends to stop completely. When temperatures are below 0°C, water in the intracellular matrix freezes, preventing movement of molecules and stopping reactions occurring. Soft tissue preservation due to freezing is not uncommon,[33] especially if bodies are buried in the permafrost,[15] where desiccation can also be a factor in preservation. The lower the temperature the smaller the degree of desiccation required to prevent putrefaction.[22]

Several examples of soft tissue preservation in glaciers have been reported. Burial next to permafrost of crew members from Sir John Franklin's expedition to find the North West passage led to exceptional preservation,[34-40] similar to Inuit remains such as the Qilakitsoq mummies.[41, 42] In two of the oldest cases of brain tissue preservation, mammoth remains found in the permafrost in Russia have been dated to ca. 40 and 53 thousand years.[43, 44]

1.2.3.3 Freeze-drying

Freeze-drying is a form of desiccation that can occur in cold climates, such as in the Arctic and Antarctic circles and at high altitudes. Ice from within a frozen body can sublime, transforming from a solid to a gas without becoming liquid, at low vapour pressures, leading to desiccation of a corpse. This can

occur in mountainous regions and has led to preservation of bodies in the Andes, such as the mummies found on Mount Llullaillaco in Chile,[45] or in glaciers, e.g. the Tyrolean Ice Man.[46-49]

1.2.3.4 Bog bodies

Soft tissue has been found preserved in bodies found in peat bogs across Northern Europe[14, 15, 50-53] and bog bodies are perhaps one of the best documented types of soft tissue preservation; nonetheless, rigorous understanding of the underlying mechanisms remains limited, in spite of much speculation and theorising. Peat is made of partially decomposed and compacted organic matter that has accumulated under water-saturated conditions and provides a unique preservation environment. Full decomposition of organic matter doesn't occur due to the anoxic conditions, the hardy nature of the plant material and the acidic environment.[54] A variety of plants are involved including sedges, shrubs and mosses, most notably *Sphagnum* peat moss. Within a peatland environment, oxygen in the stagnant water is quickly used up, along with other nutrients, and as peat accumulates the conditions become more acidic. This is due to the high cation exchange capacity of the plant material. The majority of cations and other chemicals are adsorbed by the organic material in exchange for hydrogen ions.[54]

It was generally considered that the anaerobic conditions within peat bogs prevent putrefaction as the anaerobic conditions inhibit the growth of aerobic bacteria.[52] However many of the bacteria involved in decomposition are anaerobic and within minutes of blood circulation ceasing, most human tissue becomes anoxic.[15] Peat bogs are by no means sterile, containing low but significant levels of anaerobic bacteria at deeper levels, as well as microbial activity at the surface.[55] Anaerobic bacteria that survive in peat bogs can carry

out hydrolytic breakdown reactions and in the presence of other substrates suitable for reduction (such as carbon dioxide, sulfate or nitrate) can carry out oxidative reactions. Oxidation of fatty acids in anoxic conditions is dependent on the types of bacteria present and hydrogen concentrations.[56]

The acidity of peat bogs has also been proposed to be responsible for preservation.[52] Many anaerobic putrefactive bacterial species such as *Clostridium* grow best at neutral pHs 5.5-7.5.[57] Despite the acidic reputation of bogs, a variety of pH distributions occurs depending on the peatland classification: bogs pH 3.5-4.2, poor fen pH 4-5.5, intermediate/rich fen pH 5-7.[54] The acidity level in rich fens is low enough that bacterial species can survive and in more acidic fens more specialised bacteria, acidophiles, take part in the decomposition process.

There has also been speculation about compounds from *Sphagnum* moss, possibly only released on death of the moss, possessing antibacterial properties. Sphagnol, an unidentified crystalline phenol, was extracted after boiling *Sphagnum* moss with 0.25 M NaOH proved to have bacteriostatic properties,[58] but later analysis has not been able to isolate this from living moss and it is considered unlikely to occur naturally.[59]

More recently, speculation about the effects of sphagnan, a pectin-like polymeric carbohydrate produced by *Sphagnum* moss, has held sphagnan to be responsible for the bog's preservative effect.[51] *Sphagnum* moss cell walls contain holocellulose, a combination of cellulose, hemicellulose and pectin (sometimes referred to as 'pectic acid') that acts as a cation exchanger. By absorbing the cations of salts and sequestering calcium and other multivalent ions, mineral acids are released. In dead moss, the polymer is broken down and 'pectic acid'-containing subunits, ~25% of which are D-lyxo-5-

hexosylopyranuronic acid (or trivially 5-keto-D-mannuronic acid (5-KMA)), are released. Sphagnan is associated with cell walls and has a high cation-exchange capacity due to its polyanionic character[60] and chelates metal cations essential for normal bacterial enzymatic action, for example reducing Ca^{2+} concentration by counterion-exchange.[51] Sphagnan is unstable and is converted to humic acid which also sequesters multivalent cations with high selectivity. Removal of essential micronutrients helps suppress the growth of micro-organisms.

The sphagnan structure also immobilises enzymes released from bacteria and it has been shown experimentally that pepsin, trypsin, pronase and amylases bind irreversibly with *Sphagnum* holocellulose.[61] As bacteria release enzymes to break down molecules too large to engulf, their binding and immobilisation helps prevent putrefaction.

The multiple carbonyl groups on the polysaccharide sphagnan means it can act as a tanning agent, cross-linking collagen fibres.[51, 62] Sphagnan is proposed to trap nitrogen via Schiff base formation between its carbonyls and certain amines (including ammonia, proteins and enzymes) reducing availability of bound nitrogen for bacterial growth[61] and lowering the pH of the surroundings which can prevent enzyme activity in bacteria not adapted to acidic environments.[63] However, re-examination of sphagnan has been unable to identify KMA subunits and ion-exchange capacity was attributed to GalA concentrations.[64] The exact mechanism for soft tissue survival in *Sphagnum* peat bogs, and if KMA has a role in this, is yet to be established.

1.2.3.5 Heavy metals

Enzyme denaturation by heavy metals can slow down soft tissue destruction. In areas where there are high concentrations of heavy metals (such as mercury, arsenic, copper and lead) it has even been suggested that these

heavy metals prevent total decomposition.[65] High levels of arsenic in Chilean river water that accumulate in the body during life were discussed as possibly aiding spontaneous mummification of Incan corpses buried in the Camarones River bank, preserving much soft tissue.[13] However desiccation has also been held partly responsible for this preservation.[15] Soft tissue preservation has also occurred in the presence of metallic grave goods, but only locally at low levels. Copper jewellery left in contact with the skin has led to narrow bands of flesh surviving[66] possibly due to copper ions binding to polypeptides and 'tanning' the soft tissue.

1.2.3.6 Adipocere

Adipocere is a fatty, waxy, soapy bulk also called 'grave wax' or 'corpse wax' that can form during corpse decomposition.[67] It has a range of appearances and textures and can be whitish in colour, through to grey or brown, it can range from a soft and greasy texture to hard and friable, and can smell mouldy, putrid or not at all. Adipocere formation has been called a chemical form of mummification[15] as its formation inhibits post mortem changes, can form a protective layer and can lead to soft tissue preservation. However, adipocere itself, is a product of the corpse decomposition process and its creation only occurs within conducive environments. It occurs in a variety of forms from barely visible lesions to large regions replacing areas of soft tissue.[13] The formation of adipocere has been reported to occur in a variety of environments, and can form quickly or slowly. It can also persist for very different lengths of time from 5[68] to 3350 years,[69] but can be degraded under the right conditions.

One of the first mentions of the substance was by Sir Thomas Browne in his work 'Hydriotaphia, Urn Burial' published in 1658.[70] However, it is generally

believed that Fourcroy[71, 72] and Thouret[73] were the first to scientifically report the phenomenon during their examination of exhumed of bodies from the Cemetery of the Innocents in Paris in the late eighteenth century. Fourcroy suggested after experimentation that adipocere represented a form of soap resulting from reactions of fat with ammonia and phosphate of lime.[71, 74, 75] Initial nineteenth-century chemical separation and analysis of various adipocere samples identified lime, fatty acids (palmitic, stearic, oleic or margaric), hydroxy fatty acids, cholesterol and ammonia as well as insoluble residues.[75] The insoluble residues were later identified as calcium palmitate, stearate and hydroxy stearate.[75]

Observation has shown adipocere is more likely to occur in female corpses, especially around the thighs[16] and in obese corpses[11] and doesn't occur in bodies suffering from starvation.[74] Along with the chemical evidence this agrees with the hypothesis that adipocere originates from subcutaneous fat tissues and corpses are more likely to have evidence of adipocere formation around fatty areas of the body. Despite investigation into its formation, a clear consensus on its origins has not been reached and a variety of theories for its formation have been suggested, as discussed in the following sections.

Saponification

A saponification theory of fatty acids has been suggested as the mechanism for adipocere formation. Hydrolysis of the ester bonds of triacylglycerides post-mortem can occur due to enzyme activity (either internal or bacterial lipases) or without, provided the fats are in a mildly acidic aqueous solution. Removal of a proton from the carboxylic acid means the fatty acid can take on sodium or potassium ions present in the environment (interstitial fluids, ambient water) at neutral or slightly alkaline pH, yielding a salt. The sodium or

potassium can be further replaced by calcium/alkali-earth metals/bivalent metal ions (Equation 1, Figure 5), producing an insoluble, brittle soap, in a process called 'hardening'.[11] It has been noted that in areas of hard water fat, oil and grease deposits in sewers are more insoluble, have higher melting points and have increased calcium levels having undergone saponification.[76] In a similar way, the degree of saponification in the body may be related to the mineral content of the burial soil or water, with higher mineral content leading to greater saponification. A decrease in calcium concentrations with a corresponding increase in sodium concentrations in a burial pit pore water depth profile has been correlated with adipocere formation,[77] consistent with this model of formation.

$$2\ C_{17}H_{35}COO^{-}Na^{+} + Ca^{2+} \rightarrow (C_{17}H_{35}COO^{-})_2Ca^{2+} + 2\ Na^{+}$$ **Equation 1.**

SODIUM STEARATE (SOLUBLE) CALCIUM STEARATE (INSOLUBLE)

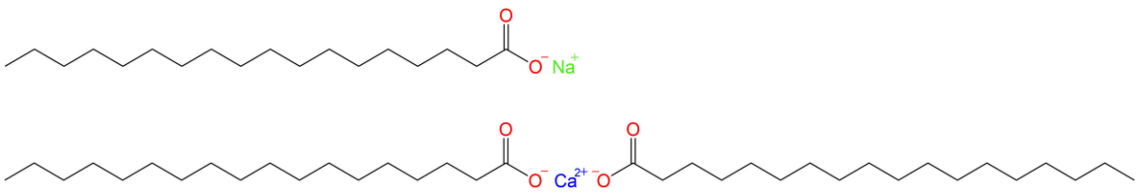

Figure 5. Stearate chemical structures: (above) sodium stearate, (below) calcium stearate

Despite early ideas, adipocere is not wholly composed of saponified fatty acids. Takatori analysed three samples of adipocere and found fatty acids from soap only constituted 2.3-34.5% by weight of the total fatty acid amount.[78]

Fat migration theory

An alternative theory of adipocere formation is that of 'fat migration'. The triacylglycerides are freed from cells by the decomposition of supporting

structures allowing them to migrate. In wet conditions and over long periods of time the triacylglycerides are hydrolysed.[75] Once hydrolysed, the smaller fatty-acid products and glycerol are rapidly lost to the surroundings by diffusion or gravitational separation[69] and the remaining larger fatty acids congeal to form adipocere. In peat bogs as part of the tanning process, crosslinking between amino acid groups on collagen molecules may lead to tissue contraction physically squeezing lipids out, after which hydrolysis of fatty acids can occur.[57] This theory does not fully explain the different proportions of saturated and unsaturated fatty acids found before and after adipocere forms, and suggests enzymes and bacteria only play a secondary role.

Hydrogenation theory

The hydrogenation theory suggests that fatty acids are freed from triacylglyerols by hydrolysis in adipose tissue and the resulting liquid mixture containing mainly unsaturated fatty acids undergoes hydrogenation to form saturated fatty acids. This process is mediated by bacteria and includes *β*-oxidation process to convert unsaturated oleic to saturated palmitic acid. Unlike the triacylglycerols which are liquid at body temperature the higher melting point of these saturated fatty acids means they remain solid, forming an insoluble air-tight shell, preventing further soft tissue decomposition.[18]

Experiments by den Dooren de Jong using a two phase system of olive oil and water inoculated with soil bacteria and left under anaerobic conditions produced a whitish crust with components that, when separated and identified by GC-MS, were similar to adipocere.[74] A similar experiment with triolein (glyceryl trioleate) and water showed that oleic acid could be converted to palmitic acid by bacteria.[74]

Analysis of adipocere

After the initial identification of adipocere a limited number of studies were made during the eighteenth and early nineteenth century that tried to clarify its composition.[75] Chemical methods of identification and separation were employed with a range of soaps and fatty acids being isolated (see Table 2). In addition to soaps, further analysis has isolated a range of components also found in adipocere (Table 3).

Using GC-MS[78] it was possible to identify the structure of 10-hydroxy octadecanoic acid (10-hydroxy stearic acid) as a component of adipocere but it was not possible to confirm the presence of 9-hydroxy stearic acid and it was proposed this was in fact 10-hydroxy palmitic acid. Small amounts of a derivative of linoleic acid, 10-hydroxy-12-octadecenoate, have been detected in adipocere but not in comparable quantities to linoleic acid, suggesting further breakdown or other microbiological conversions of this fatty acid occur.[78]

Takatori produced several papers showing production of hydroxy fatty acids and oxo fatty acids plays a role in the formation of adipocere; hydroxy fatty acids and oxo fatty acids are synthesised by bacterial enzymes. In addition, cholesterol and epicoprostanol (an isomer of coprostanol, a form of hydrogenated cholesterol) have been reported in adipocere samples.[79]

Table 2. Percentage composition of 'Hard Clean Adipocere Wax' determined by a variety of chemical methods.[75]

Component	Percentage by weight
Palmitic acid	67.52
Stearic acid	3.3
Oleic acid	5.24
-Hydroxy stearic acid	9.48
-Hydroxy stearic acid	6.32
Stearin and palmitin	1.21
Olein	0.16
Unsaponified matter	0.87
Calcium soaps	4.41
Protein	0.665
Ash	0.578
Humus and undetermined	0.247

Conditions for formation of adipocere

Adipocere formation is affected by a wide variety of burial characteristics, including the composition of the corpse, the method of burial, and the conditions of the resting place, including anaerobic conditions, humidity, temperature, sand the oil conditions. Water potentially promotes saponification as it reduces the rate of oxidative degradation of fatty acids, increasing their availability to, at low pH, produce salts. The formation of hydroxy and oxo fatty acids (with higher melting points than their corresponding straight chain fatty acids) is thought to stabilise adipocere.[78]

Table 3. Chemicals found in adipocere

Abbreviation*	Chemical constituent	Reference
C12:0	Lauric acid (dodecanoic acid)	
C14:1	Myristoleic acid	80
C14:0	Myristic acid (tetradecanoic acid)	
C16:1	Palmitoleic acid (*cis*-9-hexadecanoic acid)	
C16:0	Palmitic acid (hexadecanoic acid)	
C17:1	Heptadecenoic acid	80
C18:2	Linoleic acid (*cis,cis*-9-12-octadecadienoic acid)	
C18:1	Oleic acid (*cis*-9-octoadecanoic acid)	
C18:0	Stearic acid (octadecanoic acid)	
C20:0	Arachidic acid (eicosanoic acid)	
	Cholesterol	79
	Epicoprostanol	79
	9-hydroxystearic acid	75
	10-hydroxystearic acid 10-hydroxypalmitic 10-oxopalmitic/or margaric acid	80, 81
	9-hydroxyoctadecanoic acid	
	10-hydroxyhexadecanoic acid	
	10-hydroxyoctadecanoic acid	
10-OHODA	10-ketooctadecanoic acid	
10-OHHDA	10-ketohexadecanoic acid	

* carbon count : number of double bonds

Extensive investigation of burials after the Second World War led to some key observations regarding adipocere formation.[16] Moisture in the environment was reported to be conducive to adipocere formation but water from within the

body's tissues was sufficient. Anaerobic conditions were also conducive, but adipocere could also form under aerobic conditions.[16] Experiments have shown that soil type affects the formation[82] of adipocere, but that extremes of pH inhibit its formation.[83] Clothing has also been suggested to increase adipocere formation by increasing moisture content around the body.[16, 84]

Decomposition of adipocere

Adipocere can persist for extended periods of time in a stable environment but can decompose.[18, 85] Fatty acids can be oxidised into aldehydes and ketones, but this is prevented in anaerobic environments and adipocere deposits can remain for considerable periods of time. It has been shown to persist over 1600 years even with changing water levels.[86] Converting fats to fatty acids lowers the pH of the tissue, which can reduce bacterial growth, enhancing preservation.

1.2.3.7 Fossil fuels

Whilst the above-described forms of preservation can occur over periods up to thousands of years, on a geological timescale soft tissue preservation doesn't occur without considerable chemical transformation. Fossil formation tends to preserve the 'hard parts' (bones/teeth/scales/shell), by a process of mineralisation. It can be argued that the longest lasting form of soft tissue preservation, although undergoing much alteration, is that which results in the formation of fossil fuels. Whilst the origins of coal, oil and gas are mostly plant based, these contain many of the same precursor components as most other living matter – including lipids, proteins, carbohydrates and so on. With fossil fuels, the original organic material comes from zooplankton, algae etc. The original material's nature as organic is retained in the fossil fuels, with the presence of predominantly C, H, O, N, S atoms in a hydrocarbon framework.

When biomass (in large quantities) is submerged in anoxic water then incorporated into sediments and subjected to high temperatures and pressures over long periods of time the organic matter undergoes a series of transformations called diagenesis.[87] This leads to kerogen formation, a form of insoluble organic matter found in oil shales, and with further heat and pressure causing additional chemical change (catagenesis) produces petroleum and gas.[88] These organic mixtures can survive for millions of years.[87]

1.3 Brain Preservation

Some specific instances of brain preservation have been described in the literature and limited chemical analyses have been carried out. Of these, most of the methods of preservation are those described above.

However, some reported brain preservations do not fall easily into any of the categories of preservation mechanisms surveyed in this introduction. For instance, brain tissue found within a skull in South Africa came from an environment which was not considered dry enough for standard desiccation or wet enough for adipocere formation, and yet was preserved.[89]

Four examples of brain tissue have survived from Seyitömer Höyük, Turkey. The remains were found in a burnt layer of sediment and it has been speculated that the bodies were rapidly buried due to tectonic activity. A subsequent fire removed oxygen from the rubble and boiled the brains in their own fluids.[90] Lack of water and oxygen were proposed to have prevented enzyme activity and the high concentrations of potassium, magnesium and aluminium would have promoted saponification to form adipocere.[90] It would have been ideal if samples from these unusually preserved brains could have been analysed during this project. However, this proved impossible to arrange.

In some cases of soft tissue preservation, a combination of processes has been shown to occur. In the Cova des Pas, Minorca, an early Iron Age funerary complex, soft tissue remains including brain matter (Figure 6) show evidence that both desiccation and adipocere formation have occurred. It has been suggested the multiple corpses, including wrappings, induced an anaerobic and moist environment, in which adipocere formed in some instances but a climatic

increase in temperature and drop in moisture led to dehydration of tissue as well.[91, 92]

Figure 6. Preserved brain soft tissue from the Cova des Pas site (Minorca, Bronze Age) [39]

There have been some instances of brain preservation within wet springs such as at Windover farm in USA.[93] Here, although the bodies had been skeletonised, soft tissue within the skulls was observed. The brains had shrunk but showed some large structural features, and histological investigation showed microscopic detail consistent with brain matter.[94] This description highlights similarities with the York brain (for more details see 2.1.1).[1] One of the suggested mechanisms for lone brain matter survival is that unlike many other internal organs the brain is enclosed by a protective membrane (the meninges) as well as the skull, which provide it with greater physical protection.[14] This also isolates the brain somewhat from bacteria, although autolysis can still occur. Isolated brain remains have also been found in a mass burial of cattle and pig carcasses (interned due to the 1967 foot and mouth outbreak, UK)[77] and it has been hypothesised that the skull itself creates a microclimate which allows brain preservation when other soft tissue was lost.[95]

There are several examples of brains from waterlogged sites, such as the York brain, surviving when all other soft tissue has been lost. These are summarised by O'Connor[1] to include: in a flooded limestone cave in Warm Mineral Springs, Florida, USA, in a cemetery in Little Salt Spring, Florida, USA, in a swampy pond in Windover, Florida, USA, in 6 m deep flood debris, Zihl Canal, Switzerland, in frequently flooded graves in Svenborg, Denmark, in a waterlogged grave in Sandwell, UK, in waterlogged graves from an Augustinian Friary, Hull, UK, in a Roman riverside burial in Scole, UK and a child burial within a wet clay environment in Quimper-Bretagne, France. For a summary of the chemical investigations carried out on these remains, see Table 4.

The York brain was found in an isolated skull which had been removed from the body.[1] If removal of the head occurred at the time of death, this may have prevented the intestinal fauna reaching the brain and so delayed putrefaction. Blood would have drained out leading to fluid loss and potential desiccation. If burial of the head occurred quickly, this may have protected against some microbial access and so prevented environmental putrefactive organisms from infecting the head.[18] Lipids make up approximately 10-12% of the wet weight of fresh brain.[3] Notably the York brain remains yielded a much lower percentage of solvent extractable lipidic content (0.8–1.1% of wet weight) and the material identified from this extract is not consistent with adipocere formation.[1]

Although there is a range of natural soft tissue preservation mechanisms known/postulated, none of these fully explains the instances of isolated brain tissue remains in otherwise skeletonised bodies. In the case of waterlogged burials, adipocere formation has occurred in some cases, and may well play a role in brain preservation,[96] but did not occur in the York brain example.[1]

Table 4. Summary of scientific analyses that have occurred on selected surviving brain masses

Where	How many	Age (years BP)	Method of brain preservation	Method of analysis	Compounds Found
Heslington, York, UK[1]	1 adult	2469 ± 34 BP (673-482 BC)	Unknown, possibly waterlogged pit	Radiocarbon dating of skull CT and MRI imaging, light microscopy, SEM and TEM, 3D laser scanning DNA (unpublished), amino acid and proteomic analysis 1D-TLC of lipid extract (made using the Folch[97, 98] wash method) Thermal desorption and pyrolysis GC-MS MALDI FT-ICR MS (unpublished)	C:N ratio was 6.3 (n=2) 5% of total tissue was hydrolysable amino acids, AA racemization levels D/L > 0.06 except for Asx Peptides from myelin proteolipid protein (lipophilin) and claudin-11 (oligodendrocyte-specific protein) identified Solvent soluble lipids were 0.8-1.1% wet weight Coprostanone, trace cholesterol Hydroxyfatty acids, aldehydes, thiophenes low levels of sterols/stanones Series of 2-hydroxyfatty acids (C22:0 – C25:0 and C24:1) High molecular weight, long chain organic material

Where	How many	Age (years BP)	Method of brain preservation	Method of analysis	Compounds Found

Windover pond, Brevard County, Florida, USA[94, 99-101]	4 adults + 1 subadult with recognisable preserved/replaced brain tissue 1 adult + 3 subadults with 'amorphous brain tissue mixed with peat'	6,990±70 BP	Fluctuating water level in peat pond (aqueous environment)	Accelerator- mass spectrometry of isolated collagen (dating) x-ray imaging, computerised axial tomography and proton magnetic resonance imaging, light and transition and scanning electron microscopy Nucleic acid extraction	Human mtDNA present
Cova des Pas, Minorca[91, 92, 102]	Three within funerary cave site	~ 3000 BP	Adipocere and desiccation	Light microscopy Scanning electron microscopy Transmission electron microscopy GC-MS	Lauric acid Myristic acid Pentadecanoic acid Palmitoleic acid Palmitic acid Linoleic acid Oleic acid 10 Hydroxy palmitic acid Stearic acid 10-Hydroxy stearic acid

Where	How many	Age (years BP)	Method of brain preservation	Method of analysis	Compounds Found

57

Kirguilyakh brook, Kolyma river basin, Magadan district and Timyr peninsula in Khatanga river basin[43, 44]	2 (mammoths)	~40,000 and ~53,000 BP	Frozen mummification	2-D TLC Transform fatty acids to methyl esters analyse by GLC TLC Lipids extracted by column chromatography, separated by TLC, underwent acid methanolysis – sphingosine bases transformed into trimethylsylil derivatives, analysed by GC Chromatogram – orcin reaction, colocimetric test on sulphate group with azur A 'resorcinal method', purified by alkaline hydrolysis, chromatographed on a Sephadex column TLC) and GLC	No glycerophospholipids Sphingomyelin detected 18 fatty acids detected – stearic major saturated, nervonic major unsaturated Cerebrosides and sulfocerebrosides – (hydroxyl fatty acid fraction and normal fatty acid fraction) Sphingosine bases identified by comparison with standard prep 4-sphingenine and sphinganine Gangliosides – sialic acid Monosialogangliosides (di-/tri)- Cholesterol and cholesterol esters

Where	**How many**	**Age (years BP)**	**Method of brain preservation**	**Method of analysis**	**Compounds Found**

58

Tyrolean Iceman, Similaun glacier, South Tyrol, Italy[46-49, 103-107]	1 (male)	~5300 BP	High altitude freezing (desiccation)	Homogenised, 30min @ 100°C in 1ml of 7.5 N NaOH/methanol (1:1 v/v), add 2ml methanol/ 6 N HCl (4.6:5.4 v/v) heat 10 min @ 80°C ... GLC -MS Accelerator mass spectrometry (dating) Sample of cerebral cortex taken desiccated, immersed in cold fixative, held under vacuum, fixed in resin – light and electron microscopy	Fatty acids: Myristic acid (14:0) Palmitoleic acid (16:1) Palmitic acid (16:0) Linoleic acid (18:2) Oleic acid (18:1) 10-hydroxypalmitic acid (16:0 10OH) Stearic acid (18:0) Arachidonic acid (20:4) 10-Hydroxystearic acid (18:0 10OH) Staining with Sudan black for lipids – reacted positively with myelin remains (unsaturated lipids and periodic acid-Schiff-reactive carbohydrates detected with electron microscopy)

Where	**How many**	**Age (years BP)**	**Method of brain preservation**	**Method of analysis**	**Compounds Found**

Hampton Road, Droitwich, Worcestershire[1][08]	1 NB notes others including one found in 1843	1,500-2,000 BP	Waterlogged site	Observation only No mention of chemical analysis	Bog burial rich in cholestrine
Quimper-Bretagne, North-western France[96]	1 formalin fixed brain (child – 18 month old)	~800 BP	Salt and fresh water, acidic clay soil environment	Macroscopic observation aDNA extraction MRI CT scanning GC-MS (65mg tissue) extracted using Makristathis method	Fatty acid composition evaluated: Ginkgolic acid (13:0) Myristic acid (14:0) Pentadecanoic acid (15:0) Palmitic acid (16:0) Heptadecanoic acid (17:0) Oleic acid (18:1) Stearic acid (18:0) 10-hydroxy stearic acid (18:0 1OH) ((Eicosenoic acid (20:1) found only in modern brain comparison)) Ancient brain high conc. Sat fatt acid, low unsat. Fat acid

Where	**How many**	**Age (years BP)**	**Method of brain preservation**	**Method of analysis**	**Compounds Found**

Warm Mineral Springs, Sarasota County, Florida[93]	Under sediment in cave under water – antibiotic activity of sediment/spring water?	10,000 BP ± 200 years	Suggested adipocere	Macroscopic investigation and light microscopic Positive Salkowski and Lieberman-Burchard reactions	Cholesterol, esters, phytosterols (assumed due to staining?)
Svenborg, Denmark[109]	56 of 74 skulls contained intracranial masses	714-410 BP	Adipocere, frequent floods, alkaline reaction of soil, exclusion of air in clay	Light microscopy Scanning electron microscopy Qualitative lipid analysis	Phospholipids, Neutral lipids and fatty acids cholesterol
Loshin site, Dubrinishte Billage, Bankso Community, Sofia District[95]	2 (inside intact skulls), 5 other brain structures (1 almost whole, others fragments)	10-0 BP	Microclimate within cranial cavity? Rapid evaporation of intracellular brain fluid	Elementary atomic spectral analysis (2g desiccated under IR for 10 days, cleaned, ground, homogenised with pure carbon powder (1:1) Electron microscopy	Similar Ca, Cu, Pb content of mummified brain compared to a modern brain Less P, Na but more Mn, Si, Al, Ti in the mummified remains

61

1.4 Mass Spectrometry

The analytical technique used to explore the components of the brain lipid extracts was high resolution mass spectrometry. This method was chosen because using the spectra it is possible to calculate the molecular weight of the sample components to 3 dp and so determine their likely empirical formulae. This then provides an insight into the component's chemistry. This section provides a short overview of the history of this technique and details of the particular instrument and ionization method used.

1.4.1 OVERVIEW/HISTORY

Mass spectrometry has developed into a powerful analytical tool from its beginnings over a century ago as a means of investigating anode and cathode rays.

At the fundamental level, a modern mass spectrometer combines a method of sample introduction, a technique to ionise molecules (or atoms) from the sample, a device that can separate and measure the mass-to-charge ratio (m/z) of the resulting ions (mass analyser) and a way of determining each ion's abundance. They often include a method of selecting a specific ion and a fragmentation method, which can be used to provide important structural information. The resulting data are transferred to a processing unit where they are analysed and then depicted as a series of peaks in a mass spectrum. A brief schematic of this arrangement is shown in Figure 7..

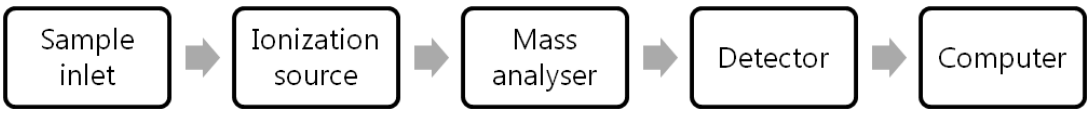

Figure 7. Schematic representation of the elements of a mass spectrometer

Advances in each of these elements have improved the resolution, limit of detection, mass accuracy and mass range over which these instruments can operate. The range of analytes that can be examined has expanded both in terms of mass and complexity, and the types of experiments that can be carried out have increased the amount of information that can be collected. The technique has become increasingly important and has expanded, facilitating the generation of entirely new fields of study.

JJ Thomson developed the first apparatus that measured mass-to-charge ratios of ions, going on to determine the mass of the electron, for which he won the 1906 Nobel Prize in Physics. His first 'parabola spectrograph' used parallel electronic and magnetic fields to deflect atoms and molecules with detection by photographic plates.[110] Further refinements to the apparatus were made by various scientists over the first few decades of the twentieth century.

The instrumentation was primarily used by physicists who were interested in the discovery and separation of atomic isotopes and AO Nier's use of mass spectrometry to separate ^{235}U in 1939[111] was a major development of the atomic age and highlighted the technique. It was also applied early on to small organic molecules.[112]

The time-of-flight mass analyser was proposed by WE Stephens[113] in 1946 and designed in 1948.[114] Other analysers, such as ion cyclotron resonance,[115] quadrupole and ion trap[116, 117] were designed and built, although it was a while

before these were developed commercially. More recently the Orbitrap, an ion trap using an electrostatic quadro-logarithmic field based on the Kingdon trap,[118] was designed by AA Makarov.[119]

The range of available ionisation approaches has expanded to include electron ionisation,[120] chemical ionisation, field desorption, atmospheric pressure chemical ionisation, plasma desorption, inductively coupled plasma, thermospray, matrix-assisted laser desorption/ionisation, electrospray, and nanoelectrospray. Mass spectrometers have been coupled to gas chromatographs, liquid chromatographs, high performance and ultra-performance liquid chromatographs.

The ability to ionise large molecules without fragmentation and the development of analysers with increased mass ranges meant that in the 1980s and 90s mass spectrometry took on a very much more significant role in the biological sciences.[121]

1.4.2 Ionisation: Matrix-Assisted Laser Desorption/Ionisation (MALDI)

MALDI is a soft ionisation technique which allows even large molecules to be ionised without use of the high temperatures/energies that can lead to sample degradation. Originally, laser desorption made use of a focused laser pulse to ablate the surface of usually solid material, producing gaseous ions and neutral molecules in a plume. The molecules may react together within the dense vapour and fragmentation of molecules over 500 Da typically occurs. Time-of-flight or simultaneous mass analysis is required due to the short period of ion production following the laser pulse. Ease of vaporisation and ionisation depends on the properties of the analyte. Karas and Hillenkamp first introduced

the use of organic matrices, allowing ionisation of large intact, non-labile molecules via laser ablation, in the technique named matrix-assisted laser desorption/ionisation (MALDI).[122] MALDI is now a very widely used technique that allows proteins, oligosaccharides, lipids and other species to be analysed by mass spectrometry.

The sample is mixed with an excess of organic matrix, usually whilst both are in solution, and a spot of the resulting mixture is placed on a metal plate to dry, forming a matrix/analyte 'cocrystal' in which the analyte molecules are surrounded and embedded. Matrices are chosen to absorb the energy of the laser used, and to protect the analyte from damage by the laser energy. In the most commonly-implemented approach to MALDI a UV laser is used to produce a short pulse of laser energy, and small conjugated organic acids are the most common matrices. Absorption of the laser energy by the matrix molecules is believed to cause the matrix to desorb and ionise. Desorption of the matrix leads to co-desorption of the analyte, initially as a neutral, into a plume the develops just above the plate, as a result of the laser pulse. While the exact mechanism of ionisation is not well understood, it is proposed that in the plume, collisions between matrix ions and analyte molecules result in charge transfer reactions, that ionise some of the analyte species.

MALDI is widely adopted for a wide range of analyses, including of lipids, other lipidic compounds, for which it has been employed in this thesis (2.4, 3.3). It is rapid and conveniently tolerant of a range of contaminants that can affect ionisation efficiencies when using other ionisation approaches. However, due to the process of cocrystalisation and ionisation, which depends on desorption from the matrix/sample spot surface, this means the technique can suffer from poor spot to spot reproducibility.

1.4.3 MASS ANALYSERS

After the ions have been produced they are separated by their *m/z* ratios, in the mass analyser. A variety of different principles can be manipulated to cause ion separation, exploiting combinations of static and dynamic magnetic and/or electric fields, depending on which of a range of analyser designs is to be used. The performance of the mass analyser can be described in terms of how well it separates ions and how well it assigns their *m/z* values.

The mass accuracy afforded by the mass analyser is described as the difference between the true and measured *m/z* values, and is expressed in millimass units (mmu) or, for high accuracies, more conveniently in parts per million (ppm). Mass resolution is the ability of the mass analyser to yield distinct signals from ions with small *m/z* differences; resolving power, R =m/Δm, where *m/z* is the mass of the ion, and Δm the difference in *m/z* values between two ions being separated.

1.4.3.1 Fourier-transform ion cyclotron resonance

Fourier-transform ion cyclotron resonance mass spectrometry (FT-ICR MS) is a technique in which a mass analyser confines ions within a static, uniform magnetic field and records the electric current induced by cycling of the ions after excitation. Fourier transformation is used to convert the time-dependent signal into a frequency-dependent signal, which is then used to generate a mass spectrum.

Ions are trapped within a 'Penning' trap, first built by Hans G. Dehmelt. Dehmelt, along with Wolfgang Paul, won a share of the 1989 Nobel Prize in Physics for their work on ion trapping.[117] Hipple, Sommer and Thomas first described the application of ion cyclotron resonance (ICR) in mass spectrometry

in 1949[115] and the first use of Fourier transformation in conjunction with ICR was reported by Comisarow and Marshall in 1974.[123]

1.4.3.2 Ion cyclotron motion

If an ion is placed in a static, uniform magnetic field it is subject to centripetal force:

$$\boldsymbol{F} = q\boldsymbol{v} \times \boldsymbol{B_0}$$

Equation 2.

where q is the ionic charge, $\mathbf{v}$ the velocity and $\mathbf{B_0}$ the magnetic field. As $\mathbf{v}$ and $\mathbf{B_0}$ are vectors, the cross-product term ($\mathbf{F}$) is perpendicular to the $\mathbf{vB}$ plane (see Figure 8).[124]

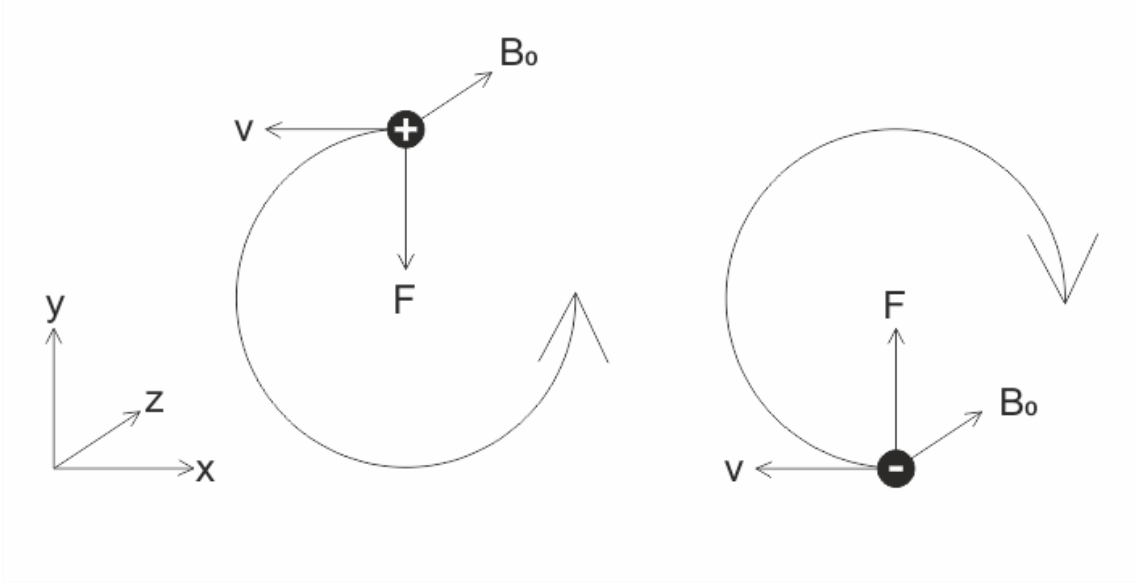

Figure 8. Ion cyclotron motion. The magnetic field (B_0) provides a perpendicular force (F) to the ions' motion (v), creating a circular motion.

This means the ion moves with a circular trajectory. It is therefore also subject to centrifugal force $\mathbf{F}'$:

$$\boldsymbol{F'} = \frac{m\boldsymbol{v}^2}{r}$$

Equation 3.

where m is the mass of the ion and r is the radius of the trajectory.[124] When these forces are in balance the trajectory is stable, and as

$$q\boldsymbol{B_0} = \frac{m\boldsymbol{v}}{r}$$

Equation 4.

the frequency of the ion completing a full circle (ϑ) in the xy plane can be given by:

$$\vartheta = \frac{\boldsymbol{v_{xy}}}{2\pi r}$$

Equation 5.

Angular velocity (ω) about the $\mathbf{B}$ or z-axis is then:

$$\omega = \frac{\boldsymbol{v_{xy}}}{r}$$

Equation 6.

Then, with substitution, the "cyclotron" motion of the ion can be shown to have a frequency ω_c related to its mass to charge ratio (m/q) and independent of its velocity.

$$\omega_c = 2\pi\vartheta = \frac{q}{m}\boldsymbol{B_0}$$

Equation 7.

With rearrangement, the radius of the ion's cyclotron motion path can be determined,[124]

$$r_c = \frac{m\boldsymbol{v_{xy}}}{q\boldsymbol{B_0}}$$

Equation 8.

remembering that:

$$q = ze$$

Equation 9.

where z is the charge number and e is the charge constant.

1.4.3.3 Observations from these equations

These equations show that an ion's cyclotron frequency is inversely proportional to its *m/z* ratio and the magnetic field strength. Ions with high *m/z* values orbit at lower frequencies than ions with smaller *m/z* values. Correspondingly the radii of heavy ions are larger than those of light ions, provided velocities are equal and within a uniform magnetic field. As the magnetic field is kept constant in an ICR cell, measuring the ion's frequency can be used to determine its *m/z*. If the magnetic field strength is very large and the velocity is very low, the cyclotron frequency is high and the radius of motion small, effectively 'trapping' the ions. All ions of the same *m/z* have the same cyclotron frequency independent of their velocity. The ions' velocity is directly proportional to radius of the cyclotron orbit, so that an increase in velocity (higher kinetic energy) leads to an increase in trajectory radius.[124]

1.4.3.4 Ion cyclotron resonance

Ion cyclotron motion is not useful until the ions are excited to a large enough radius to be detected, by irradiation with an oscillating electric field of the same frequency (in resonance) as their rotation.

Assume an ion in a magnetic field is placed between two infinite parallel electrodes as shown in Figure 9. If a potential, or voltage, V, is used to form a sinusoidal waveform $(\boldsymbol{E}_R(t))$ and applied to one plate, and a second voltage which is 180° out of phase with this waveform $(\boldsymbol{E}_L(t))$ is applied to the second plate, the opposing potential waves generate an oscillating electric field. The electric field, $\boldsymbol{E}(t)$, can be described using **i** and **j** unit vectors parallel to the x and y axis:

$$\boldsymbol{E}(t) = E_0 \cos \omega_c t \boldsymbol{j} = \boldsymbol{E}_L(t) + \boldsymbol{E}_R(t)$$

Equation 10.

Where:

$$\boldsymbol{E}_L(t) = \frac{E_0}{2} \cos \omega t \boldsymbol{j} - \frac{E_0}{2} \sin \omega t \boldsymbol{i}$$

Equation 11.

$$\boldsymbol{E}_R(t) = \frac{E_0}{2} \cos \omega t \boldsymbol{j} + \frac{E_0}{2} \sin \omega t \boldsymbol{i}$$

Equation 12.

and E_0 is generated by applying $+V_0$ and $-V_0$ to opposite electrodes:

$$E_0 = \frac{2V_0}{d}$$

Equation 13.

where d is the distance between the electrodes.[124]

The ion absorbs power, A(t):

$$A(t) = force \cdot velocity = \ z\boldsymbol{E}(t) \cdot \boldsymbol{v_{xy}}$$

Equation 14.

This resonant absorption increases the kinetic energy of the ions, increasing their orbital radius and allowing their detection (see 1.4.3.7). If the ion kinetic energy is increased enough to overcome the ion dissociation threshold, then with the increased frequency of ion collision intramolecular bonds can be broken. Fragmentation due to collisions with neutral collision gas molecules is called collision induced dissociation (CID), but only occurs at sufficient pressure, lower pressures decrease the likelihood of collision. Excitation can also lead to expulsion of ions by increasing the orbital radius until it is larger than that of the trap.

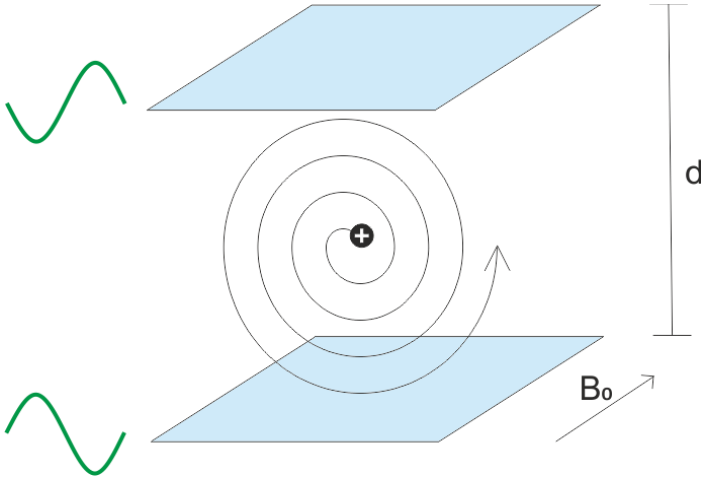

Figure 9. Resonant excitation. If the oscillating electric field has the same frequency as the ion's cyclotron frequency then the ion is excited, leading to an increase in orbital radius

When a group of ions of the same m/z are introduced into the magnetic field they are not all in phase; despite having the same ω_c their random energy distribution means that they are scattered along the circular trajectory path. When the resonance frequency is applied, all the ions are excited at the same

time and as the radius increases they are brought in phase, to travel in packets (Figure 10).

1.4.3.5 Ion cyclotron cell geometry

There is a variety of geometries the ICR cell can take but the principles of their operation remain essentially the same. A cell can be represented by a cube, within a magnetic field, composed of three pairs of opposing electrode plates: for trapping, excitation and detection. The magnetic field is generated by a superconducting magnet. Ions are introduced into the cell along the axis of the magnetic field, *z*. The trapping plates are perpendicular to the magnetic field and have a small voltage (~1 V) applied to them, causing a potential well,

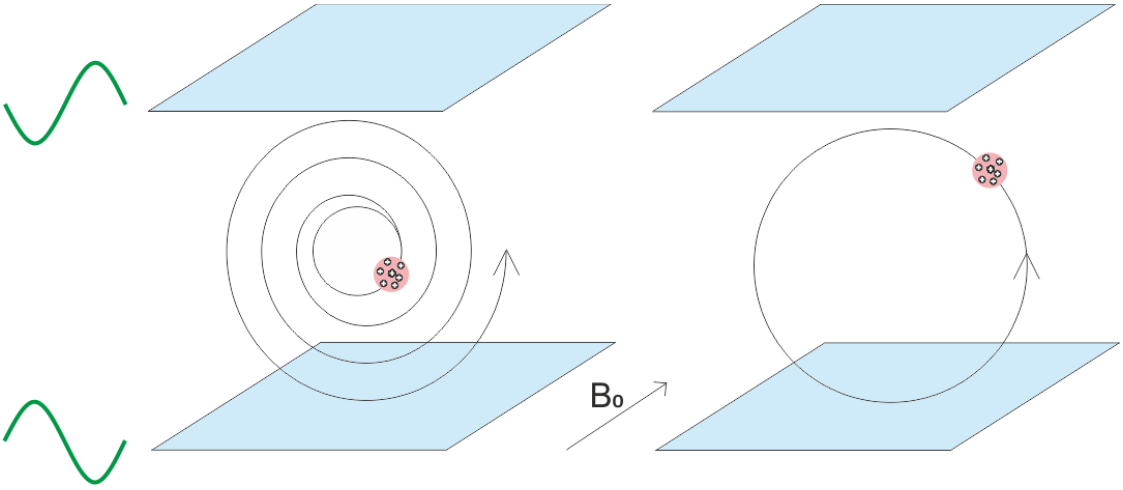

Figure 10. Resonant excitation of ions travelling in phase

preventing ions from leaving the cell along the z axis. The ions consequently rotate around the z axis in the xy plane (cyclotron motion) and move up and down the z axis.

The electrically connected detector plates are positioned parallel to the magnetic field. If an ion packet passes close to one of the plates it attracts or repels the electrons in the plate, depending on the ions' charge, thereby inducing a current, known as the image current. When the sinusoidal

alternating currents for each of the different *m/z* values in the ion packet are combined, an image current for the combined ion population is produced. The cyclotron frequency of each ion, and thus its *m/z,* can be determined from the image current. Initially when the ions enter the cell their radius of motion is small compared to the cell dimensions and they do not pass close enough to the detector plates to form a significant image current. It is only after excitation and the increase in radius that they pass close enough to be detected.

The excitation plates are also positioned parallel to the magnetic field (as per Figure 11) and, when required, a small radiofrequency voltage of the same frequency as the ions' cyclotron motion is applied. Statistically, when the ions are out of phase the current induced by an ion passing one plate is cancelled out by an ion of the same *m/z* passing the opposite plate. Again, it is only after excitation when the ions are travelling with spatial coherence that an image current can be produced.

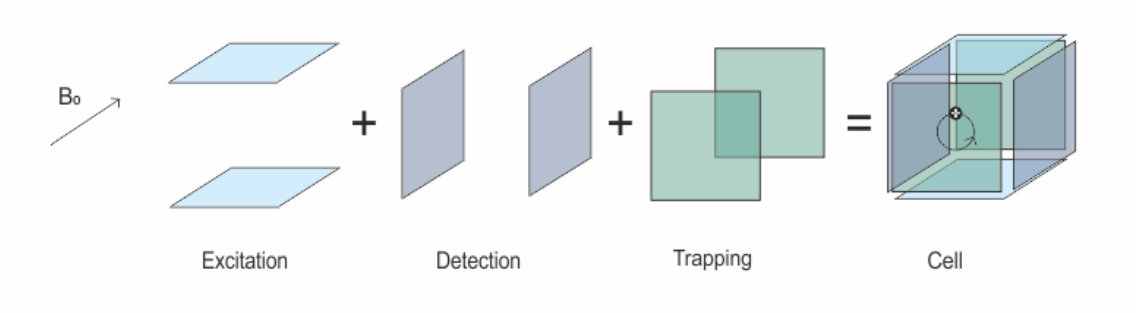

Figure 11. Geometry of a simple ion cyclotron resonance 'cell'

1.4.3.6 Broadband resonance

If we think of the energy absorbed by the ion as kinetic energy and take into account the time the ion is exposed to the excitation frequency, T_{exc}:

$$Energy = q\boldsymbol{E}(t) \cdot \boldsymbol{v_{xy}} \times T_{exc} = \frac{1}{2} m \boldsymbol{v_{xy}}^2$$

Equation 15.

On rearrangement of Equation 15 and substituting from Equation 8 then:

$$q\boldsymbol{E}(t) \cdot \frac{rq\boldsymbol{B_0}}{m} \times T_{exc} = \frac{1}{2}m\left(\frac{rq\boldsymbol{B_0}}{m}\right)^2$$

Equation 16.

so that:

$$r_{exc} = \frac{E_0 T_{exc}}{2\boldsymbol{B_0}}$$

Equation 17.

because:

$$\mathrm{E}_0 = 4\ \mathrm{E(t)}$$

Equation 18.

This means that after excitation the new radius, r_{exc}, is independent of m/z. This is very useful as it means that ions of any m/z undergoing excitation (i.e. increasing in kinetic energy due to resonance with the electric field) with a set V end up with the same radius of motion, *but* will have frequencies that depend on their m/z ratios.

In order to simultaneously excite all m/z values, so-called broadband excitation (using a range of excitation frequencies and a uniform voltage) is used; this is accomplished using stored waveform inverse Fourier transform (SWIFT). This makes use of inverse Fourier transformation (FT)[c]; after the m/z

[c] The Fourier transform (FT) is a mathematical function that can be used to decompose complex wave patterns detected in the time domain and convert them into intensities in the frequency domain. Inverse FT converts the frequency function to the time function.

range for excitation is chosen, the required cyclotron frequencies (Equation 7.) (that depend on the magnetic field strength of the instrument) are calculated using inverse FT. Once an amplitude for the excitation has been determined, the inverse FT is performed to generate a radio frequency (rf) excitation voltage waveform. On the instrument used in this project, a frequency sweep rather than broadband excitation is used as an alternative means of exciting all the ions.

Once the voltage is applied, the ions across the chosen *m/z* range are all excited to the same extent. As the excitation magnitude is proportional to the excited ions' cyclotron radii (Equation 17) which is in turn proportional to the cyclotron signal magnitude, the image current signal detected from a constant amplitude excitation voltage reflects the ions' abundance accurately.

1.4.3.7 Image current detection

As the excited ions travel along their radial path, the image current is detected by the electrodes. Ions of different *m/z* values travel with different cyclotron frequencies and thus together the population of ions induces a complex image current, called a 'transient', which is a compilation of all these frequencies (Figure 12). The transient signal is collected in the time domain and FT is required for conversion into the frequency domain. From the frequencies, the *m/z* values can be obtained and the intensities reflect the ion abundance so a mass spectrum can be compiled.

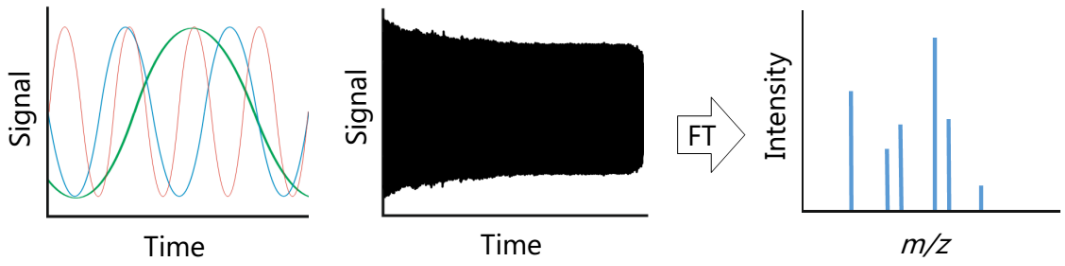

Figure 12. Signal processing (L-R): the varying cyclotron frequencies are detected as changes in voltage over time, a complex image current is built up, this transient signal undergoes Fourier transformation from time to the frequency domain – which then provides *m/z* information

1.4.3.8 Accuracy and resolution

FT-ICR is renowned for having high mass accuracy (down to 0.5 ppm) and resolution (>10 million resolving power),[125] which makes it ideal for this study, as it allows the assignment of empirical formulae to the brain residues, based on accurate mass determinations. The high resolution ensures that even weak signals can be resolved from interfering background signals. Since FT originates in the time domain, resolution is dependent on observation time and this is linked to the signal disappearance time. Resolution is proportional to the number of times a spatially coherent packet of ions complete a full circle in the ICR cell (Equation 5).

$$Theoretical\ resolution\ = \frac{\vartheta T_{aq}}{2}$$

Equation 19.

where T_{aq} is the acquisition time or transient length. For a given T_{aq}, resolution is proportional to $\mathbf{B}$ and inversely proportional to m/z. In order to achieve the theoretical resolution, the ions have to maintain their cyclotron motion and coherence for the duration of the measured transient length. The greater the magnetic field strength, the greater the mass resolution, in fact the highest mass to charge ratio that can be resolved in the ICR cell increases with $\mathbf{B}^2$.

Ion-molecule collisions slow the motion of ions, leading to signal disappearance. Collisional damping, reducing the energy of the ions through collision with inert gas molecules, reduces the axial and cyclotron motion. In order to minimise such reduction in cyclotron motion, and thus increase resolution, the cell in the instrument used for this research is placed under very high vacuum ~5^{-10} mbar (~5^{-8} Pa) so collisional damping is very low. As well as high resolution FT-ICR has high mass accuracy (the difference between the calculated and measured mass is very small). Accurate mass determination is an important way of verifying chemical composition and is partly dependent on high resolution. Using this instrument allows the calculation of accurate masses of components within a complex mixture, without the need for separation steps (during which information may be lost) and with a high degree of confidence.

1.4.4 PROTEOMICS

1.4.4.1 Introduction

Proteins are macromolecules made up of amino acid subunits connected by peptide bonds. The three dimensional structure of proteins is a result of, among other things, the sequence of the amino acids in the backbone, with twenty-two different proteinogenic amino acids occurring in nature. Proteins have a range of functions from structural roles, acting as catalysts, to transportation agents and molecular messengers.

Proteomics is the study of protein expression and employs a range of techniques and experiments including mapping where in a cell/organ/organism proteins are expressed, and monitoring how protein abundance changes with time or between genetically altered/diseased/etc. and normal cells, tissues or organisms. Determining the mass of a protein and its amino acid sequence has been a key way of identifying proteins. Until the development of desorption

ionization techniques and later electrospray ionisation and MALDI, large biomolecules were not amenable to analysis by mass spectrometry as they were required to be gaseous, and most were too large and heat labile to be brought into the gas phase for ionisation. Techniques such as electrophoresis and chromatography were imprecise approaches to molecular mass estimation of proteins, because properties other than mass affect the results. The introduction of soft ionization techniques coupled with high resolution mass analysers has enabled mass spectrometric analysis of large molecular weight biomolecules with high mass accuracy. Mass spectrometric fragmentation of proteins/peptides provides information about the amino acid sequence of the protein or its constituent peptides and significantly aids identification.

There are two strategies for protein mass spectrometric identification: top-down sequencing which involves fragmentation of intact proteins (which is not relevant to this study and is not discussed further), and bottom-up analysis. Bottom-up analysis commonly involves an extraction step, can involve sub-fractionation of complex protein mixtures, enzymatic digestion of protein mixtures to form peptides that are of a size that is amenable to analysis, mass spectrometric analysis (which can include product ion analysis of the peptide fragments) and identification. This method was used to test the ambiguous Villiers Street sample for evidence of brain related proteins. Proteomic methods are well reviewed.[126, 127]

1.4.4.2 Fractionation

A method for simplifying protein extracts (by removing some non-protein contaminants and inducing fractionation) is to use a sodium dodecyl sulfate polyacrylamide gel and carry out electrophoresis (SDS-PAGE). After solubilising the proteins in the sample by boiling in a buffer containing the detergent SDS,

which denatures the protein, the sample is equilibrated in a buffer solution containing an agent to reduce disulfide bonds to aid in protein denaturation. The negatively charged SDS molecules bind to the proteins via hydrophobic interactions in rough proportion to the protein's length, giving the proteins an overall negative charge. The proteins are then loaded into the polyacrylamide gel. The application of an electric field (electrophoresis) across the gel causes the negatively charged proteins to be attracted to the anode, forcing molecules to migrate through the gel matrix. The gel itself is formed using a polymerisation reaction which forms a crosslinked matrix with pores, the size of which can be altered by varying the ratio of reagents.[128] In general, smaller molecules move more easily through the pores in the gel and so travel faster and therefore further than larger molecules, effectively separating the proteins by size. Once the proteins have been separated they can be stained to visualise where they are within the gel and excised. Common stains are Coomassie brilliant blue or silver nitrate. After the bands have been excised they are washed to remove unbound components and reagents, and iodoacetamide plus a reducing agent is added to alkylate thiol groups, irreversibly preventing disulphide bonds from reforming.

1.4.4.3 Digestion

In order to produce peptides of a convenient size for mass spectrometric analysis, the intact proteins are chemically or enzymatically cleaved. Trypsin is an enzyme widely used for this purpose for a number of reasons. It has a well-defined specificity, consistently cleaving the peptide bond on the C-terminal side of the amino acids arginine and lysine (provided they are not followed by proline). As these amino acids appear regularly within proteins (with a combined occurrence of approximately 10%), the average length of peptides produced is ten amino acids. This is a good size for mass spectrometry analysis

as most analysers can provide good resolution in this *m/z* range, and this size is also readily amenable to collisional activation for sequencing. Because trypsin cleaves after basic amino acids the peptides produced are readily protonated. This means they readily accept hydrogen ions to produce charged species that can be detected by mass spectrometry. Conveniently, methods for in-SDS gel digestion have been developed, and are widely used.

1.4.4.4 Mass spectrometry and fragmentation

After digestion of the proteins, the peptides released can be analysed by mass spectrometry to determine size. Collision induced dissociation and product ion analysis can then be used to generate and record sequence ions formed on cleavage of the peptide backbone. After ionisation, the first mass analyser in a tandem mass spectrometer is used to select the *m/z* value of the peptide to be fragmented; it then typically undergoes collision induced dissociation and the fragment ions are then separated on the basis of their *m/z* values using the tandem instrument's second mass analyser. In the LC-TOF/TOF mass spectrometer used for the proteomics experiment in the work presented in this thesis, a spectrum of peptides present in a sample was recorded in so-called MS mode and then the MALDI laser energy increased, providing excess energy and causing the ions to fragment after leaving the ion source. A filter on the first TOF analyser leads to isolation of a precursor ion on the basis of its velocity (related to its *m/z*) and the second TOF analyser then records the fragmentation spectrum. However the product ion spectrum is produced and recorded, it provides structurally diagnostic information as peptides fragment via established and predictable pathways. Fragmentation most readily occurs at the peptide bonds along the amino acid backbone and is described by nomenclature introduced by Roepstorff[129, 130] and refined by Biemann.[131]

After fragmentation, if the charge is associated with the N-terminal end of the peptide then the resulting ions are given the labels a, b, c depending on which bond is broken, and numbered according to how many amino acids the fragment contains. If the charge is associated with the carboxyl end then fragments are labelled x, y or z – again, numbered to indicate the number of amino acids in the fragment.

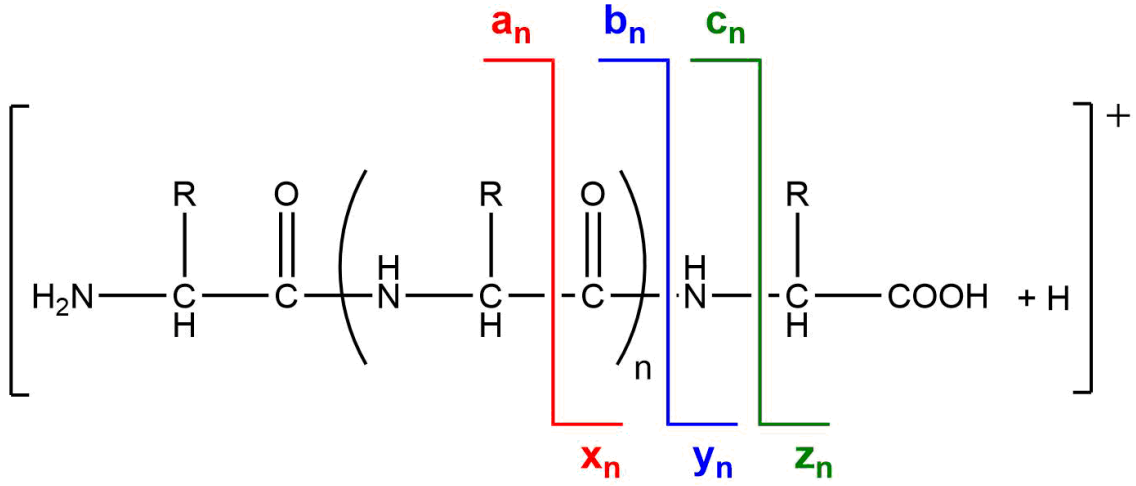

Figure 13. Peptide showing main backbone fragmentation patterns and standard nomenclature labelling, which indicates the charged species produced

The mass difference between ions in the same series (b_n, y_n) is characteristic of which amino acid occupied the relevant position in the sequence. These spectra are often complicated and can be interpreted manually or with the aid of computer algorithms.

1.4.4.5 Database searching

Peptide mass fingerprinting (PMF) is a technique where once the masses of the peptides have been determined, they can be used to identify the original protein(s) from which they came. This assumes unique proteins have unique sets of peptides (with unique sets of peptide masses). Algorithms are used to match peptide mass fingerprints determined experimentally, using mass

spectrometry to mass analyse protein digests, and those predicted using a search engine such as MASCOT,[132-134] which predicts enzyme cleavage products and their masses, for protein sequences in protein sequence databases. Generally matching several peptides at high mass accuracy from the same protein is required to determine its identity using PMF approaches.

Protein sequence databases can comprise data derived from experimentally-determined protein sequences from literature or computational analysis and/or sequences computer-predicted from genomic data. The *m/z* values of peptides produced on enzymatic digestion of the protein sequences are predicted by search engines and then matches in the protein sequence database are examined in the first step of data analysis when tandem mass spectrometric data are available. MASCOT uses an algorithm that screens databases for predicted peptides of similar size to the peptide *m/z* values measured in the mass spectrum. It then measures the similarity of the fragmentation spectra recorded to predicted fragment patterns, that are based on our understanding of how peptides fragment on tandem MS. MASCOT then presents the closest matches as potential sequences and the protein(s) these are found in. Confidence scores are provided to enable the user to assess the quality and reliability of the peptide sequence matches, and thus the protein identification; proteins identified on the basis of single peptide matches need to be considered critically, as 'one hit wonders' as these have become known, require manual validation. Manual validation of borderline or other controversial matches is also required.

1.5 Aims of the Thesis

After the discovery of the ancient brain remains in York and as part of the subsequent (unpublished) investigation, Dr Martin Rumsby, Department of Biology, University of York, produced organic lipid extracts of the material using the Folch wash method.[97, 98] The resulting extracts were analysed by Dr Rumsby using 1D TLC (and co-analysing authentic standards) and MALDI FT-ICR MS in the Centre of Excellence in Mass Spectrometry, to determine whether surviving brain lipids, or lipids representative of adipocere were detectable. The TLC data hinted at some brain-typical lipids, but also showed evidence of an intense high molecular mass residue, that did not migrate on the plates. FT-ICR mass spectrometric signals consistent with the families of glycolipids, phospholipids and sphingomyelin(s) typical of brain tissue were not observed, and neither were signals indicating the presence of the hydroxy fatty acids of the adipocere literature. Instead, a series of large, presumably water-insoluble organic species with limited nitrogen or oxygen content were identified. This discovery was contrary to expectations and does not match any of the literature reports of waxy residues associated with decaying/preserved remains.

The main aim of this investigation was to determine whether the occurrence of such apolar residues is unique to the 'York brain' or whether similar chemical species were to be found in other ancient brain remains. If these were unique to the 'York brain' the aim was to try and identify if there were any other residues that all or some brain remains had in common. If any residues occur commonly, is their occurrence related to the age of the brain? If compounds can be identified, this will give insight into the chemistry of the components across ancient brains and so to determine if they can be linked to preservation or decomposition processes.

The objectives of the study:

- Obtain appropriate samples (2.1)
    - Demonstrate using proteomic analysis that the Villiers Street sample is indeed brain, as its appearance raised some doubt (2.2, 3.2)
- Prepare lipid extracts (2.3)
- Use a high resolution mass spectrometry technique used to detect lipid-derived ions (2.4)
- Devise a procedure for analysis and comparison of mass spectrometric data (3.3)
- Compare the spectra and determine those signals that reoccur (2.4.1, 3.3)
- Identify potential chemical formulae (2.4.2, 3.3)
- Summarise and compare the findings between contexts and sites in this study (3.3.1)
- Compare this study's results with current literature on preserved soft tissue (4)

2 EXPERIMENTAL

This chapter provides details of the samples gathered for analysis along with the extract preparation technique and a description of the mass spectrometry method used for all the ancient brain lipid analyses. It also details the proteomics experiment used to test the ambiguous brain sample.

2.1 Samples

The samples analysed in the work presented in this thesis included a modern mouse brain sample, in order to trial the extraction method (provided by Dr Megan Cosgrove, Department of Biology, University of York), an extract of a modern human brain (provided by Dr Martin Rumsby, Department of Biology, University of York), and a range of archaeological and historical samples derived from the Biological Anthropological Research Centre (BARC), University of Bradford collection.

Brains (Table 5) from the BARC collection were essential to the work presented in this thesis. The specific examples were selected on Dr O'Connor's recommendation, because they were largely indisputably brain material, because it was possible for some study of sample replicates, and to allow the samples taken to span a range of sites, ages, and site geologies (for images of the samples see Appendix I: Photos of Ancient Brain Remains). However, unfortunately, soil samples from the different sites had not been taken and archived (this is because the facility was originally an anthropological resource, curating human remains, and so sampling relevant to an archaeo/geochemical study such as this one was not the object of the original sampling and curation). The sites from which brains were included were York, Hull, Blackpool and Villiers Street.

Surface oil samples were collected from Heslington, York at the approximate position of the original brain recovery for control purposes.

2.1.1 YORK

The research described in this thesis was undertaken following the surprising find of preserved brain matter on a local archaeological site (grid ref SE636506) and primary analysis of its chemical composition. The University of York decided to extend its campus in 2004 onto Heslington East,[135] an area 3 km south-east of the centre of York. A previous investigation[136] had provided some information on the site including a geophysical survey.[137] This new development presented the opportunity to conduct archaeological excavations which were initially carried out by the York Archaeological Trust, starting in late 2007, but then succeeded by Onsite Archaeology and the Department of Archaeology at the University of York. The northern part of this survey explored the presence of settlement. During the excavation of area A1 (Figure 15) in the summer of 2008, the remains of a human skull were found (Figure 14).

The site is situated over a layer of Bunter and Keuper sandstone and a glacial moraine forms a hill in the north of site. The soil is a mixture of glaciofluvial silts, sands, gravels and boulder clay, with an area of peat on the south-western edge of the site. There is a series of Iron Age features, including linear ditches, well points and Iron Age pits, that were not due to typical waste and have been suggested to be ceremonial. It was in one of the pits that the skull was found. Radiocarbon dating of collagen from the mandible was given as 519 ± 34 BC.

After removal of the skull from the original context[d] it was examined further and found that the void within the cranium was not empty. Endoscopy was used to show there was a mass within the skull that did not appear to be residual soil. While the skull was intact, a conventional CT scan and MRI were recorded to observe the mass *in situ*, revealing sulci and gyri, as well as internal voids, although these analyses weren't able to distinguish white and grey matter. The skull was taken to the University of York's Department of Biology where it was opened using a bone saw and the cranial masses removed. After delicate cleaning, the five major brain masses were photographed. Samples were taken from a single brain mass for consistency, and to preserve the remaining sections for later study.

Figure 14. (Clockwise, top to bottom): The skull as found (York Archaeological Trust), brain mass viewed using endoscope (Sonia O'Conner), brain fragment in storage at BARC, brain fragment after removal from skull and cleaning (Sonia O'Conner)

[d] In archaeology 'context' is a technical term that not only refers to an item but the surrounding soil and site, i.e. the stratigraphic layer within which it is found.

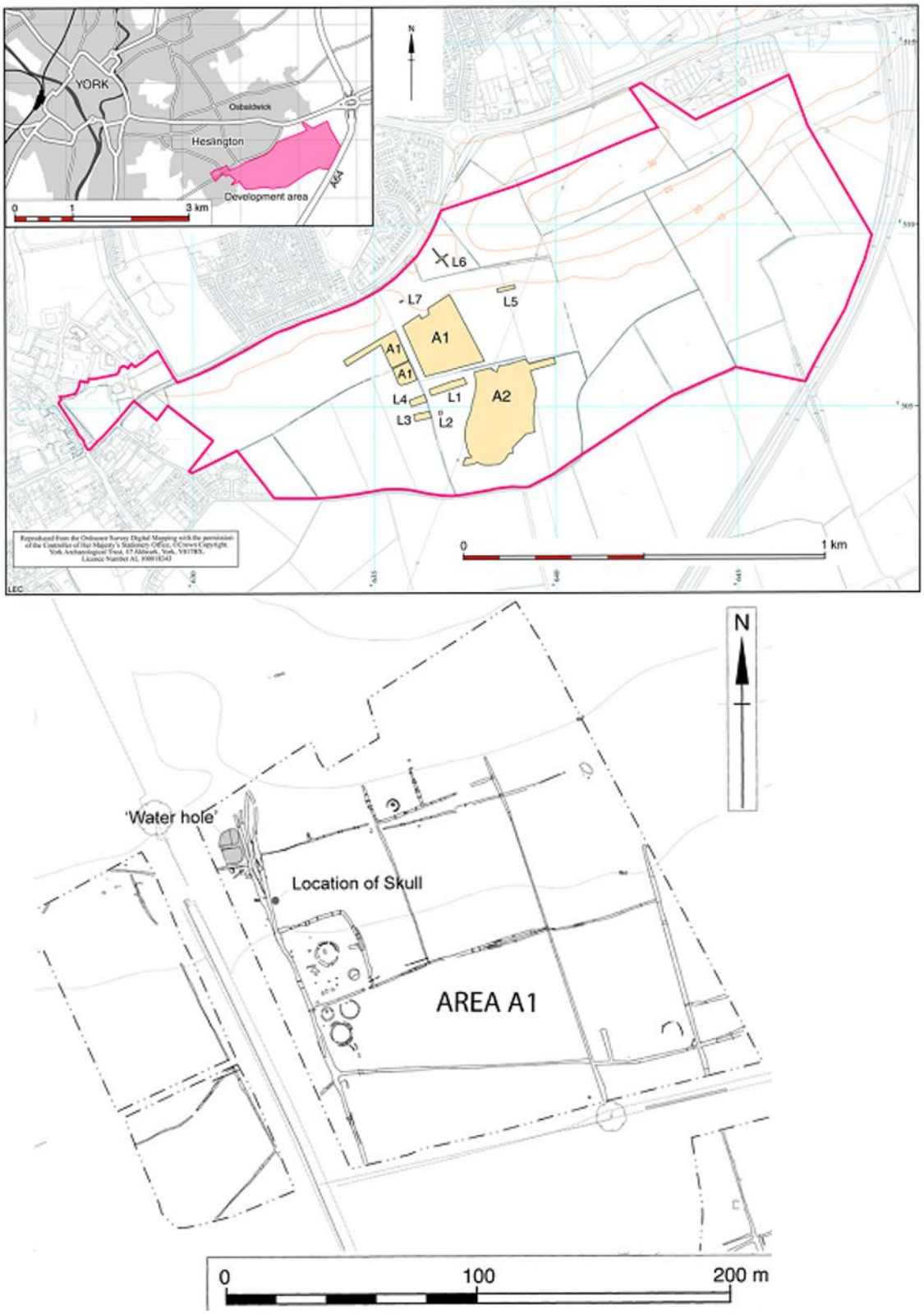

Figure 15. Above: the location of the Heslington East development and the major archaeological excavation sites, below: the location of the excavated skull.[1]

The cranial masses clearly visually resembled brain matter (Figure 14). A transmission electron microscope was used to examine finer details and observed structures resembling degraded myelin sheaths, but was unable to identify other cell or matrix structures. A few bacterial spores were observed but no other indications of putrefactive bacteria or fungi.

A variety of chemical analyses were undertaken. The C:N ratio of the brain tissue was measured as 6.3 (n=2), indicating retention of nitrogen within the remaining brain masses, suggested to be degraded protein or from potential cyanobacterial colonisation. A higher ratio of matter characterised as protein was found within the brain mass than within the sediments surrounding the skull. Amino acid racemisation analysis was undertaken in order to ascertain the likelihood of protein preservation, with 10 amino acids analysed. Despite picking five samples that appeared different, the amino acid concentrations were found to be consistent. However, only 5% of dry brain tissue was made up of hydrolysable amino acids, indicating that nitrogen retention was not solely due to proteinaceous matter. The brain matter was shown to be depleted in polar amino acids and enriched in hydrophobic amino acids. The level of racemisation was consistent with low levels of protein breakdown, with the acidic amino acid asparagine/aspartic acid having higher D/L levels, which may be due to protein refolding to form stacked β-sheets.[138, 139]

A proteomics experiment detected two proteins associated with nerve cells. Three peptide sequences matched the myelin proteolipid protein (lipophilin) version in human/other mammals, which may play a role in maintenance of myelin sheaths. A single peptide sequence was also identified for the tight junction protein claudin-11 (oligodendrocyte-specific protein) present in humans/orangutans, a protein occurring between layers of myelin sheath.

The lipid content of the brain had been reduced, with only 0.82-1.14% (wet weight as compared to 17.1% of modern rat brain) being solvent extractable. Thin layer chromatography (TLC) of the extracted brain lipids was run in the solvent system chloroform/methanol 185:15 (v/v) and resulted in bands migrating similarly to hydroxy-fatty acid GalC in rat brain and an authentic GalC standard, as well as trace bands migrating similarly to authentic fatty acid and cholesterol standards. A very non-polar, dark brown band found only in the ancient brain lipid extract was also revealed. In a more polar TLC solvent, chloroform/methanol/water 100:40:6 (v/v), trace bands were identified that migrated similarly to sphingomyelin and phosphatidylcholine in a modern rat brain control extract. The lipid extract of the York brain did not display strong bands for the expected phospholipids or cholesterol.

MALDI FT-ICR MS analysis of the same lipid extract as analysed by TLC was carried out in a 2,5-dihydroxybenzoic acid (DHB) matrix at medium and very high mass resolutions. Signals were observed in three main areas *m/z* 300, 550 and 800, but these results were not consistent with the TLC results. Despite the observed signals falling into the expected regions, the signals around *m/z* 800 were for components with an odd number of nitrogen atoms, inconsistent with sphingomyelins, phosphatidylcholines and galactocerebrosides. Peaks in the *m/z* 550 and 300 regions were for components too small to be the compounds suggested by the TLC results, but could possibly derive from their breakdown products. What was very noticeable in the spectra instead of the expected lipids was a series of high molecular weight signals, corresponding to long chain organic compounds with a heterogeneity in degree of unsaturation. It is this hydrophobic component that this thesis sets out to investigate.

2.1.2 HULL MAGISTRATES COURT

A new Magistrates Courts building was proposed for Kingston upon Hull, with construction due to start in August 1995. The site designated for the development was on the north side of Garrison Road at its junction with Market Place at NGR TA 101 285. This site was of exceptional archaeological interest due to its location in the 'Old Town' and that it was proposed to encompass part of a medieval Augustinian Friary and its cemetery, several medieval tenements, potentially the 1806 Town Hall and the 1796 House of Correction. The archaeological work was undertaken by Humberside Archaeology Unit (later Humber Archaeology Partnership); excavation began in May 1994 and continued through the spring and summer.

The underlying geology of the Old Town is largely alluvial warp with some reclaimed soils on the eastern edge, whereas to the north and east there are glacial tills. Due to dramatic fluctuations in sea levels and as Hull itself sits at the confluence of the rivers Humber and Hull, the area has been subject to flooding. Prior to the drainage in the 18th and 19th centuries, much of the surroundings were marshland. Test bores made on site showed a stratification of about 16 m of soft alluvial clay (warp), sand and peat over glacial clay, sand and gravel to a depth of about 30 m under which lay chalk bedrock. The standing groundwater level was indicated to be about 2 m above ordnance datum and when samples were analysed, they had pH values of 7.7 to 7.9.

Interestingly, the report states "Organic preservation was excellent in all of the lower layers, as waterlogged conditions were encountered at a depth of about 0.50 m beneath the level at which machine clearance had stopped: anaerobic conditions were also occasionally found in the topmost layers of archaeological deposits, but as the watering of the upper deposits was more

variable, preservation of organic material was generally poorer." "The quality of preservations of bones, coffins, associated costume and dress fittings…[was] surprisingly good."[140, 141]

The friary was founded in 1316-7 when Geoffrey de Hotham and John de Wetwang obtained a licence and plot of land for a friary; the friary was dissolved in 1540. The excavation of the friary and its cemetery uncovered 180 grave cuts and 44 coffins (Figure 16). The grave cuts were mainly individual but multiple intercutting graves were found within the friary's church site. Preliminary inspection of the coffin timbers indicates that these are from the mid to late 14th century, with dendrochronology revealing no timbers later than AD 1400[e], and stratigraphy suggests later burials were predominantly in shrouds. The initial assessment of the skeletal remains of 244 individuals from articulated burials, of which 207 were relatively complete, has been made. The remains of males, females, juveniles and two foetuses, one *in utero*, have been identified. Degenerative joint disease has been discovered on a third of adults indicating older individuals. In addition, the remains of a minimum of 56 individuals were recovered as disarticulated human bones based on the number of left proximal femurs discovered.

From these burials, twenty masses were found within cranial cavities and Dr Sonia O'Connor, Lead Conservator, suggested these were brain remains. These remains were carefully placed in individual plastic receptacles and given to BARC where they were then deposited in a cold store. Samples were taken

[e] The timbers from coffin 696 appeared to have been felled in AD 1347 and coffin 848 includes some timbers felled in AD 1362.

from some of the brain remains for planned DNA analysis and kept in stoppered glass vials. These pre-prepared samples were then provided for this survey.

2.1.3 BLACKPOOL

BARC provided a sample of brain matter discovered during the excavation of burial ground at St John the Evangelist, Church Street/Abingdon Street, Blackpool, Lancashire (centred SD 3490 0303). This was undertaken in 2009 as Blackpool Borough Council planned to redevelop this area with a pedestrian zone, fountain and artwork. It was originally believed that the churchyard had previously been cleared (according to church records in 1927 and 1954). However, funerary remains including coffins and bones were discovered.

The St John the Evangelist Church was founded in 1821 and after additions to the original building a new church finished construction on the site in 1878. The churchyard is located close to the town centre of Blackpool and prior to redevelopment consisted of flagstone paving, several walled gardens, a couple of gravestones and a monument to individuals removed from the graveyard in 1927.

Studies have shown that the underlying geology of the area comprises of Permo-Triassic sandstones which are masked by deep drift deposits of post glacial till and alluvium.[142] The topsoil is mainly fine sand and gravel. Given the damp heavy clay burial environment and on-site observations, the site was considered to be likely to include well-preserved organic material.

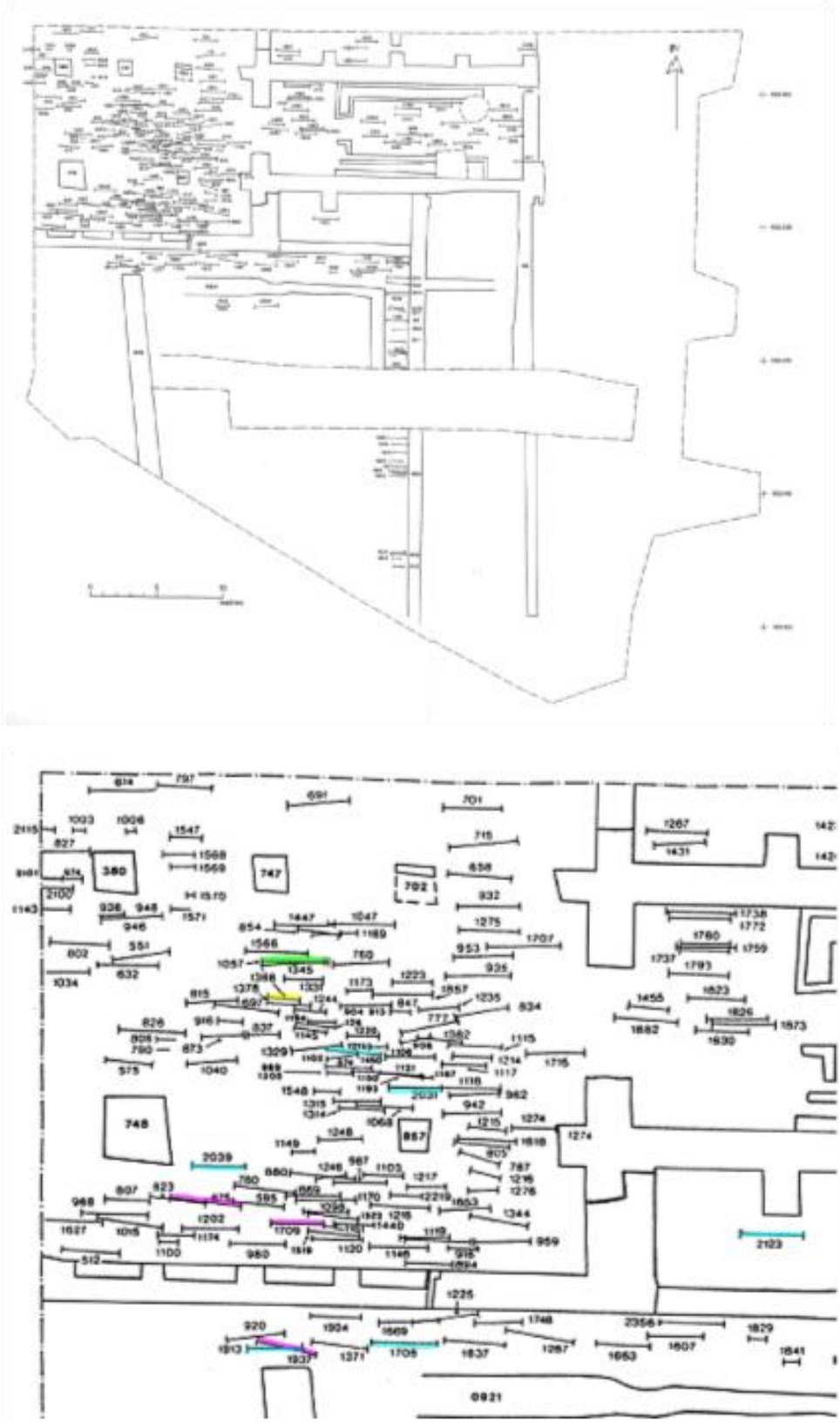

Figure 16. Above: Map showing distribution of burials within the Hull Friary precinct. Below: Plan with burials from which surviving brain remains were used in this study are highlighted; green = juvenile, blue = male, pink = female, yellow = adult (unsexed)

During the excavation to the required depth for redevelopment, 73 graves were found, 53 of which were grave cuts. Nine coffins at the edge of the disturbance were exposed, recorded and left *in situ*. Only where deep excavation (up to 2 m below ground level) was required, were the remnants of seven individuals and a well-preserved single burial removed for later reburial. The burial was of a fishtail coffin (Figure 17) containing the complete skeleton of a 25-35 year old woman (skeleton 117).

During examination of skeleton 117, a mass was identified within the skull which was suggested likely to be brain after examination by forensic pathologist Dr Jenny Robinson at the University of Central Lancashire, Preston. Dr Sonia O'Connor at Bradford University confirmed this and it was placed in cold-storage at BARC.

Figure 17. Fishtail coffin 116 *in situ*, containing skeleton 117, looking north-west.[143]

2.1.4 VILLIERS STREET CRYPT

Information about this site has yet to be published. The project is currently ongoing and work is being carried out at BARC at the University of Bradford involving Dr Jo Buckberry, Dr Andrew Wilson, Rob Janaway and Louise Brown. Despite repeated attempts to obtain further information, only limited details are available about this site and sample at this time. The site was excavated and human remains were found. The sample selected was assigned: Site: VSS A, Vault: 2, Context: 2464, Sample: 446, and labelled with the description: "spongy organic matter from endocranial area" and is believed to be from a 19th century burial. There was a question, based on this samples' appearance, whether it was indeed brain material. Consequently, a proteomic analysis, similar to that performed on the original York brain sample was carried out, in an attempt to produce molecular evidence of the material's origin.

Table 5. Sample summary table, in descending date order

Site	Burial Age	Archaeological sample site code	Archaeological context label	Bulk sample label	Physical Sample Description		Aliquot sample label	Label in thesis
					Colour	Texture		
York	673-482 BC	Hes Brain Unit C	2619	Y1	Cream coloured interior with darker brown exterior	Spongy and fibrillose	Y1a	Y1a
Hull	Mid to late 14th century	Hull	SK1709 Vault 1872	H1	Brown with areas of cream and tan	Dense, compressed layers, fibrillous, wet	H1a	H1a
					Creamy white-brown	Waxy paste, wet	H1b	H1b
		Hull HMC94	0675	H2	Creamy grey-brown	Firm lumps with granular inclusions and flakes	H2a	H2a
		Hull Brain	SK1057	H3	Pale cream to dark brown with dark orange patch	Irregular, waxy, laminous chunks, very wet	H3a	H3a
		Hull Skull	1368	H4	Chocolate brown with small areas of lighter cream	Large lumps of moist fibrous with smaller granules	H4a	H4a
		Hull HMC	1450 'Brain'	H5	Cream, tan, brown and rust	Sponge-like with fibrous channels	H5a	H5a
		Hull 1708	1871	H6	Creamy brown with grey areas	Chunks were hard, dry and layered also granules	H6a	H6a

Site	Burial Age	Archaeological sample site code	Archaeological context label	Bulk sample label	Physical Sample Description		Aliquot sample label	Label in thesis
					Colour	Texture		
Hull	Mid to late 14th century	HMC	SK1913	H7	Black and dark brown-grey with rust flecks	Very hard, dry matrix with crystalline sandy granules	H7a	H7a
		Hull HMC 94	1937	H8	Creamy pale brown with darker brown patches	Firm and fibrous, clay-like, wet	H8a	H8a
		HMC94	1937 Hull 1+2	H9	Generally tan with rust orange and dark grey areas	Firm, hard mousse with granules, wet	H9a	H9a
		Hull	SK2031	H10	Creamy brown with grey areas	Dry, hard laminous chunks and silty particles	H10a	H10a
		Hull HMC94	SK2039	H11	Light-mid tan	Soggy, matted fibrous lumps with silty particles	H11a	H11a
		Hull Brain	SK2123	H12	Mottled brown, ranging from pale cream, tan and rusty orange-red	Moist and crumbled, larger lumps appear laminous	H12a	H12a
		Hull	2123	H13	Grey-brown, ranging from creamy to dark	Firm, matted layers of tiny fibres with spongy texture	H13a	H13ai *
								H13aii *

Site	Burial Age	Archaeological sample site code	Archaeological context label	Bulk sample Label	Physical Sample Description		Aliquot sample label	Label in thesis
					Colour	Texture		
Hull	Mid to late 14th century	HMC	SK2123 'Red Sample'	H14	Grey-brown with rusty orange	Loose silty particles with larger crystalline granules (resembled soil)	H14a	H14a
		HMC	SK2123 'Red Sample'	H14	Rusty orange with grey surface	Gritty solid	H14b	H14bi
								H14bii *
Villiers Street	19th century	VSS-A	446	V1	Peach layer with mottled brown and layer	Peach layer appears spongy and laminous, the brown is granulated, wet	V1a	V1a
Blackpool	19th century (1821 – 1927)	SJB09	SK117	B1	Dark brown	Firm and spongy 'paste' with fibrous indications	B1a	B1a

Grey = All from the same archaeological sample context * Due to volume of filtrate and dried down in separate vessels i and ii

2.2 Proteomic Analysis of Villiers Street Sample

This proteomic analysis was carried out at the Bioscience Technology Facility Proteomics Laboratory, Department of Biology, University of York, by Rachel Bates and Dr Adam Dowle, who carried out the original analysis on the York brain.

Following a generally-accepted LC-MS/MS data-dependent approach for shotgun proteomic analyses,[1, 144-146] 15.6 mg of the Villiers Street brain sample was added to 25 µL NuPAGE™ LDS sample buffer, 10 µL NuPage™ reducing agent solution and 65 µL water. The solid tissue was homogenised in solution, using a Potter-Elvejhem glass-teflon homogeniser, at room temperature, rotating at approximately 200 rpm. Protein from the resulting brain suspension was solubilised with heating at 70°C for 10 mins before running into a 7 cm NuPAGE™ Novex™ 10% Bis-Tris gel (Life Technologies) at 200 V for 6 mins. Gels were stained with SafeBLUE protein stain (NBS biologicals) for a minimum of 1 h before destaining with ultrapure water for a minimum of 1 h. In-gel tryptic digestion was performed after reduction with dithioerythritol and *S*-carbamidomethylation with iodoacetamide. Gel pieces were washed twice with aqueous 50% (v/v) acetonitrile (Fisher Chemicals, HPLC grade) containing 25 mM ammonium bicarbonate, then once with acetonitrile and dried in a vacuum concentrator for 20 min.[144] Sequencing-grade, modified porcine trypsin (Promega) was dissolved in 50 mM acetic acid (Sigma Aldrich), then diluted 5-fold with 25 mM ammonium bicarbonate to give a final trypsin concentration of 0.02 µg/µL. Gel pieces were rehydrated by adding 25 µL of trypsin solution, and after 10 min enough 25 mM ammonium bicarbonate solution was added to cover the gel pieces. Digests were incubated overnight at 37°C. Peptides were extracted by washing three times with aqueous 50% (v/v) acetonitrile containing

0.1% (v/v) trifluoroacetic acid (Fisher Chemical, LC/MS grade), before drying in a vacuum concentrator and reconstituting in aqueous 0.1% (v/v) trifluoroacetic acid for LC-MS analysis.[144]

LC-MS/MS: Samples were loaded onto a nanoAcquity™ UPLC system (Waters) equipped with a nanoAcquity™ Symmetry C18, 5 µm trap (180 µm x 20 mm Waters) and a nanoAcquity™ HSS T3 1.8 µm C18 capillary column (75 mm x 250 mm, Waters).[147] The trap wash solvent was 0.1% (v/v) aqueous formic acid (Fisher Chemical, LC/MS grade) and the trapping flow rate was 10 µL/min. The trap was washed for 5 min before switching flow to the capillary column. Separation used a gradient elution of two solvents (solvent A: aqueous 0.1% (v/v) formic acid; solvent B: acetonitrile containing 0.1% (v/v) formic acid). The capillary column flow rate was 300 nL/min and the column temperature was 60 °C. The gradient profile had two linear steps: 2-30 % B over 125 min, then 30-50 % B over 5 min. All runs then proceeded to wash with 95 % solvent B for 2.5 min. The column was returned to initial conditions and re-equilibrated for 25 min before subsequent injections.

The nanoLC system was interfaced with a maXis™ HD LC-MS/MS system (Bruker Daltonics) with a CaptiveSpray™ ionisation source (Bruker Daltonics).[145] Positive ESI-MS and product ion spectra were acquired using AutoMSMS mode. Instrument control, data acquisition and processing were performed using Compass 1.7 software (microTOF control, Hystar and DataAnalysis, Bruker Daltonics). Instrument settings were: ion spray voltage: 1,450 V, dry gas: 3 L/min, dry gas temperature 150°C, ion acquisition range: *m/z* 150-2,000, MS spectra rate: 2 Hz, MS/MS spectra rate: 2 Hz at 2,500 cts to 12 Hz at 250,000 cts, cycle time: 1 s, quadrupole low mass: *m/z* 300, collision RF: 1,400 Vpp, transfer time 120 ms. The collision energy and isolation width settings were automatically calculated using the AutoMSMS fragmentation table, absolute

threshold 200 counts, preferred charge states: 2 – 4, singly charged ions excluded. A single product ion spectrum was acquired for each precursor and former target ions were excluded for 0.8 min unless the precursor intensity increased fourfold.[146]

Database Searching: Product ion spectra were searched against the human subset of the UniProt™ database (20259 sequences; 11329622 residues) using a locally-running copy of the Mascot™ program (Matrix Science Ltd., version 2.5.1), through the Bruker ProteinScape™ interface (version 2.1). Search criteria specified: enzyme, trypsin; fixed modifications, carbamidomethyl (C); variable modifications, deamidation (N,Q), oxidation (M), Gln -> pyro-Glu (N-term Q), and Glu -> pyro-Glu (N-term E); peptide tolerance, 10 ppm; MS/MS tolerance, 0.1 Da; instrument, ESI-QUAD-TOF. Peptides with an expect score of 0.05 or lower were accepted, as this is the default significance threshold.[134, 148]

2.3 Organic Extraction of Samples (mouse brain, modern human brain, archaeological brains, soil, solvent blank)

The initial sample from the York brain had been treated using the Folch wash method[97, 98] to extract the lipidic fraction. In order to make comparable extracts, the same method was employed on all of the archaeological brain samples. A modern mouse brain sample was prepared for comparison with ancient brain material extracts. In addition, Dr Martin Rumsby (Department of Biology, University of York) provided a lipid extract prepared in this manner of a sample of modern human brain tissue for comparison.

All solvents, HPLC grade water, dichloromethane and chloroform, and LC-MS grade methanol, were purchased from either Sigma Aldrich or Fisher Chemicals. All glassware was washed thoroughly with detergent and hot water twice, and then rinsed with tap water followed by deionised water twice, before rinsing with methanol, with chloroform and then finally three times with 2:1 (v/v) chloroform/methanol. To remove the meninges, the mouse brain matter sample only was rinsed with a small volume of cold 0.15 M NaCl solution, and blotted briefly on filter paper to dry. The weight of each brain or soil sample was recorded before and after lyophilisation, which typically required around 12 hours to dry the samples completely.

Prior to extraction, the lyophilised brain tissue was homogenised in chloroform/methanol 2:1 (v/v) to a final volume 20 times the volume of the tissue sample, e.g. the homogenate from 1 g of tissue was extracted using a volume of 20 mL using a Potter-Elvejhem glass-teflon homogeniser, at room temperature, rotating at approximately 200 rpm. For the soil sample, instead of

using the homogeniser, a ball mill was used, and the soil pulverised dry, and then resuspended in 2:1 (v/v) chloroform/methanol, in which it was agitated. The extracts were filtered through 12 cm glass fibre filter circles prewetted with chloroform/methanol 2:1 (v/v). 0.1 M KCl solution was added to the filtrate in a volume that was 20% of the filtrate volume, e.g. for 20 mL solvent, 4 mL 0.1 M KCl was used. This was well mixed and allowed to stand overnight at room temperature to resolve the two phases. The lower phase is composed of chloroform/methanol/water in the proportions 86:14:1 (by volume) and contains virtually all of the lipids, while the upper phase consists of the same solvents in the proportions 3:48:47 (by volume). The upper phase was removed, and solids at the interface were also removed by carefully rinsing three times with the removed upper phase, which was then discarded. The solvent was removed from the lower phase under nitrogen. The samples were weighed and stored in sterile glass sample vials under nitrogen at -20 °C prior to analysis.

A reagent blank was also prepared, which underwent all steps of the above but without solid matter (brain or soil) being included. After the final drying step, the residue was resuspended in sufficient amounts of 2:1 (v/v) chloroform/methanol solution to give a dilution of 1 mg/mL ahead of mass spectrometric analysis.

Standards used were galactocerebrosides, from bovine brain ~99%, 25 mg/mL in chloroform/methanol/water 19:10:1 (v/v), sphingomyelin from bovine brain, 1 mg/mL in chloroform/methanol 1:1 (v/v), and L-α-phosphatidylcholine, Type XVI-E, 0.5 mg/mL in dichloromethane/methanol 1:1 (v/v) (Sigma Aldrich).

Table 5 (2.1) shows a summary of the samples and extracts prepared for this study. Each extract was spotted on the MALDI plate three times and a mass spectrum recorded from each spot (2.4). As well as spotting the extracts of the

archaeological samples, the reagent blank, and a Folch wash extract of a soil sample from close to the Heslington (York) site, were each spotted three times as controls. Finally, the DHB matrix solution alone was spotted three times. It should be noted that these control spots were separate to an earlier series of matrix spots that were analysed to generate a master list of matrix signals for comparison.

2.4 Recording Spectra

The original York brain extract had been analysed in the same mass spectrometry facility (Centre of Excellence in Mass Spectrometry, York) several years before the work described in this thesis. At that time, the FT-ICR instrument was a Bruker Daltonics Apex ultra[1] , which was subsequently significantly upgraded ahead of the work described here. The instrument used for the work described in this thesis has considerably better performance specifications than the instrument used for the original analyses. The Bruker solariX XR has hexapole ion optics which increased transmission of ions into the cell, meaning ion sensitivity is much improved and has a ParaCell ion cell which allows for much higher resolution measurements.[149-151]

1 µL of matrix solution (2,5-dihydroxybenzoic acid (DHB) 10 mg/mL in 1:1 (v/v) acetonitrile: 0.1% aqueous formic acid) was applied to a Bruker MTP AnchorChip™ 400/384 MALDI sample plate and allowed to air dry.1 µL of brain or soil extract solution (with concentration of 1 mg/mL) was spotted on top of the matrix spot and allowed to air dry. Samples were spotted in triplicate.

Samples were analysed using MALDI in the positive mode using a Fourier transform-ion cyclotron resonance (FT-ICR) mass spectrometer. The 9.4 T solariX FT mass spectrometer (Bruker Daltonics) was equipped with a smartbeam™ nitrogen Nd:YAG laser (355 nm). Mass spectra were recorded over the *m/z* range 300 – 2000, acquiring 10 scans, of 2000 laser shots each, with a laser power setting of 30 %. Calibration was carried out using Bruker Peptide Calibration Standard II (PCSII). Data processing was performed using Bruker ftmsControl 2.1.0 (Build 98) software.

2.4.1 PEAK SELECTION

The software used was Bruker Compass DataAnalysis 4.4 (x64) containing DataAnalysis Version 4.4.200 (Build 102.47.2299) (64-bit). Each of the PCSII spectra was calibrated internally against the appropriate reference mass list. The adjusted PCSII spectra were then used as external calibrants for the eight sample spectra recorded spatially closest to the standard spot. After each spectrum had been calibrated appropriately, peak selection took place. This varied for each spectrum depending on signal strength and the background intensity. Peaks were selected using the MassList tool, with peak finder to calculate peak position selected, and parameters set as in Table 6:

Table 6. MassList selection parameters

Parameter	Chosen setting
Instrument type	Default (Fourier transform)
Peak finder	FTMS
S/N threshold	4
Relative intensity threshold (base peak)	0.1% (0.01%)*
Absolute intensity threshold	100000

* For DHB matrix only spots, to ensure all matrix derived signals were accounted for.

2.4.2 PEAK IDENTIFICATION

The Chemistry SmartFormula tool in the Bruker Compass DataAnalysis 4.4 software was used to generate empirical formulae for the signals meeting the intensity, signal:noise, and relative intensity thresholds (see 3.3.1).

The parameters used to provide a range of applicable empirical formulae that were then screened manually are shown in Table 7. For *m/z* values < 2000, the elements C, H, N and O are considered implicitly in the calculations unless

restricted explicitly in the parameters, where all other elements must be specified.

Table 7. Chemistry Smartformula parameters

Parameter	Chosen setting	
Lower Formula	—	
Upper Formula	$N_9O_9P_3S_3$	
Positive ions	$M+H^+$, $M+NH_4^+$, $M+Na^+$, $M+K^+$	
Charge (if not assigned)	1	
Maximum no. of formulae	10	
Relative Intensity Threshold	1%	
Electron configuration	even	
Limit: mSigma	600	
Tolerance	6 ppm	
Check rings plus double bonds	Minimum 0	Maximum 20
Filter H/C ratio	Minimum 0	Maximum 10

3 RESULTS

This chapter reports the results from the mass spectrometric analysis of a modern mouse and human brain extract as well as lipid standards, used to confirm that the components of the York brain lipid extracts were not consistent with fresh lipids. The results from the proteomics experiment of the ambiguous Villiers Street sample are also described (3.2). The majority of this chapter is composed of tables summarising the most intense reoccurring non-matrix signals found in the ancient brain lipid extract mass spectra, and the potential chemical formulae that they have been assigned.

3.1 Standards, Mouse Brain and Modern Human Brain Lipid Extracts

Positive ion MALDI spectra of commercial authentic standards of phosphatidylcholines (PC), sphingomyelins (SM), and galactocerebrosides (GalC), all lipids expected to be isolated from undecayed brain material using a Folch wash,[97, 98] were recorded. The data, together with proposed compositional assignments, for phosphatidylcholines, phospholipids that have a choline head group, are shown in Figure 19, with ion structures in Figure 18.

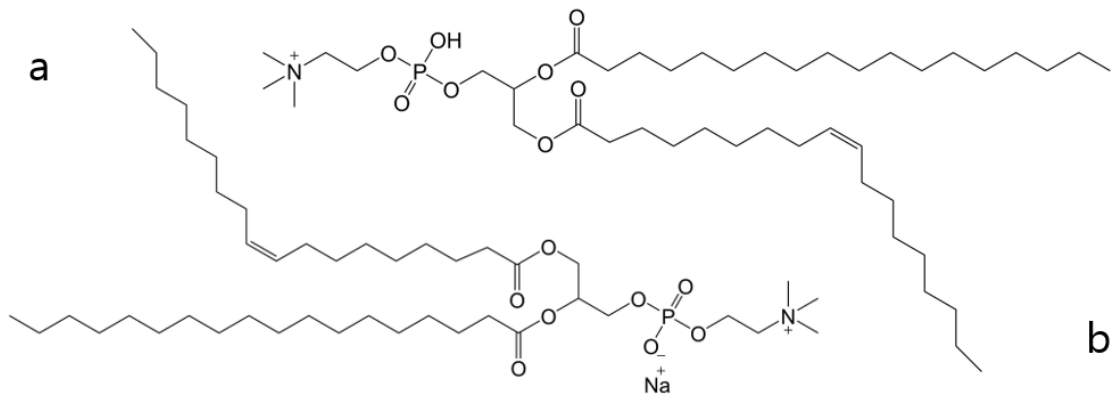

Figure 18. (a) $[PC + Na]^+$ and (b) $[PC]^+$ ions

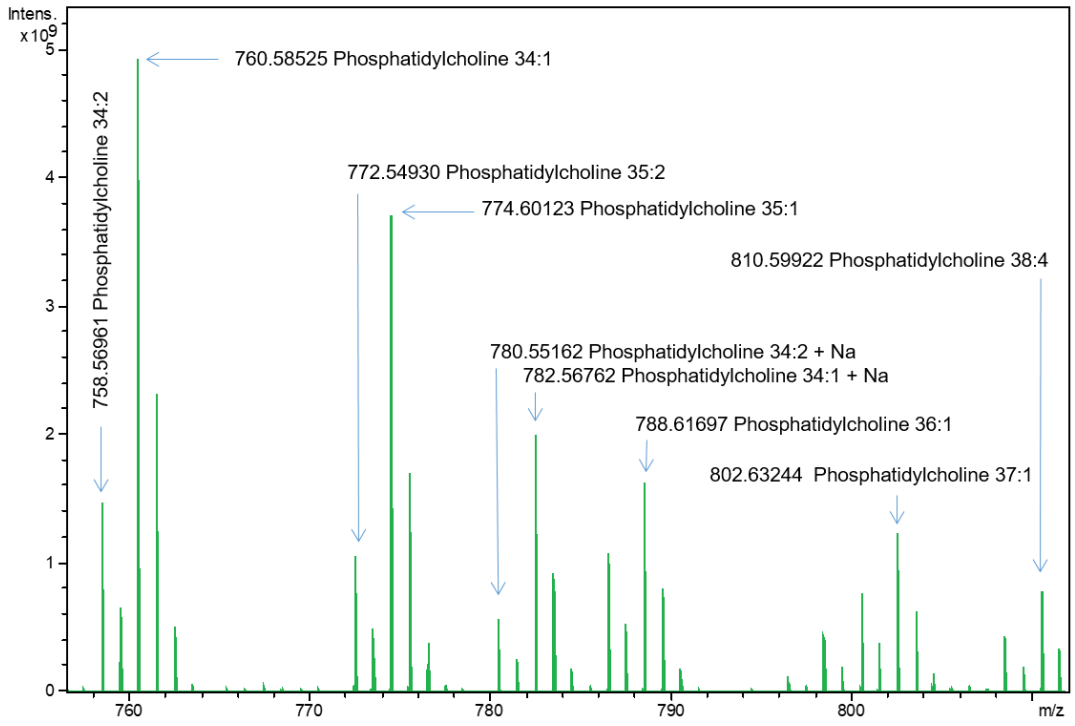

Figure 19. Above: MALDI mass spectrum of phosphatidylcholine (PC) standard

The spectrum with proposed compositional assignments for sphingomyelins, sphingolipids found in the membranes of the myelin sheath around nerve cell axons, is shown in Figure 20 and SM ion in Figure 21.

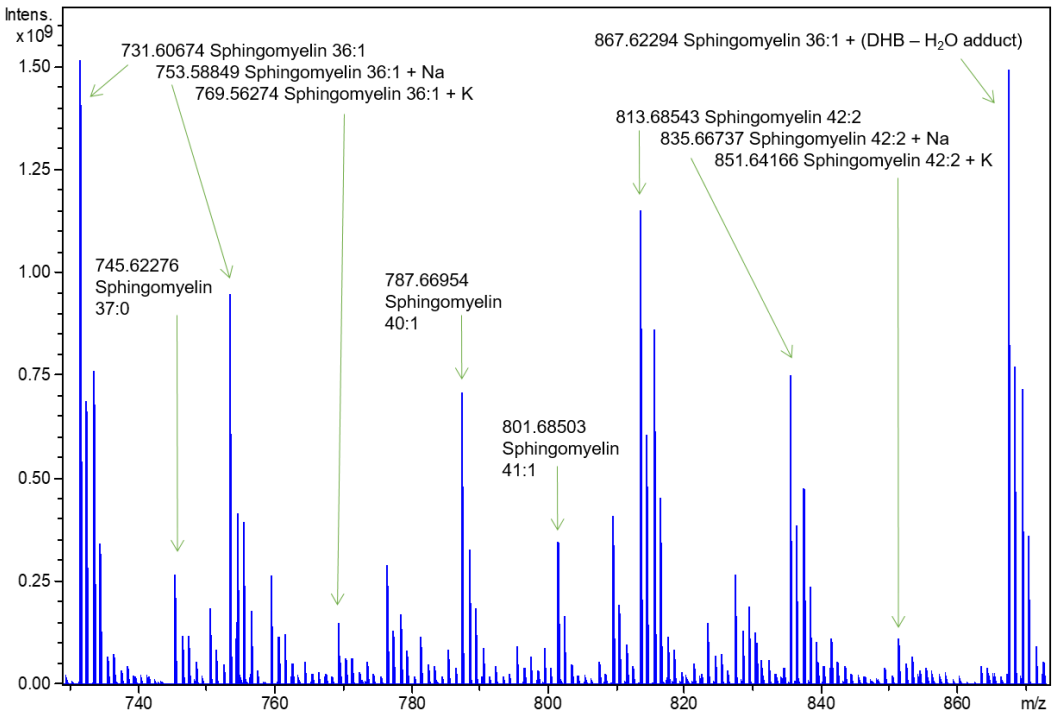

Figure 20. Above: MALDI mass spectrum of sphingomyelin (SM) standard.

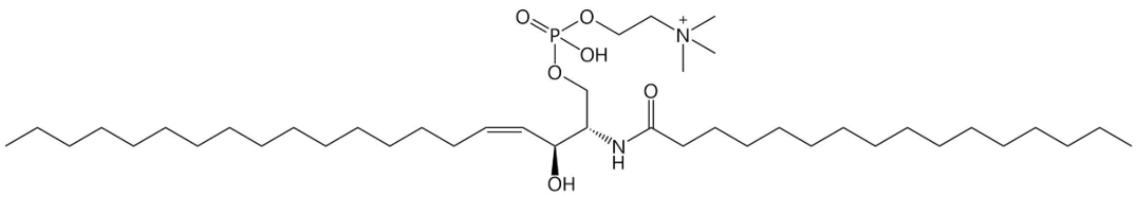

Figure 21. Example of a SM ion

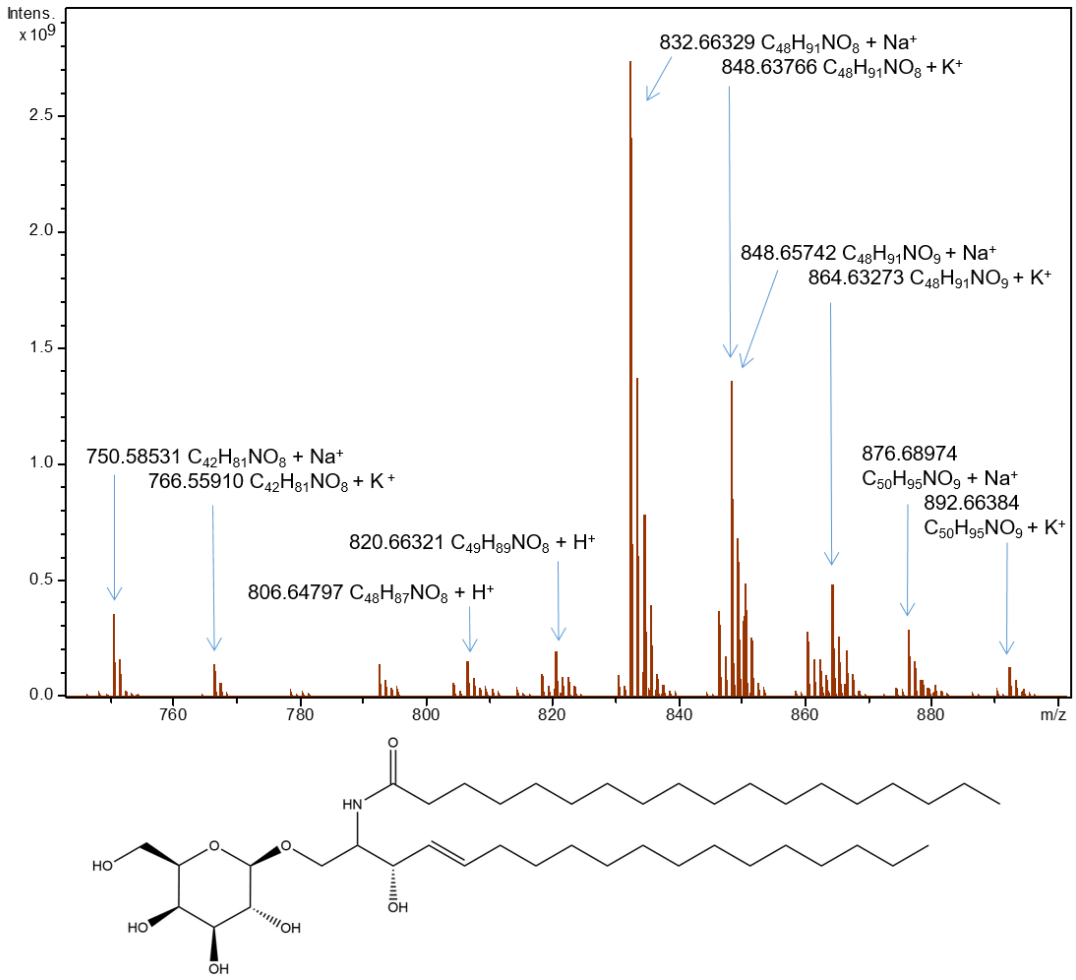

Figure 22. Above: MALDI mass spectrum of galactocerebrosides (GalC) standard. Below: An example galactocerebroside

The spectrum with proposed compositional assignments for galactocerebrosides, a marker for oligodendrocytes in the brain, is shown in Figure 22.

The equivalent MALDI mass spectra produced from the modern human and mouse brain lipid extracts (Figure 23) show a range of PC, SM, and GalC components, standard signals typical of brain lipids.

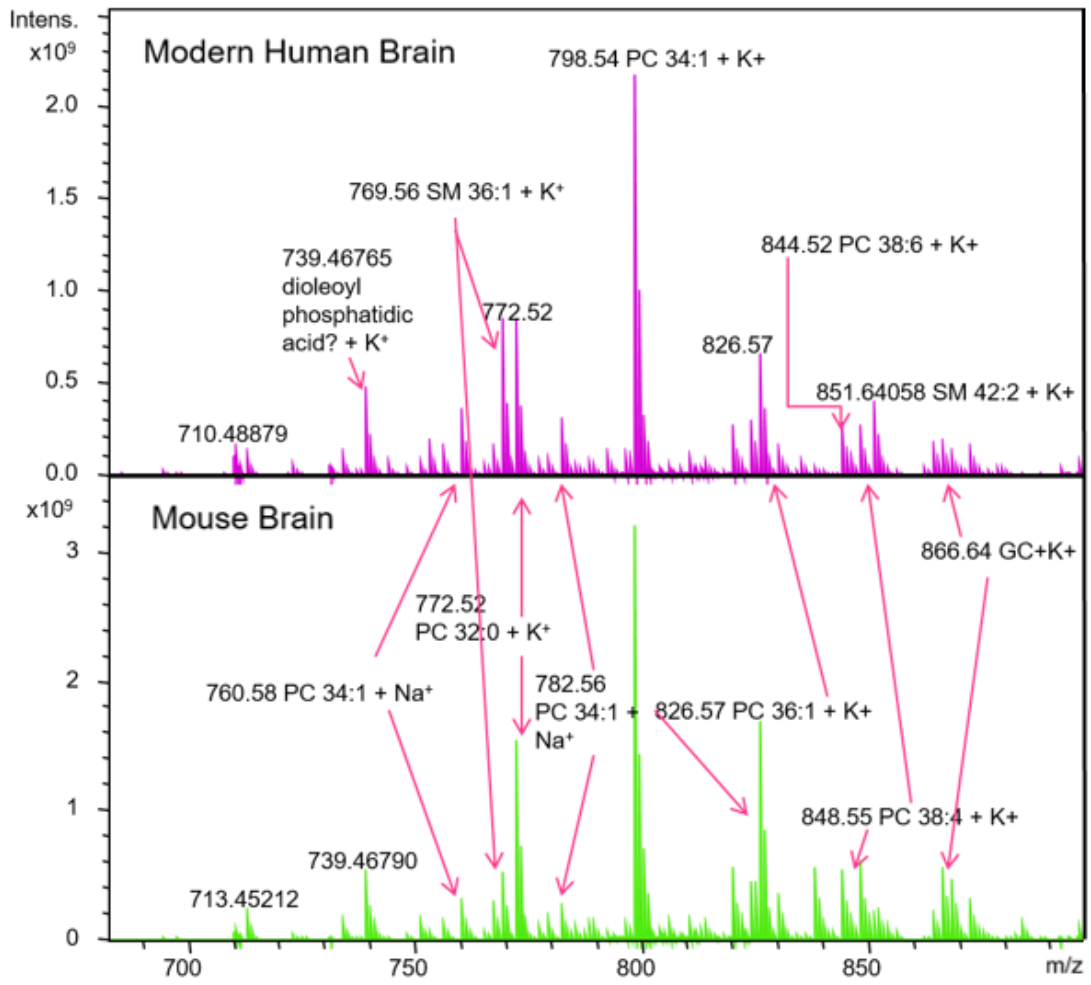

Figure 23. Human and mouse brain mass spectra

Whilst producing signals consistent with typical brain lipid components, the spectra of these extracts of modern brains do not contain peaks with the same *m/z* as those found in the extracts of the original York brain.

3.2 Protein ID From Villiers Street Sample

Because there was some question, based on the appearance of the material sampled, whether sample V1 was indeed brain material, a proteomic analysis, similar to that performed of the original York brain, was carried out. This analysis was carried out in collaboration with, and under the supervision of, the same scientists in the Bioscience Technology Facility Proteomics laboratory who carried out the original analysis.

After protein extraction, digestion and liquid chromatography-tandem mass spectrometry (LC-MS/MS) analysis, a single peptide match was made to myelin proteolipid protein, see Figure 24. This protein (moreover the same peptide), was also detected in the York brain and plays an important role in the formation and maintenance of the multilamellar structure of myelin found in the central nervous system. A single peptide match was also made to another neural protein, SLIT and NTRK-like protein 4 (Figure 25), which is expressed in the cerebral cortex of the brain.

The matches were made with short, single peptide sequences and a significant amount of keratin contamination was present, as would be normal for samples that have been handled without taking the precaution of specifically excluding keratin. It would be desirable to complete an additional proteomics analysis after removing a surface layer from the organic sample. Whilst the peptide matches were short, the distinctive nature of the proteins they came from give confidence to the claim that the sample is ancient brain remains.

Protein View: P60201

Myelin proteolipid protein OS=Homo sapiens GN=PLP1 PE=1 SV=2

Database:	UniProt_human_SP
Score:	27
Nominal mass (M_r):	30855
Calculated pI:	8.71

Sequence similarity is available as an NCBI BLAST search of P60201 against nr.

Search parameters

MS data file:	1322932390543297 9.mgf
Enzyme:	Trypsin: cuts C-term side of KR unless next residue is P.
Fixed modifications:	Carbamidomethyl (C)
Variable modifications:	Deamidated (NQ), Gln->pyro-Glu (N-term Q), Glu->pyro-Glu (N-term E), Oxidation (M)

Protein sequence coverage: 2%

Matched peptides shown in ***bold red***.

```
  1 MGLLECCARC LVGAPFASLV ATGLCFFGVA LFCGCGHEAL TGTEKLIETY
 51 FSKNYQDYEY LINVIHAFQY VIYGTASFFF LYGALLLAEG FYTTGAVRQI
101 FGDYKTTICG KGLSATVTGG QKGRGSRGQH QAHSLERVCH CLGKWLGHPD
151 KFVGITYALT VVWLLVFACS AVPVYIYFNT WTTCQSIAFP SKTSASIGSL
201 CADARMYGVL PWNAFPGKVC GSNLLSICKT AEFQMTFHLF IAAFVGAAAT
251 LVSLLTFMIA ATYNFAVLKL MGRGTKF
```

Figure 24. Mascot report showing myelin proteolipid protein peptide match found in sample V1 (this same sequence was also found in the proteomic analysis of the York brain)[1]

Protein View: Q8IW52

SLIT and NTRK-like protein 4 OS=Homo sapiens GN=SLITRK4 PE=2 SV=1

Database:	UniProt_human_SP
Score:	30
Nominal mass (M_r):	95355
Calculated pI:	7.95

Sequence similarity is available as an NCBI BLAST search of Q8IW52 against nr.

Search parameters

MS data file:	13229323905432979.mgf
Enzyme:	Trypsin: cuts C-term side of KR unless next residue is P.
Fixed modifications:	Carbamidomethyl (C)
Variable modifications:	Deamidated (NQ), Gln->pyro-Glu (N-term Q), Glu->pyro-Glu (N-term E), Oxidation (M)

Protein sequence coverage: 0%

Matched peptides shown in ***bold red***.

```
  1 MFLWLFLILS ALISSTNADS DISVEICNVC SCVSVENVLY VNCEKVSVYR
 51 PNQLKPPWSN FYHLNFQNNF LNILYPNTFL NFSHAVSLHL GNNKLQNIEG
101 GAFLGLSALK QLHLNNNELK ILRADTFLGI ENLEYLQADY NLIKYIERGA
151 FNKLHKLKVL ILNDNLISFL PDNIFRFASL THLDIRGNRI QKLPYIGVLE
201 HIGRVVELQL EDNPWNCSCD LLPLKAWLEN MPYNIYIGEA ICETPSDLYG
251 RLLKETNKQE LCPMGTGSDF DVRILPPSQL ENGYTTPNGH TTQTSLHRLV
301 TKPPKTTNPS KISGIVAGKA LSNRNLSQIV SYQTRVPPLT PCPAPCFCKT
351 HPSDLGLSVN CQEKNIQSMS ELIPKPLNAK KLHVNGNSIK DVDVSDFTDF
401 EGLDLLHLGS NQITVIKGDV FHNLTNLRRL YLNGNQIERL YPEIFSGLHN
451 LQYLYLEYNL IKEISAGTFD SMPNLQLLYL NNNLLKSLPV YIFSGAPLAR
501 LNLRNNKFMY LPVSGVLDQL QSLTQIDLEG NPWDCTCDLV ALKLWVEKLS
551 DGIVVKELKC ETPVQFANIE LKSLKNEILC PKLLNKPSAP FTSPAPAITF
601 TTPLGPIRSP PGGPVPLSIL ILSILVVLIL TVFVAFCLLV FVLRRNKKPT
651 VKHEGLGNPD CGSMQLQLRK HDHKTNKKDG LSTEAFIPQT IEQMSKSHTC
701 GLKESETGFM FSDPPGQKVV MRNVADKEKD LLHVDTRKRL STIDELDELF
751 PSRDSNVFIQ NFLESKKEYN SIGVSGFEIR YPEKQPDKKS KKSLIGGNHS
801 KIVVEQRKSE YFELKAKLQS SPDYLQVLEE QTALNKI
```

Figure 25. Mascot report showing SLIT and NTRK-like protein 4 peptide match

3.3 Comparison of Spectra of Ancient Brain Lipid Extracts

The 17 different archaeological specimens came from 14 different archaeological contexts[f] over four separate sites. For each separate archaeological specimen (labelled Y1, B1 etc, Table 5) a lipid extraction procedure using a Folch wash was performed (2.3). For those samples for which there was sufficient material, duplicate extracts were made (e.g. H12a and H12b), and for those where the volume of the filtrate was large, they were split across two sample vials (e.g. H13a i/H13a ii).

The mass spectra were analysed using Bruker DataAnalysis software. After identifying peaks using the MassList function (see 2.4.1for parameters), the data were analysed using the SmartFormula function, which assigns empirical formulae on the basis of accurate *m/z* measurements, and also uses isotopic signal intensities. The empirical formulae assigned were screened manually, to ensure a good match of the measured and simulated isotopic envelopes for each suggested formula, and to ensure the empirical formulae were realistic before proceeding.

For each series of sample MALDI spot replicates, the resulting *m/z* values for the first spot were arranged in order of decreasing signal-to-noise ratio and compared first with the data in a similar list obtained from the original master list of matrix signals. Peaks that had the same *m/z* values to within 2 d.p. were assigned as deriving from matrix background and were removed from the list.

[f] Three of the samples were taken from the same single skeleton; two more samples also came from a single skeleton. Since these had been subsampled and archived separately, they have been handled separately here too, while remaining mindful of the common origin of the samples.

The remaining *m/z* values were presumed to correspond not to matrix background but to sample-specific signals; the top five S:N peaks were inspected to determine that the they were the monoisotopic signals, and not deriving from other signals in the isotopic envelope.

The resulting list of signals and their proposed empirical formulae were then compared with those signals from all the other specimens and their replicates, to determine whether they were also observed in other samples. Signals were considered to match if the *m/z* values were within 2 ppm of each other; the mass accuracy performance of the mass spectrometer was such that mass accuracies are typically below 1 ppm, and almost always within 2 ppm – this 2 ppm cut-off was thus chosen to be conservative enough to include all potential matches. A check was then carried out to establish whether this process had missed including high intensity peaks due to some samples giving spectra with high noise, which could have meant intense signals did not meet the S:N cut-off for inclusion. The five most intense peaks from the *m/z* list for each sample were assessed in this way. If these *m/z* values had not been included in the original list, they were added and also compared with the *m/z* value lists for all samples and replicates. In addition to these three further signals that were identified during the initial analysis of the MALDI mass spectrum of the York brain were also included.

The data were compiled into Tables for each empirical formula, arranged by sample age vertically.

3.3.1 KEY SIGNALS IDENTIFIED AS A RESULT OF MASS SPECTRAL COMPARISONS

Each of the following tables presents one of the empirical formulae assigned to each of the components in a variety of compound classes, and summarises the mass spectrometric evidence for this component from each of sample spots analysed (1, 2, or 3) for each of the sample extracts. The samples are listed in descending date order, with the oldest sample (from York) at the top. The tables give the *m/z* value at which the component was identified in each of the sample spots, the *m/z* error (difference in ppm between the measured and theoretical *m/z* for this empirical formula), and then gives the absolute intensity of the signal, its intensity as a percent of the most intense signal in the *m/z* range considered (*m/z* 303 -3000), the S:N ratio for the signal, and the mass resolution of that signal. To make the data easier to comprehend, heat map colouring has been used to highlight high, medium, and low values for each of the variables reported, with dark green being the highest values, and dark red the lowest (see legend to tables). Where signals were not detected, their absence is marked by a blank cell. This colour coding allows the most intense signals to be identified 'at a glance' – they are in shades of green.

Table Legend	
10	Highest values
9	
8	
7	
6	
5	
4	
3	
2	
1	
0	Lowest values
	Not detected

The data presented in Table 8 show that a peak at *m/z* 371, assigned an empirical formula $[C_{27}H_{46}] + H^+$ (a purely hydrocarbon residue with five double bond equivalents (dbe)), occurred in several of the extracts, most notably in samples H1, H5, H6 and H10. Whilst this component is not present in samples from across all sites, being absent from Villiers Street samples (C19th), there are indications of its presence in the York remains (Iron Age), Hull samples (C14th) and the Blackpool remains (C19th), suggesting that it occurs across all the time periods represented by the sites from which samples have been analysed. Its absence from the original York brain extract analysis may be explained by the upgrade to the mass spectrometer that took place between the original analysis and the current analyses. The residue is not detected in the Villiers Street sample or in H14. Whilst the relative intensity of this signal in some of the spectra is low (under 1.0 %) the *m/z* error is less than one ppm, the S:N values are high, as is the resolution. The table also clearly shows that the residue is not detected in DHB matrix alone nor in the soil controls or the solvent blank.

Table 8. Summary of signal at *m/z* 371. C_xH_y

Calculated *m/z*	371.36723 C27H47						
Sample designation + MALDI replicate no.	Measured *m/z*	Error [ppm]	Present	S:N	Intensity	Rel. Int. %	Resolution
Y1a 1	371.36674	1.26	Yes	7.7	1059558	0.4	150657
Y1a 2			No				
Y1a 3	371.36722	0.03	Yes	7.2	1016271	0.3	283785
Original Heslington			No				
H1a 1	371.36726	-0.10	Yes	1485.6	161548096	16.3	213606
H1a 2	371.36716	0.19	Yes	1713.3	178478768	44.7	213659
H1a 3	371.36712	0.30	Yes	465.3	48796764	7.4	214398
H1b 1	371.36696	0.73	Yes	349.8	36754136	4.3	214496
H1b 2	371.36692	0.84	Yes	249.2	25610290	6.7	210282
H1b 3	371.36326	0.89	Yes	292.1	30516188	7.2	212935
H2a 1	371.36692	0.83	Yes	336.8	35224688	6.5	214529
H2a 2	371.36713	0.27	Yes	223.9	24157752	7.3	213653
H2a 3	371.36698	0.67	Yes	173.5	17930234	5.1	215739
H3a 1	371.36715	0.22	Yes	264.1	28327398	5.1	215552
H3a 2	371.36719	0.11	Yes	141.5	15346917	2.5	211919
H3a 3	371.36712	0.30	Yes	77.1	8325893	1.1	217070
H4a 1	371.36735	-0.32	Yes	184.3	19194676	1.1	214245
H4a 2	371.36725	-0.05	Yes	202.2	21295320	2.4	213850
H4a 3	371.36718	0.12	Yes	403.6	42386056	5.1	213495
H5a 1	371.36696	0.72	Yes	340.8	34862620	18.3	214578
H5a 2	371.36701	0.58	Yes	322.0	33428428	11.0	213408
H5a 3	371.36701	0.58	Yes	300.8	31434910	3.6	212022
H6a 1	371.36716	0.18	Yes	796.9	83953880	11.3	214477
H6a 2	371.36715	0.20	Yes	732.8	76508592	10.4	213556
H6a 3	371.36716	0.18	Yes	1016.1	107124200	11.4	215023
H7a 1	371.36702	0.56	Yes	207.2	22087590	5.4	213065
H7a 2	371.36712	0.30	Yes	210.7	22758882	3.6	212961
H7a 3	371.36703	0.52	Yes	362.9	38427096	5.7	213244
H8a 1	371.36719	0.10	Yes	302.5	32146176	5.5	213492
H8a 2	371.36716	0.19	Yes	224.7	23231216	5.4	207449
H8a 3	371.36709	0.38	Yes	286.2	29772980	5.8	212849
H9a 1	371.36727	-0.12	Yes	286.8	29935876	3.7	213052
H9a 2	371.36732	-0.25	Yes	598.1	62373828	7.2	214871
H9a 3	371.36717	0.16	Yes	85.2	9060308	2.0	220730
H10a 1	371.36719	0.11	Yes	159.1	16857612	2.8	213560
H10a 2	371.36707	0.41	Yes	253.3	25955170	13.3	211151
H10a 3	371.36716	0.19	Yes	595.8	62973608	17.1	213406
H11a 1	371.36727	-0.12	Yes	221.0	23149630	10.1	212403
H11a 2	371.36727	-0.12	Yes	92.7	10058427	1.3	219297
H11a 3	371.36706	0.45	Yes	89.8	9164518	7.0	220474
H12a 1	371.36737	-0.44	Yes	41.4	4627903	1.0	207602
H12a 2	371.36731	-0.23	Yes	57.9	6385782	1.3	220140
H12a 3	371.36739	-0.44	Yes	40.4	4536027	1.1	219614
H13aii 1	371.36734	-0.30	Yes	46.1	5135555	1.3	213684
H13aii 2	371.36737	-0.38	Yes	36.7	4075661	1.0	222278
H13aii 3	371.36708	0.39	Yes	21.6	2493963	0.4	221076
H14a 1			No				
H14a 2			No				
H14a 3			No				
H14bi 1			No				
H14bi 2			No				
H14bi 3			No				
V1a 1			No				
V1a 2			No				
V1a 3			No				
B1a 1	371.36738	-0.14	Yes	27.9	3173883	0.6	215223
B1a 2	371.36706	0.45	Yes	23.0	2634959	0.9	223936
B1a 3	371.36695	0.74	Yes	14.7	1772013	0.4	221042
DHB 1			No				
DHB 2			No				
DHB 3			No				
Soil 3a 1			No				
Soil 3a 2			No				
Soil 3a 3			No				
Soil 3b 1			No				
Soil 3b 2			No				
Soil 3b 3			No				
Solvent 1			No				
Solvent 2			No				
Solvent 3			No				

The data indicating the presence of singly nitrogenated hydrocarbon species are summarised in Table 9 and Table 10.

The most abundant signal (by average intensity) consistent with the protonated molecule ($M+H^+$) of a singly nitrogenated hydrocarbon species was observed at a nominal *m/z* value of 518 (Table 9). This component was assigned an empirical formula of $[C_{36}H_{71}N] + H^+$, consistent with an organic compoundwith 36 C atoms, two degrees of unsaturation/double bond equivalents (i.e. rings or double bonds), and a single N atom. The heat map colouration of the table makes it easy to see that this component is not observed in the spectra of the matrix alone, either of the soil extracts, or in the solvent blank. Its presence is most strongly detected in the extract of sample H12 but it was also an intense ion in the spectra of several of the other Hull sample extracts. It is not universally detected, being limited to detection in the H1, H5, H8, H9, and H14 extracts; it was not detected in extracts of H6 and H10. The spectra of the York extracts have intense *m/z* 518 signals, comparable in intensity to that in many of the Hull sample spectra. In the Villiers Street sample extract, there are low intensity peaks but its presence in the Blackpool sample spectra confirms that this component is present in much younger brain samples. Again the *m/z* error in these signals is generally under 1 ppm, giving confidence in the quality of the data and their assignment.

After the signal at *m/z* 518, the next most abundant signal for a mononitrogenated hydrocarbon was that at nominal *m/z* 490.

Table 9. Summary of signal at *m/z* 518. C_xH_yN

Calculated *m/z*	518.56593	C36H72N					
Sample designation + MALDI replicate no.	Measured *m/z*	Error [ppm]	Present	S:N	Intensity	Rel. Int. %	Resolution
Y1a 1	518.56597	-0.08	Yes	291.80	39821152	13.20	153227
Y1a 2	518.56583	-0.08	Yes	241.20	31666116	11.60	155029
Y1a 3	518.56591	0.04	Yes	243.20	33440106	9.70	152725
Original Heslington	518.56563	0.57	Yes	11.70	1422465	1.10	96197
H1a 1	518.56586	0.12	Yes	15.90	2481151	0.20	163731
H1a 2	518.56576	0.32	Yes	10.30	1513142	0.40	177880
H1a 3			No				
H1b 1	518.56556	0.71	Yes	15.30	2178036	0.30	168946
H1b 2	518.56550	0.82	Yes	9.30	1405594	0.40	124590
H1b 3	518.56540	1.02	Yes	13.90	1954995	0.50	144105
H2a 1	518.56543	0.97	Yes	277.60	33704532	6.20	153627
H2a 2	518.56557	0.68	Yes	116.40	16241737	4.90	151052
H2a 3	518.56562	0.59	Yes	129.60	15083922	4.20	154909
H3a 1	518.56580	0.24	Yes	364.50	49211336	8.90	152930
H3a 2	518.56592	0.01	Yes	252.20	34841612	5.70	152657
H3a 3	518.56576	0.32	Yes	162.80	20472262	2.70	154289
H4a 1	518.56604	-0.21	Yes	208.10	32376338	1.90	153122
H4a 2	518.56617	-0.47	Yes	243.90	38279608	4.40	153547
H4a 3	518.56604	-0.21	Yes	703.80	105716680	12.70	153133
H5a 1	518.56630	-0.75	Yes	4.20	744853	0.40	174453
H5a 2	518.56568	0.48	Yes	5.90	982994	0.30	163365
H5a 3	518.56541	1.00	Yes	11.20	1732423	0.20	165822
H6a 1			No				
H6a 2			No				
H6a 3			No				
H7a 1	518.56581	0.22	Yes	92.30	11830667	2.90	154108
H7a 2	518.56596	-0.07	Yes	83.90	11338334	1.80	153464
H7a 3	518.56576	0.33	Yes	125.30	16093076	2.40	157133
H8a 1			No				
H8a 2			No				
H8a 3	518.56557	0.68	Yes	5.50	984952	0.20	186590
H9a 1			No				
H9a 2	518.56588	0.09	Yes	8.10	1473977	0.20	170385
H9a 3			No				
H10a 1			No				
H10a 2			No				
H10a 3			No				
H11a 1	518.56623	-0.58	Yes	248.40	32313812	14.10	152639
H11a 2	518.56616	-0.44	Yes	118.00	15985381	2.10	154562
H11a 3	518.56583	0.18	Yes	91.60	10354617	8.00	153353
H12a 1	518.56635	-0.81	Yes	1141.50	167784208	37.30	153151
H12a 2	518.56640	-0.90	Yes	2178.20	320249056	65.10	152346
H12a 3	518.56634	-0.79	Yes	1237.70	184214928	45.80	153455
H13aii 1	518.56629	-0.70	Yes	372.60	52974428	13.40	153637
H13aii 2	518.56629	-0.71	Yes	383.60	52235528	13.40	152103
H13aii 3	518.56607	-0.27	Yes	263.60	33609248	5.70	153904
H14a 1			No				
H14a 2	518.56585	0.14	Yes	10.10	1793395	0.20	166879
H14a 3			No				
H14bi 1			No				
H14bi 2			No				
H14bi 3	518.56636	-0.83	Yes	60.60	10536869	0.20	155908
V1a 1	518.56602	0.03	Yes	83.50	12275678	0.60	154176
V1a 2	518.56599	-0.13	Yes	79.70	10876827	1.70	154603
V1a 3	518.56593	0.00	Yes	83.00	11460806	2.40	156962
B1a 1	518.56621	-0.54	Yes	1064.70	178215808	34.70	152748
B1a 2	518.56596	-0.06	Yes	437.90	60832316	19.80	151673
B1a 3	518.56569	0.45	Yes	308.30	38989648	9.10	153787
DHB 1			No				
DHB 2			No				
DHB 3			No				
Soil 3a 1			No				
Soil 3a 2			No				
Soil 3a 3			No				
Soil 3b 1			No				
Soil 3b 2			No				
Soil 3b 3			No				
Solvent 1			No				
Solvent 2			No				
Solvent 3			No				

A second signal consistent with the protonated molecule ($M+H^+$) of a singly nitrogenated hydrocarbon species was observed at a nominal *m/z* value of 490 (Table 10). This component was assigned an empirical formula of $[C_{34}H_{67}N] + H^+$, consistent with an organic compound with 34 C atoms, just one degree of unsaturation, and a single N atom. The heat map colouration of the table makes it easy to see that this component is not observed in the spectra of the matrix alone, either of the soil extracts, or in the solvent blank. It is however, observed in the spectra of most of the samples, with the exception of H6, H8, H10 and H14, and is observed, albeit at low intensity in the spectra of extracts of H1, H5 and H9, as well as the original York brain extract. Notably, it is identified in brain extracts of brains that represent the full range of ages sampled, from the extracts made in this work of the York brain (Iron Age), in some of the Hull Magistrate Court samples (C14th), as well as in Blackpool and Villiers Street samples, which are only a couple of hundred years old. It is noteworthy that the *m/z* accuracies of these data are very high – with one exception, always below 1 ppm – and that, even for low intensity signals, the mass resolution remains very high, giving good confidence in the assignment of these data.

Table 10. Summary of signal at *m/z* 490. C_xH_yN

Calculated *m/z*	490.53452	C34H68N					
Sample designation + MALDI replicate no.	Measured *m/z*	Error [ppm]	Present	S:N	Intensity	Rel. Int. %	Resolution
Y1a 1	490.53462	0.01	Yes	428.9	55384392	18.4	160134
Y1a 2	490.53452	0.22	Yes	377.7	47148336	17.3	162002
Y1a 3	490.53461	0.04	Yes	373.6	48573028	14.1	162076
Original Heslington	490.53402	1.24	Yes	8.1	1013508	0.8	105171
H1a 1	490.53447	0.33	Yes	18.9	2756671	0.3	173766
H1a 2	490.53449	0.28	Yes	12.7	1745210	0.4	185366
H1a 3			No				
H1b 1	490.53404	1.20	Yes	18.1	2432171	0.3	167332
H1b 2	490.53436	0.55	Yes	12.2	1690521	0.4	185389
H1b 3	490.53397	1.34	Yes	14.7	1978319	0.5	175921
H2a 1	490.53418	0.91	Yes	210.3	24788954	4.6	162422
H2a 2	490.53432	0.62	Yes	90.8	12086521	3.6	162943
H2a 3	490.53434	0.58	Yes	94.9	10841534	3.1	165344
H3a 1	490.53452	0.22	Yes	327.1	42092952	7.6	161973
H3a 2	490.53462	0.01	Yes	215.6	28313744	4.6	160814
H3a 3	490.53447	0.31	Yes	159.9	19403852	2.6	160753
H4a 1	490.53473	-0.20	Yes	114.7	16607238	1.0	162409
H4a 2	490.53485	-0.45	Yes	126.8	18529236	2.1	163735
H4a 3	490.53472	-0.18	Yes	394.5	55258680	6.7	162892
H5a 1	490.53442	0.43	Yes	5.0	821666	0.4	206317
H5a 2	490.53435	0.57	Yes	12.4	1697411	0.6	153601
H5a 3	490.53416	0.95	Yes	9.8	1481337	0.2	174063
H6a 1			No				
H6a 2			No				
H6a 3			No				
H7a 1	490.53449	0.28	Yes	66.9	8344507	2.0	165337
H7a 2	490.53457	0.11	Yes	55.0	7211294	1.1	167817
H7a 3	490.53445	0.35	Yes	80.7	10073580	1.5	166828
H8a 1			No				
H8a 2			No				
H8a 3			No				
H9a 1			No				
H9a 2	490.53471	-0.17	Yes	7.3	1277265	0.1	163369
H9a 3	490.53461	0.03	Yes	5.9	996838	0.2	201186
H10a 1			No				
H10a 2			No				
H10a 3			No				
H11a 1	490.53487	-0.49	Yes	202.4	25198196	11.0	162441
H11a 2	490.53486	-0.48	Yes	92.2	11967970	1.6	163980
H11a 3	490.53457	0.11	Yes	69.8	7775120	6.0	163415
H12a 1	490.53499	-0.74	Yes	357.6	49381640	11.0	161465
H12a 2	490.53502	-0.81	Yes	652.2	89941288	18.3	160478
H12a 3	490.53499	-0.73	Yes	376.8	52596028	13.1	161445
H13aii 1	490.53492	-0.61	Yes	197.6	26610480	6.7	161997
H13aii 2	490.53490	-0.55	Yes	165.1	21455778	5.5	160532
H13aii 3	490.53474	-0.24	Yes	135.6	16719509	2.8	162693
H14a 1			No				
H14a 2			No				
H14a 3			No				
H14bi 1			No				
H14bi 2			No				
H14bi 3			No				
V1a 1	490.53474	-0.23	Yes	45.8	6465144	0.3	170860
V1a 2	490.53472	-0.18	Yes	56.4	7427034	1.2	164819
V1a 3	490.53467	-0.08	Yes	54.6	7278893	1.6	164456
B1a 1	490.53487	-0.50	Yes	347.7	53424928	10.4	161321
B1a 2	490.53464	-0.02	Yes	169.7	22398784	7.3	161041
B1a 3	490.53442	0.43	Yes	119.4	14660145	3.4	163923
DHB 1			No				
DHB 2			No				
DHB 3			No				
Soil 3a 1			No				
Soil 3a 2			No				
Soil 3a 3			No				
Soil 3b 1			No				
Soil 3b 2			No				
Soil 3b 3			No				
Solvent 1			No				
Solvent 2			No				
Solvent 3			No				

In addition to mononitrogenated hydrocarbons Table 11 shows evidence the most abundant signal (by average intensity) consistent with the protonated molecule ($M+H^+$) of a dinitrogenated hydrocarbon species at *m/z* 487, assigned an empirical formula $[C_{34}H_{50}N_2] + H^+$. The component with 11 double bond equivalents, was detected in nearly all of the sample extracts with the exceptions of the York samples (both the original and current) and H1, H14 and V1. This is very highly unsaturated compared to the original brain lipids; it may be the result of condensation of a number of small unsaturated molecules. This compound wasn't detected in any of the controls (DHB, soil or solvent). The fact that it was not detected in the oldest sample may indicate that if it is a chemical present due to the decomposition or preservation processes, it has undergone further chemical changes over a longer period of time. This does not explain its absence from H1 and H14 or V1. It is notably present in samples H4, H8 and H10 and B1 at high intensities but can also be detected in most other samples with confidence.

Table 11. Summary of signal at *m/z* 487. $C_xH_yN_2$

Calculated *m/z*	487.40468	C34H51N2					
Sample designation + MALDI replicate no.	Measured *m/z*	Error [ppm]	Present	S:N	Intensity	Rel. Int. %	Resolution
Y1a 1			No				
Y1a 2			No				
Y1a 3			No				
Original Heslington			No				
H1a 1			No				
H1a 2			No				
H1a 3			No				
H1b 1			No				
H1b 2	487.40427	0.84	Yes	10.4	1482708	0.4	184178
H1b 3	487.40448	0.40	Yes	8.3	1235430	0.3	213565
H2a 1			No				
H2a 2			No				
H2a 3	487.40420	0.97	Yes	8.8	1247844	0.4	168992
H3a 1	487.40459	0.17	Yes	42.8	5757612	1.0	168433
H3a 2	487.40473	-0.11	Yes	58.1	7836520	1.3	159838
H3a 3	487.40444	0.48	Yes	25.2	3289503	0.4	165985
H4a 1	487.40472	-0.09	Yes	2288.4	326055392	19.0	162924
H4a 2	487.40486	-0.37	Yes	1766.5	254412912	29.1	163501
H4a 3	487.40472	-0.09	Yes	1804.4	251727424	30.3	163238
H5a 1	487.40433	0.71	Yes	67.1	7676542	4.0	167887
H5a 2	487.40442	0.52	Yes	88.9	10529521	3.5	166556
H5a 3	487.40439	0.58	Yes	113.6	14238334	1.6	164032
H6a 1	487.40461	0.13	Yes	437.8	54723252	7.4	163738
H6a 2	487.40459	0.19	Yes	503.0	61639288	8.4	162907
H6a 3	487.40460	0.16	Yes	416.7	52525964	5.6	163364
H7a 1	487.40461	0.14	Yes	76.9	9544381	2.3	160690
H7a 2	487.40465	0.06	Yes	67.4	8770599	1.4	168240
H7a 3	487.40452	0.32	Yes	68.1	8538995	1.3	162514
H8a 1	487.40466	0.03	Yes	982.3	131166160	22.6	163037
H8a 2	487.40485	-0.35	Yes	720.8	89030888	20.6	161588
H8a 3	487.40458	0.19	Yes	798.5	97172640	18.8	162536
H9a 1	487.40470	-0.04	Yes	628.9	84759304	10.5	162395
H9a 2	487.40468	0.00	Yes	544.7	74275672	8.6	162646
H9a 3	487.40454	0.29	Yes	359.1	44110740	9.7	161912
H10a 1	487.40463	0.09	Yes	1200.1	150049920	25.1	163471
H10a 2	487.40448	0.40	Yes	980.1	111422568	57.1	162020
H10a 3	487.40461	0.14	Yes	1977.7	254626912	69.2	163104
H11a 1	487.40491	-0.49	Yes	801.5	98948720	43.2	162879
H11a 2	487.40489	-0.43	Yes	530.9	67548592	8.8	163162
H11a 3	487.40461	0.13	Yes	272.6	29591570	22.7	163792
H12a 1	487.40500	-0.67	Yes	883.3	121549352	27.0	162843
H12a 2	487.40498	-0.61	Yes	745.2	102729224	20.9	162421
H12a 3	487.40499	-0.64	Yes	1036.0	144104224	35.8	163393
H13aii 1	487.40494	-0.54	Yes	249.1	33477306	8.5	162733
H13aii 2	487.40493	-0.51	Yes	221.5	28688376	7.4	162124
H13aii 3	487.40485	-0.36	Yes	189.0	23195892	3.9	164558
H14a 1			No				
H14a 2			No				
H14a 3			No				
H14bi 1	487.40505	-0.76	Yes	11.8	1974477	0.2	175886
H14bi 2	487.40524	-1.16	Yes	8.9	1519081	0.2	208375
H14bi 3			No				
V1a 1			No				
V1a 2			No				
V1a 3			No				
B1a 1	487.40490	-0.46	Yes	798.8	122348976	23.8	162950
B1a 2	487.40465	0.05	Yes	771.9	100887160	32.9	161853
B1a 3	487.40443	0.49	Yes	653.1	78924800	18.5	163374
DHB 1			No				
DHB 2			No				
DHB 3			No				
Soil 3a 1			No				
Soil 3a 2			No				
Soil 3a 3			No				
Soil 3b 1			No				
Soil 3b 2			No				
Soil 3b 3			No				
Solvent 1			No				
Solvent 2			No				
Solvent 3			No				

A second dinitrogenated hydrocarbon was detected at *m/z* 411 (Table 12). This signal assigned $[C_{28}H_{46}N_2] + H^+$, for a component with 7 double bond equivalents, occurred with highest intensities in samples H5 and H12, moderate intensities in H4, H11, H13 and B1 and was detected at low levels in other Hull samples as well as in Y1. Whilst this component is not present in samples from across all sites, being absent from Villiers Street samples, there are indications of its presence in the York remains and the Blackpool remains, suggesting that it occurs across all the time periods. This compound is also highly unsaturated compared to standard brain lipids. Again, its absence from the original York brain extract may be explained by the upgrade to the mass spectrometer that took place between the original analysis and the current analyses. However, this compound wasn't detected in all of the current project's York replicates and so its absence may be due to the inherent variability of MALDI. The component is clearly not detected in several of the Hull samples, e.g. H1 and H6 or in the Villiers Street sample. Whilst the relative intensity of this signal in some of the spectra is low (under 1.0 %) the *m/z* error is less than one ppm, the S:N values are high, as is the resolution. The table also clearly shows that the residue is not detected in DHB matrix alone nor in the soil controls or the solvent blank.

Table 12. Summary of signal at *m/z* 411. $C_xH_yN_2$

Calculated *m/z*	411.37338	C28H47N2					
Sample designation + MALDI replicate no.	Measured *m/z*	Error [ppm]	Present	S:N	Intensity	Rel. Int. %	Resolution
Y1a 1			No				
Y1a 2	411.37292	1.11	Yes	5.4	842786	0.3	206063
Y1a 3	411.37337	0.02	Yes	4.0	702962	0.2	288638
Original Heslington			No				
H1a 1			No				
H1a 2			No				
H1a 3			No				
H1b 1	411.37298	0.97	Yes	8.5	1176617	0.1	232644
H1b 2	411.37299	0.93	Yes	5.4	822725	0.2	259660
H1b 3	411.37293	1.07	Yes	7.3	1035378	0.2	194370
H2a 1			No				
H2a 2			No				
H2a 3	411.37344	-0.16	Yes	5.1	782367	0.2	132343
H3a 1	411.37335	0.07	Yes	29.3	3522732	0.6	212736
H3a 2	411.37328	0.23	Yes	14.2	1850830	0.3	220418
H3a 3			No				
H4a 1	411.37345	-0.18	Yes	251.5	28452994	1.7	193377
H4a 2	411.37347	-0.23	Yes	158.7	18259868	2.1	193819
H4a 3	411.37338	-0.01	Yes	154.3	17635520	2.1	193987
H5a 1	411.37307	0.74	Yes	725.2	75432024	39.6	192208
H5a 2	411.37313	0.59	Yes	959.2	101894848	33.5	193273
H5a 3	411.37311	0.65	Yes	918.1	99596392	11.4	191164
H6a 1			No				
H6a 2			No				
H6a 3			No				
H7a 1			No				
H7a 2			No				
H7a 3			No				
H8a 1			No				
H8a 2			No				
H8a 3	411.37316	0.51	Yes	7.5	1061967	0.2	206352
H9a 1			No				
H9a 2			No				
H9a 3			No				
H10a 1			No				
H10a 2			No				
H10a 3	411.37327	0.26	Yes	5.3	841586	0.2	237774
H11a 1	411.37349	-0.29	Yes	113.0	12484020	5.5	195255
H11a 2	411.37350	-0.31	Yes	36.9	4342552	0.6	190894
H11a 3	411.37331	0.15	Yes	46.6	4964630	3.8	204384
H12a 1	411.37355	-0.43	Yes	1302.9	147542336	32.8	192690
H12a 2	411.37354	-0.39	Yes	1252.5	142142672	28.9	192790
H12a 3	411.37354	-0.40	Yes	1201.2	136865392	34.0	193352
H13aii 1	411.37352	-0.35	Yes	372.1	42066632	10.7	193203
H13aii 2	411.37350	-0.31	Yes	383.2	42355268	10.9	191246
H13aii 3	411.37343	-0.13	Yes	297.7	32427694	5.5	192997
H14a 1			No				
H14a 2			No				
H14a 3			No				
H14bi 1			No				
H14bi 2			No				
H14bi 3			No				
V1a 1			No				
V1a 2			No				
V1a 3			No				
B1a 1	411.37350	-0.30	Yes	298.2	34873896	6.8	192815
B1a 2	411.37332	0.14	Yes	236.1	26238866	8.6	192278
B1a 3	411.37320	0.23	Yes	222.4	24130730	5.6	193478
DHB 1			No				
DHB 2			No				
DHB 3			No				
Soil 3a 1			No				
Soil 3a 2			No				
Soil 3a 3			No				
Soil 3b 1			No				
Soil 3b 2			No				
Soil 3b 3			No				
Solvent 1			No				
Solvent 2			No				
Solvent 3			No				

The data presented in Table 13 show an unusual peak at *m/z* 405, which was detected at an extremely high intensity in sample H1 (specifically replicate 1, but also in replicate 2) and it's only present in one other spectrum, one of the replicates of H5. Whilst its presence is rare in the data from this selection of brain samples, the signal has high resolution and S:N ratios. This peak was assigned an empirical formula $[C_{27}H_{24}N_4] + H^+$, or possibly $[C_{27}H_{21}N_3] + NH_4^+$. Since the other components have ionised as $M+H^+$ species, if this compound behaves similarly, this would be consistent with a very highly unsaturated species (18 double bond equivalents) which is probably highly aromatic. As the signal wasn't detected in the spectra of the youngest or oldest sample extracts, only in those from Hull, it could be hypothesized that this compound is created during the decomposition process and then undergoes further chemical changes at this specific site. However, its absence from the majority of samples (as well as a larger than 1 ppm *m/z* error in replicate H1a 2) may indicate that this component is probably not a significant decomposition product. Its relatively high level of functionalisation and very high level of unsaturation when compared to the majority of the components identified in these preserved brains, mark it out as rather different from most of the largely hydrocarbon species, with little or no functionalisation.

Table 13. Summary of signal at *m/z* 405. $C_xH_yN_4$

Calculated *m/z*	405.20737 C27H25N4						
Sample designation + MALDI replicate no.	Measured *m/z*	Error [ppm]	Present	S:N	Intensity	Rel. Int. %	Resolution
Y1a 1			No				
Y1a 2			No				
Y1a 3			No				
Original Heslington			No				
H1a 1	405.20733	0.11	Yes	442.2	50097424	5.0	196634
H1a 2	405.20788	-1.25	Yes	2.8	555152	0.1	216967
H1a 3			No				
H1b 1			No				
H1b 2			No				
H1b 3			No				
H2a 1			No				
H2a 2			No				
H2a 3			No				
H3a 1			No				
H3a 2			No				
H3a 3			No				
H4a 1			No				
H4a 2			No				
H4a 3			No				
H5a 1	405.20732	0.13	Yes	4.0	665646	0.3	188022
H5a 2			No				
H5a 3			No				
H6a 1			No				
H6a 2			No				
H6a 3			No				
H7a 1			No				
H7a 2			No				
H7a 3			No				
H8a 1			No				
H8a 2			No				
H8a 3			No				
H9a 1			No				
H9a 2			No				
H9a 3			No				
H10a 1			No				
H10a 2			No				
H10a 3			No				
H11a 1			No				
H11a 2			No				
H11a 3			No				
H12a 1			No				
H12a 2			No				
H12a 3			No				
H13aii 1			No				
H13aii 2			No				
H13aii 3			No				
H14a 1			No				
H14a 2			No				
H14a 3			No				
H14bi 1			No				
H14bi 2			No				
H14bi 3			No				
V1a 1			No				
V1a 2			No				
V1a 3			No				
B1a 1			No				
B1a 2			No				
B1a 3			No				
DHB 1			No				
DHB 2			No				
DHB 3			No				
Soil 3a 1			No				
Soil 3a 2			No				
Soil 3a 3			No				
Soil 3b 1			No				
Soil 3b 2			No				
Soil 3b 3			No				
Solvent 1			No				
Solvent 2			No				
Solvent 3			No				

A series of singly nitrogenated hydrocarbon compounds was detected that also contained a single oxygen atom, Table 14 to Table 28. Table 14 details a compound assigned $[C_{35}H_{47}NO] + H^+$ at *m/z* 498, a component with 13 double bond equivalents. The signal in the spectra of all B1 replicates has high intensity and S:N and it is found consistently with moderate intensities in H4, H8, H9, H10, H11 and H12. It was not detected at all in the York or Villiers Street sample extracts and it is also absent from several of the Hull sample spectra. It was detected in one replicate soil control and one replicate solvent blank spectrum. However, it was not observed consistently in the soil and solvent controls, and when it was detected, it was at low intensity and S:N, while in the sample extract spectra, the signal was much more consistently observed, and at higher S:N and relative intensity, which enhance the confidence in these observations. Interestingly, the soil blank MALDI spot in which this signal was potentially identified, was adjacent on the MALDI plate to one of the H10a replica spots, and so cross contamination is not out of the question. However, the solvent blank spot containing a weak signal at this *m/z* was not close enough to any of the sample spots for this to provide an explanation for its detection in this control.

Table 14. Summary of signal at *m/z* 498. C_xH_yNO

Calculated *m/z*	498.37304	C35H48NO					
Sample designation + MALDI replicate no.	Measured *m/z*	Error [ppm]	Present	S:N	Intensity	Rel. Int. %	Resolution
Y1a 1			No				
Y1a 2			No				
Y1a 3			No				
Original Heslington			No				
H1a 1			No				
H1a 2			No				
H1a 3			No				
H1b 1			No				
H1b 2			No				
H1b 3			No				
H2a 1			No				
H2a 2			No				
H2a 3			No				
H3a 1	498.37297	0.15	Yes	93.4	12371798	2.2	161902
H3a 2	498.37300	0.09	Yes	57.6	7869396	1.3	159409
H3a 3	498.37279	0.51	Yes	14.9	2079054	0.3	169821
H4a 1	498.37309	-0.09	Yes	300.5	43907008	2.6	159731
H4a 2	498.37319	-0.30	Yes	343.7	50708700	5.8	159403
H4a 3	498.37308	-0.08	Yes	280.7	40112968	4.8	159821
H5a 1	498.37245	-0.77	Yes	9.2	1290371	0.7	148181
H5a 2	498.37263	0.83	Yes	11.0	1556298	0.5	199344
H5a 3	498.37293	0.22	Yes	14.9	2132928	0.2	172150
H6a 1	498.37302	0.00	Yes	21.4	2971680	0.4	160841
H6a 2	498.37295	0.19	Yes	36.2	4741415	0.6	170986
H6a 3	498.37288	0.32	Yes	24.8	3429661	0.4	171027
H7a 1	498.37285	0.16	Yes	5.3	920662	0.2	195598
H7a 2			No				
H7a 3	498.37279	0.51	Yes	7.5	1201021	0.2	163199
H8a 1	498.37303	0.03	Yes	297.2	40481716	7.0	159960
H8a 2	498.37313	-0.18	Yes	113.7	14451217	3.4	157320
H8a 3	498.37290	0.29	Yes	171.6	21326776	4.1	159811
H9a 1	498.37306	-0.04	Yes	554.5	75987400	9.4	159303
H9a 2	498.37305	-0.02	Yes	733.2	101554536	11.7	159259
H9a 3	498.37292	-0.25	Yes	98.1	12387393	2.7	158669
H10a 1	498.37294	0.20	Yes	51.0	6723750	1.1	157292
H10a 2	498.37300	0.09	Yes	57.5	6846523	3.5	159325
H10a 3	498.37294	0.20	Yes	237.0	31166148	8.5	159868
H11a 1	498.37327	-0.46	Yes	158.3	19991648	8.7	159498
H11a 2	498.37317	-0.26	Yes	45.7	6146589	0.8	159258
H11a 3	498.37302	0.04	Yes	47.6	5418922	4.2	166002
H12a 1	498.37341	-0.74	Yes	90.3	12894373	2.9	163365
H12a 2	498.37338	-0.67	Yes	94.8	13539916	2.8	160536
H12a 3	498.37336	-0.64	Yes	72.5	10523685	2.6	163683
H13aii 1	498.37332	-0.57	Yes	58.7	8230004	2.1	160446
H13aii 2	498.37328	-0.48	Yes	48.8	6632260	1.7	155472
H13aii 3	498.37321	-0.33	Yes	30.1	3963297	0.7	164656
H14a 1			No				
H14a 2			No				
H14a 3			No				
H14bi 1	498.37337	-0.66	Yes	10.6	1830832	0.2	125929
H14bi 2	498.37309	-0.09	Yes	6.6	1212998	0.2	197235
H14bi 3			No				
V1a 1			No				
V1a 2			No				
V1a 3			No				
B1a 1	498.37323	-0.38	Yes	1303.1	203859920	39.7	159206
B1a 2	498.37299	0.10	Yes	592.3	78603744	25.6	158822
B1a 3	498.37278	0.53	Yes	367.1	44940512	10.5	160232
DHB 1			No				
DHB 2			No				
DHB 3			No				
Soil 3a 1			No				
Soil 3a 2			No				
Soil 3a 3			No				
Soil 3b 1			No				
Soil 3b 2	498.37391	-1.75	Yes	5.6	1156363	0.1	120372
Soil 3b 3			No				
Solvent 1			No				
Solvent 2			No				
Solvent 3	498.37391	-1.74	Yes	5.6	1156363	0.1	120372

Table 15 shows the data for the compound assigned $[C_{35}H_{49}NO] + H^+$ at *m/z* 500, for a compound with 12 double bond equivalents. This signal is clearly absent from the spectra of the extracts of the York and Villiers Street samples as well as H1, H2 and H14. It is also undetected in the DHB, soil and solvent controls. This signal has a significant intensity and S:N in the youngest sample (B1) but is also present consistently within most of the Hull sample extracts (and their replicates), with a minority having low relative intensities (< 0.5%). The strength of the signal in the B1 extract could indicate that there is proportionally more of this compound in younger brains and this concentration decreases with age, leading to its non-detection in the oldest samples, but the absence from the other young sample, Villiers Street, is not consistent with this suggestion. Alternatively, the conditions leading to the preservation of the brain in the sample from the Blackpool site may have been unusual and led to the production of this component only at this site.

Table 15. Summary of signal at *m/z* 500. C_xH_yNO

Calculated *m/z*	500.38869 C35H50NO						
Sample designation + MALDI replicate no.	Measured *m/z*	Error [ppm]	Present	S:N	Intensity	Rel. Int. %	Resolution
Y1a 1			No				
Y1a 2			No				
Y1a 3			No				
Original Heslington			No				
H1a 1			No				
H1a 2			No				
H1a 3			No				
H1b 1			No				
H1b 2			No				
H1b 3			No				
H2a 1			No				
H2a 2			No				
H2a 3			No				
H3a 1	500.38867	0.05	Yes	207.6	27132620	4.9	160046
H3a 2	500.38871	-0.03	Yes	76.0	10302716	1.7	164345
H3a 3	500.38845	0.49	Yes	26.5	3471247	0.5	179327
H4a 1	500.38880	-0.21	Yes	344.7	50330268	2.9	159133
H4a 2	500.38889	-0.39	Yes	469.1	69104888	7.9	159181
H4a 3	500.38877	-0.16	Yes	414.8	59124008	7.1	159756
H5a 1	500.38845	0.48	Yes	16.4	2089044	1.1	165065
H5a 2	500.38839	0.61	Yes	23.6	3022508	1.0	176876
H5a 3	500.38827	0.84	Yes	19.8	2747358	0.3	167912
H6a 1	500.38857	0.36	Yes	34.9	4671451	0.6	166912
H6a 2	500.38865	0.08	Yes	41.8	5428440	0.7	170431
H6a 3	500.38858	0.22	Yes	50.7	6713170	0.7	163704
H7a 1	500.38856	0.52	Yes	5.0	888157	0.2	223967
H7a 2	500.38776	1.86	Yes	6.2	1072385	0.2	182336
H7a 3	500.38873	-0.07	Yes	9.8	1483579	0.2	135382
H8a 1	500.38869	0.00	Yes	304.9	41521500	7.1	159093
H8a 2	500.38881	-0.23	Yes	101.7	12957818	3.0	159347
H8a 3	500.38861	0.17	Yes	134.3	16754881	3.2	159149
H9a 1	500.38873	-0.09	Yes	507.6	69586752	8.6	158456
H9a 2	500.38874	-0.10	Yes	1032.0	142825200	16.5	158724
H9a 3	500.38852	0.34	Yes	55.0	7067208	1.6	158809
H10a 1	500.38861	0.36	Yes	27.3	3729970	0.6	172110
H10a 2	500.38860	0.18	Yes	62.5	7418223	3.8	163413
H10a 3	500.38862	0.14	Yes	189.7	25001586	6.8	158945
H11a 1	500.38895	-0.52	Yes	133.4	16894804	7.4	161311
H11a 2	500.38898	-0.58	Yes	29.5	4068340	0.5	154626
H11a 3	500.38870	-0.02	Yes	42.6	4873773	3.7	164338
H12a 1	500.38905	-0.72	Yes	154.0	21783994	4.8	160786
H12a 2	500.38905	-0.72	Yes	192.9	27240834	5.5	159009
H12a 3	500.38901	-0.64	Yes	123.1	17672758	4.4	159347
H13aii 1	500.38901	-0.64	Yes	132.0	18135424	4.6	161335
H13aii 2	500.38902	-0.66	Yes	79.0	10551573	2.7	158252
H13aii 3	500.38881	-0.23	Yes	68.8	8701489	1.5	159704
H14a 1			No				
H14a 2			No				
H14a 3			No				
H14bi 1	500.38876	-0.15	Yes	7.2	1344219	0.1	168860
H14bi 2	500.38855	0.28	Yes	7.9	1398281	0.2	168155
H14bi 3			No				
V1a 1			No				
V1a 2			No				
V1a 3			No				
B1a 1	500.38892	-0.46	Yes	2311.5	361371808	70.4	158624
B1a 2	500.38866	0.05	Yes	710.6	94241648	30.7	157111
B1a 3	500.38847	0.45	Yes	458.2	56014704	13.1	159814
DHB 1			No				
DHB 2			No				
DHB 3			No				
Soil 3a 1			No				
Soil 3a 2			No				
Soil 3a 3			No				
Soil 3b 1			No				
Soil 3b 2			No				
Soil 3b 3			No				
Solvent 1			No				
Solvent 2			No				
Solvent 3			No				

The peak at *m/z* 530, shown in Table 16, was assigned the empirical formula $[C_{36}H_{67}NO] + H^+$, for a component with only four double bond equivalents. The strength of the signal in the spectra of the original York sample extract meant this component was flagged during the original investigation as worthy of further consideration. This is corroborated by its consistent presence and signal strength in the current analysis of the York brain, sample Y1. This compound was also found consistently across all the other samples excepting H14 and a replicate of H1. It wasn't detected in the DHB matrix control, soil controls or solvent blank. The largest measured *m/z* error was 1.48 ppm in H1b 2 but the majority was less than 1 ppm. The S:N ratios were generally high and resolution was good for all samples. This compound was one of significant interest as it appears to be part of series of related residues with four degrees of unsaturation, differing by $(CH_2)_n$ which include the following: Table 17, Table 19, Table 20, Table 26 and Table 28. The high intensity signal in the mass spectra from Y1a potentially suggests this residue occurs in older brains in higher concentrations. In theory, this may be due to an increase in its production as the brain remains age, or a decrease in the concentration of other chemical species.

Table 16. Summary of signal at *m/z* 530. C_xH_yNO

Calculated *m/z*	530.52954 C36H68NO						
Sample designation + MALDI replicate no.	Measured *m/z*	Error [ppm]	Present	S:N	Intensity	Rel. Int. %	Resolution
Y1a 1	530.52950	0.08	Yes	584.5	80591432	26.8	150582
Y1a 2	530.52935	0.37	Yes	670.0	88561008	32.5	149879
Y1a 3	530.52946	0.16	Yes	640.3	88799592	25.8	150278
Original Heslington	530.52900	1.02	Yes	479.7	50985892	40.9	92430
H1a 1			No				
H1a 2	530.52928	0.50	Yes	19.4	2629318	0.7	166237
H1a 3	530.52915	0.74	Yes	12.4	1794931	0.3	151515
H1b 1	530.52916	0.71	Yes	19.4	2719762	0.3	152767
H1b 2	530.52876	1.48	Yes	9.2	1401022	0.4	174242
H1b 3	530.52898	1.05	Yes	14.6	2052777	0.5	151105
H2a 1	530.52907	0.90	Yes	47.5	6056076	1.1	149760
H2a 2	530.52911	0.82	Yes	44.9	6540455	2.0	151643
H2a 3	530.52916	0.71	Yes	43.2	5249764	1.5	159194
H3a 1	530.52934	0.38	Yes	72.2	10109357	1.8	152973
H3a 2	530.52947	0.13	Yes	67.0	9606948	1.6	149936
H3a 3	530.52919	-1.27	Yes	31.6	4246692	0.6	148517
H4a 1	530.52952	0.05	Yes	329.5	52149244	3.0	148961
H4a 2	530.52966	-0.23	Yes	294.9	47176184	5.4	150696
H4a 3	530.52955	-0.05	Yes	289.2	44428988	5.4	150830
H5a 1	530.52906	0.92	Yes	88.1	10304791	5.4	153278
H5a 2	530.52914	0.76	Yes	113.2	13882830	4.6	152891
H5a 3	530.52917	0.70	Yes	159.2	21021916	2.4	150402
H6a 1	530.52943	0.20	Yes	94.0	12661483	1.7	150295
H6a 2	530.52937	0.32	Yes	80.7	10686020	1.5	148960
H6a 3	530.52935	0.37	Yes	98.1	13335409	1.4	151015
H7a 1	530.52925	0.54	Yes	27.3	3736447	0.9	154999
H7a 2	530.52944	0.19	Yes	26.6	3833124	0.6	153936
H7a 3	530.52920	0.64	Yes	25.1	3490295	0.5	166549
H8a 1	530.52946	0.16	Yes	29.0	4473086	0.8	159428
H8a 2	530.52972	-0.33	Yes	26.3	3742018	0.9	153840
H8a 3	530.52930	0.45	Yes	24.3	3408682	0.7	163767
H9a 1	530.52935	0.35	Yes	41.8	6403425	0.8	148423
H9a 2	530.52954	0.00	Yes	37.0	5782653	0.7	152184
H9a 3	530.52910	0.84	Yes	23.7	3355259	0.7	160992
H10a 1	530.52943	0.21	Yes	18.6	2757147	0.5	159827
H10a 2	530.52933	0.40	Yes	29.2	3724636	1.9	153369
H10a 3	530.52939	0.28	Yes	72.4	10255432	2.8	152398
H11a 1	530.52977	-0.42	Yes	166.3	21992668	9.6	150703
H11a 2	530.52976	-0.41	Yes	109.9	15090892	2.0	147548
H11a 3	530.52949	0.10	Yes	55.8	6452659	5.0	155467
H12a 1	530.52987	-0.61	Yes	180.3	27221394	6.1	151115
H12a 2	530.52988	-0.63	Yes	193.7	29261544	5.9	149304
H12a 3	530.52983	-0.53	Yes	175.8	26898016	6.7	149736
H13aii 1	530.52980	-0.48	Yes	216.6	31399490	8.0	150612
H13aii 2	530.52979	-0.47	Yes	216.7	30056904	7.7	149694
H13aii 3	530.52966	-0.22	Yes	147.9	19187624	3.3	149535
H14a 1			No				
H14a 2			No				
H14a 3			No				
H14bi 1	530.52984	-0.57	Yes	10.9	1987392	0.2	173883
H14bi 2	530.52996	-0.79	Yes	6.1	1220058	0.2	187282
H14bi 3			No				
V1a 1	530.52950	0.08	Yes	52.7	7989736	0.4	149353
V1a 2	530.52954	0.01	Yes	63.9	8886556	1.4	154021
V1a 3	530.52943	0.22	Yes	53.8	7629571	1.6	152212
B1a 1	530.52969	-0.28	Yes	106.6	18547068	3.6	149703
B1a 2	530.52948	0.12	Yes	78.9	11380443	3.7	151030
B1a 3	530.52922	0.61	Yes	72.3	9461597	2.2	149041
DHB 1			No				
DHB 2			No				
DHB 3			No				
Soil 3a 1			No				
Soil 3a 2			No				
Soil 3a 3			No				
Soil 3b 1			No				
Soil 3b 2			No				
Soil 3b 3			No				
Solvent 1			No				
Solvent 2			No				
Solvent 3			No				

Table 17 shows the data for another component that was flagged up during in the initial analysis of the York brain. It was assigned $[C_{37}H_{69}NO] + H^+$, is detected at *m/z* 544, and corresponds to a compound with four double bond equivalents. The largest signal (both by S:N/intensity/relative intensity) was found in the York sample but its detection in the H13 extract is comparable. There were moderately strong signals found in H4, H5, H6, H11 and H12 and B1. The regularity of occurrence indicates that this residue is either present at burial or formed early on in the decomposition process as it appears in the youngest brain samples (Blackpool and Villiers Street). The stronger signal in the York sample suggests it may occur in older brains in higher levels. This may be due to an increase in its formation over time or a decrease in the concentration in other compounds over *m/z* 310 due to their gradual breakdown or leaching into the soil surroundings. The peak is detected in all samples excluding H14a and the DHB matrix control. There are signals at similar *m/z* values in the spectra of the soil extract (Soil 3a replicate 2 and Soil 3b replicate 2). However, the *m/z* values for the signals in the control extract spectra have much larger ppm errors than those in the brain sample spectra. Moreover, the mean measured *m/z* value for this signal in the spectra of brain samples is 544.54519, and that of the controls is 544.54609. The standard deviation of this mean for the brain samples is 0.0003165 and that for the control is 0.00002828. 544.54519+0.000633 = *m/z* 544.54582 whereas 544.54609–0.00005656 = *m/z* 544.54603. There is no overlap of these values for plus or minus 2 standard deviations, suggesting that even though the mass error is below 2 ppm, the compound detected in the soil control is probably not the same as that in the brain extracts.

Table 17. Summary of signal at *m/z* 544. C_xH_yNO

Calculated *m/z*	544.54519 C37H70NO						
Sample designation + MALDI replicate no.	Measured *m/z*	Error [ppm]	Present	S:N	Intensity	Rel. Int. %	Resolution
Y1a 1	544.54527	-0.15	Yes	140.6	20176056	6.7	146451
Y1a 2	544.54511	0.15	Yes	158.8	21758054	8.0	148560
Y1a 3	544.54514	0.09	Yes	142.8	20613106	6.0	147040
Original Heslington	544.54461	1.06	Yes	113.8	12454207	10.0	90161
H1a 1			No				
H1a 2	544.54536	-0.31	Yes	3.0	653862	0.2	123484
H1a 3			No				
H1b 1			No				
H1b 2	544.54492	0.50	Yes	5.1	920416	0.2	182425
H1b 3	544.54527	-0.14	Yes	5.7	985137	0.2	171164
H2a 1	544.54453	1.22	Yes	8.9	1390393	0.3	154266
H2a 2	544.54467	0.95	Yes	9.2	1615743	0.5	162595
H2a 3	544.54502	0.31	Yes	8.4	1262362	0.4	159622
H3a 1	544.54503	0.30	Yes	10.4	1762706	0.3	181524
H3a 2	544.54541	-0.40	Yes	6.7	1258964	0.2	183172
H3a 3			No				
H4a 1	544.54520	-0.02	Yes	41.7	7147420	0.4	149181
H4a 2	544.54548	-0.53	Yes	45.0	7766289	0.9	147006
H4a 3	544.54528	-0.17	Yes	47.4	7833278	0.9	149848
H5a 1	544.54485	0.64	Yes	11.8	1643725	0.9	152202
H5a 2	544.54469	0.92	Yes	15.4	2166416	0.7	169209
H5a 3	544.54481	0.71	Yes	23.0	3365806	0.4	143021
H6a 1	544.54499	0.38	Yes	10.4	1695376	0.2	174408
H6a 2	544.54514	0.10	Yes	8.4	1397108	0.2	166809
H6a 3	544.54506	0.23	Yes	14.8	2309027	0.2	151092
H7a 1	544.54566	-0.62	Yes	7.2	1219644	0.3	151930
H7a 2			No				
H7a 3			No				
H8a 1	544.54548	-0.53	Yes	10.2	1825746	0.3	146944
H8a 2	544.54523	-0.71	Yes	5.4	1033240	0.2	170638
H8a 3	544.54498	0.39	Yes	8.3	1378563	0.3	176309
H9a 1	544.54472	0.86	Yes	8.3	1555361	0.2	129795
H9a 2	544.54529	-0.17	Yes	11.3	2032671	0.2	150567
H9a 3	544.54532	-0.24	Yes	5.8	1060435	0.2	178360
H10a 1	544.54502	0.11	Yes	6.6	1195704	0.2	142683
H10a 2	544.54482	0.69	Yes	5.1	897407	0.5	148255
H10a 3	544.54498	0.39	Yes	16.9	2697258	0.7	145066
H11a 1	544.54552	-0.60	Yes	33.2	4735247	2.1	155552
H11a 2	544.54538	-0.35	Yes	21.1	3224963	0.4	156639
H11a 3	544.54510	0.17	Yes	7.3	1092411	0.8	170320
H12a 1	544.54563	-0.80	Yes	48.6	7830229	1.7	151210
H12a 2	544.54567	-0.87	Yes	50.9	8189959	1.7	147947
H12a 3	544.54566	-0.87	Yes	65.1	10517305	2.6	146639
H13aii 1	544.54559	-0.73	Yes	165.5	24829956	6.3	146215
H13aii 2	544.54559	-0.74	Yes	131.8	18941330	4.9	144905
H13aii 3	544.54544	-0.45	Yes	100.4	13423244	2.3	149392
H14a 1			No				
H14a 2			No				
H14a 3			No				
H14bi 1	544.54556	-0.67	Yes	14.8	2668246	0.3	160560
H14bi 2	544.54574	-1.00	Yes	10.9	1967243	0.3	151185
H14bi 3			No				
V1a 1	544.54526	-0.13	Yes	116.9	17912242	0.8	148024
V1a 2	544.54524	-0.09	Yes	121.8	17098916	2.7	146678
V1a 3	544.54515	0.07	Yes	114.5	16319851	3.5	148890
B1a 1	544.54547	-0.51	Yes	41.9	7823133	1.5	146739
B1a 2	544.54515	0.08	Yes	31.5	4870244	1.6	148014
B1a 3	544.54468	0.95	Yes	23.4	3327673	0.8	146577
DHB 1			No				
DHB 2			No				
DHB 3			No				
Soil 3a 1			No				
Soil 3a 2	544.54607	-1.61	No	4.5	1083350	0.1	190946
Soil 3a 3			No				
Soil 3b 1			No				
Soil 3b 2	544.54611	-1.69	No	7.9	1698374	0.1	170408
Soil 3b 3			No				
Solvent 1			No				
Solvent 2			No				
Solvent 3			No				

The peak detected at *m/z* 556 shown in Table 18 was assigned $[C_{38}H_{69}NO] + H^+$ for a species with five double bond equivalents. As the table shows, this was a very intense signal in the spectrum of the York sample extracts (both original and current) and it was detected in all brain sample extracts except H14a, although less consistently in the sample replicates than some of the already described peaks. It was found in all samples of all age ranges and the strength of the signal in the oldest sample shows similar trends to those for *m/z* 544, Table 16. This compound also appears to be part of series of related residues with five degrees of unsaturation, differing by $(CH_2)_n$ which also includes Table 22 and Table 25.

Table 18. Summary of signal at *m/z* 556. C_xH_yNO

Calculated *m/z*	556.54519	C38H70NO					
Sample designation + MALDI replicate no.	Measured *m/z*	Error [ppm]	Present	S:N	Intensity	Rel. Int. %	Resolution
Y1a 1	556.54531	-0.21	Yes	190.3	27592560	9.2	143035
Y1a 2	556.54509	0.18	Yes	169.7	23537144	8.6	143893
Y1a 3	556.54518	0.03	Yes	185.9	27141152	7.9	144101
Original Heslington	556.54448	1.28	Yes	92.1	10123522	8.1	89172
H1a 1			No				
H1a 2	556.54508	0.19	Yes	7.9	1269616	0.3	167708
H1a 3			No				
H1b 1			No				
H1b 2	556.54484	0.64	Yes	10.5	1605118	0.4	167777
H1b 3	556.54579	-1.07	Yes	6.2	1063330	0.3	144240
H2a 1			No				
H2a 2	556.54496	0.42	Yes	6.5	1247567	0.4	173378
H2a 3			No				
H3a 1	556.54548	-0.52	Yes	10.1	1732414	0.3	154700
H3a 2	556.54497	0.40	Yes	9.6	1708312	0.3	158342
H3a 3			No				
H4a 1	556.54528	-0.16	Yes	46.2	8047631	0.5	144983
H4a 2	556.54553	-0.61	Yes	53.1	9301514	1.1	143896
H4a 3	556.54528	-0.17	Yes	54.8	9170112	1.1	145404
H5a 1	556.54448	1.29	Yes	8.8	1304689	0.7	163183
H5a 2	556.54504	0.28	Yes	12.3	1805993	0.6	154030
H5a 3	556.54484	0.63	Yes	21.1	3158168	0.4	155081
H6a 1	556.54545	-0.46	Yes	11.4	1854317	0.3	168865
H6a 2	556.54504	0.28	Yes	11.5	1835675	0.2	162426
H6a 3	556.54512	0.14	Yes	14.8	2345594	0.2	145198
H7a 1	556.54526	-0.12	Yes	7.2	1237168	0.3	157223
H7a 2	556.54527	-0.15	Yes	10.2	1720146	0.3	177413
H7a 3	556.54523	-0.07	Yes	9.5	1554178	0.2	171563
H8a 1	556.54531	-0.21	Yes	7.4	1432542	0.2	138074
H8a 2	556.54543	-0.43	Yes	10.1	1683020	0.4	154129
H8a 3	556.54523	-0.07	Yes	7.9	1353104	0.3	145502
H9a 1	556.54525	-0.11	Yes	5.6	1170813	0.1	163380
H9a 2	556.54519	0.00	Yes	6.7	1356580	0.2	182715
H9a 3	556.54523	-0.06	Yes	5.9	1086777	0.2	182607
H10a 1			No				
H10a 2			No				
H10a 3	556.54539	-0.35	Yes	10.4	1794935	0.5	151499
H11a 1	556.54552	-0.59	Yes	31.0	4506060	2.0	147499
H11a 2	556.54562	-0.77	Yes	16.1	2554999	0.3	148580
H11a 3	556.54512	0.13	Yes	6.6	1017594	0.8	182675
H12a 1	556.54567	-0.85	Yes	34.5	5756682	1.3	144336
H12a 2	556.54562	-0.77	Yes	35.9	5985424	1.2	148229
H12a 3	556.54567	-0.85	Yes	40.1	6729918	1.7	146088
H13aii 1	556.54561	-0.76	Yes	82.3	12706139	3.2	145014
H13aii 2	556.54550	-0.55	Yes	64.9	9617823	2.5	142674
H13aii 3	556.54543	-0.43	Yes	41.7	5815345	1.0	155588
H14a 1			No				
H14a 2			No				
H14a 3			No				
H14bi 1	556.54556	-0.66	Yes	6.7	1417965	0.2	164571
H14bi 2	556.54477	0.76	Yes	4.3	993245	0.2	145133
H14bi 3			No				
V1a 1	556.54520	-0.02	Yes	42.6	6837569	0.3	147813
V1a 2	556.54530	-0.20	Yes	35.2	5227246	0.8	144314
V1a 3	556.54512	1.57	Yes	27.5	4210110	0.9	153397
B1a 1	556.54553	-0.61	Yes	53.6	10167584	2.0	141766
B1a 2	556.54523	-0.08	Yes	42.6	6576177	2.1	144047
B1a 3	556.54495	0.44	Yes	21.6	3136757	0.7	148382
DHB 1			No				
DHB 2			No				
DHB 3			No				
Soil 3a 1			No				
Soil 3a 2			No				
Soil 3a 3			No				
Soil 3b 1			No				
Soil 3b 2			No				
Soil 3b 3			No				
Solvent 1			No				
Solvent 2			No				
Solvent 3			No				

Table 19 shows the detection of a signal at *m/z* 558. This was assigned to a component with four double bond equivalents, and empirical formula $[C_{38}H_{71}NO] + H^+$. This table shows very similar trends to those for the two preceding components (Table 17 and Table 18) and so similar comments can be applied. It is again detected in all the brain samples barring H14a (and is only detected in one replicate of H1) and is absent from the controls. There is a moderate S:N and intensity to signals from samples H4, H5 H12, H13, V1 and B1.

Table 19. Summary of signal at *m/z* 558. C_xH_yNO

Calculated *m/z*	558.56084	C38H72NO					
Sample designation + MALDI replicate no.	Measured *m/z*	Error [ppm]	Present	S:N	Intensity	Rel. Int. %	Resolution
Y1a 1	558.56085	-0.01	Yes	1110.8	159625264	53.1	142865
Y1a 2	558.56067	0.31	Yes	1090.3	149629296	55.0	143243
Y1a 3	558.56077	0.12	Yes	1088.7	157439088	45.7	143617
Original Heslington	558.56026	1.05	Yes	873.1	94157008	75.6	87715
H1a 1			No				
H1a 2	558.56077	0.12	Yes	6.1	1049438	0.3	174316
H1a 3			No				
H1b 1	558.56050	0.31	Yes	11.1	1727585	0.2	128351
H1b 2	558.56087	-0.04	Yes	8.8	1392002	0.4	160831
H1b 3	558.56030	0.96	Yes	10.7	1617816	0.4	158563
H2a 1	558.56029	0.99	Yes	37.1	4919893	0.9	149422
H2a 2	558.56041	0.77	Yes	27.7	4319181	1.3	151084
H2a 3	558.56039	0.82	Yes	34.3	4317231	1.2	155241
H3a 1	558.56074	0.18	Yes	35.0	5264343	1.0	149480
H3a 2	558.56078	0.11	Yes	33.9	5217418	0.9	135438
H3a 3	558.56060	0.43	Yes	19.6	2826460	0.4	151724
H4a 1	558.56082	0.05	Yes	297.4	50143060	2.9	142078
H4a 2	558.56106	-0.39	Yes	307.8	52394160	6.0	142616
H4a 3	558.56088	-0.08	Yes	271.3	44152576	5.3	143131
H5a 1	558.56036	0.87	Yes	64.6	7783827	4.1	144229
H5a 2	558.56038	0.82	Yes	83.5	10586600	3.5	146427
H5a 3	558.56041	0.78	Yes	140.6	19303958	2.2	142235
H6a 1	558.56071	0.24	Yes	80.2	11257412	1.5	144463
H6a 2	558.56074	0.19	Yes	71.1	9783883	1.3	145019
H6a 3	558.56068	0.29	Yes	78.5	11151778	1.2	144206
H7a 1	558.56051	0.59	Yes	20.0	2898578	0.7	148982
H7a 2	558.56073	0.20	Yes	19.5	2999906	0.5	152111
H7a 3	558.56058	0.47	Yes	10.8	1725413	0.3	167098
H8a 1	558.56074	0.19	Yes	29.1	4702760	0.8	149772
H8a 2	558.56088	-0.07	Yes	25.0	3714770	0.9	146374
H8a 3	558.56064	0.35	Yes	21.6	3171967	0.6	157060
H9a 1	558.56080	0.07	Yes	32.4	5300551	0.7	145983
H9a 2	558.56077	0.13	Yes	31.4	5216105	0.6	149792
H9a 3	558.56053	0.55	Yes	29.7	4276939	0.9	147776
H10a 1	558.56074	0.18	Yes	23.3	3509045	0.6	145465
H10a 2	558.56050	0.62	Yes	20.8	2807935	1.4	152314
H10a 3	558.56062	0.40	Yes	43.0	6469685	1.8	144063
H11a 1	558.56120	-0.64	Yes	71.7	10024988	4.4	145543
H11a 2	558.56104	-0.35	Yes	45.1	6629130	0.9	146484
H11a 3	558.56065	0.35	Yes	17.6	2260702	1.7	166019
H12a 1	558.56121	-0.66	Yes	221.5	35195940	7.8	142736
H12a 2	558.56126	-0.75	Yes	197.5	31446502	6.4	141796
H12a 3	558.56120	-0.64	Yes	180.5	29143880	7.2	141578
H13aii 1	558.56117	-0.58	Yes	150.9	23037694	5.8	143284
H13aii 2	558.56120	-0.64	Yes	136.8	19940652	5.1	143465
H13aii 3	558.56099	-0.26	Yes	89.7	12156266	2.1	143851
H14a 1			No				
H14a 2			No				
H14a 3			No				
H14bi 1	558.56121	-0.66	Yes	11.8	2241476	0.2	150275
H14bi 2	558.56064	0.37	Yes	12.1	2192303	0.3	147320
H14bi 3			No				
V1a 1	558.56081	0.06	Yes	93.7	14658965	0.7	140067
V1a 2	558.56079	0.10	Yes	102.0	14570216	2.3	139146
V1a 3	558.56072	0.22	Yes	96.6	13991797	3.0	142003
B1a 1	558.56102	-0.33	Yes	174.8	32371388	6.3	142334
B1a 2	558.56077	0.13	Yes	139.1	20781066	6.8	143432
B1a 3	558.56054	0.54	Yes	76.8	10386214	2.4	146367
DHB 1			No				
DHB 2			No				
DHB 3			No				
Soil 3a 1			No				
Soil 3a 2			No				
Soil 3a 3			No				
Soil 3b 1			No				
Soil 3b 2			No				
Soil 3b 3			No				
Solvent 1			No				
Solvent 2			No				
Solvent 3			No				

Table 20 summarises the data for the peak at *m/z* 586, assigned to a component with four double bond equivalents, and empirical formula $[C_{40}H_{75}NO] + H^+$. In the original analysis of the York brain this peak was considered worth further investigation. The relative intensity of the peaks in the mass spectra of the current project's extract spectral replicates also indicate this component is of significance. It is again detected in all the brain sample extracts barring H1a and H14. It is not detected as consistently across all the replicates of H1b, H2a, H8, H9, H10 and H11. There is a moderate S:N and intensity to signals from samples H4, H5 H12, H13, V1 and B1. The detection in the soil sample has an error of over 2 ppm and is thus not likely to represent the same component.

As well as high intensity and S:N in the spectra of the York sample extract, the mass spectra of the most modern brain extracts, V1 and B1, also have evidence of this component.

Table 20. Summary of signal at *m/z* 586. C_xH_yNO

Calculated *m/z*	586.59214	C40H76NO					
Sample designation + MALDI replicate no.	Measured *m/z*	Error [ppm]	Present	S:N	Intensity	Rel. Int. %	Resolution
Y1a 1	586.59197	0.29	Yes	68.5	10490418	3.5	136664
Y1a 2	586.59188	0.46	Yes	61.4	8975159	3.3	139511
Y1a 3	586.59200	0.24	Yes	65.4	10080365	2.9	138362
Original Heslington	586.59153	1.05	Yes	81.9	9352824	7.5	82856
H1a 1			No				
H1a 2			No				
H1a 3			No				
H1b 1	586.59172	0.72	Yes	9.4	1541106	0.2	153914
H1b 2	586.59184	0.52	Yes	4.6	886641	0.2	126937
H1b 3			No				
H2a 1	586.59151	1.09	Yes	11.0	1689596	0.3	160726
H2a 2	586.59183	0.53	Yes	6.1	1216948	0.4	169246
H2a 3			No				
H3a 1	586.59199	0.26	Yes	14.7	2416219	0.4	130516
H3a 2	586.59212	0.03	Yes	12.3	2124965	0.3	150307
H3a 3	586.59211	0.06	Yes	9.4	1528387	0.2	166201
H4a 1	586.59196	0.32	Yes	30.1	5459820	0.3	143370
H4a 2	586.59224	-0.16	Yes	36.1	6644937	0.8	139500
H4a 3	586.59210	0.06	Yes	37.3	6516075	0.8	137172
H5a 1	586.59199	0.27	Yes	4.7	837641	0.4	201918
H5a 2	586.59153	1.05	Yes	10.2	1568340	0.5	168872
H5a 3	586.59165	0.84	Yes	16.6	2590945	0.3	144839
H6a 1	586.59161	0.91	Yes	16.7	2622870	0.4	131475
H6a 2	586.59206	0.15	Yes	15.5	2397025	0.3	159087
H6a 3	586.59188	0.45	Yes	20.1	3121493	0.3	153147
H7a 1	586.59165	0.83	Yes	10.8	1737815	0.4	159140
H7a 2	586.59205	0.15	Yes	12.7	2107650	0.3	139778
H7a 3	586.59189	0.43	Yes	7.6	1322478	0.2	156807
H8a 1	586.59189	0.43	Yes	5.0	1084959	0.2	183098
H8a 2			No				
H8a 3			No				
H9a 1			No				
H9a 2	586.59184	0.51	Yes	6.0	1265257	0.1	181108
H9a 3	586.59127	1.49	Yes	6.5	1184628	0.3	175493
H10a 1			No				
H10a 2			No				
H10a 3	586.59157	0.98	Yes	13.9	2334757	0.6	141880
H11a 1	586.59254	-0.67	Yes	15.7	2485167	1.1	155574
H11a 2	586.59202	0.22	Yes	10.2	1767988	0.2	149860
H11a 3			No				
H12a 1	586.59252	-0.65	Yes	27.6	4779750	1.1	143270
H12a 2	586.59259	-0.76	Yes	24.7	4300603	0.9	147667
H12a 3	586.59248	-0.57	Yes	23.0	4085564	1.0	134904
H13aii 1	586.59224	-0.16	Yes	26.3	4410983	1.1	135998
H13aii 2	586.59241	-0.46	Yes	33.0	5167604	1.3	128464
H13aii 3	586.59232	-0.31	Yes	23.3	3465378	0.6	142066
H14a 1			No				
H14a 2			No				
H14a 3			No				
H14bi 1			No				
H14bi 2			No				
H14bi 3			No				
V1a 1	586.59208	0.11	Yes	60.3	9784428	0.4	133513
V1a 2	586.59212	0.05	Yes	62.0	9273187	1.5	137155
V1a 3	586.59189	0.43	Yes	63.2	9511151	2.0	135585
B1a 1	586.59230	-0.27	Yes	39.5	7665599	1.5	139725
B1a 2	586.59201	0.22	Yes	31.3	4981626	1.6	141208
B1a 3	586.59173	0.71	Yes	29.9	4268915	1.0	139506
DHB 1			No				
DHB 2			No				
DHB 3			No				
Soil 3a 1			No				
Soil 3a 2			No				
Soil 3a 3			No				
Soil 3b 1			No				
Soil 3b 2	586.59342	-2.18	No	4.4	1185460	0.1	148197
Soil 3b 3			No				
Solvent 1			No				
Solvent 2			No				
Solvent 3			No				

Table 21 summarises details of the peak observed at *m/z* 726 in the spectra. This was assigned a composition of $[C_{50}H_{95}NO] + H^+$ which has a high degree of saturation with only three double bond equivalents. This peak was noted in the original mass spectra of the York brain extract as belonging to the hydrocarbon chains with limited functionality. It occurs in the spectra of the new York sample extracts and is observed in the data from samples from across all sites, but only at low relative intensities within the other sample spectra. It was not detected within the H14a extract.

The peaks at similar *m/z* values in the soil and solvent sample have an error of over 2 ppm for this empirical formula, and so it is unlikely that these signals are due to the same chemical compound.

Table 21. Summary of signal at *m/z* 726. C_xH_yNO

Calculated *m/z*	726.74844	C50H96NO					
Sample designation + MALDI replicate no.	Measured *m/z*	Error [ppm]	Present	S:N	Intensity	Rel. Int. %	Resolution
Y1a 1	726.74855	0.13	Yes	188.1	32257322	10.7	110694
Y1a 2	726.74827	0.52	Yes	190.1	30493344	11.2	110574
Y1a 3	726.74844	0.27	Yes	201.2	34526444	10	110691
Original Heslington	726.74802	0.86	Yes	34.2	4418276	3.5	71627
H1a 1	726.74857	0.10	Yes	13.1	2252367	0.2	117629
H1a 2	726.74819	0.62	Yes	11.1	1851458	0.5	124308
H1a 3	726.74742	1.68	Yes	13	2006036	0.3	114214
H1b 1	726.7478	1.15	Yes	32.2	4881003	0.6	110264
H1b 2	726.74834	0.42	Yes	24.8	3702691	1	107434
H1b 3	726.74805	0.82	Yes	21.8	3264448	0.8	108939
H2a 1	726.74765	1.36	Yes	24.3	3530924	0.7	116154
H2a 2	726.74758	1.47	Yes	26.9	4322752	1.3	112665
H2a 3	726.74784	1.10	Yes	23.8	3334535	0.9	119312
H3a 1	726.74858	0.09	Yes	11.6	1966484	0.4	120995
H3a 2	726.74909	-0.61	Yes	10.8	1914474	0.3	117605
H3a 3	726.74797	0.93	Yes	6.1	1118661	0.1	141724
H4a 1	726.7484	0.33	Yes	46	8198388	0.5	112737
H4a 2	726.74873	-0.12	Yes	55.8	11040459	1.3	115034
H4a 3	726.74857	0.10	Yes	68.2	12378662	1.5	110288
H5a 1	726.74784	1.11	Yes	30.1	4000006	2.1	113171
H5a 2	726.74816	0.66	Yes	48.0	6622318	2.2	114753
H5a 3	726.74784	1.11	Yes	57.7	8518377	1.0	112878
H6a 1			No				
H6a 2	726.74856	0.11	Yes	2.9	708902	0.1	194568
H6a 3			No				
H7a 1	726.74819	0.62	Yes	9.7	1723820	0.4	107317
H7a 2	726.74872	-0.11	Yes	12.7	2284632	0.4	113296
H7a 3	726.74805	0.82	Yes	9.1	1637223	0.2	129032
H8a 1	726.74873	-0.11	Yes	13.6	2382552	0.4	123778
H8a 2	726.74853	0.15	Yes	15.3	2528610	0.6	119258
H8a 3	726.74891	-0.37	Yes	9.4	1609829	0.3	102010
H9a 1	726.74842	0.31	Yes	16.8	2812948	0.3	120668
H9a 2	726.74835	0.40	Yes	16.0	2692511	0.3	118304
H9a 3	726.74907	-0.59	Yes	5.5	1055526	0.2	102715
H10a 1			No				
H10a 2			No				
H10a 3	726.74777	1.20	Yes	7.5	1409001	0.4	120770
H11a 1	726.74896	-0.44	Yes	121.3	18688024	8.2	110217
H11a 2	726.74901	-0.50	Yes	66.8	10462792	1.4	111333
H11a 3	726.74852	0.17	Yes	37.6	4793903	3.7	113711
H12a 1	726.74923	-0.81	Yes	66.3	11558565	2.6	113415
H12a 2	726.74922	-0.79	Yes	58.9	10101910	2.1	111972
H12a 3	726.74919	-0.75	Yes	63.5	11224271	2.8	112780
H13aii 1	726.74908	-0.60	Yes	292.6	50483152	12.8	110154
H13aii 2	726.74907	-0.59	Yes	233.9	37342444	9.6	110158
H13aii 3	726.74891	-0.36	Yes	168.2	25222694	4.3	108814
H14a 1			No				
H14a 2			No				
H14a 3			No				
H14bi 1	726.74881	-0.23	Yes	8.4	1692047	0.2	123020
H14bi 2	726.7489	-0.36	Yes	7.7	1479274	0.2	118878
H14bi 3			No				
V1a 1	726.74852	0.17	Yes	278.5	47007488	2.1	110513
V1a 2	726.74855	0.12	Yes	283.1	47039084	7.5	109457
V1a 3	726.74838	0.37	Yes	249	39843428	8.5	109751
B1a 1	726.74884	-0.28	Yes	34.1	6204785	1.2	115516
B1a 2	726.74842	0.31	Yes	18.8	3082339	1	116442
B1a 3	726.74755	1.51	Yes	16.3	2470869	0.6	102186
DHB 1			No				
DHB 2			No				
DHB 3			No				
Soil 3a 1	726.75157	2.19	No	4.8	1483061	0.2	127295
Soil 3a 2			No				
Soil 3a 3			No				
Soil 3b 1			No				
Soil 3b 2	726.75132	2.55	No	7.7	2138567	0.1	113853
Soil 3b 3			No				
Solvent 1			No				
Solvent 2			No				
Solvent 3			No				

Table 22 summarises the results for the peak at *m/z* 752. This was assigned an empirical composition of $[C_{52}H_{97}NO] + H^+$, for a species with 5 double bond equivalents. The signal was detected in all sample spectra except that of H14 (a and b) and not in any of the matrix, soil or solvent controls. The signal (both S:N and intensity) was particularly high in sample H13, but was also found in the York replicates, H4, H5, H11, H12, V1 and B1. It is present across samples of all age ranges and so appears a persistent product of degradation. Resolution is good across spectra, S:N is generally good and error in ppm is less than 2 ppm.

Table 22. Summary of signal at *m/z* 752. C_xH_yNO

Calculated *m/z*	752.7649	C52H98NO					
Sample designation + MALDI replicate no.	Measured *m/z*	Error [ppm]	Present	S:N	Intensity	Rel. Int. %	Resolution
Y1a 1	752.76433	-0.05	Yes	426.7	73668544	24.5	105567
Y1a 2	752.76402	0.36	Yes	420.9	67828184	24.9	106701
Y1a 3	752.76421	0.10	Yes	443.9	76703072	22.3	106317
Original Heslington	752.76361	0.91	Yes	60.3	7758606	6.2	66434
H1a 1	752.76475	-0.61	Yes	8.8	1619584	0.2	120356
H1a 2	752.76368	0.81	Yes	13.3	2173432	0.5	117617
H1a 3	752.76320	1.45	Yes	11.4	1797412	0.3	122605
H1b 1	752.76328	1.35	Yes	31.5	4816499	0.6	106867
H1b 2	752.76384	0.60	Yes	25.9	3885211	1.0	108995
H1b 3	752.76356	0.98	Yes	28.4	4187793	1.0	107836
H2a 1	752.76346	1.11	Yes	12.8	2022146	0.4	117214
H2a 2	752.76374	0.74	Yes	13.2	2273174	0.7	118379
H2a 3	752.76313	1.55	Yes	10.7	1677798	0.5	122242
H3a 1	752.76413	0.22	Yes	22.2	3471432	0.6	107427
H3a 2	752.76443	-0.18	Yes	18.2	3003837	0.5	116743
H3a 3	752.76334	1.26	Yes	6.1	1130954	0.1	136898
H4a 1	752.76432	-0.04	Yes	135.0	23369060	1.4	106931
H4a 2	752.76469	-0.52	Yes	189.9	37208404	4.3	106641
H4a 3	752.76435	-0.08	Yes	216.4	38957276	4.7	105896
H5a 1	752.76349	1.07	Yes	72.2	9313175	4.9	107654
H5a 2	752.76368	0.81	Yes	114.9	15633533	5.1	107344
H5a 3	752.76362	0.89	Yes	156.2	22740582	2.6	107626
H6a 1	752.76422	0.10	Yes	12.9	2152843	0.3	119309
H6a 2	752.76413	0.22	Yes	10.8	1815405	0.2	127140
H6a 3	752.76412	0.24	Yes	10.0	1725341	0.2	120773
H7a 1	752.76419	0.14	Yes	13.5	2302561	0.6	118180
H7a 2	752.76384	0.60	Yes	23.0	3912797	0.6	109845
H7a 3	752.76379	0.67	Yes	13.4	2292341	0.3	109801
H8a 1	752.76408	0.29	Yes	34.1	5497035	0.9	109311
H8a 2	752.76417	0.16	Yes	25.3	3992475	0.9	110081
H8a 3	752.76422	0.10	Yes	22.9	3479412	0.7	107879
H9a 1	752.76422	0.10	Yes	25.7	4099817	0.5	113987
H9a 2	752.76417	0.16	Yes	26.0	4150653	0.5	105196
H9a 3	752.76384	0.60	Yes	14.4	2294619	0.5	110249
H10a 1	752.76380	0.65	Yes	10.6	1843016	0.3	118218
H10a 2	752.76377	0.70	Yes	9.3	1487996	0.8	141662
H10a 3	752.76399	0.40	Yes	18.6	3009613	0.8	113704
H11a 1	752.76478	-0.65	Yes	284.8	43903752	19.2	105371
H11a 2	752.76467	-0.50	Yes	137.2	21398716	2.8	106700
H11a 3	752.76413	0.21	Yes	77.2	9624112	7.4	106374
H12a 1	752.76501	-0.95	Yes	183.0	31192322	6.9	106398
H12a 2	752.76507	-1.03	Yes	179.1	29878288	6.1	107225
H12a 3	752.76495	-0.87	Yes	172.4	29808460	7.4	106172
H13aii 1	752.76490	-0.81	Yes	765.2	132357272	33.5	106471
H13aii 2	752.76490	-0.80	Yes	602.9	96410632	24.8	105206
H13aii 3	752.76461	-0.42	Yes	434.8	65290308	11.1	106389
H14a 1			No				
H14a 2			No				
H14a 3			No				
H14bi 1			No				
H14bi 2			No				
H14bi 3			No				
V1a 1	752.76433	-0.05	Yes	115.5	19818032	0.9	107190
V1a 2	752.76432	-0.03	Yes	124.9	21224710	3.4	106302
V1a 3	752.76408	0.29	Yes	104.2	16995128	3.6	107427
B1a 1	752.76463	-0.45	Yes	111.4	19365608	3.8	106561
B1a 2	752.76416	0.17	Yes	71.0	10748262	3.5	107421
B1a 3	752.76386	0.58	Yes	35.2	4983908	1.2	111195
DHB 1			No				
DHB 2			No				
DHB 3			No				
Soil 3a 1			No				
Soil 3a 2			No				
Soil 3a 3			No				
Soil 3b 1			No				
Soil 3b 2			No				
Soil 3b 3			No				
Solvent 1			No				
Solvent 2			No				
Solvent 3			No				

This signal at *m/z* 754 was very strong in the spectra of the Villiers Street sample replicates and also in H13 and Y1a extract spectra, as shown in Table 23. The *m/z* was assigned the empirical formula $[C_{52}H_{99}NO] + H^+$ which has 3 double bond equivalents. In the sample spectra the relative intensities and S:N for this *m/z* are not strong in H1, H3, H6, H7, H8, H9, H10 and H14b but it is only undetected in H14a. Although there were signals present in the soil controls at similar *m/z* values, these were over 2.5 ppm from the calculated value, and so are not likely to be from the same compound. This component is a regular presence across all sample ages and sites.

Table 23. Summary of signal at *m/z* 754. C_xH_yNO

Calculated *m/z*	754.77994	C52H100NO					
Sample designation + MALDI replicate no.	Measured *m/z*	Error [ppm]	Present	S:N	Intensity	Rel. Int. %	Resolution
Y1a 1	754.77980	0.19	Yes	490.6	84655504	28.2	105069
Y1a 2	754.77955	0.52	Yes	469.3	75596128	27.8	105439
Y1a 3	754.77973	0.28	Yes	524.4	90554136	26.3	105889
Original Heslington	754.77971	0.31	Yes	67.5	8652561	6.9	69242
H1a 1	754.77966	0.37	Yes	32.5	5086482	0.5	112584
H1a 2	754.77945	0.66	Yes	32.7	4871734	1.2	103651
H1a 3	754.77916	1.04	Yes	35.2	4926191	0.7	110306
H1b 1	754.77911	1.11	Yes	91.4	13381085	1.6	107191
H1b 2	754.77914	1.07	Yes	83.7	11830387	3.1	107114
H1b 3	754.77885	1.45	Yes	67.5	9505623	2.2	104517
H2a 1	754.77887	1.42	Yes	85.1	11662285	2.2	107772
H2a 2	754.77889	1.39	Yes	82.1	12449746	3.8	105555
H2a 3	754.77921	0.97	Yes	69.0	9183530	2.6	106226
H3a 1	754.77974	0.27	Yes	32.8	4982619	0.9	108321
H3a 2	754.78013	-0.25	Yes	35.0	5480909	0.9	103353
H3a 3	754.77963	0.41	Yes	22.4	3304082	0.4	112079
H4a 1	754.77976	0.24	Yes	111.8	19415652	1.1	107738
H4a 2	754.78002	-0.10	Yes	168.8	33123336	3.8	103464
H4a 3	754.77983	0.15	Yes	180.7	32590134	3.9	105319
H5a 1	754.77893	1.35	Yes	49.5	6483523	3.4	112279
H5a 2	754.77917	1.03	Yes	73.0	10049272	3.3	107497
H5a 3	754.77914	1.07	Yes	103.2	15139778	1.7	106352
H6a 1	754.77967	0.36	Yes	51.5	7661674	1.0	105992
H6a 2	754.77963	0.42	Yes	36.8	5419710	0.7	107452
H6a 3	754.77945	0.65	Yes	44.7	6593364	0.7	108663
H7a 1	754.77983	0.15	Yes	14.8	2492023	0.6	116360
H7a 2	754.77962	0.43	Yes	18.7	3245657	0.5	114700
H7a 3	754.77937	0.76	Yes	17.6	2906985	0.4	108057
H8a 1	754.77973	0.29	Yes	42.9	6827325	1.2	108756
H8a 2	754.77987	0.10	Yes	32.6	5049735	1.2	104566
H8a 3	754.77951	0.58	Yes	37.4	5470523	1.1	108442
H9a 1	754.77974	0.26	Yes	51.1	7839163	1.0	107956
H9a 2	754.77967	0.37	Yes	52.4	8036458	0.9	105481
H9a 3	754.77935	0.78	Yes	23.5	3550127	0.8	110000
H10a 1	754.77972	0.30	Yes	8.6	1545106	0.3	126633
H10a 2	754.77936	0.77	Yes	7.9	1303633	0.7	127930
H10a 3	754.77951	0.58	Yes	14.9	2480514	0.7	111549
H11a 1	754.78030	-0.48	Yes	306.2	47180304	20.6	104591
H11a 2	754.78026	-0.42	Yes	173.2	26921368	3.5	105226
H11a 3	754.77977	0.23	Yes	100.1	12395763	9.5	105932
H12a 1	754.78051	-0.75	Yes	208.7	35527060	7.9	105727
H12a 2	754.78053	-0.78	Yes	213.5	35546456	7.2	105171
H12a 3	754.78049	-0.73	Yes	204.2	35230968	8.8	106881
H13aii 1	754.78039	-0.59	Yes	694.6	120171928	30.4	104979
H13aii 2	754.78041	-0.62	Yes	566.9	90670336	23.3	104627
H13aii 3	754.78020	-0.34	Yes	398.4	59863876	10.2	105733
H14a 1			No				
H14a 2			No				
H14a 3			No				
H14bi 1	754.78025	-0.40	Yes	13.8	2553951	0.3	114424
H14bi 2	754.78107	-1.50	Yes	5.0	1084193	0.2	130873
H14bi 3			No				
V1a 1	754.77981	0.17	Yes	1752.4	295897120	13.5	105688
V1a 2	754.77984	0.13	Yes	1819.1	304607584	48.4	105580
V1a 3	754.77968	0.35	Yes	1527.4	244459808	52.2	105801
B1a 1	754.78010	-0.21	Yes	115.9	20149168	3.9	106195
B1a 2	754.77979	0.21	Yes	79.8	12033674	3.9	104920
B1a 3	754.77943	0.68	Yes	58.9	8132372	1.9	108494
DHB 1			No				
DHB 2			No				
DHB 3			No				
Soil 3a 1	754.78185	-2.53	No	5.3	1610655	0.2	115689
Soil 3a 2	754.78293	-3.96	No	4.3	1386710	0.1	114284
Soil 3a 3	754.78289	-3.91	No	4.0	1270467	0.3	144028
Soil 3b 1	754.78347	-4.67	No	7.1	2077755	0.3	110540
Soil 3b 2	754.78250	-3.39	No	7.7	2184976	0.1	114641
Soil 3b 3			No				
Solvent 1			No				
Solvent 2			No				
Solvent 3			No				

Table 24 summarises the results of the mass spectra in respect to the signal at *m/z* 778. The assigned compound $[C_{54}H_{99}NO] + H^+$ has six double bond equivalents and is most strongly detected in the extracts of H13 and Y1. It was not detected in the sample extracts from H2, H14 (a or b) or any of the controls. The S:N and relative signal intensity in the original York analysis are moderate, as they are in extracts of H4, H5, H11 and H12. In the other samples where this component is detected, the relative intensities are much lower, but resolution remains good.

Table 24. Summary of signal at *m/z* 778. C_xH_yNO

Calculated *m/z*	778.77994 C54H100NO						
Sample designation + MALDI replicate no.	Measured *m/z*	Error [ppm]	Present	S:N	Intensity	Rel. Int. %	Resolution
Y1a 1	778.77990	0.06	Yes	390.1	67360424	22.4	102664
Y1a 2	778.77962	0.41	Yes	365.8	58931428	21.6	102333
Y1a 3	778.77980	0.18	Yes	408.2	70545168	20.5	102638
Original Heslington	778.77916	1.01	Yes	62.3	8010677	6.4	63985
H1a 1			No				
H1a 2	778.78036	-0.54	Yes	7.0	1295196	0.3	129064
H1a 3	778.81537	1.23	Yes	34.4	4832168	0.7	106708
H1b 1	778.77914	1.03	Yes	16.0	2606084	0.3	113727
H1b 2	778.77962	0.41	Yes	8.3	1465614	0.4	101770
H1b 3	778.77849	1.86	Yes	13.0	2090258	0.5	86795
H2a 1			No				
H2a 2			No				
H2a 3			No				
H3a 1	778.81601	1.33	Yes	18.3	2918281	0.5	100553
H3a 2	778.78017	-0.29	Yes	5.7	1167948	0.2	112514
H3a 3	778.81584	1.38	Yes	10.8	1758802	0.2	115267
H4a 1	778.77986	0.10	Yes	174.1	29999554	1.8	102322
H4a 2	778.78022	-0.35	Yes	258.3	50702156	5.8	101725
H4a 3	778.77997	-0.03	Yes	279.5	50453408	6.1	102511
H5a 1	778.77905	1.14	Yes	75.9	9857823	5.2	104703
H5a 2	778.77921	0.94	Yes	126.4	17326014	5.7	103056
H5a 3	778.77916	1.00	Yes	178.2	26043088	3.0	102863
H6a 1	778.77887	1.38	Yes	10.2	1778931	0.2	110465
H6a 2	778.77916	1.01	Yes	3.9	861289	0.1	172087
H6a 3	778.77846	1.91	Yes	6.9	1284320	0.1	117092
H7a 1	778.77986	0.11	Yes	5.6	1156241	0.3	149365
H7a 2	778.77911	1.07	Yes	5.8	1246278	0.2	132704
H7a 3	778.77968	0.33	Yes	7.0	1354547	0.2	125866
H8a 1	778.77988	0.08	Yes	33.7	5456989	0.9	105420
H8a 2	778.77978	0.21	Yes	20.2	3264597	0.8	114258
H8a 3	778.77968	0.34	Yes	20.1	3101994	0.6	107561
H9a 1	778.77979	0.19	Yes	27.2	4322449	0.5	101277
H9a 2	778.77958	0.47	Yes	21.8	3534004	0.4	105277
H9a 3	778.77907	1.12	Yes	5.3	1054638	0.2	123219
H10a 1	778.77973	0.28	Yes	4.2	930679	0.2	119081
H10a 2	778.77864	1.67	Yes	8.9	1441490	0.7	111403
H10a 3	778.77986	0.11	Yes	20.0	3228944	0.9	104399
H11a 1	778.78045	-0.65	Yes	295.5	45627888	19.9	101639
H11a 2	778.78036	-0.53	Yes	165.6	25906332	3.4	102751
H11a 3	778.77968	0.34	Yes	77.0	9645057	7.4	103626
H12a 1	778.78066	-0.93	Yes	197.6	33389980	7.4	102683
H12a 2	778.78063	-0.89	Yes	200.4	33164114	6.7	102209
H12a 3	778.78060	-0.84	Yes	187.6	32149282	8.0	102369
H13aii 1	778.78052	-0.74	Yes	907.6	156401504	39.6	102470
H13aii 2	778.78053	-0.76	Yes	716.9	114516608	29.4	102093
H13aii 3	778.78026	-0.41	Yes	472.8	70994632	12.0	102765
H14a 1			No				
H14a 2			No				
H14a 3			No				
H14bi 1			No				
H14bi 2			No				
H14bi 3			No				
V1a 1	778.78002	-0.10	Yes	30.2	5444243	0.2	104506
V1a 2	778.77999	-0.06	Yes	34.0	6027291	1.0	106477
V1a 3	778.77989	0.06	Yes	21.7	3805239	0.8	113907
B1a 1	778.78039	-0.57	Yes	132.7	23072326	4.5	101963
B1a 2	778.77979	0.20	Yes	80.7	12240507	4.0	103406
B1a 3	778.77944	0.65	Yes	39.2	5543994	1.3	109361
DHB 1			No				
DHB 2			No				
DHB 3			No				
Soil 3a 1			No				
Soil 3a 2			No				
Soil 3a 3			No				
Soil 3b 1			No				
Soil 3b 2			No				
Soil 3b 3			No				
Solvent 1			No				
Solvent 2			No				
Solvent 3			No				

The next assigned compound, in Table 25, has two more hydrogens than that of the previous compound, shown in Table 24. The ion is assigned as $[C_{54}H_{101}NO] + H^+$, for a component with five double bond equivalents, and it has a similar detection pattern. The peak in the mass spectra of H13 and Y1 has high S:N and relative intensity %, with moderate detection in sample extracts H4, H5, H11 and H12, as well as the original York analysis. It is also not detected in H14 (a and b) and the controls. A significant difference is that this more saturated compound is detected in the H2 extract, although at low intensity, while $[C_{54}H_{99}NO] + H^+$ is not.

Table 25. Summary of signal at *m/z* 780. C_xH_yNO

Calculated *m/z*	780.79564	C54H102NO					
Sample designation + MALDI replicate no.	Measured *m/z*	Error [ppm]	Present	S:N	Intensity	Rel. Int. %	Resolution
Y1a 1	780.79543	0.2	Yes	390.2	67344560	22.4	99152
Y1a 2	780.79516	0.55	Yes	372.8	59974812	22.0	100076
Y1a 3	780.79536	0.3	Yes	412.2	71201024	20.7	99868
Original Heslington	780.79539	0.26	Yes	63.5	8160934	6.6	66553
H1a 1			No				
H1a 2	780.79527	0.41	Yes	6.4	1212323	0.3	119013
H1a 3	780.79508	0.66	Yes	7.3	1269893	0.2	101784
H1b 1	780.79465	1.21	Yes	32.4	4963456	0.6	107704
H1b 2	780.79497	0.8	Yes	25.4	3821912	1.0	108165
H1b 3	780.79511	0.62	Yes	20.6	3131251	0.7	110765
H2a 1	780.79431	1.65	Yes	11.0	1786668	0.3	108270
H2a 2	780.7944	1.52	Yes	11.1	1950390	0.6	108663
H2a 3	780.79551	0.11	Yes	14.7	2216821	0.6	94994
H3a 1	780.79491	0.88	Yes	14.2	2343575	0.4	108909
H3a 2	780.79612	-0.67	Yes	15.7	2661083	0.4	102652
H3a 3	780.79604	-0.57	Yes	7.5	1323180	0.2	102442
H4a 1	780.79548	0.15	Yes	117.6	20354596	1.2	98755
H4a 2	780.79576	-0.22	Yes	172.2	34080160	3.9	97840
H4a 3	780.79551	0.11	Yes	197.9	35985784	4.3	99296
H5a 1	780.79459	1.28	Yes	38.9	5251653	2.8	104169
H5a 2	780.79476	1.06	Yes	66.4	9331768	3.1	96140
H5a 3	780.79463	1.24	Yes	89.2	13282311	1.5	95236
H6a 1	780.79520	0.5	Yes	25.2	3933120	0.5	105004
H6a 2	780.79532	0.35	Yes	19.4	3013675	0.4	113579
H6a 3	780.79505	0.69	Yes	17.9	2831277	0.3	106470
H7a 1	780.79477	1.05	Yes	11.5	2030156	0.5	106694
H7a 2	780.79541	0.24	Yes	9.6	1828654	0.3	122821
H7a 3	780.79509	0.65	Yes	12.4	2161055	0.3	114274
H8a 1	780.79535	0.31	Yes	23.6	3934348	0.7	104116
H8a 2	780.79581	-0.27	Yes	15.0	2520926	0.6	122981
H8a 3	780.79554	0.06	Yes	16.1	2550287	0.5	116011
H9a 1	780.79510	0.63	Yes	27.3	4339803	0.5	102642
H9a 2	780.79559	0.01	Yes	21.4	3467007	0.4	106878
H9a 3	780.79530	0.38	Yes	7.1	1304991	0.3	105529
H10a 1	780.79567	-0.09	Yes	6.9	1328621	0.2	130816
H10a 2	780.79543	0.21	Yes	5.4	994568	0.5	145630
H10a 3	780.79526	0.43	Yes	13.6	2300607	0.6	109385
H11a 1	780.79601	-0.53	Yes	219.7	34058292	14.9	98519
H11a 2	780.79591	-0.41	Yes	116.3	18396864	2.4	101570
H11a 3	780.79543	0.2	Yes	66.1	8356096	6.4	101024
H12a 1	780.79627	-0.86	Yes	180.3	30241376	6.7	99894
H12a 2	780.79626	-0.85	Yes	187.2	30769116	6.3	99853
H12a 3	780.7962	-0.77	Yes	170.1	28951846	7.2	99372
H13aii 1	780.79608	-0.63	Yes	615.8	105855152	26.8	98466
H13aii 2	780.79608	-0.63	Yes	495.9	79279040	20.4	97652
H13aii 3	780.79583	-0.3	Yes	314.4	47327236	8.0	99116
H14a 1			No				
H14a 2			No				
H14a 3			No				
H14bi 1			No				
H14bi 2			No				
H14bi 3			No				
V1a 1	780.79546	0.17	Yes	190.9	32510822	1.5	100934
V1a 2	780.79544	0.2	Yes	206.7	34960308	5.6	101686
V1a 3	780.79533	0.34	Yes	161.9	26124596	5.6	102621
B1a 1	780.79590	-0.4	Yes	135.5	23628180	4.6	99439
B1a 2	780.79537	0.29	Yes	91.6	13927549	4.5	100472
B1a 3	780.79501	0.74	Yes	47.0	6631984	1.6	105959
DHB 1			No				
DHB 2			No				
DHB 3			No				
Soil 3a 1			No				
Soil 3a 2			No				
Soil 3a 3			No				
Soil 3b 1			No				
Soil 3b 2			No				
Soil 3b 3			No				
Solvent 1			No				
Solvent 2			No				
Solvent 3			No				

Table 26 shows the next assigned compound, $[C_{54}H_{103}NO] + H^+$, with four double bond equivalents represents the product of a further hydrogenation of the compounds assigned in Table 24 and Table 25. This signal was noted to be of interest in the original mass spectrum of the York brain extract. The mass spectra for the extracts show this signal has a particularly high relative intensity in the V1 extract replicates, but similar S:N and relative intensities as the previous more unsaturated compounds in extracts Y1, H11, H12 and H13. Comparing the relative intensities across the three tables, there appears to be an increase in signal intensity as the compound becomes more dehydrogenated. As well as being detected in H2, there is limited detection in the H14b replicates. It is only not detected in the controls and H14a.

Table 26. Summary of signal at *m/z* 782. C_xH_yNO

Calculated *m/z*	782.81124	C54H104NO					
Sample designation + MALDI replicate no.	Measured *m/z*	Error [ppm]	Present	S:N	Intensity	Rel. Int. %	Resolution
Y1a 1	782.81124	0.00	Yes	347.4	59990716	20.0	98480
Y1a 2	782.81093	0.39	Yes	301.4	48553044	17.8	98889
Y1a 3	782.81117	0.10	Yes	351.8	60815600	17.6	99169
Original Heslington	782.81115	0.12	Yes	43.6	5673239	4.6	68508
H1a 1	782.81113	0.15	Yes	26.6	4185579	0.4	105204
H1a 2	782.81060	0.83	Yes	28.9	4327643	1.1	95253
H1a 3	782.81058	0.84	Yes	20.4	2995034	0.5	105446
H1b 1	782.81046	1.00	Yes	70.5	10416510	1.2	104420
H1b 2	782.81056	0.87	Yes	75.4	10715092	2.8	104048
H1b 3	782.81024	1.28	Yes	65.5	9259270	2.2	104009
H2a 1	782.81018	1.36	Yes	105.9	14428024	2.7	102485
H2a 2	782.81040	1.08	Yes	88.2	13179877	4.0	103113
H2a 3	782.81045	1.02	Yes	74.5	9967049	2.8	104465
H3a 1	782.81085	0.51	Yes	39.6	5946287	1.1	104433
H3a 2	782.81120	0.05	Yes	93.0	14105720	2.3	100461
H3a 3	782.81077	0.60	Yes	42.1	5969549	0.8	107376
H4a 1	782.81133	-0.11	Yes	83.0	14459533	0.8	99105
H4a 2	782.81156	-0.41	Yes	114.2	22724094	2.6	98644
H4a 3	782.81135	-0.13	Yes	124.7	22803036	2.7	98940
H5a 1	782.81011	1.44	Yes	20.1	2854253	1.5	112783
H5a 2	782.81066	0.75	Yes	36.1	5210999	1.7	98493
H5a 3	782.81030	1.21	Yes	48.7	7395334	0.8	95208
H6a 1	782.81108	0.21	Yes	129.1	18782768	2.5	102241
H6a 2	782.81104	0.26	Yes	99.0	14107183	1.9	102932
H6a 3	782.81093	0.40	Yes	105.4	15134702	1.6	102428
H7a 1	782.81066	0.74	Yes	21.2	3468954	0.8	105510
H7a 2	782.81133	-0.12	Yes	25.4	4281226	0.7	109391
H7a 3	782.81095	0.37	Yes	21.7	3539613	0.5	107685
H8a 1	782.81118	0.08	Yes	27.7	4548611	0.8	109072
H8a 2	782.81098	0.34	Yes	21.1	3419310	0.8	109812
H8a 3	782.81107	0.22	Yes	22.7	3472824	0.7	100383
H9a 1	782.81111	0.17	Yes	40.9	6343755	0.8	104196
H9a 2	782.81127	-0.04	Yes	39.1	6070769	0.7	101302
H9a 3	782.81096	0.36	Yes	12.2	2020358	0.4	128034
H10a 1	782.81014	1.40	Yes	6.4	1255920	0.2	114036
H10a 2	782.81126	-0.03	Yes	5.4	996257	0.5	146467
H10a 3	782.81153	-0.37	Yes	11.4	1978501	0.5	112383
H11a 1	782.81173	-0.62	Yes	183.6	28526206	12.5	97810
H11a 2	782.81178	-0.69	Yes	125.2	19784938	2.6	100522
H11a 3	782.81108	0.21	Yes	62.0	7860355	6.0	100926
H12a 1	782.81207	-1.06	Yes	195.7	32793128	7.3	99515
H12a 2	782.81208	-1.07	Yes	210.6	34578280	7.0	99283
H12a 3	782.81197	-0.93	Yes	183.3	31166000	7.7	99931
H13aii 1	782.81188	-0.81	Yes	456.8	78608888	19.9	98951
H13aii 2	782.81185	-0.78	Yes	400.2	64043792	16.4	98080
H13aii 3	782.81158	-0.43	Yes	275.4	41502024	7.0	99184
H14a 1			No				
H14a 2			No				
H14a 3			No				
H14bi 1	782.81160	-0.45	Yes	13.7	2528055	0.3	99977
H14bi 2	782.81109	0.19	Yes	9.5	1758204	0.3	112277
H14bi 3			No				
V1a 1	782.81126	-0.02	Yes	2988.2	503781568	23.0	102002
V1a 2	782.81126	-0.02	Yes	3270.4	547980864	87.1	101610
V1a 3	782.81110	0.19	Yes	2674.7	426458976	91.0	101948
B1a 1	782.81177	-0.67	Yes	138.7	24166634	4.7	98189
B1a 2	782.81114	0.16	Yes	93.1	14152196	4.6	98707
B1a 3	782.81068	0.72	Yes	76.8	10628778	2.5	102557
DHB 1			No				
DHB 2			No				
DHB 3			No				
Soil 3a 1			No				
Soil 3a 2			No				
Soil 3a 3			No				
Soil 3b 1			No				
Soil 3b 2			No				
Soil 3b 3			No				
Solvent 1			No				
Solvent 2			No				
Solvent 3			No				

The peak at *m/z* 806 (Table 27) was assigned $[C_{56}H_{103}NO] + H^+$, which has six double bond equivalents. The S:N and intensities for this signal were high in the extracts of Y1 and H13. However, this was undetected in more of the sample extracts, H2, H3, H7 and H14 (a and b). It was detected at very low S:N and intensity in a replicate 2 of the DHB matrix control, which may indicate this is a contaminant from the background. However, the spot for one of the H12a replicates was adjacent on the MALDI plate to this DHB matrix replicate, so cross contamination is a possibility.

Table 27. Summary of signal at *m/z* 806. C_xH_yNO

Calculated *m/z*	806.81128 C56H104NO						
Sample designation + MALDI replicate no.	Measured *m/z*	Error [ppm]	Present	S:N	Intensity	Rel. Int. %	Resolution
Y1a 1	806.81132	-0.10	Yes	199.6	34618480	11.5	95204
Y1a 2	806.81092	0.40	Yes	168.1	27198022	10	95721
Y1a 3	806.81129	-0.06	Yes	191.7	33285500	9.7	95855
Original Heslington	806.81052	0.89	Yes	28.6	3893619	3.1	69262
H1a 1			No				
H1a 2			No				
H1a 3	806.81057	0.84	Yes	5.2	991526	0.2	85547
H1b 1			No				
H1b 2	806.81039	1.06	Yes	11.3	1879741	0.5	103704
H1b 3	806.81139	-0.18	Yes	7.8	1384163	0.3	123218
H2a 1			No				
H2a 2			No				
H2a 3			No				
H3a 1			No				
H3a 2			No				
H3a 3			No				
H4a 1	806.81132	-0.09	Yes	91.3	15863463	0.9	95968
H4a 2	806.81179	-0.68	Yes	117.8	23533906	2.7	94509
H4a 3	806.81147	-0.28	Yes	137.8	25280648	3.0	93538
H5a 1	806.81057	0.84	Yes	21.9	3116550	1.6	100200
H5a 2	806.81036	1.10	Yes	44.1	6357947	2.1	89742
H5a 3	806.81053	0.88	Yes	61.4	9298555	1.1	93743
H6a 1			No				
H6a 2	806.81080	0.54	Yes	5.7	1117940	0.2	120346
H6a 3			No				
H7a 1			No				
H7a 2			No				
H7a 3			No				
H8a 1	806.81119	0.07	Yes	14.5	2555500	0.4	103037
H8a 2	806.81144	-0.24	Yes	13.2	2278880	0.5	100403
H8a 3	806.81102	0.28	Yes	12.9	2124854	0.4	99218
H9a 1	806.81129	-0.06	Yes	8.4	1569667	0.2	131874
H9a 2	806.81178	-0.67	Yes	12.5	2166260	0.3	103426
H9a 3			No				
H10a 1			No				
H10a 2	806.81118	0.08	Yes	8.8	1442273	0.7	97051
H10a 3	806.81162	-0.47	Yes	8.9	1623309	0.4	103593
H11a 1	806.81190	-0.82	Yes	134.7	21056150	9.2	94694
H11a 2	806.81177	-0.65	Yes	71.7	11541954	1.5	97057
H11a 3	806.81118	0.08	Yes	30.8	4074215	3.1	99682
H12a 1	806.81210	-1.06	Yes	102.7	17233316	3.8	94743
H12a 2	806.81207	-1.02	Yes	103.3	17000718	3.5	91352
H12a 3	806.81191	-0.83	Yes	93.8	15995995	4	94194
H13aii 1	806.81195	-0.87	Yes	378.1	64897644	16.4	92064
H13aii 2	806.81195	-0.88	Yes	286.3	45899668	11.8	91575
H13aii 3	806.81167	-0.53	Yes	182.7	27649572	4.7	92523
H14a 1			No				
H14a 2			No				
H14a 3			No				
H14bi 1			No				
H14bi 2			No				
H14bi 3			No				
V1a 1	806.81156	-0.39	Yes	23.3	4273189	0.2	104924
V1a 2	806.81116	0.11	Yes	26.8	4848030	0.8	95753
V1a 3	806.81103	0.26	Yes	20.6	3612513	0.8	96643
B1a 1	806.81201	-0.96	Yes	104.2	18306010	3.6	97238
B1a 2	806.81127	-0.03	Yes	62.1	9609020	3.1	96390
B1a 3	806.81049	0.93	Yes	29.3	4281017	1	100946
DHB 1			No				
DHB 2	806.81129	-0.06	Yes	4.3	846707	0.1	135576
DHB 3			No				
Soil 3a 1			No				
Soil 3a 2			No				
Soil 3a 3			No				
Soil 3b 1			No				
Soil 3b 2			No				
Soil 3b 3			No				
Solvent 1			No				
Solvent 2			No				
Solvent 3			No				

Table 28 provides information on the peak detected at *m/z* 810, a peak of interest in the original York brain extract mass spectrum. This was assigned $[C_{56}H_{107}NO] + H^+$, for a component with four double bond equivalents. The signal was strongest in the spectra of the V1 extract, with it being the largest peak in the spectrum for the second replicate. It was detected in the spectra for the extracts from all sites and ages except sample H14a. There were signals detected in the soil controls at a similar *m/z*, but the error was 2.49 ppm or over and so these are considered not to be the same compound. It was absent in the DHB control and solvent blank spectra.

Table 28. Summary of signal at *m/z* 810. C_xH_yNO

Calculated *m/z*	810.84254	C56H108NO					
Sample designation + MALDI replicate no.	Measured *m/z*	Error [ppm]	Present	S:N	Intensity	Rel. Int. %	Resolution
Y1a 1	810.84233	0.27	Yes	142.4	24788378	8.2	93571
Y1a 2	810.84203	0.64	Yes	111.5	18156236	6.7	94293
Y1a 3	810.84221	0.41	Yes	132.8	23175538	6.7	94408
Original Heslington	810.84280	-0.32	Yes	12.6	1855672	1.5	76148
H1a 1	810.84196	0.71	Yes	15.0	2488284	0.3	96108
H1a 2	810.84130	1.53	Yes	16.1	2553660	0.6	100332
H1a 3	810.84153	1.25	Yes	12.9	2009284	0.3	108744
H1b 1	810.84166	1.09	Yes	49.3	7401927	0.9	100501
H1b 2	810.84190	0.79	Yes	62.4	8934655	2.3	97586
H1b 3	810.84142	1.39	Yes	46.0	6598793	1.6	101548
H2a 1	810.84137	1.45	Yes	81	11117049	2.1	99629
H2a 2	810.84151	1.27	Yes	54.7	8254321	2.5	101017
H2a 3	810.84182	0.89	Yes	46.4	6351511	1.8	98920
H3a 1	810.84230	0.30	Yes	82.3	11987285	2.2	98970
H3a 2	810.84242	0.16	Yes	165.4	24918002	4.1	98279
H3a 3	810.84198	0.69	Yes	54.0	7578724	1.0	100467
H4a 1	810.84218	0.45	Yes	43.5	7733853	0.5	93635
H4a 2	810.84275	-0.26	Yes	59.3	12037681	1.4	94139
H4a 3	810.84241	0.17	Yes	54.3	10178638	1.2	88052
H5a 1			No				
H5a 2	810.84207	0.59	Yes	9.0	1548306	0.5	116355
H5a 3	810.84190	0.79	Yes	9.4	1697815	0.2	116640
H6a 1	810.84223	0.38	Yes	178.6	25922602	3.5	98782
H6a 2	810.84215	0.48	Yes	160.9	22765422	3.1	97725
H6a 3	810.84211	0.53	Yes	148.7	21217556	2.3	97797
H7a 1	810.84233	0.27	Yes	26.1	4222385	1.0	97698
H7a 2	810.84229	0.32	Yes	34.9	5763031	0.9	95394
H7a 3	810.84212	0.52	Yes	26.4	4252615	0.6	100271
H8a 1	810.84225	0.36	Yes	9.7	1824275	0.3	105385
H8a 2	810.84218	0.45	Yes	9.0	1662391	0.4	108333
H8a 3	810.84213	0.51	Yes	6.4	1209018	0.2	117585
H9a 1	810.84176	0.96	Yes	18.8	3092587	0.4	93088
H9a 2	810.84254	0.01	Yes	15.9	2674640	0.3	103727
H9a 3	810.84230	0.31	Yes	6.2	1188789	0.3	110478
H10a 1	810.84178	0.94	Yes	5.8	1191476	0.2	113527
H10a 2			No				
H10a 3	810.84259	-0.06	Yes	4.6	995528	0.3	123728
H11a 1	810.84292	-0.47	Yes	64.8	10312926	4.5	92703
H11a 2	810.84280	-0.32	Yes	47.4	7747941	1.0	97910
H11a 3	810.84256	-0.02	Yes	15.5	2201723	1.7	106303
H12a 1	810.84322	-0.84	Yes	143.5	23934950	5.3	96448
H12a 2	810.84329	-0.92	Yes	135.8	22238334	4.5	94800
H12a 3	810.84310	-0.69	Yes	114.6	19453778	4.8	98430
H13aii 1	810.84309	-0.67	Yes	195.8	33783372	8.6	94268
H13aii 2	810.84296	-0.52	Yes	180.6	29076606	7.5	94747
H13aii 3	810.84280	-0.31	Yes	134.0	20364778	3.5	95955
H14a 1			No				
H14a 2			No				
H14a 3			No				
H14bi 1	810.84301	-0.57	Yes	19.0	3380178	0.4	107018
H14bi 2	810.84315	-0.74	Yes	13.1	2296497	0.4	107286
H14bi 3			No				
V1a 1	810.84242	0.15	Yes	3186.3	536857920	24.5	98365
V1a 2	810.84242	0.16	Yes	3752.3	629071296	100.0	98209
V1a 3	810.84226	0.36	Yes	2874.2	457445408	97.6	98518
B1a 1	810.84287	-0.40	Yes	133.9	23415848	4.6	95795
B1a 2	810.84210	0.55	Yes	76.9	11826751	3.9	95949
B1a 3	810.84172	1.02	Yes	71.7	10013132	2.3	99926
DHB 1			No				
DHB 2			No				
DHB 3			No				
Soil 3a 1	810.84632	-4.65	No	4.7	1492056	0.2	100608
Soil 3a 2			No				
Soil 3a 3	810.84646	-4.83	No	4.6	1414755	0.3	103464
Soil 3b 1	810.84574	-3.94	No	4.7	1531803	0.2	92510
Soil 3b 2	810.84456	-2.49	No	6.2	1835816	0.1	114693
Soil 3b 3			No				
Solvent 1			No				
Solvent 2			No				
Solvent 3			No				

As well as compounds with C_xH_yNO general formulae, some signals were consistent with a $C_xH_yN_2O$ formula. Table 29 shows the information for the peak found in the mass spectra at *m/z* 501, which as $[C_{34}H_{48}N_2O] + H^+$ would have 11 double bond equivalents. This gave a very strong signal (S:N, intensity and relative intensity %) in the extract of B1 spectral replicates, and to a lesser extent in those of H4, H8, H9, H10 and H11. It was only detected in a single replicate of the extracts of H1 (a and b), H14b. The signal strengths (S:N and relative intensity) were low in Y1 and H2 extract mass spectra but resolution was consistently over 150,000. This component was not detected in the original York brain analysis (this may be due to the subsequent upgrade of the mass spectrometer), nor in the spectra of extracts of H14a and V1. This peak was also not found in any of the control spectra.

Table 29. Summary of signal at *m/z* 501. $C_xH_yN_2O$

Calculated *m/z*	501.38394	C34H49N2O					
Sample designation + MALDI replicate no.	Measured *m/z*	Error [ppm]	Present	S:N	Intensity	Rel. Int. %	Resolution
Y1a 1	501.38389	-0.07	Yes	16.3	2402691	0.8	161818
Y1a 2	501.38382	-0.34	Yes	12.8	1889729	0.7	166731
Y1a 3	501.38397	0.46	Yes	13.4	2042641	0.6	168129
Original Heslington			No				
H1a 1			No				
H1a 2	501.38449	-1.10	Yes	2.6	581602	0.1	240146
H1a 3			No				
H1b 1			No				
H1b 2			No				
H1b 3	501.38302	1.83	Yes	8.0	1218321	0.3	111354
H2a 1	501.38358	0.73	Yes	16.8	2250828	0.4	157396
H2a 2	501.38342	1.05	Yes	8.1	1358659	0.4	215983
H2a 3	501.38371	0.45	Yes	17.5	2231431	0.6	158511
H3a 1	501.38388	0.11	Yes	245.6	32058080	5.8	158965
H3a 2	501.38396	-0.05	Yes	379.6	50277868	8.2	157511
H3a 3	501.38378	0.32	Yes	179.2	21896552	2.9	160503
H4a 1	501.38400	-0.11	Yes	2016.5	293033088	17.1	157962
H4a 2	501.38413	-0.36	Yes	1503.7	220870912	25.3	158392
H4a 3	501.38400	-0.11	Yes	1366.2	194081040	23.4	158459
H5a 1	501.38356	0.77	Yes	91.6	10446816	5.5	158850
H5a 2	501.38362	0.63	Yes	114.2	13555837	4.5	156890
H5a 3	501.38360	0.68	Yes	169.2	21311908	2.4	157715
H6a 1	501.38386	0.16	Yes	160.8	20492628	2.8	157848
H6a 2	501.38385	0.18	Yes	199.8	24914852	3.4	157186
H6a 3	501.38384	0.20	Yes	142.2	18320072	1.9	158486
H7a 1	501.38384	0.21	Yes	112.9	14009299	3.4	158628
H7a 2	501.38387	0.14	Yes	105.3	13681324	2.2	157518
H7a 3	501.38383	0.22	Yes	117.4	14662607	2.2	160924
H8a 1	501.38392	0.04	Yes	2751.9	372404512	64.0	158094
H8a 2	501.38411	-0.32	Yes	1786.9	222973904	51.7	157305
H8a 3	501.38384	0.20	Yes	1932.6	237312992	45.9	158213
H9a 1	501.38397	-0.07	Yes	5307.5	724846080	89.7	157518
H9a 2	501.38396	-0.03	Yes	4371.1	603998912	69.7	157788
H9a 3	501.38381	0.26	Yes	2376.7	293602944	64.7	157644
H10a 1	501.38390	0.09	Yes	1059.8	134094080	22.4	158537
H10a 2	501.38376	0.35	Yes	857.5	98248616	50.3	157657
H10a 3	501.38386	0.16	Yes	1669.4	217762432	59.2	158611
H11a 1	501.38421	-0.55	Yes	701.6	87634632	38.3	158165
H11a 2	501.38416	-0.44	Yes	440.0	56690156	7.4	159422
H11a 3	501.38386	0.15	Yes	221.9	24268884	18.7	160173
H12a 1	501.38431	-0.74	Yes	244.9	34460576	7.7	157795
H12a 2	501.38429	-0.70	Yes	210.0	29641590	6.0	156462
H12a 3	501.38429	-0.69	Yes	285.5	40589544	10.1	157319
H13aii 1	501.38421	-0.53	Yes	141.7	19447234	4.9	159652
H13aii 2	501.38423	-0.57	Yes	137.2	18119688	4.7	157840
H13aii 3	501.38411	-0.33	Yes	107.2	13409798	2.3	161162
H14a 1			No				
H14a 2			No				
H14a 3			No				
H14bi 1			No				
H14bi 2	501.38467	-1.46	Yes	6.7	1233117	0.2	171717
H14bi 3			No				
V1a 1			No				
V1a 2			No				
V1a 3			No				
B1a 1	501.38415	-0.42	Yes	3111.8	486390528	94.8	157626
B1a 2	501.38393	0.02	Yes	1850.2	244920112	79.9	157374
B1a 3	501.38368	0.51	Yes	1296.5	157998512	37.0	158867
DHB 1			No				
DHB 2			No				
DHB 3			No				
Soil 3a 1			No				
Soil 3a 2			No				
Soil 3a 3			No				
Soil 3b 1			No				
Soil 3b 2			No				
Soil 3b 3			No				
Solvent 1			No				
Solvent 2			No				
Solvent 3			No				

The mass spectra of the B1 extract showed a strong signal at *m/z* 511, another $C_xH_yN_2O$ compound. This was assigned $[C_{35}H_{46}N_2O] + H^+$, which has 14 double bond equivalents; data are summarised in Table 30. The signal strength (S:N and relative intensity %) was reasonably high in the mass spectra for H4, H8, H9, H10 and H11. It was only detected in a single replicate of the extracts from H7 and H14b. The component was undetected in the extracts from H1 (a and b), H2, H14a, V1 and the controls.

Table 30. Summary of signal at *m/z* 511. $C_xH_yN_2O$

Calculated *m/z*	511.3682	C35H47N2O					
Sample designation + MALDI replicate no.	Measured *m/z*	Error [ppm]	Present	S:N	Intensity	Rel. Int. %	Resolution
Y1a 1	511.36817	0.24	Yes	17.3	2603937	0.9	166091
Y1a 2	511.36815	0.28	Yes	21.6	3056176	1.1	148507
Y1a 3	511.36813	0.31	Yes	23.2	3403985	1.0	165440
Original Heslington			No				
H1a 1			No				
H1a 2			No				
H1a 3			No				
H1b 1			No				
H1b 2			No				
H1b 3			No				
H2a 1			No				
H2a 2			No				
H2a 3			No				
H3a 1	511.36811	0.35	Yes	53.3	7359524	1.3	160570
H3a 2	511.36818	0.21	Yes	67.0	9353036	1.5	155282
H3a 3	511.36814	0.30	Yes	20.8	2832432	0.4	164117
H4a 1	511.36824	0.10	Yes	1423.9	215397248	12.6	155976
H4a 2	511.36833	-0.07	Yes	1094.3	167304528	19.1	156212
H4a 3	511.36822	0.14	Yes	1008.3	148566576	17.9	156375
H5a 1	511.36792	0.73	Yes	26.2	3219502	1.7	158908
H5a 2	511.36801	0.54	Yes	32.1	4065488	1.3	172763
H5a 3	511.36791	0.74	Yes	49.3	6557568	0.8	155379
H6a 1	511.36815	0.27	Yes	53.2	7127318	1.0	161444
H6a 2	511.36817	0.24	Yes	96.5	12432997	1.7	158504
H6a 3	511.36811	0.36	Yes	60.2	8104588	0.9	162805
H7a 1	511.36829	0.00	Yes	7.0	1148330	0.3	158355
H7a 2			No				
H7a 3			No				
H8a 1	511.36823	0.12	Yes	306.0	42943512	7.4	155066
H8a 2	511.36837	-0.16	Yes	250.0	32226264	7.5	154821
H8a 3	511.36815	0.27	Yes	253.9	32108700	6.2	156066
H9a 1	511.36821	0.15	Yes	738.7	104524016	12.9	155551
H9a 2	511.36822	0.13	Yes	644.6	92389856	10.7	155685
H9a 3	511.36811	0.35	Yes	419.5	53220488	11.7	155658
H10a 1	511.36819	0.20	Yes	231.0	30156976	5.0	154934
H10a 2	511.36807	0.44	Yes	175.7	20658758	10.6	153183
H10a 3	511.36814	0.30	Yes	393.8	52964896	14.4	157352
H11a 1	511.36848	-0.36	Yes	280.4	36016992	15.7	157242
H11a 2	511.36841	-0.24	Yes	161.3	21464910	2.8	155765
H11a 3	511.36821	0.16	Yes	88.6	9961659	7.7	156718
H12a 1	511.36855	-0.51	Yes	182.1	26569232	5.9	155501
H12a 2	511.36856	-0.52	Yes	155.9	22816386	4.6	156445
H12a 3	511.36856	-0.53	Yes	176.3	26052172	6.5	157708
H13aii 1	511.36847	-0.36	Yes	137.0	19368080	4.9	157656
H13aii 2	511.36851	-0.43	Yes	153.9	20844876	5.4	158229
H13aii 3	511.36838	-0.18	Yes	111.8	14268247	2.4	158678
H14a 1			No				
H14a 2			No				
H14a 3			No				
H14bi 1	511.36845	-0.30	Yes	6.5	1285992	0.1	173408
H14bi 2			No				
H14bi 3			No				
V1a 1			No				
V1a 2			No				
V1a 3			No				
B1a 1	511.36836	-0.14	Yes	893.7	146298032	28.5	155562
B1a 2	511.36820	0.19	Yes	544.7	74469312	24.3	155621
B1a 3	511.36797	0.63	Yes	339.4	42435668	9.9	156079
DHB 1			No				
DHB 2			No				
DHB 3			No				
Soil 3a 1			No				
Soil 3a 2			No				
Soil 3a 3			No				
Soil 3b 1			No				
Soil 3b 2			No				
Soil 3b 3			No				
Solvent 1			No				
Solvent 2			No				
Solvent 3			No				

Table 31 provides information on the peak at *m/z* 513, assigned $[C_{35}H_{48}N_2O] + H^+$ which has 13 double bond equivalents. This has a strong signal (S:N and relative intensity) in the spectra for H4, H9, H11 and B1. It was undetected in H1 (a and b), H14a, V1 and the controls (the compound in solvent replicate 2 is assumed to be different due to the large ppm error).

All of the $C_xH_yN_2O$ compounds appear to be prevalent (high relative intensity) in the B1 extract replicate spectra. This may indicate that these compounds are found in higher concentrations in younger brains, or that concentrations of other lipids are lower. Their absence from all of the V1 spectra however is not consistent with this suggestion. Alternatively, these compounds may indicate an additional distinctiveness of the Blackpool burial environment.

Table 31. Summary of signal at *m/z* 513. $C_xH_yN_2O$

Calculated *m/z*	513.38394	C35H49N2O					
Sample designation + MALDI replicate no.	Measured *m/z*	Error [ppm]	Present	S:N	Intensity	Rel. Int. %	Resolution
Y1a 1	513.38357	0.73	Yes	6.1	1104160	0.4	181265
Y1a 2	513.38394	0.00	Yes	5.2	949921	0.3	156204
Y1a 3	513.38370	0.46	Yes	10.5	1698526	0.5	172241
Original Heslington			No				
H1a 1			No				
H1a 2			No				
H1a 3			No				
H1b 1			No				
H1b 2			No				
H1b 3			No				
H2a 1	513.38367	0.53	Yes	12.6	1780915	0.3	181389
H2a 2	513.38347	0.91	Yes	9.3	1543646	0.5	201391
H2a 3	513.38315	1.55	Yes	6.3	984570	0.3	191874
H3a 1	513.38381	0.25	Yes	397.7	53003976	9.6	154414
H3a 2	513.38390	0.08	Yes	618.5	83887368	13.7	154391
H3a 3	513.38374	0.38	Yes	223.6	27752276	3.7	155712
H4a 1	513.38391	0.06	Yes	4630.1	699732800	40.9	155149
H4a 2	513.38403	-0.18	Yes	3591.0	548323648	62.7	155585
H4a 3	513.38390	0.07	Yes	3648.5	536799232	64.7	155529
H5a 1	513.38347	0.91	Yes	50.2	5916634	3.1	162372
H5a 2	513.38358	0.70	Yes	63.4	7765494	2.6	163540
H5a 3	513.38358	0.70	Yes	90.4	11783916	1.4	153992
H6a 1	513.38383	0.22	Yes	195.8	25472972	3.4	158476
H6a 2	513.38379	0.30	Yes	289.6	36757696	5.0	155157
H6a 3	513.38379	0.30	Yes	225.7	29593050	3.1	155364
H7a 1	513.38383	0.41	Yes	21.0	2881421	0.7	155662
H7a 2	513.38965	0.04	Yes	7.3	1245665	0.2	180935
H7a 3	513.38376	0.36	Yes	30.3	4072024	0.6	161928
H8a 1	513.38388	0.12	Yes	792.0	110680232	19.0	155136
H8a 2	513.38406	-0.22	Yes	627.7	80471672	18.7	154708
H8a 3	513.38381	0.25	Yes	622.6	78334560	15.2	154924
H9a 1	513.38390	0.08	Yes	2476.7	349772384	43.3	155132
H9a 2	513.38388	0.11	Yes	2279.0	325910368	37.6	154950
H9a 3	513.38376	0.36	Yes	1380.7	174521888	38.5	154908
H10a 1	513.38383	0.22	Yes	145.8	19143954	3.2	156920
H10a 2	513.38368	0.51	Yes	120.3	14234548	7.3	155233
H10a 3	513.38384	0.20	Yes	264.2	35622460	9.7	155955
H11a 1	513.38415	-0.41	Yes	1163.5	148525648	64.9	155093
H11a 2	513.38411	-0.33	Yes	608.1	80140032	10.5	156401
H11a 3	513.38386	0.15	Yes	367.1	40425964	31.1	156606
H12a 1	513.38424	-0.58	Yes	459.1	66534492	14.8	154800
H12a 2	513.38422	-0.55	Yes	421.4	61162732	12.4	154295
H12a 3	513.38422	-0.54	Yes	491.3	72042160	17.9	155432
H13aii 1	513.38416	-0.43	Yes	399.1	55871320	14.2	155446
H13aii 2	513.38420	-0.51	Yes	375.2	50387700	12.9	154635
H13aii 3	513.38409	-0.28	Yes	274.9	34669252	5.9	156754
H14a 1			No				
H14a 2			No				
H14a 3			No				
H14bi 1	513.38416	-0.42	Yes	8.2	1529179	0.2	162801
H14bi 2	513.38410	-0.32	Yes	5.7	1117081	0.2	179585
H14bi 3			No				
V1a 1			No				
V1a 2			No				
V1a 3			No				
B1a 1	513.38406	-0.20	Yes	3139.5	513161056	100.0	154806
B1a 2	513.38385	0.18	Yes	2249.0	306540608	100.0	154395
B1a 3	513.38364	0.60	Yes	1692.2	210444000	49.3	155653
DHB 1			No				
DHB 2			No				
DHB 3			No				
Soil 3a 1			No				
Soil 3a 2			No				
Soil 3a 3			No				
Soil 3b 1			No				
Soil 3b 2			No				
Soil 3b 3			No				
Solvent 1			No				
Solvent 2	513.3822	3.39	No	5.1	1237239	0.2	97793
Solvent 3			No				

A curious signal was found in the mass spectra for a single replicate of H1 a, at *m/z* 463, shown in Table 32. This was assigned $[C_{30}H_{30}N_4O] + H^+$, a highly unsaturated species with 18 double bond equivalents. This had a very high S:N ratio and so was selected for comparison with other extracts but did not appear in any other spectra, including the controls. Is this an anomaly or contaminant?

Table 32. Summary of signal at *m/z* 463. $C_xH_yN_4O$

Calculated *m/z*	463.24924 C30H31N4O						
Sample designation + MALDI replicate no.	Measured *m/z*	Error [ppm]	Present	S:N	Intensity	Rel. Int. %	Resolution
Y1a 1			No				
Y1a 2			No				
Y1a 3			No				
Original Heslington			No				
H1a 1	463.24921	0.07	Yes	1146.9	143583792	14.5	172029
H1a 2			No				
H1a 3			No				
H1b 1			No				
H1b 2			No				
H1b 3			No				
H2a 1			No				
H2a 2			No				
H2a 3			No				
H3a 1			No				
H3a 2			No				
H3a 3			No				
H4a 1			No				
H4a 2			No				
H4a 3			No				
H5a 1			No				
H5a 2			No				
H5a 3			No				
H6a 1			No				
H6a 2			No				
H6a 3			No				
H7a 1			No				
H7a 2			No				
H7a 3			No				
H8a 1			No				
H8a 2			No				
H8a 3			No				
H9a 1			No				
H9a 2			No				
H9a 3			No				
H10a 1			No				
H10a 2			No				
H10a 3			No				
H11a 1			No				
H11a 2			No				
H11a 3			No				
H12a 1			No				
H12a 2			No				
H12a 3			No				
H13aii 1			No				
H13aii 2			No				
H13aii 3			No				
H14a 1			No				
H14a 2			No				
H14a 3			No				
H14bi 1			No				
H14bi 2			No				
H14bi 3			No				
V1a 1			No				
V1a 2			No				
V1a 3			No				
B1a 1			No				
B1a 2			No				
B1a 3			No				
DHB 1			No				
DHB 2			No				
DHB 3			No				
Soil 3a 1			No				
Soil 3a 2			No				
Soil 3a 3			No				
Soil 3b 1			No				
Soil 3b 2			No				
Soil 3b 3			No				
Solvent 1			No				
Solvent 2			No				
Solvent 3			No				

Table 33 displays the data for the peak at *m/z* 502 assigned $[C_{34}H_{47}NO_2]$ + H^+. This is the first of several compounds that have multiple oxygen atoms but only a single nitrogen atom. It has 12 double bond equivalents and so is highly unsaturated. This compound appears at high relative intensity and S:N in some of the Hull brain sample extract spectra, especially H4, H8, H9, H10, H11. Conversely it is entirely absent from spectra from H1 (a and b) and H14a and is only in certain replicates of H2 and H14b. Aside from the Hull brain extracts this component is not detected in any of the York extracts (modern or the original York analysis) or the Villiers Street brain extracts. It does appear in the Blackpool extracts which indicates it can form within a shorter time period.

Table 33. Summary of signal at *m/z* 502. $C_xH_yNO_2$

Calculated *m/z*	502.36796	C34H48NO2					
Sample designation + MALDI replicate no.	Measured *m/z*	Error [ppm]	Present	S:N	Intensity	Rel. Int. %	Resolution
Y1a 1			No				
Y1a 2			No				
Y1a 3			No				
Original Heslington			No				
H1a 1			No				
H1a 2			No				
H1a 3			No				
H1b 1			No				
H1b 2			No				
H1b 3			No				
H2a 1	502.36752	0.87	Yes	18.9	2516526	0.5	167992
H2a 2			No				
H2a 3			No				
H3a 1	502.36784	0.24	Yes	400.3	52690288	9.6	158300
H3a 2	502.36793	0.05	Yes	632.0	84588688	13.8	157966
H3a 3	502.36776	0.38	Yes	205.1	25248654	3.3	159710
H4a 1	502.36793	0.05	Yes	7745.7	1.147E+09	67.0	158028
H4a 2	502.36804	-0.16	Yes	5844.3	874623744	100.0	158093
H4a 3	502.36791	0.08	Yes	5743.1	829623040	100.0	158502
H5a 1	502.36753	0.05	Yes	112.9	12887130	6.8	159384
H5a 2	502.36763	0.66	Yes	163.5	19446794	6.4	158636
H5a 3	502.36760	0.71	Yes	280.0	35478088	4.1	159373
H6a 1	502.36784	0.23	Yes	322.9	41345768	5.6	158164
H6a 2	502.36782	0.28	Yes	482.9	60447724	8.2	158554
H6a 3	502.36782	0.27	Yes	335.2	43286172	4.6	158684
H7a 1	502.36776	0.17	Yes	33.2	4351545	1.1	166500
H7a 2	502.36772	0.47	Yes	32.3	4440354	0.7	162242
H7a 3	502.36775	0.40	Yes	42.5	5536963	0.8	158558
H8a 1	502.36790	0.12	Yes	2668.6	366584576	63.0	158081
H8a 2	502.36806	-0.21	Yes	1461.0	184594768	42.8	157303
H8a 3	502.36782	0.26	Yes	1659.4	206019904	39.9	157990
H9a 1	502.36794	0.04	Yes	4538.6	630138816	78.0	157771
H9a 2	502.36792	0.08	Yes	4158.0	584311872	67.4	158060
H9a 3	502.36780	0.31	Yes	2444.8	305363904	67.3	158245
H10a 1	502.36787	0.18	Yes	1120.9	143489104	24.0	158731
H10a 2	502.36776	0.38	Yes	947.7	109377208	56.0	157195
H10a 3	502.36784	0.22	Yes	1978.0	261348368	71.0	158862
H11a 1	502.36817	-0.42	Yes	1815.2	228869696	100.0	158513
H11a 2	502.36812	-0.34	Yes	846.3	110075264	14.4	158841
H11a 3	502.36787	0.17	Yes	699.5	76348072	58.7	158924
H12a 1	502.36824	-0.56	Yes	365.4	52134524	11.6	158153
H12a 2	502.36823	-0.55	Yes	303.7	43425892	8.8	158668
H12a 3	502.36822	-0.52	Yes	357.2	51567952	12.8	158524
H13aii 1	502.36819	-0.46	Yes	296.2	40925820	10.4	159638
H13aii 2	502.36821	-0.50	Yes	321.9	42682904	11.0	156927
H13aii 3	502.36810	-0.29	Yes	256.1	31981334	5.4	158463
H14a 1			No				
H14a 2			No				
H14a 3			No				
H14bi 1	502.36835	-0.78	Yes	10.0	1766020	0.2	158994
H14bi 2	502.36789	0.13	Yes	12.9	2116527	0.3	181016
H14bi 3			No				
V1a 1			No				
V1a 2			No				
V1a 3			No				
B1a 1	502.36809	-0.26	Yes	1115.4	178460000	34.8	157496
B1a 2	502.36790	0.11	Yes	672.0	90445040	29.5	158218
B1a 3	502.36767	0.56	Yes	470.3	58074100	13.6	158870
DHB 1			No				
DHB 2			No				
DHB 3			No				
Soil 3a 1			No				
Soil 3a 2			No				
Soil 3a 3			No				
Soil 3b 1			No				
Soil 3b 2			No				
Soil 3b 3			No				
Solvent 1			No				
Solvent 2			No				
Solvent 3			No				

The details for the peak at *m/z* 514 are shown in Table 34. This signal was assigned to $[C_{35}H_{47}NO_2] + H^+$, for a compound with 13 double bond equivalents. It has a similar empirical formula to the compound in Table 33, but is a degree more unsaturated. The strongest presence of this peak occurred in the spectra from the Blackpool brain extract and it was most evident in H9 and H11 of the Hull extracts. This compound was entirely undetected in the York sample and in certain Hull samples, H1 (a and b) and H2. It was only detected, and at low intensities and S:N, in some replicates of the following sample extracts: H5, H8, H14 (a and b) and V1.

Table 34. Summary of signal at *m/z* 514. $C_xH_yNO_2$

Calculated *m/z*	514.36796 C35H48NO2						
Sample designation + MALDI replicate no.	Measured *m/z*	Error [ppm]	Present	S:N	Intensity	Rel. Int. %	Resolution
Y1a 1			No				
Y1a 2			No				
Y1a 3			No				
Original Heslington			No				
H1a 1			No				
H1a 2			No				
H1a 3			No				
H1b 1			No				
H1b 2			No				
H1b 3			No				
H2a 1			No				
H2a 2			No				
H2a 3			No				
H3a 1	514.36793	0.05	Yes	88.2	11984656	2.2	155049
H3a 2	514.36809	-0.26	Yes	81.0	11246054	1.8	153211
H3a 3	514.36784	0.22	Yes	25.4	3401542	0.4	158791
H4a 1	514.36808	-0.24	Yes	407.1	61789488	3.6	154369
H4a 2	514.36826	-0.60	Yes	296.0	45469016	5.2	155438
H4a 3	514.36808	-0.24	Yes	254.5	37720032	4.5	153758
H5a 1			No				
H5a 2	514.36735	1.18	Yes	15.4	2100786	0.7	150159
H5a 3	514.36754	0.81	Yes	15.1	2208481	0.3	169330
H6a 1	514.36801	-0.11	Yes	26.5	3692367	0.5	154496
H6a 2	514.36797	-0.02	Yes	28.1	3821399	0.5	154650
H6a 3	514.36796	0.00	Yes	25.8	3637353	0.4	163567
H7a 1	514.36790	0.11	Yes	8.0	1282543	0.3	168797
H7a 2	514.34842	-0.19	Yes	5.6	1023196	0.2	214214
H7a 3	514.36835	-0.77	Yes	7.7	1252034	0.2	169434
H8a 1			No				
H8a 2	514.36819	-0.46	Yes	148.8	19298170	4.5	151887
H8a 3	514.36790	0.10	Yes	176.0	22345908	4.3	155437
H9a 1	514.36808	-0.24	Yes	531.0	75226112	9.3	154024
H9a 2	514.36803	-0.13	Yes	598.0	85730048	9.9	154411
H9a 3	514.36783	0.24	Yes	181.3	23164522	5.1	154545
H10a 1	514.36795	0.01	Yes	77.4	10297115	1.7	152155
H10a 2	514.36775	0.41	Yes	73.9	8850307	4.5	153336
H10a 3	514.36792	0.07	Yes	198.6	26851648	7.3	153549
H11a 1	514.36830	-0.67	Yes	153.3	19819648	8.7	154280
H11a 2	514.36820	-0.48	Yes	55.2	7543373	1.0	153609
H11a 3	514.36793	0.06	Yes	56.3	6424413	4.9	158314
H12a 1	514.36835	-0.76	Yes	102.1	15030200	3.3	155364
H12a 2	514.36839	-0.85	Yes	84.8	12554708	2.6	151841
H12a 3	514.36835	-0.78	Yes	92.1	13754643	3.4	155484
H13aii 1	514.36831	-0.68	Yes	67.2	9647407	2.4	157098
H13aii 2	514.36830	-0.67	Yes	59.4	8218304	2.1	154490
H13aii 3	514.36816	-0.40	Yes	46.4	6081523	1.0	162265
H14a 1			No				
H14a 2	514.36836	-0.78	Yes	6.1	1186333	0.2	152243
H14a 3			No				
H14bi 1	514.36831	-0.70	Yes	14.8	2511742	0.3	163932
H14bi 2	514.36796	-0.02	Yes	14.8	2421333	0.4	168189
H14bi 3			No				
V1a 1			No				
V1a 2			No				
V1a 3	514.36775	0.41	Yes	7.2	1248831	0.3	156146
B1a 1	514.36826	-0.59	Yes	1335.3	218444224	42.6	154101
B1a 2	514.36800	-0.09	Yes	735.7	100474872	32.8	153211
B1a 3	514.36773	0.44	Yes	500.0	62379800	14.6	154951
DHB 1			No				
DHB 2			No				
DHB 3			No				
Soil 3a 1			No				
Soil 3a 2			No				
Soil 3a 3			No				
Soil 3b 1			No				
Soil 3b 2			No				
Soil 3b 3			No				
Solvent 1			No				
Solvent 2			No				
Solvent 3			No				

The data for a strong peak in the spectrum of brain sample extract H1a at *m/z* 464 are as shown in Table 35. This signal was assigned the formula $[C_{27}H_{39}NO_3] + K^+$, due to the isotope pattern, which has nine degrees of unsaturation. Like the compound in Table 32 this had a very high S:N ratio and so was selected for comparison with other extracts but did not appear in any other spectra, including the controls.

Table 35. Summary of signal at *m/z* 464. $C_xH_yNO_3$

Calculated *m/z*	464.25693 C27H39KNO3						
Sample designation + MALDI replicate no.	Measured *m/z*	Error [ppm]	Present	S:N	Intensity	Rel. Int. %	Resolution
Y1a 1			No				
Y1a 2			No				
Y1a 3			No				
Original Heslington			No				
H1a 1	464.25693		Yes	628.0	78751896	7.9	170723
H1a 2			No				
H1a 3			No				
H1b 1			No				
H1b 2			No				
H1b 3			No				
H2a 1			No				
H2a 2			No				
H2a 3			No				
H3a 1			No				
H3a 2			No				
H3a 3			No				
H4a 1			No				
H4a 2			No				
H4a 3			No				
H5a 1			No				
H5a 2			No				
H5a 3			No				
H6a 1			No				
H6a 2			No				
H6a 3			No				
H7a 1			No				
H7a 2			No				
H7a 3			No				
H8a 1			No				
H8a 2			No				
H8a 3			No				
H9a 1			No				
H9a 2			No				
H9a 3			No				
H10a 1			No				
H10a 2			No				
H10a 3			No				
H11a 1			No				
H11a 2			No				
H11a 3			No				
H12a 1			No				
H12a 2			No				
H12a 3			No				
H13aii 1			No				
H13aii 2			No				
H13aii 3			No				
H14a 1			No				
H14a 2			No				
H14a 3			No				
H14bi 1			No				
H14bi 2			No				
H14bi 3			No				
V1a 1			No				
V1a 2			No				
V1a 3			No				
B1a 1			No				
B1a 2			No				
B1a 3			No				
DHB 1			No				
DHB 2			No				
DHB 3			No				
Soil 3a 1			No				
Soil 3a 2			No				
Soil 3a 3			No				
Soil 3b 1			No				
Soil 3b 2			No				
Soil 3b 3			No				
Solvent 1			No				
Solvent 2			No				
Solvent 3			No				

The peak in the mass spectra at *m/z* 518 (Table 36) was assigned the empirical formula $[C_{34}H_{47}NO_3] + H^+$, with 12 double bond equivalents. This is similar to the compound in Table 33, but with an additional oxygen atom. It has a comparable detection pattern, appearing at high relative intensity and S:N in some of the Hull extracts, especially H8, H9, H10, H11, but less so in H4 than the compound in Table 33. It, too, is entirely absent from H1 (a and b) and H14a and is only in certain replicates of H14b, but is additionally entirely absent from H2. Aside from the Hull extracts this component is not detected in any of the York extracts (modern or the original York analysis) or the Villiers Street extracts. It is also detected in the Blackpool extracts.

Table 36. Summary of signal at *m/z* 518. $C_xH_yNO_3$

Calculated *m/z*	518.36287	C34H48NO3					
Sample designation + MALDI replicate no.	Measured *m/z*	Error [ppm]	Present	S:N	Intensity	Rel. Int. %	Resolution
Y1a 1			No				
Y1a 2			No				
Y1a 3			No				
Original Heslington			No				
H1a 1			No				
H1a 2			No				
H1a 3			No				
H1b 1			No				
H1b 2			No				
H1b 3			No				
H2a 1			No				
H2a 2			No				
H2a 3			No				
H3a 1	518.36266	0.40	Yes	88.9	12232569	2.2	157888
H3a 2	518.36276	0.22	Yes	163.5	22690870	3.7	155489
H3a 3	518.36262	0.49	Yes	56.1	7239467	1.0	158566
H4a 1	518.36282	0.11	Yes	642.3	99304624	5.8	153847
H4a 2	518.36293	-0.12	Yes	487.1	76158800	8.7	155104
H4a 3	518.36281	0.11	Yes	594.8	89382760	10.8	155130
H5a 1	518.36241	0.88	Yes	90.7	10535260	5.5	154855
H5a 2	518.36252	0.68	Yes	132.3	16045343	5.3	155676
H5a 3	518.36243	0.85	Yes	149.4	19501960	2.2	156184
H6a 1	518.36268	0.37	Yes	121.1	16043446	2.2	154896
H6a 2	518.36266	0.40	Yes	198.3	25539116	3.5	157781
H6a 3	518.36265	0.42	Yes	122.1	16335090	1.7	158021
H7a 1	518.36248	0.75	Yes	15.3	2199416	0.5	194175
H7a 2	518.36224	1.22	Yes	14.9	2257825	0.4	177772
H7a 3	518.36218	1.33	Yes	13.2	1956058	0.3	172887
H8a 1	518.36276	0.21	Yes	892.8	126657896	21.8	153869
H8a 2	518.36296	-0.18	Yes	497.9	64706840	15.0	153772
H8a 3	518.36269	0.35	Yes	682.0	86748960	16.8	154132
H9a 1	518.36282	0.10	Yes	1386.0	199198384	24.7	153484
H9a 2	518.36277	0.19	Yes	944.4	137582016	15.9	153737
H9a 3	518.36263	0.46	Yes	877.5	112297096	24.7	153835
H10a 1	518.36272	0.28	Yes	646.2	84869960	14.2	153989
H10a 2	518.36258	0.56	Yes	457.5	53783308	27.6	154534
H10a 3	518.36270	0.32	Yes	1079.1	146589392	39.8	154249
H11a 1	518.36306	-0.37	Yes	736.5	95239560	41.6	154023
H11a 2	518.36302	-0.29	Yes	381.7	51036116	6.7	154481
H11a 3	518.36276	0.21	Yes	237.3	26383118	20.3	154936
H12a 1	518.36317	-0.58	Yes	149.6	22258102	5.0	157616
H12a 2	518.36315	-0.53	Yes	135.1	20151558	4.1	155582
H12a 3	518.36310	-0.44	Yes	139.0	20961076	5.2	155018
H13aii 1	518.36308	-0.40	Yes	52.9	7772386	2.0	162563
H13aii 2	518.36311	-0.46	Yes	62.6	8773785	2.3	157950
H13aii 3	518.36303	-0.30	Yes	32.6	4403227	0.7	167652
H14a 1			No				
H14a 2			No				
H14a 3			No				
H14bi 1	518.36276	0.21	Yes	7.6	1468192	0.2	206577
H14bi 2	518.36307	-0.38	Yes	5.8	1153138	0.2	216090
H14bi 3			No				
V1a 1			No				
V1a 2			No				
V1a 3			No				
B1a 1	518.36298	-0.21	Yes	143.2	24241152	4.7	156444
B1a 2	518.36273	0.28	Yes	92.9	13132001	4.3	155952
B1a 3	518.36249	0.73	Yes	71.5	9261392	2.2	160343
DHB 1			No				
DHB 2			No				
DHB 3			No				
Soil 3a 1			No				
Soil 3a 2			No				
Soil 3a 3			No				
Soil 3b 1			No				
Soil 3b 2			No				
Soil 3b 3			No				
Solvent 1			No				
Solvent 2			No				
Solvent 3			No				

A multiply oxygenated, mono-nitrogenated compound detected in the oldest sample (York) spectra is found at *m/z* 564. A summary of the spectral information for this signal is provided in Table 37. The peak was assigned the formula $[C_{36}H_{69}NO_3] + H^+$, with only three double bond equivalents; this is the most saturated component identified of this class of compound. This component is detected in all sample extracts. It is not detected in the DHB matrix and the peaks in the soil controls and solvent blank replicates are over 2.5 ppm from the calculated *m/z* and so are not considered to be the same component.

In the first replicate of the current York extract the peak had the highest relative intensity, and is also very high in the other two replicates, but it has a low relative intensity % in the original York analysis. This may be due to the instrument upgrades or due to the additional time (before the current extract was made) that the brain sample has spent out of its burial environment and in cold storage, where further chemical changes may have taken place.

In the spectra of all the other sample extracts the relative intensity of the signal is generally low (less than 1%), but all *m/z* values were within an error margin of 1.5 ppm, and the signals have good resolution. The signal is not always detected across all replicates, but only in H14a is it only identified in a single replicate. With such low relative intensities, it may appear in other replicates but would have been excluded using the current screening criteria.

Table 37. Summary of signal at *m/z* 564. $C_xH_yNO_3$

Calculated *m/z*	564.5351	C36H70NO3					
Sample designation + MALDI replicate no.	Measured *m/z*	Error [ppm]	Present	S:N	Intensity	Rel. Int. %	Resolution
Y1a 1	564.53510	-0.14	Yes	2064.2	300621824	100.0	140835
Y1a 2	564.53492	0.18	Yes	1671.4	232160384	85.3	141016
Y1a 3	564.53503	-0.02	Yes	1953.8	286345344	83.1	141489
Original Heslington	564.53446	0.99	Yes	35.7	4123617	3.3	87473
H1a 1	564.53485	0.31	Yes	16.4	2712414	0.3	147223
H1a 2	564.53463	0.69	Yes	13.0	1919697	0.5	164774
H1a 3			No				
H1b 1	564.53457	0.80	Yes	32.8	4571409	0.5	142282
H1b 2	564.53496	0.10	Yes	18.3	2610413	0.7	126762
H1b 3	564.53460	0.74	Yes	24.3	3345208	0.8	145493
H2a 1	564.53440	1.09	Yes	27.3	3729277	0.7	146562
H2a 2	564.53459	0.77	Yes	16.4	2712781	0.8	148130
H2a 3	564.53449	0.95	Yes	13.9	1925929	0.5	160252
H3a 1	564.53484	0.32	Yes	36.2	5497974	1.0	152486
H3a 2	564.53505	-0.06	Yes	30.8	4835127	0.8	138429
H3a 3	564.53424	1.39	Yes	9.8	1575588	0.2	132229
H4a 1	564.53510	-0.14	Yes	99.1	17229292	1.0	140893
H4a 2	564.53529	-0.48	Yes	71.6	12675803	1.4	144168
H4a 3	564.53519	-0.30	Yes	82.0	13801866	1.7	142343
H5a 1	564.53462	0.72	Yes	43.9	5416951	2.8	146895
H5a 2	564.53466	0.63	Yes	60.8	7854402	2.6	142963
H5a 3	564.53473	0.52	Yes	79.7	11195468	1.3	141238
H6a 1	564.53506	0.07	Yes	11.4	1879858	0.3	158702
H6a 2	564.53482	0.36	Yes	12.6	1991295	0.3	146572
H6a 3	564.53467	0.61	Yes	18.2	2852124	0.3	162523
H7a 1	564.53438	1.14	Yes	7.6	1302116	0.3	160893
H7a 2	564.53524	-0.38	Yes	8.0	1425992	0.2	172349
H7a 3	564.53499	0.05	Yes	8.6	1448073	0.2	149014
H8a 1	564.53496	0.10	Yes	30.6	5000042	0.9	145666
H8a 2	564.53541	-0.69	Yes	29.3	4351590	1.0	139463
H8a 3	564.53492	0.18	Yes	20.0	2988841	0.6	155747
H9a 1	564.53520	-0.31	Yes	16.3	2864749	0.4	157521
H9a 2	564.53522	-0.36	Yes	18.3	3221405	0.4	166940
H9a 3	564.53472	0.53	Yes	7.2	1278939	0.3	189045
H10a 1	564.53512	-0.17	Yes	6.9	1257855	0.2	166956
H10a 2	564.53459	0.77	Yes	10.9	1619946	0.8	150187
H10a 3	564.53483	0.33	Yes	27.0	4234809	1.2	154984
H11a 1	564.53539	-0.65	Yes	34.9	5090939	2.2	149031
H11a 2	564.53543	-0.73	Yes	21.6	3367782	0.4	145466
H11a 3			No				
H12a 1	564.53555	-0.94	Yes	35.3	5964161	1.3	147560
H12a 2	564.53542	-0.71	Yes	34.6	5864499	1.2	141797
H12a 3	564.53547	-0.79	Yes	31.3	5399150	1.3	153234
H13aii 1	564.53550	-0.85	Yes	44.2	7073855	1.8	146663
H13aii 2	564.53530	-0.49	Yes	44.7	6820341	1.8	142995
H13aii 3	564.53537	-0.61	Yes	34.7	4937962	0.8	145157
H14a 1			No				
H14a 2	564.53493	0.16	Yes	10.3	1965286	0.3	148810
H14a 3			No				
H14bi 1	564.53553	-0.90	Yes	12.7	2410267	0.3	159603
H14bi 2	564.53543	-0.73	Yes	7.6	1508035	0.2	169366
H14bi 3			No				
V1a 1			No				
V1a 2	564.53552	-0.89	Yes	11.1	1875552	0.3	145011
V1a 3	564.53475	0.48	Yes	6.4	1227756	0.3	172431
B1a 1	564.53537	-0.62	Yes	65.0	12500726	2.4	143053
B1a 2	564.53500	0.05	Yes	39.9	6266823	2.0	148960
B1a 3	564.53480	0.39	Yes	27.6	3957757	0.9	136427
DHB 1			No				
DHB 2			No				
DHB 3			No				
Soil 3a 1			No				
Soil 3a 2			No				
Soil 3a 3	564.53689	-3.31	No	6.2	1482324	0.3	138714
Soil 3b 1			No				
Soil 3b 2	564.53650	-2.63	No	9.5	2061998	0.1	144554
Soil 3b 3			No				
Solvent 1	564.53673	-3.03	No	6.8	1721876	0.0	146498
Solvent 2			No				
Solvent 3			No				

Table 38 shows the data for the peak at *m/z* 648, assigned $[C_{42}H_{81}NO_3]$ + H^+, with three double bond equivalents. This peak is detected in the spectra of nearly all the sample extracts, if not in all the replicates, but it was not detected in the original analysis of the York brain extract. This may have been due to the change in instrumentation or additional time in storage. The strongest S:N and relative intensity % for this peak were found in the spectra for the extracts of H5, H10 and H11. It was only detected with small S:N and relative intensity % in the spectra for H1a, H14 (a and b) and V1. Most of the detections in the soil and solvent controls were over 2 ppm away from the calculated *m/z* and so are considered not to be the same compound. However, one signal fell within this error range, and so could be considered to indicate compound's presence within the soil background. However, the *m/z* value assigned is well outside the 1.5 ppm error margin within which all the other sample *m/z* values are measured, and so there must be doubt about this identification in the one soil replicate.

Table 38. Summary of signal at *m/z* 648. $C_xH_yNO_3$

Calculated *m/z*	648.62892	C42H82NO3					
Sample designation + MALDI replicate no.	Measured *m/z*	Error [ppm]	Present	S:N	Intensity	Rel. Int. %	Resolution
Y1a 1	648.62901	0.05	Yes	99.2	16093210	5.4	124633
Y1a 2	648.62883	-0.90	Yes	67.9	10491214	3.9	125730
Y1a 3	648.62895	-0.13	Yes	116.1	18842400	5.5	124709
Original Heslington			No				
H1a 1	648.62878	0.21	Yes	118.7	17780358	1.8	125538
H1a 2	648.62856	0.56	Yes	111.9	15138508	3.8	124695
H1a 3	648.62845	0.73	Yes	158.1	20621118	3.1	122342
H1b 1	648.62840	0.81	Yes	301.3	41476884	4.8	123791
H1b 2	648.62189	0.80	Yes	294.7	39214316	10.2	121074
H1b 3	648.62827	1.01	Yes	362.7	47760348	11.3	122900
H2a 1	648.62822	1.09	Yes	528.2	68771144	12.8	123001
H2a 2	648.62833	0.91	Yes	198.0	29561560	8.9	122528
H2a 3	648.62841	0.79	Yes	152.7	19130522	5.4	124318
H3a 1	648.62882	0.16	Yes	273.4	39362500	7.1	123699
H3a 2	648.62900	-0.12	Yes	340.2	50194572	8.2	121299
H3a 3	648.62858	0.53	Yes	112.4	15113936	2.0	123344
H4a 1	648.62896	-0.07	Yes	551.1	94425016	5.5	123297
H4a 2	648.62934	-0.64	Yes	267.0	49199552	5.6	123524
H4a 3	648.62907	-0.23	Yes	413.8	71159000	8.6	124023
H5a 1	648.62828	0.86	Yes	623.9	75403760	39.6	123197
H5a 2	648.62843	0.76	Yes	498.6	64293572	21.1	122844
H5a 3	648.62839	0.82	Yes	361.6	50850196	5.8	123112
H6a 1	648.62885	0.11	Yes	141.4	20141758	2.7	124575
H6a 2	648.62879	0.20	Yes	182.8	25304904	3.4	124073
H6a 3	648.62877	0.24	Yes	202.7	28714906	3.1	125073
H7a 1	648.62876	0.25	Yes	200.3	28058438	6.9	123186
H7a 2	648.62884	0.12	Yes	159.4	23852888	3.8	122674
H7a 3	648.62876	0.25	Yes	200.1	28297852	4.2	123599
H8a 1	648.62889	0.05	Yes	485.6	74201520	12.8	122968
H8a 2	648.62898	-0.08	Yes	292.0	41582808	9.6	120696
H8a 3	648.62866	0.40	Yes	368.3	50398348	9.8	121716
H9a 1	648.62881	0.18	Yes	281.8	43035688	5.3	122861
H9a 2	648.62892	0.00	Yes	268.6	41374524	4.8	123168
H9a 3	648.62845	0.72	Yes	125.9	17437172	3.8	126732
H10a 1	648.62876	0.25	Yes	165.8	23643404	4.0	123349
H10a 2	648.62846	0.71	Yes	195.8	24642084	12.6	121911
H10a 3	648.62874	0.27	Yes	652.6	94883208	25.8	123592
H11a 1	648.62930	-0.59	Yes	411.5	60014560	26.2	123145
H11a 2	648.62934	-0.65	Yes	219.9	32711356	4.3	124971
H11a 3	648.62884	0.13	Yes	133.3	15880724	12.2	126700
H12a 1	648.62955	-0.97	Yes	439.4	72870264	16.2	122843
H12a 2	648.62958	-1.02	Yes	396.2	64979128	13.2	123516
H12a 3	648.62950	-0.89	Yes	285.9	48197292	12.0	124118
H13aii 1	648.62944	-0.80	Yes	338.7	55595496	14.1	123730
H13aii 2	648.62937	-0.69	Yes	345.0	52957304	13.6	121875
H13aii 3	648.62923	-0.47	Yes	264.4	37770488	6.4	123733
H14a 1			No				
H14a 2	648.62885	0.12	Yes	10.2	1942652	0.3	141524
H14a 3			No				
H14bi 1	648.62906	-0.21	Yes	12.4	2358631	0.3	133991
H14bi 2	648.62889	0.05	Yes	6.8	1377159	0.2	128338
H14bi 3			No				
V1a 1	648.62895	0.03	Yes	88.5	14693231	0.7	124974
V1a 2	648.62905	-0.20	Yes	111.3	17534086	2.8	123787
V1a 3	648.62897	0.07	Yes	68.2	10688888	2.3	122848
B1a 1	648.62930	-0.58	Yes	219.0	39446188	7.7	122936
B1a 2	648.62880	0.19	Yes	162.8	24344622	7.9	124341
B1a 3	648.62858	0.53	Yes	224.3	29983818	7.0	124155
DHB 1			No				
DHB 2			No				
DHB 3			No				
Soil 3a 1	648.63127	-3.62	No	10.9	2638290	0.3	136532
Soil 3a 2			No				
Soil 3a 3	648.63112	-3.39	No	7.1	1803418	0.4	128716
Soil 3b 1	648.63149	-3.96	No				
Soil 3b 2	648.63061	-2.60	No				
Soil 3b 3	648.63013	-1.86	Yes	5.6	1577305	0.3	140991
Solvent 1	648.63090	-3.05	No	13.3	3275128	0.1	122879
Solvent 2	648.63125	-3.59	No	5.4	1528911	0.2	146137
Solvent 3	648.63127	-2.11	No	10.9	2638290	0.3	136532

A more highly oxygenated compound was assigned to the peak at *m/z* 584. This was assigned the formula $[C_{36}H_{73}NO_4] + H^+$, which has a single double bond equivalent. Table 39 shows that this compound was not detected in any of the controls or the youngest sample extracts, B1 and V1. It was sporadically detected in the Hull samples but the peak was most strongly seen in the spectra for Y1, with high S:N, intensities and relative intensity %s. It wasn't detected in all the Hull samples, only consistently across all replicates of H1 (a and b), H2, H4 and H5. This pattern may suggest that this is a later stage degradation product, produced after a series of other chemical changes over time, and so is more apparent in older samples. It may also indicate that some aspect of the York site was conducive to its formation or preservation within the original sample burial, and so this component appears higher in intensity. The intensity within the York sample extract compared to the Hull samples may indicate it is observed in larger quantities in the York extract, but may alternatively indicate that the abundance of other chemical compounds has decreased, so it appears more prominent.

Table 39. Summary of signal at *m/z* 584. $C_xH_yNO_4$

Calculated *m/z*	584.56124	C36H74NO4					
Sample designation + MALDI replicate no.	Measured *m/z*	Error [ppm]	Present	S:N	Intensity	Rel. Int. %	Resolution
Y1a 1	584.56131	-0.13	Yes	1368.1	203449392	67.7	136145
Y1a 2	584.56114	0.17	Yes	1182.3	167242288	61.4	136343
Y1a 3	584.56124	0.00	Yes	1441.9	215606560	62.6	136331
Original Heslington	584.56144	-0.35	Yes	14.2	1799286	1.4	93241
H1a 1	584.56126	-0.04	Yes	16.2	2700206	0.3	130673
H1a 2	584.56127	-0.06	Yes	19.3	2738609	0.7	144345
H1a 3	584.56106	0.30	Yes	11.5	1752962	0.3	128411
H1b 1	584.56088	0.61	Yes	39.9	5557330	0.6	136814
H1b 2	584.56088	0.61	Yes	28.7	3963520	1.0	135549
H1b 3	584.56076	0.82	Yes	31.4	4278210	1.0	143079
H2a 1	584.56029	1.62	Yes	11.9	1808492	0.3	158998
H2a 2	584.56023	1.72	Yes	4.9	1038248	0.3	140783
H2a 3	584.56138	-0.25	Yes	5.8	980427	0.3	182015
H3a 1	584.56100	0.40	Yes	8.0	1456096	0.3	192619
H3a 2	584.56175	-0.88	Yes	5.7	1149639	0.2	149974
H3a 3			No				
H4a 1	584.56152	-0.49	Yes	19.7	3680560	0.2	145935
H4a 2	584.56183	-1.01	Yes	12.3	2481338	0.3	161676
H4a 3	584.56152	-0.49	Yes	16.5	3071738	0.4	142030
H5a 1	584.56073	0.86	Yes	51.4	6332522	3.3	138210
H5a 2	584.56081	0.73	Yes	64.4	8365240	2.8	139116
H5a 3	584.56083	0.69	Yes	75.2	10639891	1.2	138393
H6a 1			No				
H6a 2			No				
H6a 3			No				
H7a 1			No				
H7a 2			No				
H7a 3			No				
H8a 1	584.56112	0.19	Yes	16.0	2763860	0.5	144355
H8a 2			No				
H8a 3	584.56100	0.40	Yes	9.1	1526385	0.3	163987
H9a 1			No				
H9a 2			No				
H9a 3			No				
H10a 1			No				
H10a 2			No				
H10a 3			No				
H11a 1	584.56154	-0.53	Yes	12.1	1991546	0.9	145429
H11a 2			No				
H11a 3	584.56124	-0.01	Yes	6.8	1055299	0.8	115744
H12a 1			No				
H12a 2			No				
H12a 3	584.54109	-1.88	Yes	12.7	2398897	0.6	134144
H13aii 1	584.56239	-1.97	No	5.0	1101857	0.3	181937
H13aii 2	584.56183	-1.02	Yes	4.0	905513	0.2	172240
H13aii 3			No				
H14a 1			No				
H14a 2			No				
H14a 3			No				
H14bi 1	584.56189	-1.12	Yes	6.2	1357554	0.2	167677
H14bi 2			No				
H14bi 3			No				
V1a 1			No				
V1a 2			No				
V1a 3			No				
B1a 1			No				
B1a 2			No				
B1a 3			No				
DHB 1			No				
DHB 2			No				
DHB 3			No				
Soil 3a 1			No				
Soil 3a 2			No				
Soil 3a 3			No				
Soil 3b 1			No				
Soil 3b 2			No				
Soil 3b 3			No				
Solvent 1			No				
Solvent 2			No				
Solvent 3			No				

A dinitrogenated, dioxygenated hydrocarbon was identified as likely occurring at *m/z* 527, shown in Table 40. This was assigned $[C_{35}H_{46}N_2O_2] + H^+$, which has 14 double bond equivalents and is highly unsaturated. It is a significant peak in the spectra from the H9 and B1 replicates, with high S:N, intensity and relative intensity %. It was detected in the current York extract but not the original York analysis. It was not detected in several of the Hull sample extracts (H1a and b, H2, H14a) and not in the Villiers Street extract either.

Table 40. Summary of signal at *m/z* 527. $C_xH_yN_2O_2$

Calculated *m/z*	527.36321 C35H47N2O2						
Sample designation + MALDI replicate no.	Measured *m/z*	Error [ppm]	Present	S:N	Intensity	Rel. Int. %	Resolution
Y1a 1	527.36310	0.19	Yes	15.4	2407194	0.8	155586
Y1a 2	527.36317	0.07	Yes	13.9	2121042	0.8	175514
Y1a 3	527.36293	0.52	Yes	16.5	2582634	0.7	153741
Original Heslington			No				
H1a 1			No				
H1a 2			No				
H1a 3			No				
H1b 1			No				
H1b 2			No				
H1b 3			No				
H2a 1			No				
H2a 2			No				
H2a 3			No				
H3a 1	527.36310	0.20	Yes	34.9	5038793	0.9	160418
H3a 2	527.36316	0.08	Yes	43.0	6275630	1.0	151645
H3a 3	527.36292	0.54	Yes	22.7	3132787	0.4	154295
H4a 1	527.36316	0.09	Yes	700.6	110532424	6.5	149541
H4a 2	527.36333	-0.24	Yes	562.3	89672432	10.3	150159
H4a 3	527.36317	0.06	Yes	482.5	73923080	8.9	150662
H5a 1	527.36255	1.24	Yes	21.1	2675446	1.4	157538
H5a 2	527.36284	0.69	Yes	26.7	3492171	1.1	156068
H5a 3	527.36280	0.76	Yes	44.8	6129583	0.7	153601
H6a 1	527.36306	0.27	Yes	42.4	5867731	0.8	154069
H6a 2	527.36309	0.22	Yes	56.4	7547188	1.0	154824
H6a 3	527.36306	0.27	Yes	46.5	6471623	0.7	156019
H7a 1	527.36328	-0.15	Yes	6.5	1112263	0.3	153112
H7a 2	527.36294	0.50	Yes	7.9	1353442	0.2	142440
H7a 3	527.36310	0.20	Yes	13.9	2066137	0.3	142089
H8a 1	527.36313	0.15	Yes	505.9	73038296	12.6	150279
H8a 2	527.36329	-0.15	Yes	335.8	44295324	10.3	149286
H8a 3	527.36304	0.32	Yes	367.3	47395096	9.2	150500
H9a 1	527.36318	0.04	Yes	1082.6	158351728	19.6	149933
H9a 2	527.36312	0.15	Yes	885.6	131315360	15.2	149920
H9a 3	527.36299	0.41	Yes	590.9	76607448	16.9	149109
H10a 1	527.36311	0.18	Yes	170.5	22887994	3.8	151409
H10a 2	527.36292	0.55	Yes	144.9	17364808	8.9	149823
H10a 3	527.36307	0.26	Yes	303.2	41969720	11.4	150384
H11a 1	527.36343	-0.42	Yes	271.5	35718248	15.6	151352
H11a 2	527.36342	-0.40	Yes	161.3	22009662	2.9	150180
H11a 3	527.36315	0.11	Yes	99.4	11274921	8.7	152571
H12a 1	527.36351	-0.58	Yes	111.9	17008854	3.8	151545
H12a 2	527.36355	-0.65	Yes	109.6	16683979	3.4	149207
H12a 3	527.36351	-0.58	Yes	125.3	19260306	4.8	148149
H13aii 1	527.36344	-0.45	Yes	69.5	10281454	2.6	152611
H13aii 2	527.36351	-0.58	Yes	71.3	10085382	2.6	150640
H13aii 3	527.36337	-0.31	Yes	54.5	7252952	1.2	152249
H14a 1			No				
H14a 2			No				
H14a 3			No				
H14bi 1			No				
H14bi 2	527.36394	-1.39	Yes	6.3	1239415	0.2	162114
H14bi 3			No				
V1a 1			No				
V1a 2			No				
V1a 3			No				
B1a 1	527.36334	-0.26	Yes	647.2	110952312	21.6	149627
B1a 2	527.36311	0.18	Yes	420.9	59378720	19.4	149720
B1a 3	527.36288	0.61	Yes	277.7	35532948	8.3	151445
DHB 1			No				
DHB 2			No				
DHB 3			No				
Soil 3a 1			No				
Soil 3a 2			No				
Soil 3a 3			No				
Soil 3b 1			No				
Soil 3b 2			No				
Soil 3b 3			No				
Solvent 1			No				
Solvent 2			No				
Solvent 3			No				

Table 41 shows a summary for the peak at *m/z* 731. This ion was assigned the formula $[C_{46}H_{80}N_2O_3] + Na^+$, which has eight double bond equivalents and was a high intensity peak in the H12 spectra. The peak was detected in spectra from all sites/ages and not in any of the controls. The S:N and relative intensity % were also relatively large, across all replicates in Y1, H4, H11 and H13. It was undetected in H14, a and b.

Table 41. Summary of signal at *m/z* 731. $C_xH_yN_2O_3$

Calculated *m/z*	731.60612	C46H80N2NaO3					
Sample designation + MALDI replicate no.	Measured *m/z*	Error [ppm]	Present	S:N	Intensity	Rel. Int. %	Resolution
Y1a 1	731.60606	0.08	Yes	431.3	74481144	24.8	108712
Y1a 2	731.60578	0.46	Yes	408.1	65856728	24.2	109025
Y1a 3	731.60597	0.20	Yes	417.0	72113800	20.9	109527
Original Heslington	731.60492	1.63	Yes	18.9	2545543	2.0	69233
H1a 1	731.60579	0.45	Yes	157.9	23600660	2.4	109553
H1a 2	731.60555	0.78	Yes	669.1	93945304	23.5	109367
H1a 3	731.60552	0.81	Yes	142.1	18932144	2.9	111040
H1b 1	731.60537	1.01	Yes	81.7	11980917	1.4	110406
H1b 2	731.60538	1.00	Yes	79.4	11229051	2.9	107597
H1b 3	731.60530	1.11	Yes	82.5	11543488	2.7	111401
H2a 1	731.60521	1.24	Yes	326.3	43821056	8.1	109485
H2a 2	731.60530	1.12	Yes	226.2	33912260	10.2	110110
H2a 3	731.60551	0.83	Yes	131.6	17168828	4.8	112604
H3a 1	731.60589	0.31	Yes	75.3	11045808	2.0	111672
H3a 2	731.60602	0.13	Yes	79.4	11955923	2.0	110189
H3a 3	731.60573	0.53	Yes	29.2	4200968	0.6	107295
H4a 1	731.60599	0.16	Yes	1143.8	195700720	11.4	109347
H4a 2	731.60639	-0.38	Yes	688.2	133400800	15.3	109428
H4a 3	731.60608	0.05	Yes	722.1	128661304	15.5	109866
H5a 1	731.60542	0.95	Yes	46.9	6101208	3.2	113236
H5a 2	731.60539	0.99	Yes	62.3	8541047	2.8	109447
H5a 3	731.60529	1.13	Yes	57.1	8473195	1.0	108454
H6a 1	731.60588	0.32	Yes	506.9	72430552	9.8	109233
H6a 2	731.60587	0.34	Yes	522.7	72704688	9.9	109700
H6a 3	731.60582	0.40	Yes	726.2	102298192	10.9	109572
H7a 1	731.60586	0.35	Yes	17.2	2824545	0.7	122070
H7a 2	731.60589	0.30	Yes	26.1	4390243	0.7	112877
H7a 3	731.60640	-0.38	Yes	9.6	1735542	0.3	131899
H8a 1	731.60603	0.12	Yes	72.8	11335620	1.9	109012
H8a 2	731.60628	-0.23	Yes	72.0	10719546	2.5	111715
H8a 3	731.60567	0.61	Yes	72.2	10241692	2.0	109061
H9a 1	731.60591	0.28	Yes	171.4	25518382	3.2	109426
H9a 2	731.60589	0.31	Yes	223.3	33173400	3.8	109699
H9a 3	731.60553	0.79	Yes	100.0	13973069	3.1	108370
H10a 1			No				
H10a 2			No				
H10a 3	731.60567	0.61	Yes	36.2	5544880	1.5	113529
H11a 1	731.60650	-0.53	Yes	880.7	134848896	58.9	109146
H11a 2	731.60648	-0.50	Yes	560.1	85828920	11.2	109402
H11a 3	731.60594	0.24	Yes	268.6	32620636	25.1	109396
H12a 1	731.60667	-0.76	Yes	2643.1	449381664	100.0	109316
H12a 2	731.60668	-0.78	Yes	2353.8	391142208	79.5	108873
H12a 3	731.60667	-0.76	Yes	2335.1	402325024	100.0	109486
H13aii 1	731.60658	-0.64	Yes	1697.4	294104992	74.5	109464
H13aii 2	731.60661	-0.68	Yes	1302.9	208053136	53.4	108949
H13aii 3	731.60638	-0.36	Yes	1055.4	157992192	26.8	109359
H14a 1			No				
H14a 2			No				
H14a 3			No				
H14bi 1			No				
H14bi 2			No				
H14bi 3			No				
V1a 1			No				
V1a 2	731.60624	-0.18	Yes	12.5	2434107	0.4	119751
V1a 3	731.60606	-0.29	Yes	431.3	74481144	24.8	108712
B1a 1	731.60633	-0.30	Yes	110.6	19178724	3.7	108882
B1a 2	731.60597	0.20	Yes	86.5	12937856	4.2	110062
B1a 3	731.60558	0.74	Yes	53.2	7331857	1.7	114884
DHB 1			No				
DHB 2			No				
DHB 3			No				
Soil 3a 1			No				
Soil 3a 2			No				
Soil 3a 3			No				
Soil 3b 1			No				
Soil 3b 2			No				
Soil 3b 3			No				
Solvent 1	731.60852	-3.28	No	4.0	1322414	0.0	120898
Solvent 2			No				
Solvent 3			No				

The peak at *m/z* 759, see Table 42, was assigned $[C_{48}H_{84}N_2O_3] + Na^+$, which has eight double bond equivalents and is the equivalent of the compound in Table 41 with the addition of CH_2-CH_2. It has a similar detection pattern to the smaller analogue compound summarised in Table 41, with the most prominent peak intensities being found in the spectra from the H12 extract, followed by H11 and H13. The S:N and intensities are reduced in Y1 and H4 as compared to those in the previous table and as well as being undetected in H14, a and b, it is also only detected in a single replicate from H10 and V1 (and these have errors of over 1.5 ppm), and does not appear in the original York analysis.

Table 42. Summary of signal at *m/z* 759. $C_xH_yN_2O_3$

Calculated *m/z*	759.63742	C48H84N2NaO3					
Sample designation + MALDI replicate no.	Measured *m/z*	Error [ppm]	Present	S:N	Intensity	Rel. Int. %	Resolution
Y1a 1	759.63761	-0.26	Yes	47.5	8510727	2.8	107368
Y1a 2	759.63721	0.27	Yes	39.1	6602984	2.4	109644
Y1a 3	759.63749	-0.10	Yes	43.3	7799512	2.3	103897
Original Heslington			No				
H1a 1	759.63723	0.24	Yes	20.9	3388549	0.3	110255
H1a 2	759.63694	0.62	Yes	82.6	11837839	3.0	106744
H1a 3	759.63684	0.75	Yes	16.8	2515897	0.4	117717
H1b 1	759.63751	-0.13	Yes	10.7	1846131	0.2	111040
H1b 2	759.63692	0.65	Yes	10.0	1695273	0.4	129799
H1b 3	759.63595	1.92	Yes	13.0	2078070	0.5	109826
H2a 1	759.63641	1.33	Yes	65.6	9063418	1.7	107271
H2a 2	759.63649	1.22	Yes	32.0	5052156	1.5	112804
H2a 3	759.63679	0.82	Yes	24.0	3397970	1.0	108491
H3a 1	759.63711	0.40	Yes	19.2	3049540	0.6	125398
H3a 2	759.63737	0.06	Yes	23.5	3789676	0.6	115369
H3a 3	759.63746	-0.07	Yes	9.1	1520418	0.2	132162
H4a 1	759.63748	-0.08	Yes	245.3	42194416	2.5	104982
H4a 2	759.63801	-0.79	Yes	155.9	30616924	3.5	104513
H4a 3	759.63761	-0.26	Yes	175.7	31701422	3.8	105301
H5a 1	759.63711	0.41	Yes	8.4	1346318	0.7	118240
H5a 2	759.63664	1.02	Yes	11.5	1848622	0.6	119835
H5a 3	759.63707	0.46	Yes	12.3	2092409	0.2	126682
H6a 1	759.63743	-0.02	Yes	60.3	8916724	1.2	104087
H6a 2	759.63733	0.11	Yes	57.7	8318443	1.1	104147
H6a 3	759.63715	0.34	Yes	81.5	11757740	1.3	106210
H7a 1	759.63710	0.42	Yes	7.3	1391201	0.3	101635
H7a 2	759.63725	0.22	Yes	11.7	2149101	0.3	114629
H7a 3	759.63779	-0.50	Yes	6.3	1258591	0.2	141213
H8a 1	759.63814	-0.96	Yes	5.5	1165527	0.2	134914
H8a 2	759.63782	-0.54	Yes	5.1	1071092	0.2	154618
H8a 3	759.63684	0.75	Yes	15.6	2462678	0.5	114847
H9a 1	759.63757	-0.21	Yes	19.8	3241050	0.4	106578
H9a 2	759.63741	0.01	Yes	47.9	7366484	0.9	103676
H9a 3	759.63674	0.89	Yes	20.1	3075659	0.7	101719
H10a 1			No				
H10a 2	759.68361	1.83	Yes	7.0	1199706	0.6	107767
H10a 3			No				
H11a 1	759.63797	-0.73	Yes	126.0	19614886	8.6	105231
H11a 2	759.63788	-0.61	Yes	74.6	11785283	1.5	107295
H11a 3	759.63729	0.17	Yes	39.8	5100703	3.9	113802
H12a 1	759.63823	-1.08	Yes	1949.5	329006080	73.2	105157
H12a 2	759.63824	-1.08	Yes	1905.1	314519072	63.9	104734
H12a 3	759.63823	-1.07	Yes	1564.2	267634096	66.5	105179
H13aii 1	759.63814	-0.95	Yes	533.3	92353568	23.4	104825
H13aii 2	759.63812	-0.93	Yes	366.9	58804596	15.1	104388
H13aii 3	759.63776	-0.46	Yes	316.7	47645124	8.1	104783
H14a 1			No				
H14a 2			No				
H14a 3			No				
H14bi 1			No				
H14bi 2			No				
H14bi 3			No				
V1a 1			No				
V1a 2	759.63639	1.35	Yes	4.2	1041308	0.2	154604
V1a 3			No				
B1a 1	759.63802	-0.73	Yes	96.6	16846912	3.3	105694
B1a 2	759.63736	0.08	Yes	58.9	8974776	2.9	105138
B1a 3	759.63706	0.47	Yes	42.7	5989972	1.4	107471
DHB 1			No				
DHB 2			No				
DHB 3			No				
Soil 3a 1			No				
Soil 3a 2			No				
Soil 3a 3			No				
Soil 3b 1			No				
Soil 3b 2			No				
Soil 3b 3			No				
Solvent 1			No				
Solvent 2			No				
Solvent 3			No				

Although the extracts contained a range of oxygenated and nitrogenated hydrocarbons, interestingly there were very few examples of hydrocarbons that contained only oxygen. The tentative assignment of a highly oxygenated organic compound giving a signal at *m/z* 321 is shown in Table 43, as $[C_{12}H_{26}O_7] + K^+$. This compound is fully saturated and so is suggested to be a fatty alcohol, presumably related to the fatty acids found in brains. It was a significant signal in the spectrum of the extract of sample H6, with both high S:N and relative intensity, consistent across all replicates. The peak was detected in the spectra of some other sample extracts (such as H5 and H11) but not consistently across all replicates. It is detected in both Y1 and V1 extracts but not in the extract of the youngest sample, B1. The ionisation of this compound is unusual; although salts are likely to be present within the matrix and sample, proton ionisation was observed much more consistently. However, this component is chemically quite distinct from the majority of the components detected, which were large organics, and so it is not impossible to imagine that a short fatty alcohol may behave differently. Because of the *m/z* range used for recording the spectra, it isn't possible to determine whether its protonated molecule is also formed.

Table 43. Summary of signal at *m/z* 321. $C_xH_yO_7$

Calculated *m/z*	321.13101 C12H26KO7						
Sample designation + MALDI replicate no.	Measured *m/z*	Error [ppm]	Present	S:N	Intensity	Rel. Int. %	Resolution
Y1a 1			No				
Y1a 2			No				
Y1a 3	321.13074	0.85	Yes	4.0	675447	0.2	321769
Original Heslington			No				
H1a 1			No				
H1a 2			No				
H1a 3			No				
H1b 1			No				
H1b 2			No				
H1b 3			No				
H2a 1			No				
H2a 2			No				
H2a 3			No				
H3a 1			No				
H3a 2			No				
H3a 3			No				
H4a 1			No				
H4a 2			No				
H4a 3			No				
H5a 1	321.13063	1.19	Yes	6.2	883556	0.5	221107
H5a 2	321.13060	1.29	Yes	4.5	717497	0.2	313717
H5a 3			No				
H6a 1	321.13077	0.74	Yes	4256.3	447302528	60.4	248874
H6a 2	321.13077	0.75	Yes	4340.1	451906560	61.5	248872
H6a 3	321.13077	0.74	Yes	4964.9	522470560	55.6	248835
H7a 1			No				
H7a 2			No				
H7a 3			No				
H8a 1			No				
H8a 2			No				
H8a 3			No				
H9a 1			No				
H9a 2			No				
H9a 3	321.13097	0.12	Yes	14.2	1715155	0.4	276080
H10a 1			No				
H10a 2			No				
H10a 3			No				
H11a 1			No				
H11a 2	321.13078	0.72	Yes	96.5	10469033	1.4	246020
H11a 3	321.13068	1.02	Yes	57.4	5948500	4.6	256978
H12a 1			No				
H12a 2			No				
H12a 3			No				
H13aii 1			No				
H13aii 2			No				
H13aii 3			No				
H14a 1			No				
H14a 2			No				
H14a 3			No				
H14bi 1	321.13085	0.50	Yes	36.4	4299900	0.5	239254
H14bi 2	321.13104	-0.08	Yes	6.2	946564	0.1	271734
H14bi 3			No				
V1a 1			No				
V1a 2	321.13081	0.64	Yes	10.1	1326132	0.2	260154
V1a 3			No				
B1a 1			No				
B1a 2			No				
B1a 3			No				
DHB 1			No				
DHB 2			No				
DHB 3			No				
Soil 3a 1			No				
Soil 3a 2			No				
Soil 3a 3			No				
Soil 3b 1			No				
Soil 3b 2			No				
Soil 3b 3			No				
Solvent 1			No				
Solvent 2			No				
Solvent 3			No				

A further highly oxygenated fully saturated organic compound that was identified was detected at *m/z* 365 and, like the signal at *m/z* 321, was also observed with high S:N and intensity in the data from sample H6. This was assigned $[C_{14}H_{30}O_8] + K^+$ and is shown in Table 44. Its presence was detected in several other sample extracts but not across all replicates and it was also detected in one replicate of the soil and of the solvent blank. The very high relative intensity of the signal in the H6 extract spectra suggest it may be present in high quantities in this sample - the relative intensities in the soil and solvent blank single replicates are very low.

Table 44. Summary of signal at *m/z* 365. $C_xH_yO_8$

Calculated *m/z*	365.15723	C14H30KO8					
Sample designation + MALDI replicate no.	Measured *m/z*	Error [ppm]	Present	S:N	Intensity	Rel. Int. %	Resolution
Y1a 1	365.15697	0.71	Yes	6.8	969444	0.3	186296
Y1a 2	365.15704	0.51	Yes	4.1	678823	0.2	300038
Y1a 3			No				
Original Heslington			No				
H1a 1			No				
H1a 2			No				
H1a 3	365.15691	0.87	Yes	7.7	1058937	0.2	211783
H1b 1	365.15694	0.77	Yes	13.5	1665357	0.2	263615
H1b 2			No				
H1b 3	365.15685	1.04	Yes	7.6	1044679	0.2	246899
H2a 1			No				
H2a 2			No				
H2a 3			No				
H3a 1			No				
H3a 2			No				
H3a 3	365.15664	1.59	Yes	7.7	1056455	0.1	241676
H4a 1			No				
H4a 2			No				
H4a 3			No				
H5a 1			No				
H5a 2			No				
H5a 3			No				
H6a 1	365.15708	0.39	Yes	5812.8	610774784	82.5	219108
H6a 2	365.15707	0.41	Yes	5866.4	610736448	83.1	218926
H6a 3	365.15708	0.41	Yes	6822.4	717843712	76.4	219195
H7a 1			No				
H7a 2			No				
H7a 3			No				
H8a 1			No				
H8a 2	365.15695	0.77	Yes	5.1	766377	0.2	232727
H8a 3			No				
H9a 1			No				
H9a 2			No				
H9a 3	365.15714	0.24	Yes	20.9	2407552	0.5	227532
H10a 1			No				
H10a 2			No				
H10a 3	365.15720	0.07	Yes	4.1	681059	0.2	230541
H11a 1			No				
H11a 2	365.15717	0.15	Yes	159.4	17120492	2.2	223896
H11a 3	365.15701	0.60	Yes	46.7	4889316	3.8	227741
H12a 1			No				
H12a 2			No				
H12a 3			No				
H13aii 1			No				
H13aii 2			No				
H13aii 3			No				
H14a 1			No				
H14a 2	365.15708	0.40	Yes	47.0	5425592	0.7	215935
H14a 3			No				
H14bi 1			No				
H14bi 2	365.15701	0.59	Yes	8.3	1182611	0.2	204278
H14bi 3			No				
V1a 1			No				
V1a 2	365.15704	0.51	Yes	10.0	1310916	0.2	234274
V1a 3			No				
B1a 1			No				
B1a 2			No				
B1a 3			No				
DHB 1			No				
DHB 2			No				
DHB 3			No				
Soil 3a 1			No				
Soil 3a 2			No				
Soil 3a 3			No				
Soil 3b 1			No				
Soil 3b 2			No				
Soil 3b 3	365.15777	-0.54	Yes	4.7	734890	0.1	277188
Solvent 1			No				
Solvent 2	365.15736	-0.13	Yes	9.3	1259844	0.2	262054
Solvent 3			No				

The peak at *m/z* 393, assigned $[C_{16}H_{34}O_9]$ + Na^+ for another fully saturated species, summarised in Table 45, was again a significant detection in the sample H6 extract and again in replicates of other samples, including one of the soil controls. The high relative intensity of these highly oxygenated, strongly ionised organic compounds in the extracts of H6 may indicate a unique brain chemistry or unique environment for decomposition, e.g. this may have been found in different soil conditions, have included grave goods or the original brain chemistry may have differed from that of other burials. The presence in the soil control is at very low S:N, especially when compared with that of the signal in the spectrum of the H6 extract. It is worth noting this replicate spot was adjacent on the MALDI plate to the H6 spots and so cross contamination may explain its presence in this spectra. However, the solvent control was not close enough for cross contamination to be likely.

Table 45. Summary of signal at *m/z* 393. $C_xH_yO_9$

Calculated *m/z*	393.20939 C16H34NaO9						
Sample designation + MALDI replicate no.	Measured *m/z*	Error [ppm]	Present	S:N	Intensity	Rel. Int. %	Resolution
Y1a 1			No				
Y1a 2			No				
Y1a 3			No				
Original Heslington			No				
H1a 1	393.20954	-0.09	Yes	11.2	1485710	0.1	223558
H1a 2	393.20930	0.52	Yes	12.7	1578020	0.4	213149
H1a 3	393.20920	0.75	Yes	10.3	1338047	0.2	195022
H1b 1	393.20938	0.30	Yes	19.8	2334555	0.3	216831
H1b 2	393.20927	0.59	Yes	19.9	2286593	0.6	209750
H1b 3	393.20921	0.74	Yes	10.5	1347898	0.3	278461
H2a 1			No				
H2a 2			No				
H2a 3	393.20957	-0.17	Yes	5.7	837561	0.2	148251
H3a 1			No				
H3a 2	393.20944	0.15	Yes	9.8	1307732	0.2	225386
H3a 3			No				
H4a 1			No				
H4a 2			No				
H4a 3	393.20907	1.10	Yes	7.9	1093821	0.1	220593
H5a 1			No				
H5a 2			No				
H5a 3			No				
H6a 1	393.20939	0.30	Yes	4087.1	433222240	58.5	203226
H6a 2	393.20938	0.71	Yes	2798.2	293792384	40.0	203110
H6a 3	393.20938	0.32	Yes	3152.9	334861440	35.6	202935
H7a 1			No				
H7a 2			No				
H7a 3			No				
H8a 1			No				
H8a 2	393.20908	1.09	Yes	4.6	720798	0.2	311421
H8a 3			No				
H9a 1			No				
H9a 2			No				
H9a 3		0.02	Yes				
H10a 1	393.20931	0.49	Yes	12.6	1578831	0.3	205543
H10a 2	393.20905	1.15	Yes	4.6	714468	0.4	185437
H10a 3	393.20923	0.70	Yes	9.2	1229217	0.3	255296
H11a 1			No				
H11a 2	393.20953	-0.08	Yes	119.1	12971392	1.7	200813
H11a 3	393.20934	0.42	Yes	27.4	2983954	2.3	208390
H12a 1			No				
H12a 2			No				
H12a 3	393.20937	0.34	Yes	5.6	856887	0.2	218925
H13aii 1			No				
H13aii 2			No				
H13aii 3	393.20952	-0.04	Yes	14.0	1716276	0.3	201938
H14a 1			No				
H14a 2	393.20943	0.19	Yes	33.8	4020980	0.5	213678
H14a 3			No				
H14bi 1			No				
H14bi 2			No				
H14bi 3			No				
V1a 1			No				
V1a 2			No				
V1a 3			No				
B1a 1			No				
B1a 2			No				
B1a 3			No				
DHB 1			No				
DHB 2			No				
DHB 3			No				
Soil 3a 1			No				
Soil 3a 2	393.20993	-0.43	Yes	8.0	1100845	0.1	216463
Soil 3a 3			No				
Soil 3b 1			No				
Soil 3b 2			No				
Soil 3b 3			No				
Solvent 1			No				
Solvent 2			No				
Solvent 3			No				

In addition to the 38 signals, already described, for which reasonable, unique empirical formulae could be assigned, consistent with the mass accuracy performance of the FT-ICR instrument used for these analyses, there were several more signals for which single reasonable empirical formulae could not be assigned. These were *m/z* 549.31, 629.34, 688.62. For each of these signals, more than one potential empirical formula could be proposed and it was not possible to determine which was the most likely on the basis of the data and their constraints. These signals were highlighted in the summary list of signals extracted from all the sample spectra (Table 50 in Appendix II), and then the list sorted in order of descending S:N, in order to assess the importance of the unassigned signals. The ten highest S:N unassigned signals were then further examined as follows. Instead of restricting the potential empirical formulae to those with a maximum of 9 oxygen, 9 nitrogen, 3 phosphorus and 3 sulfur atoms, all restrictions on the possible number of these heteroatoms were removed, and the assignment process for these ten signals repeated, reviewing and assessing to matches in the same way as before. Since this process was no more successful in assigning reasonable formulae consistent with the data and the constraints of their mass accuracy and isotope patterns, no further attempts were made using this approach, and we report these signals with their most likely candidate formulae, noting that we are unable from these data to differentiate between the possible formulae.

An alternative approach was attempted, by assessing the mean *m/z* errors (averaging the error over all the samples in which the signal was observed) for the different candidate formulae, to assess whether one formula gave a noticeably smaller mean *m/z* error; this approach was largely similarly unhelpful in determining the most likely formula. An exception to this was for the signal at *m/z* 549, as shown in Table 46, where the possible assignments of the signal

at *m/z* 549 are suggested as $[C_{32}H_{42}N_6] + K^+$ or $[C_{36}H_{40}N_2O_3] + H^+$, with 14 or 18 double bond equivalents respectively, both of which are highly unsaturated suggestions. The average error for the measured *m/z* in comparison to the calculated *m/z* in the mass spectra for the sample extracts of $[C_{32}H_{42}N_6] + K^+$ was -0.49 ppm whilst the average error for $[C_{36}H_{40}N_2O_3] + H^+$ was 1.19 ppm, suggesting the former formula is more likely to be correct.

Table 46 shows the *m/z* 549 compound is present across all sites except Villiers Street and occurs with highest intensity in the spectra for the H14b replicates. It also occurs with good S:N, if at lower relative intensity percentages, in other Hull samples: H3, H7, H8 and H14a.

There are signals at similar *m/z* values in the spectra of the soil extracts (Soil 3a and Soil 3b replicates). The *m/z* values for the signals in the control extract spectra have larger ppm errors than those in the brain sample spectra, principally when comparing the measured values for $[C_{32}H_{42}N_6] + K^+$. The mean measured *m/z* value for this signal in the spectra of brain samples is 549.310522 and that of the controls is 549.31183. The standard deviation of this mean for the brain samples is 0.000247869 and that for the control is 0.000170646. 549.310522+0.000495738 = *m/z* 549.3110177 whereas 549.31183-0.000341292 = *m/z* 549.3114887. There is no overlap of these values, suggesting that even though the mass error is below 2 ppm, the compound detected in the soil control is probably not the same as that in the brain extracts.

Table 46. Summary of signal at *m/z* 549. $C_{32}H_{42}N_6$ or $C_{36}H_{40}N_2O_3$

Calculated formula		C32H42KN6	C36H41N2O3					
Calculated *m/z*		549.31025	549.31117					
Sample designation + MALDI replicate no.	Measured *m/z*	Error [ppm]	Error [ppm]	Present	S:N	Intensity	Rel. Int. %	Resolution
Y1a 1	549.31067	-0.76	0.91	Yes	23.6	3636566	1.2	150441
Y1a 2	549.31046	-0.38	1.29	Yes	15.8	2435370	0.9	151763
Y1a 3	549.31057	-0.58	1.09	Yes	17.8	2837409	0.8	153692
Original Heslington				No				
H1a 1	549.31038	-0.22	1.45	Yes	20.3	3208350	0.3	150986
H1a 2	549.31013	0.22	1.89	Yes	22.2	3021558	0.8	149655
H1a 3	549.31030	-0.09	1.58	Yes	36.8	4849331	0.7	145663
H1b 1	549.31006	0.35	2.02	Yes	32.5	4442085	0.5	150407
H1b 2	549.31031	-0.11	1.56	Yes	53.3	6902780	1.8	146575
H1b 3	549.31011	0.26	1.92	Yes	50.3	6479661	1.5	149311
H2a 1	549.31001	0.44	2.10	Yes	45.0	5845618	1.1	152456
H2a 2	549.31008	0.32	1.99	Yes	33.9	5144129	1.6	142703
H2a 3	549.31017	0.15	1.82	Yes	84.5	10145661	2.9	147459
H3a 1	549.31041	-0.28	1.39	Yes	170.9	24154464	4.4	145713
H3a 2	549.31055	-0.53	1.13	Yes	384.5	55206192	9.0	144368
H3a 3	549.31030	-0.09	1.57	Yes	232.5	29986808	4.0	144771
H4a 1	549.31063	-0.69	0.98	Yes	89.8	15044741	0.9	146171
H4a 2	549.31083	-1.06	0.61	Yes	71.4	12141437	1.4	149540
H4a 3	549.31064	-0.70	0.97	Yes	54.6	8973506	1.1	150064
H5a 1	549.31046	-0.37	1.29	Yes	4.7	817542	0.4	178920
H5a 2	549.31049	-0.43	1.24	Yes	5.8	1000606	0.3	196522
H5a 3	549.31063	-0.68	0.99	Yes	13.9	2153656	0.2	168040
H6a 1	549.31048	-0.41	1.26	Yes	46.4	6558480	0.9	148195
H6a 2	549.31032	-0.12	1.55	Yes	50.2	6909570	0.9	149838
H6a 3	549.31035	-0.17	1.49	Yes	46.5	6645613	0.7	145534
H7a 1	549.31043	-0.31	1.35	Yes	244.4	31784446	7.8	145085
H7a 2	549.31044	-0.34	1.33	Yes	168.8	23321726	3.7	145801
H7a 3	549.31035	-0.18	1.49	Yes	200.7	26421936	3.9	144679
H8a 1	549.31051	-0.47	1.20	Yes	196.9	29549390	5.1	146291
H8a 2	549.31067	-0.76	0.91	Yes	186.7	25424060	5.9	145092
H8a 3	549.31046	-0.38	1.29	Yes	155.6	20734820	4.0	146778
H9a 1	549.31062	-0.68	0.99	Yes	44.6	7051877	0.9	151690
H9a 2	549.31055	-0.55	1.12	Yes	33.4	5430774	0.6	152566
H9a 3	549.31043	-0.32	1.35	Yes	52.6	7253727	1.6	152620
H10a 1	549.31051	-0.47	1.20	Yes	88.2	12291822	2.1	147157
H10a 2	549.31040	-0.27	1.40	Yes	51.2	6428672	3.3	150359
H10a 3	549.31048	-0.40	1.26	Yes	94.4	13655090	3.7	147125
H11a 1	549.31098	-1.32	0.35	Yes	58.8	8165536	3.6	149804
H11a 2	549.31072	-0.85	0.82	Yes	43.9	6376637	0.8	148616
H11a 3	549.31047	-0.39	1.28	Yes	10.9	1493800	1.1	176752
H12a 1	549.31095	-1.27	0.39	Yes	86.3	13654912	3.0	146009
H12a 2	549.31094	-1.25	0.42	Yes	73.1	11631297	2.4	146228
H12a 3	549.31096	-1.29	0.38	Yes	99.1	15859353	3.9	143775
H13aii 1	549.31103	-1.41	0.26	Yes	27.1	4325633	1.1	150926
H13aii 2	549.31090	-1.18	0.49	Yes	33.7	5063676	1.3	148502
H13aii 3	549.31084	-1.07	0.60	Yes	19.4	2830545	0.5	153750
H14a 1	549.31037	-0.20	1.46	Yes	95.3	15441758	1.1	146392
H14a 2	549.31042	-0.30	1.37	Yes	150.8	23523890	3.1	146070
H14a 3	549.31057	-0.58	1.09	Yes	143.3	26476526	1.3	146159
H14bi 1	549.31076	-0.92	0.75	Yes	1404.3	222491712	24.7	144935
H14bi 2	549.31064	-0.71	0.96	Yes	1098.1	166745312	25.6	145251
H14bi 3	549.31081	-1.02	0.65	Yes	943.6	170842448	3.4	144912
V1a 1				No				
V1a 2				No				
V1a 3				No				
B1a 1	549.31077	-0.94	0.73	Yes	95.6	17454476	3.4	145109
B1a 2	549.31059	-0.62	1.05	Yes	64.5	9646104	3.1	149430
B1a 3	549.31028	-0.04	1.63	Yes	45.4	6184485	1.4	154136
DHB 1				No				
DHB 2				No				
DHB 3				No				
Soil 3a 1	549.31178	-2.77	-1.11	Possibly	19.0	3710072	0.5	138413
Soil 3a 2	549.31188	-2.96	-1.29	Possibly	24.0	4401494	0.4	141874
Soil 3a 3	549.31201	-3.20	-1.54	Possibly	27.9	5262762	1.2	106057
Soil 3b 1	549.31175	-2.73	-1.06	Possibly	21.4	3830155	0.5	141600
Soil 3b 2	549.31156	-2.38	-0.71	Possibly	26.7	4953770	0.3	131599
Soil 3b 3	549.31200	-3.19	-1.52	Possibly	14.2	2674747	0.5	113755
Solvent 1				No				
Solvent 2				No				
Solvent 3				No				

Table 47 summarises the data for peak at *m/z* 629 with the following tentative formula possibilities: $[C_{44}H_{46}O_2] + Na^+$ with 22 degrees of unsaturation, $[C_{41}H_{50}O_3] + K^+$ with 17 degrees of unsaturation or $[C_{42}H_{40}N_6] + H^+$ with 26 degrees of unsaturation. The average error in ppm for each of these are similar in magnitude and cannot help distinguish a more likely candidate. All of these compounds are extremely unsaturated which may indicate they include a series of ring structures as well as double bonds.

Similarly to the peaks in Table 32 and Table 35, this signal *m/z* 629 was found at high intensity in the spectra of a single replicate of the H1a extract. Contrarily, it was also detected in the spectra of H4, H12 and H13 extracts. As the compound was not detected in the oldest (York) or youngest (Blackpool and Villiers Street) samples it may indicate that this is an intermediary decomposition product. Chemical changes may have occurred to the original organic matter from the brain over a longer period of time than 200 years to form this compound, and it may undergo further processes over time such that it is no longer detected in a sample over 2500 years old. Alternatively, this may be a compound linked to the environment of the Hull burials and so is a site-specific product.

Table 47. Summary of signal at *m/z* 629. $C_{44}H_{46}O_2$, $C_{41}H_{50}O_3$ or $C_{42}H_{40}N_6$

Calculated formula		C44H46NaO2	C41H50KO3	C42H41N6					
Calculated *m/z*		629.339	629.33915	629.33872					
Sample designation + MALDI replicate no.	Measured *m/z*	Error [ppm]	Error [ppm]	Error [ppm]	Present	S:N	Intensity	Rel. Int. %	Resolution
Y1a 1					No				
Y1a 2					No				
Y1a 3					No				
Original Heslington					No				
H1a 1	629.33859	0.65	0.89	0.20	Yes	455.9	67364672	6.8	125588
H1a 2					No				
H1a 3					No				
H1b 1					No				
H1b 2					No				
H1b 3					No				
H2a 1					No				
H2a 2					No				
H2a 3					No				
H3a 1					No				
H3a 2					No				
H3a 3					No				
H4a 1	629.33734	2.64	2.88	2.19	Yes	19.7	3698718	0.2	132205
H4a 2	629.33788	1.78	2.02	1.34	Yes	12.4	2573984	0.3	136832
H4a 3	629.33752	2.36	2.60	1.92	Yes	38.8	6910128	0.8	126972
H5a 1					No				
H5a 2					No				
H5a 3					No				
H6a 1					No				
H6a 2					No				
H6a 3					No				
H7a 1					No				
H7a 2					No				
H7a 3					No				
H8a 1					No				
H8a 2					No				
H8a 3					No				
H9a 1					No				
H9a 2					No				
H9a 3					No				
H10a 1					No				
H10a 2					No				
H10a 3					No				
H11a 1					No				
H11a 2					No				
H11a 3					No				
H12a 1	629.33792	1.71	1.95	1.27	Yes	9.5	1895435	0.4	159124
H12a 2	629.33845	0.87	1.11	0.43	Yes	4.2	1025458	0.2	181175
H12a 3	629.33750	2.39	2.63	1.95	Yes	8.9	1810388	0.4	158121
H13aii 1	629.33807	1.47	1.71	1.03	Yes	22.8	3993099	1.0	137073
H13aii 2	629.33813	1.38	1.62	0.94	Yes	15.6	2670132	0.7	139144
H13aii 3	629.33790	1.76	2.00	1.31	Yes	12.0	1990191	0.3	140895
H14a 1					No				
H14a 2					No				
H14a 3					No				
H14bi 1					No				
H14bi 2					No				
H14bi 3					No				
V1a 1					No				
V1a 2					No				
V1a 3					No				
B1a 1					No				
B1a 2					No				
B1a 3					No				
DHB 1					No				
DHB 2					No				
DHB 3					No				
Soil 3a 1					No				
Soil 3a 2					No				
Soil 3a 3					No				
Soil 3b 1					No				
Soil 3b 2					No				
Soil 3b 3					No				
Solvent 1					No				
Solvent 2					No				
Solvent 3					No				

The peak at 688, Table 48, has a variety of possible assignments. The most probable were $[C_{42}H_{83}NO_4] + Na^+$ with two double bond equivalents or $[C_{40}H_{77}N_7O_2] + H^+$ with six double bond equivalents. The average error for the peak measurements found in the sample extracts for the former was 0.42 ppm and for the later 0.02 ppm, which implies that $[C_{40}H_{77}N_7O_2] + H^+$ is the more likely ion to be detected.

The signal itself was detected in all sample extracts except H14a, although wasn't detected in all replicates of H14b or V1. It was found with the highest relative intensity in the Hull extracts: H2, H10 and H11.

Table 48. Summary of signal at *m/z* 688. $C_{42}H_{83}NO_4$ or $C_{40}H_{77}N_7O_2$

Calculated formula		C42H83NNaO4	C40H78N7O2					
Calculated *m/z*		688.62115	688.61875					
Sample designation + MALDI replicate no.	Measured *m/z*	Error [ppm]	Error [ppm]	Present	S:N	Intensity	Rel. Int. %	Resolution
Y1a 1	688.62108	0.51	0.10	Yes	67.6	11491469	3.8	121284
Y1a 2	688.62100	0.62	0.21	Yes	69.1	11028392	4.1	122174
Y1a 3	688.62108	0.51	0.10	Yes	65.8	11216683	3.3	119410
Original Heslington				No				
H1a 1	688.62091	0.76	0.36	Yes	57.2	8750562	0.9	118868
H1a 2	688.62091	0.76	0.35	Yes	89.9	12545136	3.1	119845
H1a 3	688.62083	0.88	0.47	Yes	146.5	19310544	2.9	116413
H1b 1	688.62073	1.02	0.61	Yes	177.8	25125248	2.9	117135
H1b 2	688.62074	1.00	0.59	Yes	280.0	37995256	9.9	115840
H1b 3	688.62058	1.23	0.82	Yes	234.7	31612422	7.5	116641
H2a 1	688.62050	1.35	0.94	Yes	521.1	68780520	12.8	116308
H2a 2	688.62056	1.27	0.86	Yes	351.4	52362708	15.8	115596
H2a 3	688.62080	0.92	0.52	Yes	452.4	57137308	16.1	116049
H3a 1	688.62111	0.46	0.05	Yes	171.5	24772174	4.5	116413
H3a 2	688.62129	0.21	-0.20	Yes	230.6	34122516	5.6	116543
H3a 3	688.62097	0.67	0.27	Yes	131.2	17684262	2.3	118959
H4a 1	688.62123	0.29	-0.11	Yes	185.2	31967150	1.9	116932
H4a 2	688.62171	-0.40	-0.81	Yes	511.6	96475264	11.0	115928
H4a 3	688.62140	0.04	-0.37	Yes	288.3	50577784	6.1	116956
H5a 1	688.62063	1.16	0.76	Yes	189.2	23374970	12.3	116477
H5a 2	688.62081	0.90	0.49	Yes	187.7	24732002	8.1	115860
H5a 3	688.62063	1.16	0.75	Yes	109.0	15706394	1.8	115774
H6a 1	688.62109	0.50	0.09	Yes	54.1	7958603	1.1	119637
H6a 2	688.62102	0.60	0.20	Yes	35.4	5176556	0.7	124260
H6a 3	688.62102	0.59	0.18	Yes	36.5	5438024	0.6	116510
H7a 1	688.62106	0.53	0.13	Yes	137.4	19790718	4.8	113715
H7a 2	688.62110	0.47	0.07	Yes	109.2	16844818	2.7	118438
H7a 3	688.62102	0.60	0.19	Yes	253.6	36580376	5.4	116856
H8a 1	688.62124	0.28	-0.13	Yes	369.8	56407932	9.7	115734
H8a 2	688.62119	0.35	-0.06	Yes	334.7	48101104	11.2	114557
H8a 3	688.62103	0.58	0.18	Yes	311.4	42881256	8.3	115958
H9a 1	688.62118	0.37	-0.04	Yes	139.0	21092652	2.6	116159
H9a 2	688.62110	0.47	0.07	Yes	150.6	22929688	2.6	116644
H9a 3	688.62087	0.81	0.41	Yes	89.2	12473297	2.7	117164
H10a 1	688.62114	0.43	0.02	Yes	501.8	71218056	11.9	115888
H10a 2	688.62082	0.88	0.48	Yes	291.3	36823888	18.9	115018
H10a 3	688.62115	0.41	0.01	Yes	440.2	64023352	17.4	115754
H11a 1	688.62173	-0.44	-0.85	Yes	300.9	45062768	19.7	116108
H11a 2	688.62168	-0.36	-0.77	Yes	119.4	18206106	2.4	116600
H11a 3	688.62125	0.26	-0.15	Yes	172.7	20769404	16.0	115847
H12a 1	688.62196	-0.76	-1.17	Yes	233.0	39354408	8.8	117214
H12a 2	688.62189	-0.67	-1.08	Yes	227.9	37841984	7.7	115474
H12a 3	688.62192	-0.71	-1.12	Yes	210.2	36003632	8.9	116500
H13aii 1	688.62177	-0.50	-0.90	Yes	71.2	12287215	3.1	117645
H13aii 2	688.62170	-0.39	-0.80	Yes	63.8	10268217	2.6	117107
H13aii 3	688.62163	-0.30	-0.70	Yes	75.0	11220745	1.9	117776
H14a 1				No				
H14a 2				No				
H14a 3				No				
H14bi 1				No				
H14bi 2	688.62198	-0.80	-1.21	Yes	5.2	1111322	0.2	141749
H14bi 3				No				
V1a 1				No				
V1a 2	688.62095	0.70	0.30	Yes	7.4	1519100	0.2	112046
V1a 3				No				
B1a 1	688.62134	0.13	-0.28	Yes	27.3	5126488	1.0	119319
B1a 2	688.62081	0.90	0.50	Yes	29.3	4627421	1.5	128269
B1a 3	688.62082	0.88	0.48	Yes	49.2	6818530	1.6	117282
DHB 1				No				
DHB 2				No				
DHB 3				No				
Soil 3a 1				No				
Soil 3a 2				No				
Soil 3a 3				No				
Soil 3b 1				No				
Soil 3b 2	688.62191	-0.70	-0.76	Yes	4.8	1424904	0.1	117820
Soil 3b 3				No				
Solvent 1				No				
Solvent 2				No				
Solvent 3				No				

Appendix II: Unidentified Compound Tables provides details of the remaining signals (excluding those from DHB) that were not assigned to formulae using this method.

Having completed analyses of all of the spectra as described above, a final analysis was carried out on a randomly chosen sample extract in order to test whether organic material with low oxygen and nitrogen content was present among signals of lower intensity/S:N. All of the spectra from the current extract of the York brain sample were considered as follows; a complete list of all signals not found in the matrix spectra was assembled, unrestricted empirical formula assignments using the Bruker software were carried out and the outcomes compared with those from the analyses described above. It is notable that even when the allowed compositions are unrestricted and all signals (rather than just the most intense ones) were considered, a significant number of *m/z* values received unique assignments, and that these were to empirical formulae that were almost always organic components with small numbers of oxygen and/or nitrogen atoms, just as for the vast majority of the assignments reported above. In other words, whatever the basis for the data analysis and screening, the results are consistent with the chloroform/methanol extracts of all the brains analysed containing functionalised organics, with small numbers of oxygen and/or nitrogen atoms.

4 DISCUSSION

Through comparing the MALDI mass spectra of the lipid extracts from the ancient brain residues, a variety of organic compounds, with varying degrees of saturation, have been identified to occur in samples across all age ranges and burial sites. By looking at the signals with the strongest S:N and intensities in the spectra, the aim was to target dominant organic-soluble/lipidic components and identify them.

The range of samples analysed supports our original hypothesis, that the presence of these components is not isolated to the beautifully preserved York brain, but also occurs in other less immediately recognisable brain remains. However, it is easy to see that even within one preserved brain, different subsamples can reflect a range of chemical compositions. Lipid extracts H12a, H13a, H14a and H14b all came from the same brain remains identified from a single skeletal burial and yet the spectra are recognisably rather different. Whilst H12a and H13a spectra appear to mirror each other closely, the compounds detected within these samples are often absent from those of the H14a extract. However, while the H14b spectra differ from those from H12a and H13a for some compounds, there remains similarity between the spectra with respect to other components. These differences may be related to the difficulty of sample recovery and soil contamination. It is hard to 'clean' an ancient brain sample without knowing if damage is being done to the brain mass and so many of the samples in storage also have associated soil matrix. However we have been unable to test the effect of this, since soil samples from the burial sites were not archived. By carefully reviewing the DHB matrix data and the solvent blank experiment, the peaks identified can be demonstrated to be unique to the samples, but lack of soil controls is an unavoidable issue. Ideally, soil samples should have been taken from the same archaeological context but

with sufficient distance from the skull/brain remains to have prevented chemicals associated with these from leaching into the control soil sample. Even though these soil samples weren't available for this analysis, the detection of so many components in the spectra of the Hull, Villiers Street and Blackpool brain remains that also occur in the exceptionally preserved York brain indicates that these compounds are unlikely to derive from the different soils surrounding these very different sites, but rather from the preserved tissue remains. A clearer knowledge of these burial environments is likely to be essential to understanding how the preservation mechanism works.

From the combined data derived from these studies, it is harder to determine if these compounds are age-related, as peak intensities in mass spectra produced by MALDI are not necessarily reflective of chemical concentrations.[152] This is due to a number of factors, including some compounds being more readily ionisable and the potential for uneven crystallisation of components within the matrix (e.g. the 'coffee-ring' effect).[153] High relative intensities in one spectrum do not necessarily mean that a component occurs in greater concentration in that mixture. When looking at the results (3.3.1), often when a peak was not detected in the youngest samples (V1a and B1a) it was also not detected in the oldest sample (Y1a), i.e. the peak was only detected in samples from the Hull Magistrates Court site. Such components may not be an indicator of age but rather a consequence of local environment.

The proteomics experiment on sample V1 is consistent with the material being brain matter, by identifying peptides that are clearly related to the CNS, myelin proteolipid protein and SLIT and NTRK-like protein 4. The level of these peptides was very low, and only single peptide matches were made to these proteins. However, the peptides were identified with expect scores lower than

0.05, and so it is possible to have confidence in these single-peptide protein identifications. Ideally, a more invasive (larger) sample of the brain remains would need to be extracted, such as from the interior of the mass, to reduce keratin contamination from the handling of the surface and potentially a more protected and therefore preserved environment, where higher protein levels may have been maintained.

The components identified from brain lipid extracts had molecular weights that varied from 321 Da to 810 Da with the majority of their mass due to carbon atoms. Many of the organic compounds included a very limited number of oxygen and nitrogen atoms, with up to five heteroatoms in total compared to more than 28 carbon atoms. However, there were three highly oxygenated species with up to nine oxygen atoms, and where no single assignment was possible higher nitrogen content (up to seven N atoms) has been proposed. There is a range of degrees of unsaturation, from zero to almost twenty double bond equivalents (dbes). Compounds with low numbers of nitrogen and oxygen atoms will be apolar in nature, and thus have low water solubilities, encouraging preservation (1.2.2.1). Those which are saturated, or have low degrees of unsaturation are probably especially apolar and so particularly resistant to chemical change. These lipids are likely to be hard waxes and insoluble in water, potentially forming a barrier to further chemical or enzymatic decomposition.

Whilst there doesn't appear to be a clear pattern relating oxygen and nitrogen content with age or site, there does appear to be a slight trend between degrees of unsaturation and age and/or site. Species with higher numbers of double bond equivalents are less consistently detected in the oldest brain extracts, but are more commonly detected in the intermediate age (Hull) brain extracts and generally in the youngest (Blackpool) brain extract. This may

be more related to site than age though, as these more unsaturated components are not always detected in the other young sample extract, from Villiers Street. It would be understandable to link this trend to age, as unsaturated organic molecules tend to be more reactive than fully saturated organic molecules[154] and so their concentrations may be expected to decrease over time.

The components of the ancient brain lipid extracts tentatively identified (3.3.1) can be provisionally grouped into classes: C_xH_y, $C_xH_yN_n$, $C_xH_yN_nO_o$, $C_xH_yO_o$, etc. shown in Table 49. The compound class with most representatives, identified in the ancient brain lipid extracts is made up of organic species containing a single oxygen and a single nitrogen atom with varying levels of unsaturation. These compounds have a wide molecular weight range from 529.923 Da to 810.457 Da and most have three to six degrees of unsaturation. For each degree of unsaturation, it is possible to propose a homologous series of components which are related by increasing numbers of CH_2 subunits. These compounds occur across all sites and brain ages, being detected in York, Hull, Blackpool and Villiers Street sample extracts. There are two additional examples in this category ($C_{35}H_{49}NO$ and $C_{35}H_{47}NO$) which are highly unsaturated (12 and 13 dbes respectively) and so are slightly lighter: 499.771 Da and 497.755 Da. These two components are not detected in the oldest brain extract (York), which suggests that they are altered over time; however, they are also not present in one of the youngest samples – from Villiers Street. All of these compounds are much larger than any of the lipids described routinely in the adipocere literature but appear to be similarly apolar and hydrophobic. They could potentially be the results of condensation reactions.[155]

More oxygenated species include $C_{36}H_{69}NO_3$ (563.939 Da) and $C_{42}H_{81}NO_3$ (648.099 Da) which both have three degrees of unsaturation. These chemicals

were identified in the mass spectra from the lipid extracts of samples from all sites. There is a possibility that these derive from ceramides (brain lipids) that have yet to be fully hydrolysed to their fatty acid constituents. Furthermore, there are more unsaturated forms of $C_xH_yNO_3$: $C_{27}H_{39}NO_3$ (425.605 Da, 9 dbe), which was only detected in a single Hull sample extract and $C_{34}H_{47}NO_3$ (517.743 Da, 12 dbe), which was detected in some Hull extracts and the youngest extract from Blackpool.

Two possibly related compounds are $C_{46}H_{80}N_2O_3$ (709.141 Da) and $C_{48}H_{84}N_2O_3$ (737.194 Da), both of which contain eight double bond equivalents and differ by C_2H_4. They have a similar detection pattern, as the associated ions are found in the spectra of all the brain lipid extracts across all ages and sites.

The compond class with the lowest molecular weight range is a series of completely saturated, highly oxidised species: $C_{12}H_{26}O_7$, $C_{14}H_{30}O_8$, $C_{16}H_{34}O_9$ (respective molecular weights: 282.383 Da, 326.383 Da, 370.436 Da). These are possibly a homologous series differing by ethylene glycol subunits (Figure 26). Signals for all three compounds were detected in the spectra of the H6a extract replicates. Whilst the smallest two compounds are detected in the old (York) and young (Villiers Street) samples, as well as in sporadically within the intermediate (Hull) samples (the largest compound was only detected in the Hull samples). This makes it difficult to interpret whether these are age or site related. It is unlikely that these components are linked to adipocere formation as they contain much more oxygen than the reported constituent of adipocere.

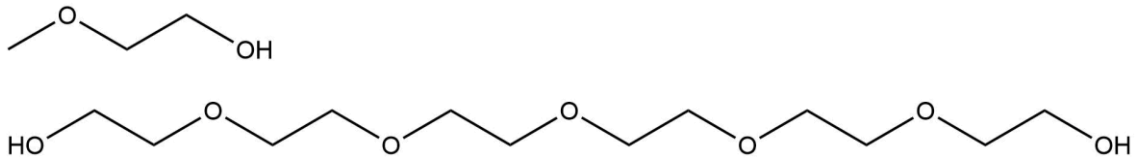

Figure 26. Above: Ethylene glycol Below: Hexaethyleneglycol (3,6,9,12,15-Pentaoxaheptadecane-1,17-diol), a possible structure for $C_{12}H_{26}O_7$

Other almost saturated compounds include the amines $C_{34}H_{67}N$ and $C_{36}H_{71}N$. These are both found in the oldest (York) and youngest (Blackpool and Villiers Street) as well as in many of the intermediate age (Hull) brain lipid extracts, suggesting that these are resistant to chemical change as discussed above. Another almost saturated compound with a similar carbon number is $C_{36}H_{73}NO_4$. The additional oxygen atoms may indicate this is a sphinganine-like residue; sphinganine is a brain lipid.[156] The related ion is not detected in the youngest lipid extract spectra but is found in the spectra from the older Hull and York brain extracts. This may suggest the chemical alteration pathway takes longer to produce this residue, or it may be that the environment of the younger sites did not support its formation.

More highly unsaturated organic residues are likely to have (arene) ring structures such as the following trio of potentially related compounds: $C_{34}H_{48}N_2O$ (11 dbe), $C_{35}H_{46}N_2O$ (14 dbe), $C_{35}H_{48}N_2O$ (13 dbe). These are found in the York, Hull and Blackpool extracts.

Table 49. Summary of the chemical identities of the brain lipid residues and their occurrence

Ion formulae	$C_{27}H_{47}$	$C_{34}H_{68}N$	$C_{36}H_{72}N$	$C_{28}H_{47}N_2$	$C_{34}H_{51}N_2$	$C_{27}H_{25}N_4$	$C_{50}H_{96}NO$	$C_{52}H_{100}NO$	$C_{36}H_{68}NO$	$C_{37}H_{70}NO$	$C_{38}H_{72}NO$	$C_{40}H_{76}NO$	$C_{54}H_{104}NO$
Calculated m/z	371.36723	490.53452	518.56593	411.37338	487.40468	405.20737	726.74844	754.77994	530.52954	544.54519	558.56084	586.59214	782.81124
Class	C_xH_y	C_xH_yN		$C_xH_yN_2$		$C_xH_yN_4$	C_xH_yNO						
Compound formulae	$C_{27}H_{46}$	$C_{34}H_{67}N$	$C_{36}H_{71}N$	$C_{28}H_{46}N_2$	$C_{34}H_{50}N_2$	$C_{27}H_{24}N_4$	$C_{50}H_{95}NO$	$C_{52}H_{99}NO$	$C_{36}H_{67}NO$	$C_{37}H_{69}NO$	$C_{38}H_{71}NO$	$C_{40}H_{75}NO$	$C_{54}H_{103}NO$
Molecular Weight	370.655	489.904	517.957	410.679	486.776	404.507	726.297	754.351	529.923	543.950	557.978	586.031	782.404
dbe of compound	5	1	2	7	11	18	3	3	4	4	4	4	4
N/C ratio	0.000	0.029	0.028	0.071	0.038	0.148	0.020	0.019	0.028	0.027	0.026	0.025	0.019
O/C ratio	0.000	0.000	0.000	0.000	0.000	0.000	0.020	0.019	0.028	0.027	0.026	0.025	0.019
H/C ratio	1.704	1.971	1.972	1.643	1.471	0.889	1.900	1.904	1.861	1.865	1.868	1.875	1.907
Y1a	Detected	Yes	Yes	Detected	No	No	Yes	Yes	Yes	Yes	Yes	Yes	Yes
Original Heslington	No	Yes	Yes	No	No	No	Yes	Yes	Yes	Yes	Yes	Yes	Yes
H1a	Yes	Detected	Detected	No	No	Detected	Yes	Yes	Detected	Detected	Detected	No	Yes
H1b	Yes	Yes	Yes	Yes	Detected	No	Yes	Yes	Yes	Detected	Yes	Detected	Yes
H2a	Yes	Yes	Yes	Detected	Detected	No	Yes	Yes	Yes	Yes	Yes	Detected	Yes
H3a	Yes	Yes	Yes	Detected	Yes	No	Yes	Yes	Yes	Detected	Yes	Yes	Yes
H4a	Yes	Yes	Yes	Yes	Yes	No	Yes	Yes	Yes	Yes	Yes	Yes	Yes
H5a	Yes	Yes	Yes	Yes	Yes	Detected	Yes	Yes	Yes	Yes	Yes	Yes	Yes
H6a	Yes	No	No	No	Yes	No	Detected	Yes	Yes	Yes	Yes	Yes	Yes
H7a	Yes	Yes	Yes	No	Yes	No	Yes	Yes	Yes	Detected	Yes	Yes	Yes
H8a	Yes	No	Detected	Detected	Yes	No	Yes	Yes	Yes	Yes	Yes	Detected	Yes
H9a	Yes	Detected	Detected	No	Yes	No	Yes	Yes	Yes	Yes	Yes	Detected	Yes
H10a	Yes	No	No	Detected	Yes	No	Detected	Yes	Yes	Yes	Yes	Detected	Yes
H11a	Yes	Yes	Yes	Yes	Yes	No	Yes	Yes	Yes	Yes	Yes	Detected	Yes
H12a	Yes	Yes	Yes	Yes	Yes	No	Yes	Yes	Yes	Yes	Yes	Yes	Yes
H13aii	Yes	Yes	Yes	Yes	Yes	No	Yes	Yes	Yes	Yes	Yes	Yes	Yes
H14a	No	No	Detected	No	No	No	No	No	No	No	No	No	No
H14bi	No	No	Detected	No	Detected	No	Detected	Detected	Detected	Detected	Detected	No	Detected
V1a	No	Yes	Yes	No	No	No	Yes	Yes	Yes	Yes	Yes	Yes	Yes
B1a	Yes	Yes	Yes	Yes	Yes	No	Yes	Yes	Yes	Yes	Yes	Yes	Yes
DHB	No	No	No	No	No	No	No	No	No	No	No	No	No
Soil 3a	No	No	No	No	No	No	No	No	No	No	No	No	No
Soil 3b	No	No	No	No	No	No	No	No	No	No	No	No	No
Solvent	No	No	No	No	No	No	No	No	No	No	No	No	No

Ion formulae	$C_{56}H_{108}NO$	$C_{38}H_{70}NO$	$C_{52}H_{98}NO$	$C_{54}H_{102}NO$	$C_{54}H_{100}NO$	$C_{56}H_{104}NO$	$C_{35}H_{50}NO$	$C_{35}H_{48}NO$	$C_{34}H_{49}N_2O$	$C_{35}H_{47}N_2O$	$C_{35}H_{49}N_2O$	$C_{30}H_{31}N_4O$
Calculated m/z	810.84254	556.54519	752.7649	780.79564	778.77994	806.81128	500.38869	498.37304	501.38394	511.3682	513.38394	463.24924
Class	C_xH_yNO								$C_xH_yN_2O$			$C_xH_yN_4O$
Compound formulae	$C_{56}H_{107}NO$	$C_{38}H_{69}NO$	$C_{52}H_{97}NO$	$C_{54}H_{101}NO$	$C_{54}H_{99}NO$	$C_{56}H_{103}NO$	$C_{35}H_{49}NO$	$C_{35}H_{47}NO$	$C_{34}H_{48}N_2O$	$C_{35}H_{46}N_2O$	$C_{35}H_{48}N_2O$	$C_{30}H_{30}N_4O$
Molecular Weight	810.457	555.962	752.335	780.388	778.372	806.425	499.771	497.755	500.759	510.754	512.770	462.587
dbe of compound	4	5	5	5	6	6	12	13	11	14	13	18
N/C ratio	0.018	0.026	0.019	0.019	0.019	0.018	0.029	0.029	0.059	0.057	0.057	0.133
O/C ratio	0.018	0.026	0.019	0.019	0.019	0.018	0.029	0.029	0.029	0.029	0.029	0.033
H/C ratio	1.911	1.816	1.865	1.870	1.833	1.839	1.400	1.343	1.412	1.314	1.371	1.000
Y1a	Yes	Yes	Yes	Yes	Yes	Yes	No	No	Yes	Yes	Yes	No
Original Heslington	Yes	Yes	Yes	Yes	Yes	Yes	No	No	No	No	No	No
H1a	Yes	Detected	Yes	Detected	Detected	Detected	No	No	Detected	No	No	Detected
H1b	Yes	Detected	Yes	Yes	Yes	Detected	No	No	Detected	No	No	No
H2a	Yes	Detected	Yes	Yes	No	No	No	No	Yes	No	Yes	No
H3a	Yes	Detected	Yes	Yes	Yes	No	Yes	Yes	Yes	Yes	Yes	No
H4a	Yes	Yes	Yes	Yes	Yes	Yes	Yes	Yes	Yes	Yes	Yes	No
H5a	Detected	Yes	Yes	Yes	Yes	Yes	Yes	Yes	Yes	Yes	Yes	No
H6a	Yes	Yes	Yes	Yes	Yes	Detected	Yes	Yes	Yes	Yes	Yes	No
H7a	Yes	Yes	Yes	Yes	Yes	No	Yes	Detected	Yes	Detected	Yes	No
H8a	Yes	Yes	Yes	Yes	Yes	Yes	Yes	Yes	Yes	Yes	Yes	No
H9a	Yes	Yes	Yes	Yes	Yes	Detected	Yes	Yes	Yes	Yes	Yes	No
H10a	Detected	Detected	Yes	Yes	Yes	Detected	Yes	Yes	Yes	Yes	Yes	No
H11a	Yes	Yes	Yes	Yes	Yes	Yes	Yes	Yes	Yes	Yes	Yes	No
H12a	Yes	Yes	Yes	Yes	Yes	Yes	Yes	Yes	Yes	Yes	Yes	No
H13aii	Yes	Yes	Yes	Yes	Yes	Yes	Yes	Yes	Yes	Yes	Yes	No
H14a	No	No	No	No	No	No	No	No	No	No	No	No
H14bi	Detected	Detected	No	No	No	No	Detected	Detected	Detected	Detected	Detected	No
V1a	Yes	Yes	Yes	Yes	Yes	Yes	No	No	No	No	No	No
B1a	Yes	Yes	Yes	Yes	Yes	Yes	Yes	Yes	Yes	Yes	Yes	No
DHB	No	No	No	No	No	Detected	No	No	No	No	No	No
Soil 3a	No	No	No	No	No	No	No	No	No	No	No	No
Soil 3b	No	No	No	No	No	No	No	No	No	No	No	No
Solvent	No	No	No	No	No	No	No	No	No	No	No	No

Ion formulae	$C_{34}H_{48}NO_2$	$C_{35}H_{48}NO_2$	$C_{27}H_{39}KNO_3$	$C_{34}H_{48}NO_3$	$C_{36}H_{70}NO_3$	$C_{42}H_{82}NO_3$	$C_{36}H_{74}NO_4$	$C_{35}H_{47}N_2O_2$	$C_{46}H_{80}N_2NaO_3$	$C_{48}H_{84}N_2NaO_3$
Calculated m/z	502.36796	514.36796	464.25693	518.36287	564.5351	648.62892	584.56124	527.36321	731.60612	759.63742
Class	$C_xH_yNO_2$		$C_xH_yNO_3$				$C_xH_yNO_4$	$C_xH_yN_2O_2$	$C_xH_yN_2O_3$	
Compound formulae	$C_{34}H_{47}NO_2$	$C_{35}H_{47}NO_2$	$C_{27}H_{39}NO_3$	$C_{34}H_{47}NO_3$	$C_{36}H_{69}NO_3$	$C_{42}H_{81}NO_3$	$C_{36}H_{73}NO_4$	$C_{35}H_{46}N_2O_2$	$C_{46}H_{80}N_2O_3$	$C_{48}H_{84}N_2O_3$
Molecular Weight	501.744	513.755	425.605	517.743	563.939	648.099	583.971	526.753	709.141	737.194
dbe of compound	12	13	9	12	3	3	1	14	8	8
N/C ratio	0.029	0.029	0.037	0.029	0.028	0.024	0.028	0.057	0.043	0.042
O/C ratio	0.059	0.057	0.111	0.088	0.083	0.071	0.111	0.057	0.065	0.063
H/C ratio	1.382	1.343	1.444	1.382	1.917	1.929	2.028	1.314	1.739	1.750
Y1a	No	No	No	No	Yes	Yes	Yes	Yes	Yes	Yes
Original Heslington	No	No	No	No	Yes	No	Yes	No	Yes	No
H1a	No	No	Detected	No	Detected	Yes	Yes	No	Yes	Yes
H1b	No	No	No	No	Yes	Yes	Yes	No	Yes	Yes
H2a	Detected	No	No	No	Yes	Yes	Yes	No	Yes	Yes
H3a	Yes	Yes	No	Yes	Yes	Yes	Detected	Yes	Yes	Yes
H4a	Yes	Yes	No	Yes	Yes	Yes	Yes	Yes	Yes	Yes
H5a	Yes	Detected	No	Yes	Yes	Yes	Yes	Yes	Yes	Yes
H6a	Yes	Yes	No	Yes	Yes	Yes	No	Yes	Yes	Yes
H7a	Yes	Yes	No	Yes	Yes	Yes	No	Yes	Yes	Yes
H8a	Yes	Detected	No	Yes	Yes	Yes	Detected	Yes	Yes	Yes
H9a	Yes	Yes	No	Yes	Yes	Yes	No	Yes	Yes	Yes
H10a	Yes	Yes	No	Yes	Yes	Yes	No	Yes	Detected	Detected
H11a	Yes	Yes	No	Yes	Detected	Yes	Detected	Yes	Yes	Yes
H12a	Yes	Yes	No	Yes	Yes	Yes	Detected	Yes	Yes	Yes
H13aii	Yes	Yes	No	Yes	Yes	Yes	Detected	Yes	Yes	Yes
H14a	No	Detected	No	No	Detected	Detected	No	No	No	No
H14bi	Detected	Detected	No	Detected	Detected	Detected	Detected	Detected	No	No
V1a	No	Detected	No	No	Detected	Yes	No	No	Detected	Detected
B1a	Yes	Yes	No	Yes	Yes	Yes	No	Yes	Yes	Yes
DHB	No	No	No	No	No	No	No	No	No	No
Soil 3a	No	No	No	No	No	No	No	No	No	No
Soil 3b	No	No	No	No	No	Detected	No	No	No	No
Solvent	No	No	No	No	No	No	No	No	No	No

Ion formulae	$C_{12}H_{26}KO_7$	$C_{14}H_{30}KO_8$	$C_{16}H_{34}NaO_9$
Calculated m/z	321.13101	365.15723	393.20939
Class	$C_xH_yO_n$		
Compound formulae	$C_{12}H_{26}O_7$	$C_{14}H_{30}O_8$	$C_{16}H_{34}O_9$
Molecular Weight	282.383	326.383	370.436
dbe of compound	0	0	0
N/C ratio	0.000	0.000	0.000
O/C ratio	1.714	1.750	1.778
H/C ratio	2.167	2.143	2.125
Y1a	Detected	Detected	No
Original Heslington	No	No	No
H1a	No	Detected	Yes
H1b	No	Detected	Yes
H2a	No	No	Detected
H3a	No	Detected	Detected
H4a	No	No	Detected
H5a	Detected	No	No
H6a	Yes	Yes	Yes
H7a	No	No	No
H8a	No	Detected	Detected
H9a	Detected	Detected	Detected
H10a	No	Detected	Yes
H11a	Detected	Detected	Detected
H12a	No	No	Detected
H13aii	No	No	Detected
H14a	No	Detected	Detected
H14bi	Detected	Detected	No
V1a	Detected	Detected	No
B1a	No	No	No
DHB	No	No	No
Soil 3a	No	No	Detected
Soil 3b	No	Detected	No
Solvent	No	Detected	No

Having determined that organic compounds with low numbers of oxygen and nitrogen atoms occur across the range of brains sampled, and that they are a consistent feature as opposed to being only found in the York brain, a literature search was undertaken to see if similar compounds had been reported elsewhere as decomposition products with longevity. Some of the formulae assigned in 3.3.1 are remarkably similar to those of substructures of kerogen, those that include saturated carbons and little functionalisation, such as that shown in Figure 27.

Kerogen is solid complex organic matter, generally found in sedimentary rocks (such as shale and mudstone), that is considered insoluble in standard organic solvents.[88] It can be associated with bitumen, often considered to be the black viscous fraction that is soluble in organic solvents.

The organic matter (OM) found in sediments is produced either as a by-product of metabolism by living organisms or from their remains on death.[157] The OM undergoes decomposition, usually by metabolic or physico-chemical

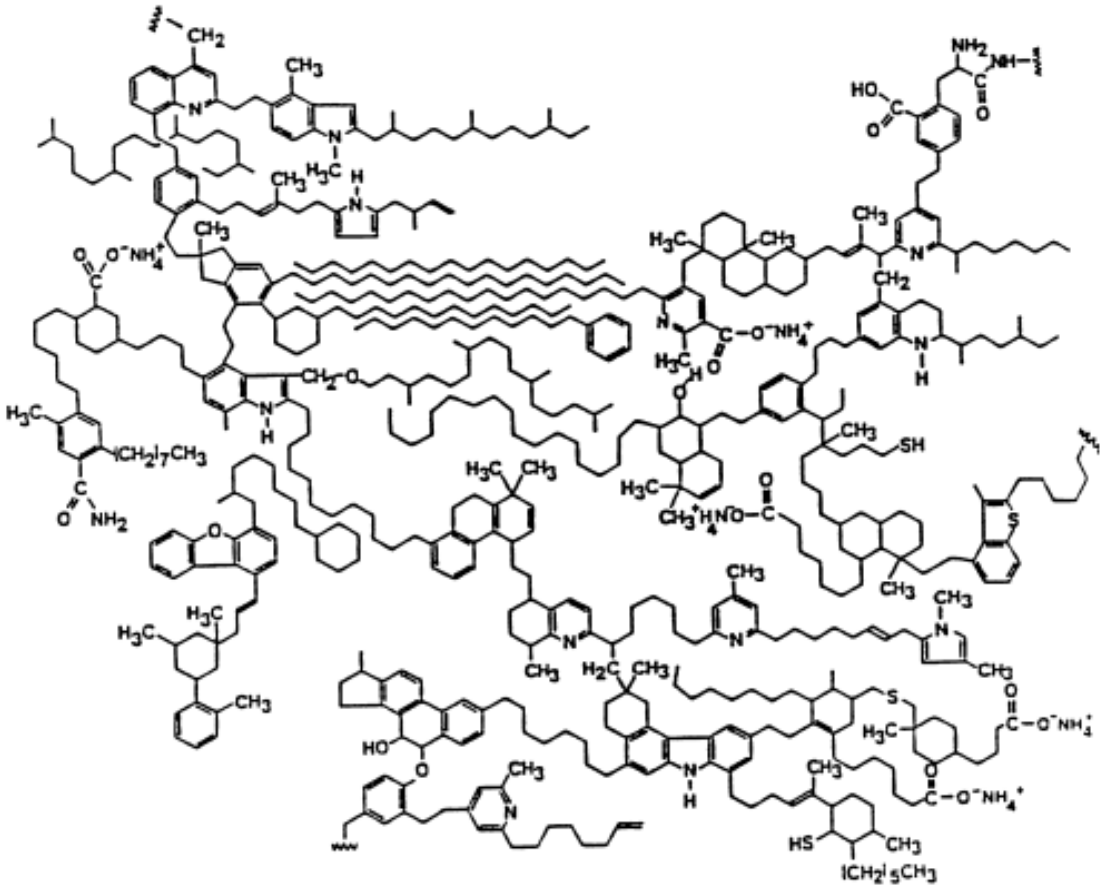

Figure 27. Structural model of Green River oil shale kerogen.[158]

processes such as oxidation and hydrolysis. This produces a range of small simple molecules: CO_2, H_2O, H_2, NH_3, N_2 and SH_2. These are reincorporated into biological organisms or the recycling processes within the environment. However, some material does not decompose easily and instead of being broken down it remains, more or less unaltered, and is incorporated into sediments. The types of OM that are preserved tend to be those that are unable to be used as energy sources by other organisms, those that may be toxic or those that undergo rapid structural changes such as polymerisation or mineralisation that then prevent enzymatic deterioration.[88] Matter that is left in environments where there are no organisms or oxygen within the sediments also tend to be preserved. There are certain types of OM that have low chemical reactivity or, by virtue of being inert have longevity and so are exploited as protective chemicals. Chemicals such as waxes and resins

(saturated hydrocarbons), chitin (a glucose derivative found, among others, in insect exoskeletons), certain pigments, isoprenoids and porphyrins, or certain metabolites such as steroids and terpenoids are examples of components liable to be preserved.[88]

Once the OM has undergone initial decomposition changes and has been incorporated into sediments, further degradation (whether microbial or chemical) can lead to recombination and polymerisation. These transformations are summarised in Figure 28.

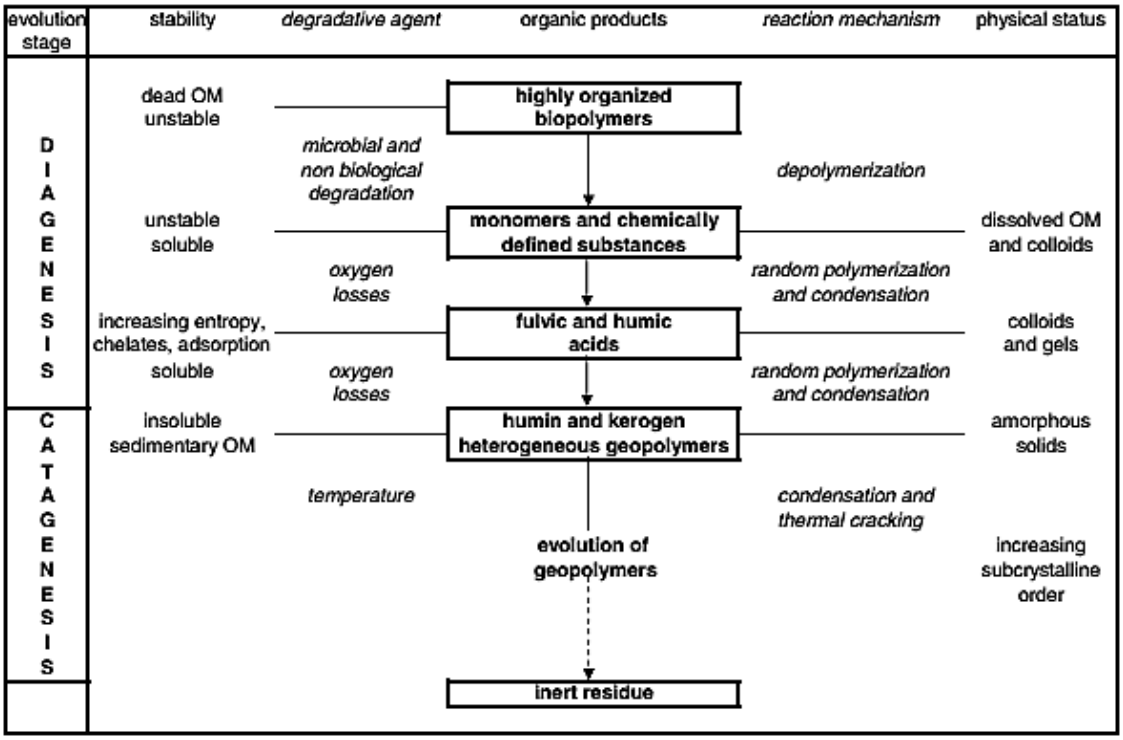

Figure 28. Schematic pathway of successive transformations of OM (taken from [159])

In kerogen formation, the organic metamorphisms are classified at different stages as diagenesis, catagenesis and metagenesis.[87] Once the organic matter is incorporated into sediments, then additional geochemical and geodynamic processes such as weathering, temperature and pressure due to changes in depth come into play.[88] Kerogen may even migrate from the

original 'source' rock to 'reservoir' rock.[160] Once kerogen is formed, generally over thousands of years, it is insoluble in most organic solvents due to the high molecular weight of its components (over 1,000 Da).[88]

This change from OM to kerogen differs both in timescale and structural complexity from the organic materials reported in this thesis, but the components we are identifying can certainly be described as resembling kerogen substructures. Comparing the hydrogen:carbon and oxygen:carbon ratios of the lipid residues (Figure 29) to van Krevelen plots of kerogen shows that the majority of points fall in the region of the plot typical of kerogen.[161]

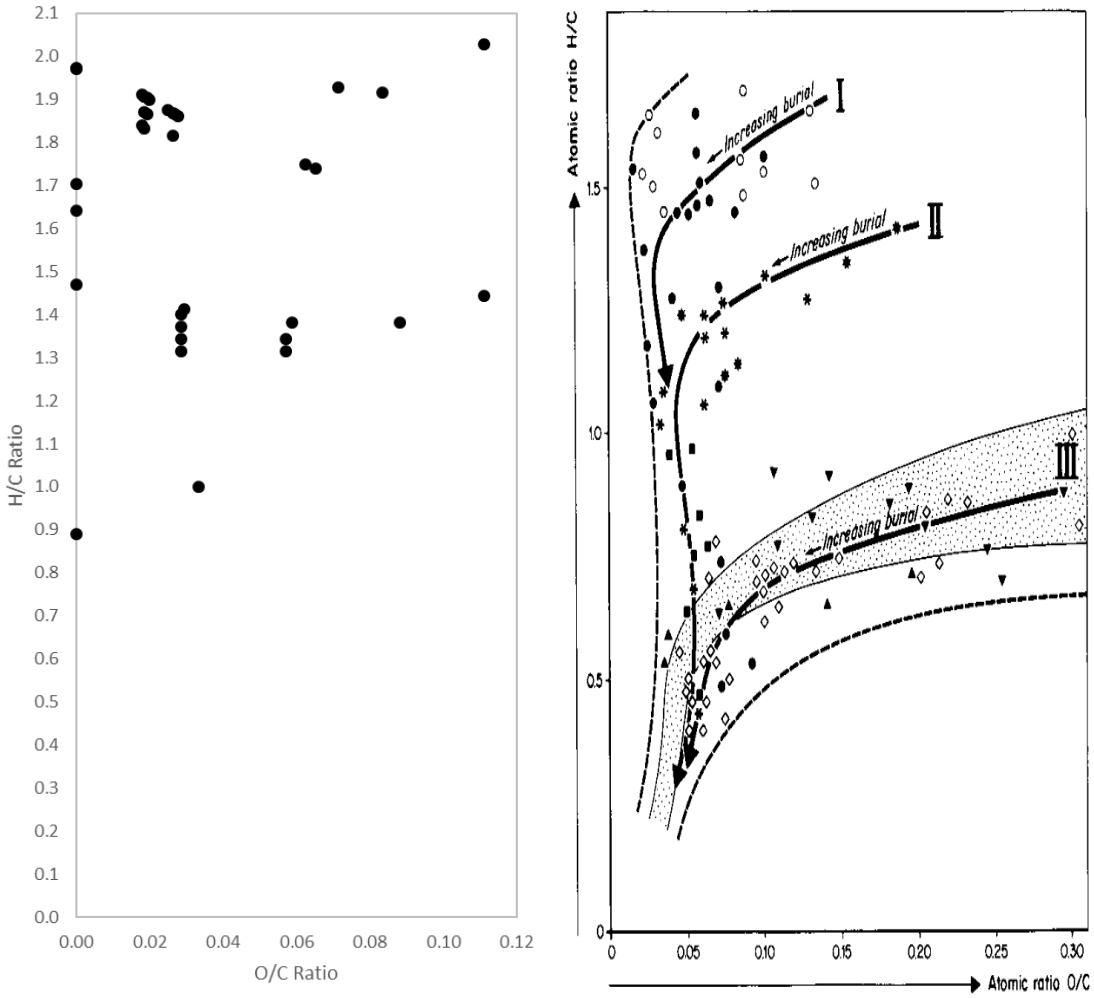

Figure 29. Left: Van Krevelen plot of ancient brain lipid residues shown in Table 49 (except the highly oxygenated $C_{12}H_{26}O_7$, $C_{14}H_{30}O_8$, $C_{16}H_{34}O_9$). Right: Van Krevelen plot of kerogen (types I, II and III)[87]

When studying kerogen, the use of organic solvents to extract 'free hydrocarbons' or associated organic matter can be carried out before Soxhlet extraction. Mixing or ultrasonic methods are then used to remove fixed kerogen from rock sources. The initial solvent extraction often follows a similar methodology to that used in the experiments presented in this thesis e.g. Farrimond et al's[162] work, in which the extracted components are described as solvent-soluble biohopanoids and geohopanoids:

"Solvent-soluble biohopanoids and geohopanoids were extracted and derivatised as outlined in Innes et al. (1997). Briefly, freeze-dried sediments were extracted with chloroform/methanol (2:1 v/v) using a Gerhardt Soxtherm apparatus, and separate aliquots of the extract were derivatised by means of three methods"[163]

Once extracted, kerogen is often analysed by GC-MS or pyrolysis GC. There are few examples of high resolution MS of kerogen, although this is a well-established approach in petroleomics, the identification of the molecular constituents of crude oil.[164-167]

Kerogen literature generally assigns kerogen as coming from marine sources or vegetation. Very little is identified as coming from mammals or higher lifeforms, although the proposed source compounds (amino acids, lipids, carbohydrates) should not be too different. Whilst kerogen has possible similarities with the components identified in the brain samples, the source differs from those commonly discussed, and it doesn't come from an entire organism but a single organ.[159] The timescale of preservation is also quite different, with the components of the ancient brain remains being produced in skeletonised burials within 200 years, as opposed to requiring the thousands of years reported for kerogen.

There is always the technical possibility that the species identified in some of the more amorphous brain matter samples are derived from organic matter found within the soil from the burial environments; the soil may be difficult to physically separate from such amorphous brain matter. However, the extraordinary preservation and definition of the York brain (it was washed and was visibly clearly a brain from which the soil could confidently be removed) meant that it was possible to be certain that the material being extracted was demonstrably from the brain material and not from the surrounding soil; compounds from this sample have been identified within most of the other brain samples. These compounds appear to fall within the kerogen formation pathway, but presumably correspond to steps that occur very early in that pathway. The organic matter is likely to be resistant to chemical change and has low water solubility, which would explain their persistence and preservation in the burial environment. In summary, these lipidic residues may thus represent the products of a common soft tissue preservation mechanism not yet generally recognised, that can allow brain material to be preserved under appropriate conditions.

5 CONCLUSION AND FURTHER WORK

Following the description of the excellent preservation of the York brain, the current investigation has sourced several ancient brain specimens from different archaeological sites for comparison. After extracting the lipidic content of these samples using the same extraction method as was used for the York brain, the high resolution mass spectrometry analysis technique allowed us to determine that all the ancient brain remains examined contained solvent-extractable organic compounds with low functionalisation. This study has demonstrated that the large lipidic residues originally identified are not unique to the York brain, but also occur in ancient brain remains from other sites and dates. However the data do not support a relationship with archaeological age as a factor, as no distinctive trends in residue occurrence have been related to the age of the original specimens. Having identified some of the chemical formulae of these residues using the high mass accuracy resulting from FT-ICR MS it has been possible to explore their chemistry.

To the best of my knowledge, such structures are not discussed within the current body of literature with regards to human body decomposition or preservation. This absence from the literature may be due to the rarity of brain samples from burials and the very limited scientific investigation into their preservation. It may also be due to the general preference for using GC-MS for archaeological investigations, rather than the high resolution MALDI FT-ICR MS method which we used for this investigation. With GC-MS it is unlikely that these heavy, un-labile, waxy residues would have been identified. Having demonstrated that these components are common to preserved brain matter, the next step will be to begin to unravel chemical mechanisms for the formation of these components. For that, information on their chemical structures (not just compound classes) is now required.

What we can conclude is that these compounds are not found within fresh brain lipid extracts (3.1), although their probable precursors are, and so are presumably formed as part of a decomposition process, presumably following a similar chemical process as takes place during kerogen formation: bio- and non-biodegradation followed by random polymerisation and condensation.[159] Once the compounds have been modified to be insoluble (in water) and resistant to chemical change, they remain preserved within the skull cavities.

It would be interesting to see the results of a similar experiment using high resolution MALDI FT-ICR MS to identify components of a classic adipocere sample. Does adipocere contain similar components to those discovered in the ancient brain remains, or is it solely composed of smaller lipids and salts? Determining whether there are components in common between the different preserved organic matter may help in understanding the preservation process itself.

The next step in a follow-up investigation would be to determine how similar the components identified in the ancient brain remains are to those found in kerogen (or associated with kerogen). MS/MS could be used to determine more detail of the molecular structures of the highlighted components. This would allow comparison with current kerogen literature but potentially it could also be used to see if any of these compounds show a similarity to those found within the living brain, i.e. are biomarkers for brain or CNS structures. As well as demonstrating provenance, this may reveal more about the chemical pathways required for the formation of the compounds found in the ancient brain extracts.

Comparison with kerogen, and the solvent-soluble OM associated with kerogen, could be achieved by performing similar extractions and analysis by

MALDI FT-ICR MS of authentic kerogen samples (e.g. Jet Rock from the Whitby Mudstone Formation). Standard tests run on kerogen and proto-kerogen, such as GC-MS, pyrolysis-GC and chemical degradation could also be carried out on the brain samples (if sufficient quantities are available), for better comparison with the existing kerogen literature. By combining these techniques, we could determine how similar the molecular structures of the solvent-extractable OM within the brain samples are, which may provide additional information on how and why the brain tissues were preserved.

A more direct method of determining why the brain tissue was preserved would be to carry out burial tests, either within the laboratory or at a body farm. The main controls would be related to tissue preservation (see introduction), temperature (a variety of temperatures similar to those of soils at appropriate burial depths), water (a range of moisture levels, especially limited hydrations), pH range, using abiotic soil and standard soils as well as more clay-like soils, and with limited oxygen levels. Having more information regarding the original burial environments of the brain samples provided would be invaluable. Either samples of fresh brain tissue would have to be placed in simulated skulls or entire burials would be required (e.g. piglet burials). The major factor would be time, as none of the samples studied were less than 100 years old; how to process burials to 'speed them up' (e.g. use of elevated heat or pressure) would need investigation if this route were to be taken. Finally, it would naturally be ideal if more preserved brains were to be discovered, or samples from other collections accessed and investigated for the presence of similar compounds to those identified here.

APPENDICES

Appendix I: Photos of Ancient Brain Remains

Figure 30. Photograph of brain mass HMC SK1709, from which sample H1 had been removed for potential DNA analysis.

Figure 31. Photograph of brain mass labelled HMC SK1913, from which H7 was sampled.

Figure 32. Photograph of HMC94 SK2039, from which H11 was sampled.

Figure 33. Photograph of brain mass labelled HMC SK2123, from which samples H12 and H13 had been sampled.

Figure 34. Photograph of brain mass HMC SK2123 which had been stored separately with the additional label 'Red sample', from which H14 was sampled.

Figure 35. Photograph of the brain mass labelled SJB09 SK117, after sample B1 was removed.

Figure 36. Photograph of the brain mass labelled VSS-A SK2463, from which V1 was sampled.

Figure 37. Photographs of ancient preserved brain matter. From (L-R) Top row: H1, B1, V1, H1. Second row: H2, H3, H4, H5. Third row: H6, H7, H8, H9. Bottom row: H10, H11, H12, H13.

Figure 38: (Figure 37 continued) H14

Appendix II: Unidentified Compound Tables

This appendix provides summary data of peaks that were unable to be assigned formula using the method described in 3.3 Comparison of Spectra of Ancient Brain Lipid Extracts. Table 50 shows the top peaks identified using S:N and intensities using the MassList data from the first replicate of each sample.

Legend
Formula assigned
Assigned (of interest)
Multiple assignments
Unassigned

Table 51 onwards provides the S:N, intensity and relative intensity % information along with the measured *m/z* values for the unassigned peaks.

Table 50. Significant peaks from the initial replicate mass spectra: the top five S:N peaks, plus top five intense peaks

Sample	S:N	*m/z*	Intensity	Resolution	Ranking	Table No.
H4a	7745.7	502.36793	1147219584	158028	#1	33
H6a	5888.6	497.23573	740723968	160132	#1	53
H6a	5812.8	365.15708	610774784	219108	#2	44
H9a	5307.5	501.38397	724846080	157518	#1	29
H4a	4630.1	513.38391	699732800	155149	#2	31
H6a	4556.0	437.23565	522658496	181733	#3	50
H9a	4538.6	502.36794	630138816	157771	#2	33
H6a	4256.3	321.13077	447302528	248874	#4	43
H6a	4087.1	393.20939	433222240	203226	#5	45
H6a	3750.1	541.26198	500162272	147294	#4 Intensity	55
V1a	3186.3	810.84242	536857920	98365	#1	28
B1a	3139.5	513.38406	513161056	154806	#1	31
B1a	3111.8	501.38415	486390528	157626	#2	29
V1a	2988.2	782.81126	503781568	102002	#2	26
H8a	2751.9	501.38392	372404512	158094	#1	29
H8a	2668.6	502.36790	366584576	158081	#2	33
H12a	2643.1	731.60667	449381664	109316	#1	41
H9a	2476.7	513.38390	349772384	155132	#3	31
H10a	2421.3	850.67377	365529600	93276	#1	72
B1a	2311.5	500.38892	361371808	158624	#3	15
H4a	2288.4	487.40472	326055392	162924	#4	11
Y1a	2064.2	564.53510	300621824	140835	#1	37
H4a	2016.5	501.38400	293033088	157962	#5	29
H12a	1949.5	759.63823	329006080	105157	#2	42
H11a	1815.2	502.36817	228869696	158513	#1	33
V1a	1752.4	754.77981	295897120	105688	#3	23
H13a	1697.4	731.60658	294104992	109464	#1	41
H1a	1485.6	371.36726	161548096	213606	#1	8
H4a	1423.9	511.36824	215397248	155976	#5	30
H14b	1404.3	549.31076	222491712	144935	#1	46
H9a	1386.0	518.36282	199198384	153484	#4	36
Y1a	1368.1	584.56131	203449392	136145	#2	39
B1a	1335.3	514.36826	218444224	154101	#4	34
B1a	1303.1	498.37323	203859920	159206	#5	14
H12a	1302.9	411.37355	147542336	192690	#3	12
Y1a	1295.2	769.56191	222809984	103772	#3	67
H5a	1294.9	866.64701	171511376	91666	#1	76
H12a	1245.2	753.58853	210274880	105944	#4	66
H13a	1224.7	769.56257	210928064	104070	#2	67
B1a	1220.0	866.64885	212526496	91464	#5 Intensity	76
H10a	1200.1	487.40463	150049920	163471	#2	11
H11a	1163.5	513.38415	148525648	155093	#2	31
H1a	1146.9	463.24921	143583792	172029	#2	32
H12a	1141.5	518.56635	167784208	153151	#5	9
H8a	1121.6	850.67390	172735088	93373	#3	72
H10a	1120.9	502.36787	143489104	158731	#3	33
Y1a	1110.8	558.56085	159625264	142865	#4	19
H10a	1104.8	857.26041	166969232	93191	#4	75
H11a	1095.9	753.58830	167992176	105784	#3	66
H9a	1082.6	527.36318	158351728	149933	#5	40
Y1a	1080.4	622.51721	167955776	128233	#5	63
Y1a	1055.2	853.65577	181226224	90679	#4 Intensity	74
H8a	982.3	487.40466	131166160	163037	#4	11
H13a	907.6	778.78052	156401504	102470	#3	24
H8a	892.8	518.36276	126657896	153869	#5	36

Sample	S:N	*m/z*	Intensity	Resolution	Ranking	Table No.
H11a	882.2	591.16932	123699448	132197	#4	62
H11a	880.7	731.60650	134848896	109146	#5	41
Orig Hes	873.1	558.56026	94157008	87715	#1	19
H5a	848.0	850.67306	111252360	93425	#2	72
H10a	817.8	836.65833	122328568	95362	#5	70
H11a	817.1	835.66685	126273656	94952	#5 Intensity	69
H13a	794.6	591.16935	124609912	133029	#4	62
H2a	793.9	850.67285	106139416	93563	#1	72
H13a	765.2	752.76490	132357272	106471	#5	22
H13a	750.0	753.58846	129733888	106310	#5 Intensity	66
H5a	725.2	411.37307	75432024	192208	#3	12
H3a	721.8	850.67377	102309128	93542	#1	72
H7a	676.1	866.64786	102886432	90979	#1	76
H14a	668.3	475.03456	91763808	166905	#1	51
H7a	635.7	850.67370	96096720	92987	#2	72
H1a	628.0	464.25693	78751896	170723	#3	35
H5a	623.9	648.62828	75403760	123197	#4	38
H2a	606.0	564.14496	76517744	140815	#2	60
H14a	565.3	541.95693	90001352	146137	#2	56
H2a	528.2	648.62822	68771144	123001	#3	38
H1b	523.1	850.67319	75562120	93427	#1	72
H2a	521.1	688.62050	68780520	116308	#4	48
V1a	503.9	866.64834	85048648	91526	#4	76
Orig Hes	479.7	530.52900	50985892	92430	#2	16
H5a	458.3	852.63134	60274400	93276	#5	73
H1a	455.9	629.33859	67364672	125588	#4	47
V1a	446.5	569.43305	70081832	139853	#5	61
H1a	442.2	405.20733	50097424	196634	#5	13
H1a	436.3	640.61474	64501928	130878	#5 Intensity	65
H2a	401.0	815.69879	53771760	97115	#5	68
H3a	400.3	502.36784	52690288	158300	#2	33
H3a	397.7	513.38381	53003976	154414	#3	31
H3a	364.5	518.56580	49211336	152930	#4	9
H14a	357.8	485.30279	50028080	163971	#3	52
H1b	349.8	371.36696	36754136	214496	#2	8
H14a	339.9	629.86603	56399184	126522	#4	64
H3a	327.1	490.53452	42092952	161973	#5	10
H14a	322.1	544.95136	51415856	146089	#5	57
H7a	315.4	968.58583	46827556	82196	#3	77
H1b	307.5	866.64723	44625348	91727	#3	76
H1b	301.3	648.62840	41476884	123791	#4	38
H7a	288.3	529.25136	36703012	147819	#4	54
H7a	266.1	848.56176	40420960	92848	#5	71
H14b	227.0	485.30310	31942806	165864	#2	52
H14b	186.0	547.33153	29765016	146472	#3	58
H1b	177.8	688.62073	25125248	117135	#5	48
H14b	162.0	541.95726	25964372	145197	#4	56
H14b	158.1	563.32646	26167880	138558	#5	59
Orig Hes	113.8	544.54461	12454207	90161	#3	17
Orig Hes	92.1	556.54448	10123522	89172	#4	18
Orig Hes	81.9	586.59153	9352824	82856	#5	20
Orig Hes		726			Of Interest	21
Orig Hes		780			Of Interest	25
Orig Hes		806			Of Interest	27

Table 51. Summary of signal at *m/z* 437

Calculated *m/z*	437.235					
Sample designation + MALDI replicate no.	Measured *m/z*	Present	S:N	Intensity	Rel. Int. %	Resolution
Y1a 1	437.23574	Yes	7.2	1106967	0.4	211025
Y1a 2		No				
Y1a 3		No				
Original Heslington		No				
H1a 1	437.23551	Yes	29.4	3780609	0.4	165392
H1a 2	437.23543	Yes	8.5	1192966	0.3	218178
H1a 3		No				
H1b 1	437.23545	Yes	24.3	2979088	0.3	179491
H1b 2	437.23555	Yes	25.2	3002469	0.8	181957
H1b 3	437.23528	Yes	18.7	2314939	0.5	194485
H2a 1		No				
H2a 2		No				
H2a 3	437.23521	Yes	4.9	779290	0.2	244220
H3a 1		No				
H3a 2		No				
H3a 3		No				
H4a 1		No				
H4a 2		No				
H4a 3		No				
H5a 1		No				
H5a 2		No				
H5a 3		No				
H6a 1	437.23565	Yes	4556.0	522658496	70.6	181733
H6a 2	437.23565	Yes	3083.2	348667840	47.5	181547
H6a 3	437.23564	Yes	3473.7	400597728	42.6	181695
H7a 1	437.23560	Yes	5.7	902597	0.2	129034
H7a 2		No				
H7a 3	437.23555	Yes	10.8	1488459	0.2	198289
H8a 1		No				
H8a 2	437.23544	Yes	4.8	796257	0.2	200980
H8a 3	437.23593	Yes	5.7	900355	0.2	206700
H9a 1		No				
H9a 2		No				
H9a 3	437.23556	Yes	14.6	1903005	0.4	157081
H10a 1	437.23566	Yes	14.7	1943232	0.3	209670
H10a 2		Yes				
H10a 3	437.23569	Yes	9.3	1353630	0.4	193526
H11a 1		No				
H11a 2	437.23587	Yes	101.7	12081922	1.6	182129
H11a 3	437.23541	Yes	14.2	1726821	1.3	182503
H12a 1		No				
H12a 2		No				
H12a 3		No				
H13aii 1		No				
H13aii 2		No				
H13aii 3	437.23577	Yes	13.6	1785287	0.3	184823
H14a 1		No				
H14a 2	437.23565	Yes	51.6	6670331	0.9	183100
H14a 3		No				
H14bi 1		No				
H14bi 2		No				
H14bi 3		No				
V1a 1		No				
V1a 2		No				
V1a 3		No				
B1a 1		No				
B1a 2		No				
B1a 3		No				
DHB 1		No				
DHB 2		No				
DHB 3		No				
Soil 3a 1	437.23843	Possibly	11.2	1710052	0.2	191227
Soil 3a 2	437.23832	Possibly	19.6	2711679	0.3	185435
Soil 3a 3	437.23826	Possibly	11.7	1772674	0.4	170985
Soil 3b 1	437.23820	Possibly	6.7	1094950	0.1	262073
Soil 3b 2	437.23834	Possibly	6.1	1063838	0.1	222850
Soil 3b 3	437.23616	Possibly	5.2	906032	0.2	340455
Solvent 1	437.23801	Possibly	15.6	2392853	0.1	188323
Solvent 2	437.23827	Possibly	7.9	1358350	0.2	169420
Solvent 3	437.23363	Possibly	5.6	991328	0.1	226739

Table 52. Summary of signal at *m/z* 475

Calculated *m/z*	475.0346					
Sample designation + MALDI replicate no.	Measured *m/z*	Present	S:N	Intensity	Rel. Int. %	Resolution
Y1a 1	475.03458	Yes	10.4	1579009	0.5	166357
Y1a 2	475.03427	Yes	12.1	1743666	0.6	176696
Y1a 3	475.03473	Yes	7.6	1228247	0.4	188633
Original Heslington		No				
H1a 1	475.03425	Yes	12.4	1858661	0.2	183474
H1a 2	475.03450	Yes	14.0	1876917	0.5	189019
H1a 3	475.03437	Yes	42.9	5214576	0.8	164896
H1b 1	475.03434	Yes	140.5	16768396	2.0	167071
H1b 2	475.03435	Yes	55.5	6599193	1.7	169894
H1b 3	475.03430	Yes	153.2	17817048	4.2	170704
H2a 1	475.03421	Yes	39.1	4760563	0.9	181877
H2a 2	475.03434	Yes	79.4	10355035	3.1	167750
H2a 3	475.03429	Yes	126.1	14153377	4.0	165351
H3a 1	475.03452	Yes	140.3	17796960	3.2	168660
H3a 2	475.03461	Yes	405.7	51732772	8.5	165538
H3a 3	475.03443	Yes	316.1	37434144	4.9	167449
H4a 1		No				
H4a 2		No				
H4a 3	475.03455	Yes	9.6	1573263	0.2	199782
H5a 1	475.03418	Yes	84.5	9501151	5.0	169266
H5a 2	475.03428	Yes	96.5	11241642	3.7	171480
H5a 3	475.03419	Yes	47.1	5940580	0.7	170437
H6a 1	475.03443	Yes	27.0	3561484	0.5	174396
H6a 2	475.03444	Yes	38.0	4815529	0.7	170050
H6a 3	475.03449	Yes	10.4	1540557	0.2	157756
H7a 1	475.03447	Yes	143.4	17262694	4.2	168048
H7a 2	475.03455	Yes	135.7	17013558	2.7	166325
H7a 3	475.03427	Yes	19.8	2625851	0.4	170658
H8a 1	475.03460	Yes	89.7	11898242	2.0	168985
H8a 2	475.03480	Yes	62.2	7756604	1.8	171583
H8a 3	475.03453	Yes	55.4	6861025	1.3	172634
H9a 1	475.03467	Yes	33.4	4625546	0.6	169686
H9a 2	475.03463	Yes	15.6	2328441	0.3	173639
H9a 3	475.03444	Yes	39.4	4981208	1.1	173955
H10a 1		No				
H10a 2		No				
H10a 3		No				
H11a 1	475.03503	Yes	7.5	1181243	0.5	168900
H11a 2		No				
H11a 3		No				
H12a 1		No				
H12a 2		No				
H12a 3		No				
H13aii 1	475.03485	Yes	4.5	856905	0.2	178372
H13aii 2		No				
H13aii 3		No				
H14a 1	475.03456	Yes	668.3	91763808	6.5	166905
H14a 2	475.03455	Yes	697.2	94010056	12.6	166657
H14a 3	475.03470	Yes	1022.8	154462192	7.4	167266
H14bi 1	475.03486	Yes	84.6	11911432	1.3	170649
H14bi 2	475.03474	Yes	73.5	10118442	1.6	171829
H14bi 3	475.03488	Yes	523.4	77456968	1.5	167423
V1a 1	475.03462	Yes	171.3	22722732	1.0	167913
V1a 2	475.03458	Yes	212.4	26594982	4.2	165439
V1a 3	475.03454	Yes	277.6	35036228	7.5	166854
B1a 1	475.03481	Yes	46.5	7093970	1.4	167036
B1a 2	475.03458	Yes	121.2	15634869	5.1	163637
B1a 3	475.03435	Yes	246.1	29340442	6.9	168656
DHB 1		No				
DHB 2		No				
DHB 3		No				
Soil 3a 1	475.03641	Possibly	9.4	1654723	0.2	189312
Soil 3a 2	475.03620	Possibly	21.0	3233749	0.3	159486
Soil 3a 3	475.03597	Possibly	23.0	3627947	0.8	166594
Soil 3b 1	475.03630	Possibly	31.0	4545242	0.6	158692
Soil 3b 2	475.03589	Possibly	4.3	908638	0.0	203344
Soil 3b 3	475.03608	Possibly	9.8	1623640	0.3	153953
Solvent 1	475.03589	Possibly	24.7	4137956	0.1	160673
Solvent 2	475.03608	Possibly	12.4	2274775	0.3	198406
Solvent 3	475.03641	Possibly	9.4	1654723	0.2	189312

Table 53. Summary of signal at *m/z* 485

Calculated *m/z*	485.3031					
Sample designation + MALDI replicate no.	Measured *m/z*	Present	S:N	Intensity	Rel. Int. %	Resolution
Y1a 1	485.30282	Yes	101.6	13172061	4.4	167046
Y1a 2	485.30262	Yes	141.6	17648636	6.5	165304
Y1a 3	485.30274	Yes	125.2	16257716	4.7	165401
Original Heslington		No				
H1a 1	485.30270	Yes	15.6	2294325	0.2	187742
H1a 2		No				
H1a 3		No				
H1b 1		No				
H1b 2	485.30262	Yes	5.0	850687	0.2	260397
H1b 3	485.30233	Yes	12.9	1756697	0.4	183301
H2a 1	485.30273	Yes	11.2	1566883	0.3	205692
H2a 2	485.30270	Yes	10.9	1679524	0.5	199141
H2a 3	485.30261	Yes	16.4	2079016	0.6	176983
H3a 1	485.30282	Yes	17.5	2485661	0.5	177997
H3a 2	485.30276	Yes	31.1	4271870	0.7	173361
H3a 3	485.30271	Yes	31.1	3957876	0.5	171866
H4a 1		No				
H4a 2		No				
H4a 3	485.30311	Yes	6.4	1159568	0.1	199473
H5a 1	485.30244	Yes	25.7	3089781	1.6	177276
H5a 2	485.30252	Yes	36.6	4462409	1.5	168386
H5a 3	485.30250	Yes	44.8	5726927	0.7	173115
H6a 1	485.30268	Yes	23.3	3135957	0.4	176985
H6a 2	485.30272	Yes	17.1	2335186	0.3	178358
H6a 3	485.30276	Yes	27.6	3702176	0.4	170254
H7a 1	485.30273	Yes	55.4	6895027	1.7	172053
H7a 2	485.30285	Yes	30.2	4048230	0.6	171569
H7a 3	485.30273	Yes	33.8	4343932	0.6	180657
H8a 1	485.30272	Yes	14.1	2138891	0.4	195873
H8a 2	485.30290	Yes	10.9	1610620	0.4	193591
H8a 3	485.30255	Yes	17.8	2406861	0.5	171928
H9a 1	485.30281	Yes	42.4	5885537	0.7	167839
H9a 2	485.30265	Yes	16.4	2473398	0.3	178418
H9a 3	485.30269	Yes	23.1	3062138	0.7	168660
H10a 1		No				
H10a 2	485.30262	Yes	10.7	1475965	0.8	191296
H10a 3	485.30298	Yes	4.2	808384	0.2	187730
H11a 1		No				
H11a 2	485.30309	Yes	11.3	1691350	0.2	163941
H11a 3	485.30295	Yes	4.0	692449	0.5	212726
H12a 1	485.30285	Yes	5.3	1005119	0.2	168486
H12a 2		No				
H12a 3		No				
H13aii 1	485.30301	Yes	13.4	2037298	0.5	177649
H13aii 2	485.30248	Yes	9.1	1427286	0.4	181061
H13aii 3	485.30283	Yes	19.0	2550473	0.4	189573
H14a 1	485.30279	Yes	357.8	50028080	3.5	163971
H14a 2	485.30281	Yes	287.0	39414380	5.3	165502
H14a 3	485.30300	Yes	330.8	51196260	2.5	163887
H14bi 1	485.30310	Yes	227.0	31942806	3.6	165864
H14bi 2	485.30292	Yes	239.2	32681550	5.0	165411
H14bi 3	485.30314	Yes	115.1	17641380	0.3	166106
V1a 1	485.30283	Yes	290.8	38933396	1.8	164404
V1a 2	485.30276	Yes	398.1	50162712	8.0	162513
V1a 3	485.30275	Yes	333.1	42467140	9.1	164696
B1a 1	485.30304	Yes	44.4	6932624	1.4	172835
B1a 2	485.30275	Yes	50.1	6713034	2.2	173812
B1a 3	485.30266	Yes	33.4	4254729	1.0	171337
DHB 1		No				
DHB 2		No				
DHB 3		No				
Soil 3a 1	485.30404	Possibly	414.1	61788532	7.8	152408
Soil 3a 2	485.30437	Possibly	159.4	23178656	2.1	162989
Soil 3a 3	485.30421	Possibly	187.9	28124302	6.2	160493
Soil 3b 1	485.30440	Possibly	290.6	41005240	5.4	160318
Soil 3b 2	485.30395	Possibly	284.9	42274620	2.2	163179
Soil 3b 3	485.30441	Possibly	100.8	14407908	2.7	164638
Solvent 1	485.30413	Possibly	71.3	11686924	0.3	171109
Solvent 2	485.30429	Possibly	84.3	14144505	1.7	167407
Solvent 3	485.30404	Possibly	414.1	61788532	7.8	152408

Table 54. Summary of signal at *m/z* 497

Calculated *m/z*	497.23573					
Sample designation + MALDI replicate no.	Measured *m/z*	Present	S:N	Intensity	Rel. Int. %	Resolution
Y1a 1	497.23554	Yes	13.5	2034204	0.7	165313
Y1a 2	497.23534	Yes	11.0	1660329	0.6	190924
Y1a 3	497.23554	Yes	12.9	1972666	0.6	180187
Original Heslington		No				
H1a 1	497.23540	Yes	9.1	1483924	0.1	137540
H1a 2		No				
H1a 3	497.23526	Yes	5.9	970688	0.1	136830
H1b 1	497.23571	Yes	29.3	3810684	0.4	167333
H1b 2	497.23594	Yes	10.8	1540608	0.4	178563
H1b 3	497.23550	Yes	14.7	2000039	0.5	181164
H2a 1		No				
H2a 2		No				
H2a 3		No				
H3a 1		No				
H3a 2	497.23556	Yes	6.3	1123307	0.2	155995
H3a 3	497.23527	Yes	8.0	1240956	0.2	210580
H4a 1		No				
H4a 2		No				
H4a 3		No				
H5a 1		No				
H5a 2		No				
H5a 3		No				
H6a 1	497.23573	Yes	5888.6	740723968	100.0	160132
H6a 2	497.23572	Yes	5956.4	734608192	100.0	159948
H6a 3	497.23571	Yes	7409.2	939987136	100.0	160135
H7a 1	497.23590	Yes	10.5	1557967	0.4	156232
H7a 2	497.23592	Yes	7.0	1169568	0.2	170710
H7a 3	497.23568	Yes	12.3	1788491	0.3	166479
H8a 1		No				
H8a 2	497.23562	Yes	5.4	959117	0.2	241084
H8a 3		No				
H9a 1		No				
H9a 2		No				
H9a 3	497.23565	Yes	32.1	4244641	0.9	167326
H10a 1		No				
H10a 2		No				
H10a 3		No				
H11a 1		No				
H11a 2	497.23603	Yes	74.5	9831020	1.3	164436
H11a 3	497.23501	Yes	7.6	1091140	0.8	113291
H12a 1	497.23359	Yes	8.9	1539347	0.3	183747
H12a 2	497.23382	Yes	8.6	1501758	0.3	192137
H12a 3	497.23396	Yes	9.6	1648004	0.4	163210
H13aii 1		No				
H13aii 2		No				
H13aii 3	497.23600	Yes	41.6	5369805	0.9	157758
H14a 1	497.23560	Yes	18.7	2973298	0.2	159905
H14a 2	497.23573	Yes	185.0	26254996	3.5	158880
H14a 3		No				
H14bi 1	497.23626	Yes	10.0	1750521	0.2	141613
H14bi 2	497.23571	Yes	16.9	2645586	0.4	155871
H14bi 3		No				
V1a 1		No				
V1a 2	497.23551	Yes	11.1	1708055	0.3	175678
V1a 3	497.23580	Yes	10.6	1665966	0.4	177455
B1a 1		No				
B1a 2		No				
B1a 3		No				
DHB 1		No				
DHB 2		No				
DHB 3		No				
Soil 3a 1	497.23678	Possibly	6.2	1269158	0.2	205487
Soil 3a 2	497.23688	Possibly	6.0	1188975	0.1	137492
Soil 3a 3	497.23683	Possibly	6.0	1227658	0.3	150631
Soil 3b 1	497.23727	Possibly	5.5	1095719	0.1	162734
Soil 3b 2	497.23653	Possibly	9.5	1765659	0.1	159697
Soil 3b 3	497.23712	Possibly	13.1	2208579	0.4	182777
Solvent 1		No				
Solvent 2	497.23744	Possibly	6.3	1391531	0.2	121999
Solvent 3	497.23678	Possibly	6.2	1269158	0.2	205487

Table 55. Summary of signal at *m/z* 529

Calculated *m/z*	529.251					
Sample designation + MALDI replicate no.	Measured *m/z*	Present	S:N	Intensity	Rel. Int. %	Resolution
Y1a 1	529.25206	Yes	13.1	2091754	0.7	144237
Y1a 2	529.25138	Yes	17.2	2550732	0.9	166898
Y1a 3	529.25163	Yes	18.7	2875921	0.8	150406
Original Heslington		No				
H1a 1		No				
H1a 2	529.25130	Yes	9.9	1484800	0.4	149745
H1a 3	529.25124	Yes	17.4	2398598	0.4	151130
H1b 1	529.25111	Yes	29.2	3942199	0.5	139226
H1b 2	529.25179	Yes	7.1	1147408	0.3	153035
H1b 3	529.25102	Yes	19.3	2615891	0.6	156450
H2a 1	529.25165	Yes	9.0	1380201	0.3	132336
H2a 2	529.25149	Yes	10.0	1682395	0.5	115368
H2a 3	529.25112	Yes	86.9	10272178	2.9	147585
H3a 1	529.25128	Yes	19.2	2903952	0.5	154594
H3a 2	529.25146	Yes	71.6	10242021	1.7	147628
H3a 3	529.25127	Yes	98.9	12674955	1.7	145125
H4a 1		No				
H4a 2	529.25193	Yes	9.6	1838171	0.2	132011
H4a 3	529.25155	Yes	21.1	3521729	0.4	154511
H5a 1	529.25100	Yes	220.9	25425224	13.4	150594
H5a 2	529.25112	Yes	267.0	32359742	10.6	150401
H5a 3	529.25107	Yes	130.4	17264238	2	151168
H6a 1	529.25133	Yes	135.5	18136326	2.4	148928
H6a 2	529.25136	Yes	144.8	18943726	2.6	149854
H6a 3	529.25135	Yes	132.5	17923218	1.9	151081
H7a 1	529.25136	Yes	288.3	36703012	9.0	147819
H7a 2	529.25140	Yes	164.9	22253920	3.5	148945
H7a 3	529.25136	Yes	53.3	7086914	1.0	156779
H8a 1	529.25144	Yes	81.4	12015359	2.1	146523
H8a 2	529.25168	Yes	50.7	6943652	1.6	154718
H8a 3	529.25134	Yes	67.4	8931793	1.7	151219
H9a 1	529.25147	Yes	238.9	35176952	4.4	149308
H9a 2	529.25139	Yes	80.3	12186672	1.4	152977
H9a 3	529.25127	Yes	333.4	43345964	9.6	148941
H10a 1	529.25140	Yes	16.7	2509974	0.4	158379
H10a 2	529.25131	Yes	7.5	1160484	0.6	193270
H10a 3		No				
H11a 1	529.25179	Yes	44.6	6107634	2.7	152589
H11a 2	529.25170	Yes	29.8	4304638	0.6	149048
H11a 3	529.25176	Yes	14.9	1922854	1.5	151313
H12a 1		No				
H12a 2		No				
H12a 3	529.25121	Yes	5.0	1062707	0.3	171861
H13aii 1	529.25210	Yes	6.9	1289925	0.3	138046
H13aii 2		No				
H13aii 3	529.25169	Yes	5.7	1015005	0.2	191652
H14a 1	529.25145	Yes	13.0	2309980	0.2	171973
H14a 2	529.25175	Yes	12.6	2186754	0.3	132612
H14a 3	529.25166	Yes	23.4	4419660	0.2	148962
H14bi 1	529.25155	Yes	13.3	2361717	0.3	160452
H14bi 2	529.25191	Yes	12.6	2172929	0.3	162496
H14bi 3		No				
V1a 1		No				
V1a 2		No				
V1a 3	529.25173	Yes	5	980375	0.2	149730
B1a 1		No				
B1a 2		No				
B1a 3		No				
DHB 1		No				
DHB 2		No				
DHB 3		No				
Soil 3a 1		No				
Soil 3a 2		No				
Soil 3a 3		No				
Soil 3b 1		No				
Soil 3b 2		No				
Soil 3b 3		No				
Solvent 1		No				
Solvent 2		No				
Solvent 3		No				

Table 56. Summary of signal at *m/z* 541.2

Calculated *m/z*	541.26198					
Sample designation + MALDI replicate no.	Measured *m/z*	Present	S:N	Intensity	Rel. Int. %	Resolution
Y1a 1	541.262	Yes	9.5	1623121	0.5	168618
Y1a 2	541.26168	Yes	9.9	1611549	0.6	155832
Y1a 3		No				
Original Heslington		No				
H1a 1		No				
H1a 2		No				
H1a 3		No				
H1b 1	541.26176	Yes	25.1	3461672	0.4	146634
H1b 2	541.2628	Yes	8	1266771	0.3	166405
H1b 3	541.26179	Yes	7	1144486	0.3	145685
H2a 1		No				
H2a 2	541.26308	Yes	14	2271481	0.7	148068
H2a 3	541.26214	Yes	4	748181	0.2	166957
H3a 1		No				
H3a 2	541.26332	Yes	9.9	1700923	0.3	181643
H3a 3	541.2615	Yes	6.7	1141705	0.2	140372
H4a 1		No				
H4a 2		No				
H4a 3		No				
H5a 1		No				
H5a 2		No				
H5a 3		No				
H6a 1	541.26198	Yes	3750.1	500162272	67.5	147294
H6a 2	541.26197	Yes	3812.3	4.97E+08	67.7	146971
H6a 3	541.26195	Yes	4634.8	6.25E+08	66.5	147182
H7a 1		No				
H7a 2		No				
H7a 3	541.26174	Yes	7.8	1301363	0.2	124849
H8a 1	541.26328	Possibly	15.2	2525386	0.4	161332
H8a 2		No				
H8a 3	541.26327	Possibly	5.8	1047538	0.2	149327
H9a 1		No				
H9a 2		No				
H9a 3	541.26182	Yes	31.3	4380332	1	157080
H10a 1		No				
H10a 2		No				
H10a 3		No				
H11a 1		No				
H11a 2	541.26245	Yes	31.1	4541274	0.6	150890
H11a 3		No				
H12a 1		No				
H12a 2		No				
H12a 3		No				
H13aii 1		No				
H13aii 2		No				
H13aii 3	541.2623	Yes	28.8	4018850	0.7	148477
H14a 1	541.26208	Yes	15.5	2739989	0.2	145577
H14a 2	541.26202	Yes	145.4	22325700	3	146335
H14a 3	541.26245	Yes	13.3	2702023	0.1	145673
H14bi 1		No				
H14bi 2	541.26224	Yes	9	1658603	0.3	142770
H14bi 3		No				
V1a 1		No				
V1a 2	541.26221	Yes	8.3	1427076	0.2	147693
V1a 3	541.26141	Yes	9.3	1585012	0.3	103022
B1a 1		No				
B1a 2		No				
B1a 3		No				
DHB 1		No				
DHB 2		No				
DHB 3		No				
Soil 3a 1	541.26394	Possibly	7.4	1609213	0.2	162618
Soil 3a 2	541.26424	Possibly	8.2	1689568	0.2	175437
Soil 3a 3		No				
Soil 3b 1	541.26342	Possibly	7	1444763	0.2	178711
Soil 3b 2		No				
Soil 3b 3	541.26397	Possibly	10.5	2030030	0.4	162607
Solvent 1		No				
Solvent 2	541.26465	Possibly	5.2	1350395	0.2	183734
Solvent 3	541.26394	Possibly	7.4	1609213	0.2	162618

Table 57. Summary of signal at *m/z* 541.9

Calculated *m/z*	541.9569					
Sample designation + MALDI replicate no.	Measured *m/z*	Present	S:N	Intensity	Rel. Int. %	Resolution
Y1a 1	541.95703	Yes	9.2	1594994	0.5	116377
Y1a 2	541.95674	Yes	10.9	1773604	0.7	164923
Y1a 3	541.95646	Yes	10.7	1822632	0.5	137092
Original Heslington		No				
H1a 1		No				
H1a 2	541.95627	Yes	9.6	1464091	0.4	160268
H1a 3	541.95665	Yes	25.7	3470953	0.5	142337
H1b 1	541.95661	Yes	40.6	5471998	0.6	143536
H1b 2	541.95694	Yes	4.4	839450	0.2	177581
H1b 3	541.95663	Yes	20.9	2867192	0.7	149396
H2a 1	541.95630	Yes	13.2	1912513	0.4	156402
H2a 2	541.95629	Yes	9.1	1608051	0.5	154895
H2a 3	541.95648	Yes	27.4	3480832	1.0	160611
H3a 1	541.95686	Yes	45.4	6633692	1.2	145853
H3a 2	541.95702	Yes	95.0	13873429	2.3	145526
H3a 3	541.95681	Yes	84.0	11016311	1.5	145087
H4a 1		No				
H4a 2		No				
H4a 3		No				
H5a 1	541.95653	Yes	29.3	3654230	1.9	148845
H5a 2	541.95686	Yes	18.0	2480734	0.8	171136
H5a 3		No				
H6a 1	541.95686	Yes	37.1	5304901	0.7	143753
H6a 2	541.95686	Yes	29.1	4129616	0.6	147879
H6a 3	541.95682	Yes	20.3	3066702	0.3	141258
H7a 1	541.95700	Yes	214.1	27887308	6.8	144280
H7a 2	541.95695	Yes	334.5	45919016	7.2	145785
H7a 3	541.95613	Yes	17.2	2533758	0.4	117288
H8a 1	541.95614	Yes	11.1	1961867	0.3	134328
H8a 2	541.95740	Yes	6.5	1170838	0.3	165421
H8a 3	541.95679	Yes	8.5	1413476	0.3	140217
H9a 1	541.95699	Yes	21.2	3507900	0.4	124278
H9a 2	541.95694	Yes	43.3	6950157	0.8	146624
H9a 3	541.95680	Yes	42.8	5952823	1.3	141470
H10a 1		No				
H10a 2		No				
H10a 3		No				
H11a 1	541.95734	Yes	4.7	928645	0.4	164923
H11a 2		No				
H11a 3		No				
H12a 1		No				
H12a 2		No				
H12a 3		No				
H13aii 1	541.95604	Yes	6.3	1247168	0.3	96371
H13aii 2		No				
H13aii 3		No				
H14a 1	541.95693	Yes	565.3	90001352	6.4	146137
H14a 2	541.95690	Yes	385.1	59543532	8.0	145378
H14a 3	541.95712	Yes	1175.7	214821568	10.3	146923
H14bi 1	541.95726	Yes	162.0	25964372	2.9	145197
H14bi 2	541.95711	Yes	266.9	40778120	6.3	145970
H14bi 3	541.95734	Yes	57.5	10717671	0.2	136143
V1a 1	541.95701	Yes	155.3	23691560	1.1	146182
V1a 2	541.95694	Yes	175.7	24547782	3.9	143763
V1a 3	541.95691	Yes	150.7	21370884	4.6	146109
B1a 1	541.95706	Yes	26.5	5067735	1.0	141072
B1a 2	541.95708	Yes	48.0	7263601	2.4	146893
B1a 3	541.95668	Yes	97.8	12984663	3.0	146920
DHB 1		No				
DHB 2		No				
DHB 3		No				
Soil 3a 1		No				
Soil 3a 2	541.95824	Possibly	6.1	1356713	0.1	120140
Soil 3a 3		No				
Soil 3b 1		No				
Soil 3b 2		No				
Soil 3b 3		No				
Solvent 1		No				
Solvent 2	541.95891	Possibly	4.0	1149615	0.1	163935
Solvent 3		No				

Table 58. Summary of signal at *m/z* 544

Calculated *m/z*	544.95136					
Sample designation + MALDI replicate no.	Measured *m/z*	Present	S:N	Intensity	Rel. Int. %	Resolution
Y1a 1		No				
Y1a 2	544.95133	Yes	5.9	1097299	0.4	193885
Y1a 3	544.9512	Yes	8.4	1500842	0.4	165936
Original Heslington		No				
H1a 1		No				
H1a 2		No				
H1a 3	544.95147	Yes	16.1	2281690	0.3	148910
H1b 1	544.95118	Yes	27.9	3854396	0.4	144536
H1b 2		No				
H1b 3	544.95131	Yes	13.8	1988360	0.5	153849
H2a 1		No				
H2a 2		No				
H2a 3	544.95106	Yes	6.8	1078549	0.3	186793
H3a 1	544.95149	Yes	26.7	4029019	0.7	143310
H3a 2	544.95163	Yes	43.8	6556992	1.1	151522
H3a 3	544.95123	Yes	49.8	6654864	0.9	149168
H4a 1		No				
H4a 2		No				
H4a 3		No				
H5a 1	544.95103	Yes	15.8	2105886	1.1	174719
H5a 2	544.95097	Yes	15.1	2136236	0.7	149760
H5a 3		No				
H6a 1	544.95143	Yes	24.3	3569477	0.5	154157
H6a 2	544.95123	Yes	16.2	2428940	0.3	162377
H6a 3	544.95154	Yes	7.9	1376126	0.1	155860
H7a 1	544.95142	Yes	112.5	14786144	3.6	146031
H7a 2	544.95142	Yes	200.0	27574838	4.3	146758
H7a 3		No				
H8a 1	544.95188	Yes	5.1	1067378	0.2	182246
H8a 2		No				
H8a 3		No				
H9a 1	544.95152	Yes	5.9	1204734	0.1	175327
H9a 2	544.95160	Yes	25.5	4217240	0.5	158316
H9a 3	544.95137	Yes	27.5	3933191	0.9	144971
H10a 1		No				
H10a 2		No				
H10a 3		No				
H11a 1		No				
H11a 2		No				
H11a 3		No				
H12a 1		No				
H12a 2		No				
H12a 3		No				
H13aii 1		No				
H13aii 2		No				
H13aii 3		No				
H14a 1	544.95136	Yes	322.1	51415856	3.6	146089
H14a 2	544.95136	Yes	240.6	37319632	5	147000
H14a 3	544.9516	Yes	721.5	131967392	6.3	145440
H14bi 1	544.95171	Yes	93.3	15086237	1.7	148477
H14bi 2	544.95159	Yes	141.6	21780156	3.3	147004
H14bi 3		No				
V1a 1	544.9515	Yes	95.4	14672339	0.7	146926
V1a 2	544.95142	Yes	96.6	13629429	2.2	142678
V1a 3	544.95142	Yes	95.5	13656124	2.9	148996
B1a 1	544.95153	Yes	12.8	2619118	0.5	159639
B1a 2	544.95155	Yes	24.9	3908161	1.3	150366
B1a 3	544.95125	Yes	58.9	7931436	1.9	150264
DHB 1		No				
DHB 2		No				
DHB 3		No				
Soil 3a 1		No				
Soil 3a 2		No				
Soil 3a 3		No				
Soil 3b 1		No				
Soil 3b 2		No				
Soil 3b 3		No				
Solvent 1		No				
Solvent 2		No				
Solvent 3		No				

Table 59. Summary of signal at *m/z* 547

Calculated *m/z*	547.33153					
Sample designation + MALDI replicate no.	Measured *m/z*	Present	S:N	Intensity	Rel. Int. %	Resolution
Y1a 1	547.33010	Yes	5.1	1028032	0.3	151431
Y1a 2		No				
Y1a 3	547.33145	Yes	6.9	1288700	0.4	166608
Original Heslington		No				
H1a 1		No				
H1a 2		No				
H1a 3		No				
H1b 1		No				
H1b 2		No				
H1b 3		No				
H2a 1		No				
H2a 2		No				
H2a 3		No				
H3a 1		No				
H3a 2	547.33165	Yes	4.7	982303	0.2	153598
H3a 3		No				
H4a 1		No				
H4a 2		No				
H4a 3		No				
H5a 1		No				
H5a 2		No				
H5a 3		No				
H6a 1	547.33217	Yes	14.3	2225132	0.3	151300
H6a 2	547.33213	Yes	22.0	3192310	0.4	145583
H6a 3	547.33226	Yes	20.4	3074150	0.3	157230
H7a 1		No				
H7a 2		No				
H7a 3		No				
H8a 1		No				
H8a 2		No				
H8a 3		No				
H9a 1		No				
H9a 2		No				
H9a 3		No				
H10a 1		No				
H10a 2		No				
H10a 3		No				
H11a 1		No				
H11a 2		No				
H11a 3		No				
H12a 1	547.33267	Yes	7.1	1416270	0.3	163035
H12a 2		No				
H12a 3	547.33322	Yes	8.7	1674021	0.4	111986
H13aii 1		No				
H13aii 2		No				
H13aii 3		No				
H14a 1	547.33107	Yes	28.3	4804970	0.3	160730
H14a 2	547.33115	Yes	31.7	5189595	0.7	149429
H14a 3	547.33131	Yes	34.9	6696388	0.3	150725
H14bi 1	547.33153	Yes	186.0	29765016	3.3	146472
H14bi 2	547.33142	Yes	151.3	23249762	3.6	146280
H14bi 3	547.33155	Yes	151.4	27694218	0.5	142764
V1a 1		No				
V1a 2		No				
V1a 3		No				
B1a 1		No				
B1a 2		No				
B1a 3		No				
DHB 1		No				
DHB 2		No				
DHB 3		No				
Soil 3a 1		No				
Soil 3a 2		No				
Soil 3a 3		No				
Soil 3b 1		No				
Soil 3b 2		No				
Soil 3b 3		No				
Solvent 1		No				
Solvent 2		No				
Solvent 3		No				

Table 60. Summary of signal at *m/z* 563

Calculated *m/z*	563.32646					
Sample designation + MALDI replicate no.	Measured *m/z*	Present	S:N	Intensity	Rel. Int. %	Resolution
Y1a 1	563.32658	Yes	5.8	1147511	0.4	158306
Y1a 2		No				
Y1a 3	563.32703	Yes	7.1	1347433	0.4	130798
Original Heslington		No				
H1a 1		No				
H1a 2		No				
H1a 3		No				
H1b 1		No				
H1b 2	563.32532	Yes	4.8	901693	0.2	144247
H1b 3		No				
H2a 1	563.32581	Yes	9.0	1599578	0.3	145335
H2a 2		No				
H2a 3		No				
H3a 1		No				
H3a 2	563.32644	Yes	22.8	3664814	0.6	134011
H3a 3	563.32641	Yes	6.5	1141200	0.2	129815
H4a 1		No				
H4a 2	563.32766	Yes	8.6	1807114	0.2	136357
H4a 3	563.32669	Yes	8.6	1739732	0.2	154575
H5a 1	563.32590	Yes	5.2	892824	0.5	188556
H5a 2		No				
H5a 3	563.32616	Yes	9.4	1593299	0.2	134747
H6a 1		No				
H6a 2	563.32570	Yes	2.0	569335	0.1	259736
H6a 3		No				
H7a 1	563.32596	Yes	6.1	1096926	0.3	205366
H7a 2	563.32677	Yes	8.5	1498567	0.2	128398
H7a 3	563.32599	Yes	9.5	1557316	0.2	138507
H8a 1	563.32650	Yes	30.0	4906865	0.8	144143
H8a 2	563.32650	Yes	19.6	3010635	0.7	137032
H8a 3	563.32701	Yes	28.5	4131415	0.8	81411
H9a 1		No				
H9a 2		No				
H9a 3		No				
H10a 1		No				
H10a 2	563.32623	Yes	11.7	1722130	0.9	157059
H10a 3	563.32636	Yes	23.7	3759657	1.0	132756
H11a 1	563.32724	Yes	5.1	1005840	0.4	116209
H11a 2		No				
H11a 3		No				
H12a 1	563.32747	Yes	10.4	1988288	0.4	116216
H12a 2	563.32736	Yes	6.1	1305675	0.3	122134
H12a 3	563.32766	Yes	7.0	1452866	0.4	130463
H13aii 1	563.32846	Yes	8.0	1547457	0.4	85006
H13aii 2	563.32721	Yes	6.4	1238477	0.3	101428
H13aii 3		No				
H14a 1	563.32555	Yes	8.8	1776410	0.1	176285
H14a 2	563.32661	Yes	11.5	2154190	0.3	123926
H14a 3	563.32576	Yes	16.0	3390225	0.2	152922
H14bi 1	563.32646	Yes	158.1	26167880	2.9	138558
H14bi 2	563.32630	Yes	86.4	13793081	2.1	141902
H14bi 3	563.32655	Yes	85.5	16479149	0.3	140704
V1a 1		No				
V1a 2		No				
V1a 3		No				
B1a 1	563.32677	Yes	6.5	1560484	0.3	170747
B1a 2	563.32666	Yes	5.6	1146761	0.4	159393
B1a 3		No				
DHB 1		No				
DHB 2		No				
DHB 3		No				
Soil 3a 1		No				
Soil 3a 2		No				
Soil 3a 3		No				
Soil 3b 1		No				
Soil 3b 2		No				
Soil 3b 3		No				
Solvent 1		No				
Solvent 2		No				
Solvent 3		No				

Table 61. Summary of signal at *m/z* 564

Calculated *m/z*	564.14495					
Sample designation + MALDI replicate no.	Measured *m/z*	Present	S:N	Intensity	Rel. Int. %	Resolution
Y1a 1		No				
Y1a 2		No				
Y1a 3		No				
Original Heslington		No				
H1a 1		No				
H1a 2		No				
H1a 3		No				
H1b 1		No				
H1b 2		No				
H1b 3	564.14476	Yes	6.6	1121938	0.3	153068
H2a 1	564.14496	Yes	606.0	76517744	14.2	140815
H2a 2	564.14505	Yes	204.0	30255750	9.1	142368
H2a 3	564.14508	Yes	403.6	48057812	13.5	140641
H3a 1	564.14541	Yes	128.4	18702668	3.4	140129
H3a 2	564.14552	Yes	240.3	35567364	5.8	141350
H3a 3	564.14526	Yes	167.9	22170340	2.9	142081
H4a 1	564.14549	Yes	55.6	9815905	0.6	144552
H4a 2	564.14573	Yes	56.1	10003723	1.1	140737
H4a 3	564.14558	Yes	62.0	10521984	1.3	140797
H5a 1		No				
H5a 2		No				
H5a 3		No				
H6a 1	564.14531	Yes	32.8	4837683	0.7	147148
H6a 2	564.14537	Yes	45.8	6476349	0.9	147263
H6a 3	564.14528	Yes	45.3	6630120	0.7	144227
H7a 1	564.14487	Yes	4.5	888019	0.2	175299
H7a 2	564.14530	Yes	5.6	1093683	0.2	177549
H7a 3	564.14543	Yes	10.0	1635315	0.2	155580
H8a 1	564.14556	Yes	46.6	7454513	1.3	140610
H8a 2	564.14568	Yes	36.2	5305143	1.2	138649
H8a 3	564.14545	Yes	34.9	4986132	1.0	137990
H9a 1		No				
H9a 2	564.14550	Yes	6.0	1266818	0.1	88970
H9a 3	564.14583	Yes	5.5	1048783	0.2	126327
H10a 1	564.14542	Yes	304.7	42793712	7.2	140738
H10a 2	564.14517	Yes	209.5	25843690	13.2	139474
H10a 3	564.14539	Yes	437.4	63876820	17.4	139934
H11a 1	564.14596	Yes	98.5	13818729	6.0	140347
H11a 2	564.14577	Yes	45.6	6775279	0.9	137577
H11a 3	564.14535	Yes	30.7	3759265	2.9	144380
H12a 1	564.14593	Yes	223.5	36087664	8.0	140549
H12a 2	564.14589	Yes	148.6	24119972	4.9	141022
H12a 3	564.14591	Yes	208.6	34197988	8.5	139777
H13aii 1	564.14585	Yes	573.5	88004664	22.3	140895
H13aii 2	564.14585	Yes	574.7	83943168	21.6	139966
H13aii 3	564.14571	Yes	402.0	54066084	9.2	141434
H14a 1		No				
H14a 2		No				
H14a 3		No				
H14bi 1		No				
H14bi 2		No				
H14bi 3		No				
V1a 1		No				
V1a 2		No				
V1a 3		No				
B1a 1	564.14581	Yes	36.8	7219441	1.4	138575
B1a 2	564.14555	Yes	29.3	4684682	1.5	147466
B1a 3	564.14519	Yes	20.8	3059296	0.7	143349
DHB 1		No				
DHB 2		No				
DHB 3		No				
Soil 3a 1		No				
Soil 3a 2		No				
Soil 3a 3		No				
Soil 3b 1		No				
Soil 3b 2		No				
Soil 3b 3		No				
Solvent 1		No				
Solvent 2		No				
Solvent 3		No				

Table 62. Summary of signal at *m/z* 569

Calculated *m/z*	569.43305					
Sample designation + MALDI replicate no.	Measured *m/z*	Present	S:N	Intensity	Rel. Int. %	Resolution
Y1a 1	569.43264	Yes	31.1	4876424	1.6	175216
Y1a 2	569.43263	Yes	45.4	6658016	2.4	153450
Y1a 3	569.43285	Yes	44.2	6841952	2	155564
Original Heslington		No				
H1a 1		No				
H1a 2	569.43211	Yes	12.1	1813734	0.5	211538
H1a 3		No				
H1b 1		No				
H1b 2		No				
H1b 3	569.43492	Yes	64.6	8427930	2	142697
H2a 1	569.43473	Yes	33	4457626	0.8	135899
H2a 2	569.43488	Yes	144.6	21552302	6.5	137867
H2a 3		No				
H3a 1		No				
H3a 2		No				
H3a 3		No				
H4a 1		No				
H4a 2		No				
H4a 3		No				
H5a 1		No				
H5a 2		No				
H5a 3		No				
H6a 1		No				
H6a 2		No				
H6a 3	569.43498	Yes	16.8	2651137	0.3	146328
H7a 1	569.43243	Yes	41.2	5752676	1.4	164501
H7a 2	569.43217	Yes	17.4	2761644	0.4	181957
H7a 3	569.43215	Yes	28.4	4104032	0.6	174650
H8a 1		No				
H8a 2		No				
H8a 3		No				
H9a 1		No				
H9a 2		No				
H9a 3		No				
H10a 1		No				
H10a 2		No				
H10a 3		No				
H11a 1		No				
H11a 2		No				
H11a 3		No				
H12a 1		No				
H12a 2		No				
H12a 3		No				
H13aii 1	569.43313	Yes	6.1	1264545	0.3	143861
H13aii 2	569.43238	Yes	4.8	943275	0.2	219659
H13aii 3		No				
H14a 1	569.43284	Yes	670.9	110471344	7.8	146835
H14a 2	569.433	Yes	550	87443544	11.7	139066
H14a 3	569.43309	Yes	651.8	124420280	6	147843
H14bi 1	569.43255	Yes	14.2	2668350	0.3	189665
H14bi 2	569.43217	Yes	15.4	2722050	0.4	190137
H14bi 3		No				
V1a 1	569.43305	Yes	446.5	70081832	3.2	139853
V1a 2	569.43304	Yes	536.3	77024264	12.2	139655
V1a 3	569.43297	Yes	386.2	56109232	12	139303
B1a 1	569.43286	Yes	65	12428485	2.4	165708
B1a 2	569.43289	Yes	57.3	8857013	2.9	155407
B1a 3	569.43258	Yes	50.6	7011653	1.6	152292
DHB 1		No				
DHB 2		No				
DHB 3		No				
Soil 3a 1	569.43407	Yes	20.5	4205710	0.5	153479
Soil 3a 2	569.43494	Yes	4.3	1120690	0.1	157629
Soil 3a 3	569.43403	Yes	6	1474274	0.3	147743
Soil 3b 1	569.43467	Yes	12.3	2474166	0.3	153480
Soil 3b 2		No				
Soil 3b 3		No				
Solvent 1	569.42859	Yes	6	1567107	0	120056
Solvent 2	569.42888	Yes	4.7	1341949	0.2	144068
Solvent 3	569.43407	Yes	20.5	4205710	0.5	153479

Table 63. Summary of signal at *m/z* 591

Calculated *m/z*	591.169					
Sample designation + MALDI replicate no.	Measured *m/z*	Present	S:N	Intensity	Rel. Int. %	Resolution
Y1a 1		No				
Y1a 2		No				
Y1a 3		No				
Original Heslington		No				
H1a 1		No				
H1a 2		No				
H1a 3		No				
H1b 1		No				
H1b 2		No				
H1b 3		No				
H2a 1	591.16841	Yes	244.7	31395072	5.8	132993
H2a 2	591.16847	Yes	95.9	14415247	4.4	132546
H2a 3	591.16852	Yes	166.4	20264962	5.7	133275
H3a 1	591.16889	Yes	129.2	18805350	3.4	134128
H3a 2	591.16894	Yes	144.2	21475952	3.5	131519
H3a 3	591.16871	Yes	90.2	12100432	1.6	131067
H4a 1	591.16899	Yes	577.8	98963216	5.8	132753
H4a 2	591.16926	Yes	919.6	162248784	18.6	132885
H4a 3	591.16903	Yes	874.3	146123056	17.6	132448
H5a 1	591.16837	Yes	16.8	2273520	1.2	141672
H5a 2	591.16841	Yes	25.2	3470382	1.1	151924
H5a 3	591.16839	Yes	44.9	6487745	0.7	135129
H6a 1	591.16883	Yes	456.9	63785704	8.6	132206
H6a 2	591.16881	Yes	458.4	62421736	8.5	132794
H6a 3	591.16880	Yes	484.3	68086376	7.2	131735
H7a 1	591.17000	Yes	4.7	941655	0.2	147094
H7a 2	591.16913	Yes	7.9	1442489	0.2	115023
H7a 3	591.16882	Yes	5.4	1040241	0.2	150992
H8a 1	591.16892	Yes	818.7	125411120	21.6	132818
H8a 2	591.16911	Yes	491.5	68730176	15.9	130735
H8a 3	591.16880	Yes	472.9	64117652	12.4	132939
H9a 1	591.16896	Yes	110.3	17383730	2.2	131784
H9a 2	591.16893	Yes	189.6	30025640	3.5	132816
H9a 3	591.16870	Yes	26.6	3912554	0.9	137603
H10a 1	591.16889	Yes	393.2	55303488	9.3	133251
H10a 2	591.16877	Yes	522.4	64423952	33.0	130912
H10a 3	591.16883	Yes	1131.3	164561568	44.7	132468
H11a 1	591.16932	Yes	882.2	123699448	54.0	132197
H11a 2	591.16924	Yes	435.6	62884676	8.2	131463
H11a 3	591.16882	Yes	224.7	26058974	20.0	132160
H12a 1	591.16943	Yes	671.3	108911080	24.2	131866
H12a 2	591.16944	Yes	570.1	92211568	18.7	131470
H12a 3	591.16940	Yes	653.2	107514992	26.7	132130
H13aii 1	591.16935	Yes	794.6	124609912	31.6	133029
H13aii 2	591.16936	Yes	712.4	105708104	27.1	132442
H13aii 3	591.16921	Yes	494.6	67790608	11.5	132918
H14a 1		No				
H14a 2		No				
H14a 3		No				
H14bi 1		No				
H14bi 2		No				
H14bi 3		No				
V1a 1		No				
V1a 2		No				
V1a 3		No				
B1a 1	591.16929	Yes	184.2	34263236	6.7	131093
B1a 2	591.16896	Yes	111.5	16899394	5.5	132506
B1a 3	591.16853	Yes	65.2	8951317	2.1	129500
DHB 1		No				
DHB 2		No				
DHB 3		No				
Soil 3a 1		No				
Soil 3a 2		No				
Soil 3a 3		No				
Soil 3b 1		No				
Soil 3b 2		No				
Soil 3b 3		No				
Solvent 1		No				
Solvent 2		No				
Solvent 3		No				

Table 64. Summary of signal at *m/z* 622

Calculated *m/z*	622.517					
Sample designation + MALDI replicate no.	Measured *m/z*	Present	S:N	Intensity	Rel. Int. %	Resolution
Y1a 1	622.51721	Yes	1080.4	167955776	55.9	128233
Y1a 2	622.51698	Yes	1119.8	164598592	60.5	128467
Y1a 3	622.51712	Yes	1101.3	171901568	49.9	128759
Original Heslington		No				
H1a 1		No				
H1a 2		No				
H1a 3		No				
H1b 1		No				
H1b 2		No				
H1b 3		No				
H2a 1		No				
H2a 2	622.51504	Possibly	8.4	1557742	0.5	141194
H2a 3		No				
H3a 1		No				
H3a 2		No				
H3a 3		No				
H4a 1		No				
H4a 2		No				
H4a 3		No				
H5a 1	622.51668	Yes	6.6	1082230	0.6	189492
H5a 2	622.51646	Yes	8.0	1321222	0.4	162074
H5a 3	622.51636	Yes	14.4	2312618	0.3	142658
H6a 1		No				
H6a 2		No				
H6a 3		No				
H7a 1	622.51932	No	5.7	1092277	0.3	143706
H7a 2	622.51568	No	7.2	1373176	0.2	119506
H7a 3		No				
H8a 1		No				
H8a 2		No				
H8a 3	622.51984	Possibly	6.1	1135327	0.2	130615
H9a 1		No				
H9a 2		No				
H9a 3		No				
H10a 1		No				
H10a 2		No				
H10a 3		No				
H11a 1		No				
H11a 2		No				
H11a 3		No				
H12a 1		No				
H12a 2		No				
H12a 3	622.51942	Possibly	4.4	1064930	0.3	144330
H13aii 1		No				
H13aii 2	622.51916	Possibly	5.2	1104555	0.3	123316
H13aii 3		No				
H14a 1		No				
H14a 2		No				
H14a 3		No				
H14bi 1	622.51720	Yes	9.5	1886734	0.2	170786
H14bi 2	622.51690	Yes	4.8	1080790	0.2	194101
H14bi 3		No				
V1a 1		No				
V1a 2	622.51975	Possibly	15.1	2602639	0.4	129462
V1a 3	622.51928	Possibly	7.1	1388996	0.3	120813
B1a 1		No				
B1a 2		No				
B1a 3		No				
DHB 1		No				
DHB 2		No				
DHB 3	622.51468	Possibly	5.5	993921	0.1	163769
Soil 3a 1	622.51686	Yes	12.5	2878020	0.4	144002
Soil 3a 2		No				
Soil 3a 3	622.51725	Yes	19.7	4214860	0.9	124802
Soil 3b 1	622.51654	Yes	6.6	1640875	0.2	143389
Soil 3b 2	622.51669	Yes	22.0	4749899	0.3	129617
Soil 3b 3		No				
Solvent 1	622.51691	Yes	60.3	13307653	0.4	123916
Solvent 2	622.51716	Yes	35.0	7789609	1.0	128528
Solvent 3	622.51686	Yes	12.5	2878020	0.4	144002

Table 65. Summary of signal at *m/z* 629

Calculated *m/z*	629.86603					
Sample designation + MALDI replicate no.	Measured *m/z*	Present	S:N	Intensity	Rel. Int. %	Resolution
Y1a 1	629.86633	Yes	35.0	5760173	1.9	134290
Y1a 2	629.86602	Yes	43.9	6758955	2.5	130047
Y1a 3	629.86612	Yes	55.7	9001892	2.6	131496
Original Heslington		No				
H1a 1		No				
H1a 2	629.86608	Yes	3.4	746192	0.2	95213
H1a 3		No				
H1b 1	629.86568	Yes	27.2	3978560	0.5	131803
H1b 2		No				
H1b 3		No				
H2a 1		No				
H2a 2		No				
H2a 3	629.86535	Yes	6.7	1111339	0.3	158642
H3a 1		No				
H3a 2	629.86614	Yes	26.7	4238130	0.7	127338
H3a 3	629.86577	Yes	44.0	6087236	0.8	129618
H4a 1		No				
H4a 2		No				
H4a 3		No				
H5a 1	629.86552	Yes	37.4	4761332	2.5	134903
H5a 2	629.86568	Yes	43.9	5891271	1.9	127945
H5a 3	629.86563	Yes	24.5	3720535	0.4	134921
H6a 1	629.86596	Yes	66.2	9556963	1.3	131555
H6a 2	629.86596	Yes	101.1	14077530	1.9	126865
H6a 3	629.86601	Yes	75.9	10936821	1.2	128562
H7a 1	629.86605	Yes	82.1	11530015	2.8	128478
H7a 2	629.86610	Yes	54.0	8167478	1.3	130737
H7a 3		No				
H8a 1		No				
H8a 2		No				
H8a 3	629.86622	Yes	9.0	1526780	0.3	132676
H9a 1	629.86600	Yes	19.2	3268006	0.4	131889
H9a 2	629.86595	Yes	8.3	1602963	0.2	138015
H9a 3	629.86588	Yes	24.8	3673080	0.8	121207
H10a 1		No				
H10a 2		No				
H10a 3		No				
H11a 1		No				
H11a 2		No				
H11a 3		No				
H12a 1		No				
H12a 2		No				
H12a 3		No				
H13aii 1	629.86665	Yes	26.5	4581207	1.2	133237
H13aii 2	629.86656	Yes	8.3	1578851	0.4	164583
H13aii 3	629.86629	Yes	15.4	2460513	0.4	146380
H14a 1	629.86603	Yes	339.9	56399184	4.0	126522
H14a 2	629.86607	Yes	134.0	21434662	2.9	127796
H14a 3	629.86626	Yes	458.0	87797424	4.2	126171
H14bi 1	629.86654	Yes	64.4	10781896	1.2	127157
H14bi 2	629.86637	Yes	85.4	13422087	2.1	130159
H14bi 3		No				
V1a 1	629.86623	Yes	65.7	10866587	0.5	128334
V1a 2	629.86614	Yes	88.0	13606567	2.2	123886
V1a 3	629.86601	Yes	99.6	15228116	3.2	127239
B1a 1	629.86642	Yes	113.3	20845060	4.1	126887
B1a 2	629.86610	Yes	54.4	8383911	2.7	130492
B1a 3	629.86578	Yes	79.1	10788137	2.5	130291
DHB 1		No				
DHB 2		No				
DHB 3		No				
Soil 3a 1		No				
Soil 3a 2	629.86879	Possibly	7.3	1788707	0.2	111769
Soil 3a 3		No				
Soil 3b 1	629.86819	Possibly	5.4	1405950	0.2	137861
Soil 3b 2		No				
Soil 3b 3	629.86479	Possibly	5.5	1494089	0.3	143606
Solvent 1		No				
Solvent 2		No				
Solvent 3		No				

Table 66. Summary of signal at *m/z* 640

Calculated *m/z*	640.61474					
Sample designation + MALDI replicate no.	Measured *m/z*	Present	S:N	Intensity	Rel. Int. %	Resolution
Y1a 1	640.6148	Yes	8.6	1684479	0.6	153314
Y1a 2		No				
Y1a 3		No				
Original Heslington		No				
H1a 1	640.61474	Yes	436.3	64501928	6.5	130878
H1a 2	640.61465	Yes	13.2	2041459	0.5	129211
H1a 3		No				
H1b 1	640.61415	Yes	14.8	2314440	0.3	146530
H1b 2	640.61441	Yes	42.9	5936727	1.5	131870
H1b 3	640.61447	Yes	19	2771344	0.7	139290
H2a 1		No				
H2a 2	640.61423	Yes	45.4	7025742	2.1	132785
H2a 3		No				
H3a 1	640.6148	Yes	95.4	13952800	2.5	133997
H3a 2	640.61495	Yes	30.3	4769589	0.8	136277
H3a 3	640.61456	Yes	50.7	6973349	0.9	133270
H4a 1		No				
H4a 2		No				
H4a 3		No				
H5a 1	640.61424	Yes	8.7	1336928	0.7	147586
H5a 2		No				
H5a 3	640.61387	Yes	7.1	1304560	0.1	126249
H6a 1	640.61453	Yes	15.6	2491423	0.3	139528
H6a 2		No				
H6a 3	640.61475	Yes	40.1	5933782	0.6	129579
H7a 1	640.61464	Yes	17.5	2715716	0.7	137718
H7a 2		No				
H7a 3	640.61478	Yes	20.1	3099943	0.5	148221
H8a 1		No				
H8a 2		No				
H8a 3	640.6146	Yes	8.5	1460387	0.3	141992
H9a 1		No				
H9a 2	640.61481	Yes	156.7	24402192	2.8	129757
H9a 3	640.61455	Yes	40	5744328	1.3	129523
H10a 1		No				
H10a 2	640.61445	Yes	11.1	1680602	0.9	154434
H10a 3	640.61445	Yes	6.5	1267390	0.3	166742
H11a 1		No				
H11a 2		No				
H11a 3		No				
H12a 1	640.61542	Yes	17.8	3266801	0.7	138743
H12a 2	640.61559	Yes	8.5	1720507	0.3	161888
H12a 3	640.61542	Yes	9.5	1928023	0.5	154998
H13aii 1	640.61555	Yes	13.6	2532585	0.6	141404
H13aii 2		No				
H13aii 3	640.61525	Yes	93.1	13392815	2.3	131342
H14a 1	640.61479	Yes	16.6	3092652	0.2	146848
H14a 2	640.61487	Yes	49	8048352	1.1	134013
H14a 3		No				
H14bi 1	640.61537	Yes	82.4	13677028	1.5	131468
H14bi 2	640.61529	Yes	29.7	4877488	0.7	139792
H14bi 3		No				
V1a 1	640.61502	Yes	14.4	2651385	0.1	133192
V1a 2		No				
V1a 3	640.61503	Yes	38.6	6145556	1.3	131648
B1a 1		No				
B1a 2	640.61474	Yes	78.8	11962818	3.9	130064
B1a 3	640.6146	Yes	7.9	1350762	0.3	132211
DHB 1		No				
DHB 2		No				
DHB 3		No				
Soil 3a 1	640.6167	Possibly	8.4	2085042	0.3	154194
Soil 3a 2	640.61707	Possibly	22.7	4889158	0.5	130113
Soil 3a 3	640.61707	Possibly	19.9	4297140	0.9	128340
Soil 3b 1	640.61724	Possibly	86.7	17537028	2.3	124292
Soil 3b 2	640.61663	Possibly	50.3	10535977	0.6	133883
Soil 3b 3		No				
Solvent 1	640.61655	Possibly	37	8386573	0.2	126640
Solvent 2	640.6168	Possibly	47.6	10482499	1.3	125004
Solvent 3	640.6167	Possibly	8.4	2085042	0.3	154194

Table 67. Summary of signal at *m/z* 753

Calculated *m/z*	753.588					
Sample designation + MALDI replicate no.	Measured *m/z*	Present	S:N	Intensity	Rel. Int. %	Resolution
Y1a 1	753.58778	Yes	805.7	138793088	46.2	105833
Y1a 2	753.58757	Yes	904.5	145378432	53.4	106049
Y1a 3	753.58776	Yes	918.3	158324240	45.9	106455
Original Heslington		No				
H1a 1	753.58757	Yes	90.2	13549418	1.4	107181
H1a 2	753.58738	Yes	558.3	78220824	19.6	105566
H1a 3	753.58740	Yes	160.7	21380882	3.2	107773
H1b 1	753.58725	Yes	53.7	7993408	0.9	106700
H1b 2	753.58719	Yes	153.2	21394932	5.6	105059
H1b 3	753.58706	Yes	103.3	14387553	3.4	107114
H2a 1	753.58702	Yes	230.1	30997508	5.7	105445
H2a 2	753.58700	Yes	316.2	47000348	14.2	105761
H2a 3	753.58734	Yes	307.1	39809972	11.2	106059
H3a 1	753.58763	Yes	39.6	5953769	1.1	104782
H3a 2	753.58781	Yes	102.7	15432182	2.5	107945
H3a 3	753.58759	Yes	73.4	10119416	1.3	107612
H4a 1	753.58774	Yes	214.0	36848588	2.2	106751
H4a 2	753.58807	Yes	1225.9	238305280	27.2	105687
H4a 3	753.58786	Yes	617.4	110513000	13.3	105873
H5a 1	753.58723	Yes	54.4	7088631	3.7	113459
H5a 2	753.58729	Yes	67.8	9355107	3.1	107582
H5a 3	753.58698	Yes	32.5	4981311	0.6	109912
H6a 1	753.58765	Yes	774.3	110668656	14.9	105904
H6a 2	753.58764	Yes	528.0	73561064	10.0	106299
H6a 3	753.58763	Yes	497.9	70247680	7.5	106329
H7a 1	753.58763	Yes	38.6	5974281	1.5	113553
H7a 2	753.58763	Yes	32.3	5350769	0.8	111383
H7a 3	753.58784	Yes	30.7	4843951	0.7	109190
H8a 1	753.58784	Yes	108.3	16739922	2.9	107566
H8a 2	753.58808	Yes	86.2	12826637	3.0	106685
H8a 3	753.58756	Yes	103.8	14634922	2.8	106768
H9a 1	753.58767	Yes	186.7	27759012	3.4	106288
H9a 2	753.58772	Yes	165.3	24640104	2.8	106629
H9a 3	753.58734	Yes	257.1	35654232	7.9	106114
H10a 1	753.58742	Yes	27.1	4205108	0.7	106129
H10a 2	753.58712	Yes	10.4	1623582	0.8	108046
H10a 3	753.58778	Yes	32.8	5069289	1.4	109972
H11a 1	753.58830	Yes	1095.9	167992176	73.4	105784
H11a 2	753.58832	Yes	416.9	64320276	8.4	105911
H11a 3	753.58785	Yes	407.6	49574784	38.1	105897
H12a 1	753.58853	Yes	1245.2	210274880	46.8	105944
H12a 2	753.58852	Yes	1335.0	220507440	44.8	105619
H12a 3	753.58847	Yes	1484.1	253942672	63.1	106059
H13aii 1	753.58846	Yes	750.0	129733888	32.9	106310
H13aii 2	753.58835	Yes	434.1	69507696	17.8	105965
H13aii 3	753.58821	Yes	665.0	99697320	16.9	106137
H14a 1		No				
H14a 2		No				
H14a 3		No				
H14bi 1		No				
H14bi 2		No				
H14bi 3		No				
V1a 1		No				
V1a 2	753.58795	Yes	12.4	2411378	0.4	121059
V1a 3	753.58747	Yes	8.2	1652947	0.4	114403
B1a 1	753.58818	Yes	63.7	11226296	2.2	107230
B1a 2	753.58765	Yes	100.6	15087912	4.9	107495
B1a 3	753.58738	Yes	89.9	12242539	2.9	107599
DHB 1		No				
DHB 2		No				
DHB 3		No				
Soil 3a 1		No				
Soil 3a 2		No				
Soil 3a 3		No				
Soil 3b 1		No				
Soil 3b 2		No				
Soil 3b 3		No				
Solvent 1		No				
Solvent 2		No				
Solvent 3		No				

Table 68. Summary of signal at *m/z* 769

Calculated *m/z*	769.561					
Sample designation + MALDI replicate no.	Measured *m/z*	Present	S:N	Intensity	Rel. Int. %	Resolution
Y1a 1	769.56191	Yes	1295.2	222809984	74.1	103772
Y1a 2	769.56167	Yes	1214.0	194787632	71.5	104049
Y1a 3	769.56187	Yes	1311.8	225905760	65.6	103891
Original Heslington	769.56116	Yes	22.1	3005843	2.4	64535
H1a 1	769.56190	Yes	13.2	2242194	0.2	99785
H1a 2	769.56148	Yes	114.0	16177983	4.1	104579
H1a 3	769.56134	Yes	18.0	2672188	0.4	122225
H1b 1	769.56127	Yes	27.3	4230631	0.5	102174
H1b 2	769.56133	Yes	26.8	4005281	1.0	99729
H1b 3	769.56136	Yes	28.8	4239769	1.0	104063
H2a 1	769.56088	Yes	41.5	5849720	1.1	104336
H2a 2	769.56125	Yes	33.8	5290571	1.6	99263
H2a 3	769.56113	Yes	64.9	8680315	2.4	103069
H3a 1	769.56190	Yes	11.4	1942237	0.4	112290
H3a 2	769.56194	Yes	40.5	6305398	1.0	101906
H3a 3	769.56154	Yes	32.7	4687603	0.6	107767
H4a 1	769.56198	Yes	164.9	28443070	1.7	103571
H4a 2	769.56221	Yes	129.7	25647918	2.9	102180
H4a 3	769.56204	Yes	220.4	39844232	4.8	103090
H5a 1	769.56107	Yes	54.6	7177302	3.8	100818
H5a 2	769.56136	Yes	74.4	10327635	3.4	103198
H5a 3	769.56114	Yes	53.2	7999048	0.9	107933
H6a 1	769.56174	Yes	702.6	100625016	13.6	103675
H6a 2	769.56172	Yes	702.6	97954016	13.3	103670
H6a 3	769.56175	Yes	693.1	97678272	10.4	103944
H7a 1	769.56167	Yes	33.8	5299575	1.3	106921
H7a 2	769.56181	Yes	24.9	4210080	0.7	107641
H7a 3	769.56102	Yes	7.6	1452542	0.2	107260
H8a 1	769.56188	Yes	34.0	5499229	0.9	104876
H8a 2	769.56217	Yes	28.9	4540595	1.1	105097
H8a 3	769.56155	Yes	30.8	4579930	0.9	101981
H9a 1	769.56182	Yes	156.4	23303694	2.9	103284
H9a 2	769.56200	Yes	69.3	10521153	1.2	105081
H9a 3	769.56140	Yes	223.7	31270500	6.9	103966
H10a 1		No				
H10a 2		No				
H10a 3	769.56311	Yes	5.1	1059364	0.3	133503
H11a 1	769.56241	Yes	447.1	68850256	30.1	102781
H11a 2	769.56240	Yes	279.2	43439776	5.7	104250
H11a 3	769.56183	Yes	130.1	16099622	12.4	106077
H12a 1	769.56272	Yes	426.7	71706432	16.0	103461
H12a 2	769.56272	Yes	327.3	53943316	11.0	103145
H12a 3	769.56265	Yes	623.7	106097096	26.4	103430
H13aii 1	769.56257	Yes	1224.7	210928064	53.4	104070
H13aii 2	769.56250	Yes	729.5	116528360	29.9	103279
H13aii 3	769.56226	Yes	852.5	127748936	21.7	103469
H14a 1		No				
H14a 2		No				
H14a 3		No				
H14bi 1		Yes				
H14bi 2		No				
H14bi 3		No				
V1a 1	769.56196	Yes	19.3	3601324	0.2	95494
V1a 2	769.56186	Yes	22.4	4088476	0.6	96613
V1a 3	769.56197	Yes	18.7	3328082	0.7	107749
B1a 1	769.56230	Yes	106.1	18520260	3.6	105594
B1a 2	769.56186	Yes	128.4	19269426	6.3	102455
B1a 3	769.56139	Yes	80.8	11098002	2.6	102177
DHB 1		No				
DHB 2		No				
DHB 3		No				
Soil 3a 1		No				
Soil 3a 2		No				
Soil 3a 3		No				
Soil 3b 1		No				
Soil 3b 2		No				
Soil 3b 3	769.56132	Yes	13.7	3872421	0.7	120132
Solvent 1		No				
Solvent 2		No				
Solvent 3		No				

Table 69. Summary of signal at *m/z* 815

Calculated *m/z*	815.698					
Sample designation + MALDI replicate no.	Measured *m/z*	Present	S:N	Intensity	Rel. Int. %	Resolution
Y1a 1	815.69986	Yes	197.5	34256788	11.4	94826
Y1a 2	815.69955	Yes	170.6	27612170	10.1	94695
Y1a 3	815.69977	Yes	193.3	33572144	9.7	95124
Original Heslington	815.69948	Yes	10.1	1540566	1.2	73052
H1a 1	815.69964	Yes	200.7	29250796	2.9	97278
H1a 2	815.69934	Yes	217.6	30386918	7.6	95560
H1a 3	815.69916	Yes	154.4	20631994	3.1	96984
H1b 1		No				
H1b 2	815.69906	Yes	113.1	15925629	4.1	94011
H1b 3	815.69895	Yes	116.8	16269584	3.8	97291
H2a 1	815.69879	Yes	401.0	53771760	10.0	97115
H2a 2	815.69898	Yes	226.2	33082456	10.0	95514
H2a 3	815.69924	Yes	128.0	16966586	4.8	97061
H3a 1	815.69998	Yes	35.1	5301382	1.0	95824
H3a 2	815.70008	Yes	45.1	7035405	1.2	98914
H3a 3	815.70016	Yes	12.6	2008788	0.3	108467
H4a 1	815.69988	Yes	934.2	159038400	9.3	95105
H4a 2	815.70020	Yes	691.4	136369200	15.6	93751
H4a 3	815.69994	Yes	674.4	122372352	14.8	94300
H5a 1	815.69903	Yes	65.3	8688625	4.6	96489
H5a 2	815.69914	Yes	99.2	13921444	4.6	97452
H5a 3	815.69901	Yes	104.6	15618298	1.8	97363
H6a 1	815.69967	Yes	144.1	20975384	2.8	93532
H6a 2	815.69960	Yes	140.6	19935904	2.7	92417
H6a 3	815.69964	Yes	180.4	25675590	2.7	93674
H7a 1	815.70006	Yes	17.4	2930005	0.7	100597
H7a 2	815.69965	Yes	23.1	3938428	0.6	101708
H7a 3	815.70028	Yes	13.4	2325344	0.3	98042
H8a 1	815.69986	Yes	84.0	13179053	2.3	96039
H8a 2	815.70032	Yes	84.1	12706084	2.9	93444
H8a 3	815.69943	Yes	70.5	10141548	2.0	95079
H9a 1	815.69986	Yes	87.7	13212759	1.6	90995
H9a 2	815.69988	Yes	208.0	30873514	3.6	94961
H9a 3	815.69941	Yes	45.2	6664728	1.5	99414
H10a 1	815.69924	Yes	11.1	1969166	0.3	105517
H10a 2	815.69927	Yes	8.9	1461140	0.7	120942
H10a 3	815.69966	Yes	58.9	8922300	2.4	97338
H11a 1	815.70034	Yes	416.7	64440508	28.2	89979
H11a 2	815.70041	Yes	267.7	42173596	5.5	92246
H11a 3	815.69964	Yes	127.5	15938101	12.3	93635
H12a 1	815.70070	Yes	524.2	86491656	19.2	92470
H12a 2	815.70071	Yes	551.7	89306696	18.2	93295
H12a 3	815.70062	Yes	375.7	62982488	15.7	91704
H13aii 1	815.70045	Yes	288.5	49608904	12.6	87735
H13aii 2	815.70047	Yes	203.4	32704778	8.4	85975
H13aii 3	815.70015	Yes	158.1	23972936	4.1	88603
H14a 1		No				
H14a 2		No				
H14a 3		No				
H14bi 1		No				
H14bi 2		No				
H14bi 3		No				
V1a 1	815.70027	Yes	27.7	5019660	0.2	96400
V1a 2	815.70003	Yes	33.5	5957636	0.9	97737
V1a 3	815.69982	Yes	30.2	5147068	1.1	94162
B1a 1	815.70060	Yes	61.6	10971319	2.1	97662
B1a 2	815.69996	Yes	36.6	5804118	1.9	97552
B1a 3	815.69939	Yes	24.6	3642149	0.9	102705
DHB 1		No				
DHB 2		No				
DHB 3		No				
Soil 3a 1		No				
Soil 3a 2		No				
Soil 3a 3		No				
Soil 3b 1		No				
Soil 3b 2		No				
Soil 3b 3		No				
Solvent 1		No				
Solvent 2		No				
Solvent 3		No				

Table 70. Summary of signal at *m/z* 835

Calculated *m/z*	835.666					
Sample designation + MALDI replicate no.	Measured *m/z*	Present	S:N	Intensity	Rel. Int. %	Resolution
Y1a 1	835.66623	Yes	314.9	54378100	18.1	95593
Y1a 2	835.66596	Yes	338	54288384	19.9	95116
Y1a 3	835.66616	Yes	366.2	63237160	18.4	95569
Original Heslington		No				
H1a 1	835.66623	Yes	36.9	5605825	0.6	96643
H1a 2	835.66571	Yes	140.8	19708226	4.9	94963
H1a 3	835.66542	Yes	42.7	5943936	0.9	97588
H1b 1	835.66576	Yes	32.6	5018995	0.6	95438
H1b 2	835.66531	Yes	61.8	8864284	2.3	97676
H1b 3	835.66527	Yes	59.5	8459346	2	96643
H2a 1	835.66509	Yes	86	11782574	2.2	97244
H2a 2	835.66529	Yes	138.2	20193596	6.1	97710
H2a 3	835.66551	Yes	110.6	14771681	4.2	97666
H3a 1		No				
H3a 2	835.66705	Yes	8.6	1619980	0.3	102985
H3a 3		No				
H4a 1	835.66637	Yes	127.1	21918690	1.3	98220
H4a 2	835.66675	Yes	934.0	184967984	21.1	95983
H4a 3	835.66640	Yes	514.8	93959776	11.3	96310
H5a 1	835.66515	Yes	27.9	3926519	2.1	97581
H5a 2	835.66560	Yes	44.8	6520961	2.1	98616
H5a 3	835.66512	Yes	23.4	3769640	0.4	104083
H6a 1	835.66601	Yes	370.9	53580880	7.2	95552
H6a 2	835.66600	Yes	229.8	32440302	4.4	96070
H6a 3	835.66604	Yes	213.8	30372508	3.2	96576
H7a 1	835.66650	Yes	12.5	2214349	0.5	103031
H7a 2	835.66588	Yes	11.2	2090992	0.3	106919
H7a 3	835.66670	Yes	9.6	1769096	0.3	100489
H8a 1	835.66602	Yes	97.0	15202560	2.6	97024
H8a 2	835.66658	Yes	76.9	11695727	2.7	95582
H8a 3	835.66606	Yes	91.8	13162577	2.5	96274
H9a 1	835.66626	Yes	141.8	21155372	2.6	96775
H9a 2	835.66615	Yes	107.0	16042073	1.9	96650
H9a 3	835.66565	Yes	81.0	11764275	2.6	96247
H10a 1	835.66644	Yes	26.1	4227808	0.7	99995
H10a 2	835.66573	Yes	9.6	1561807	0.8	119537
H10a 3	835.66628	Yes	32.9	5153113	1.4	110067
H11a 1	835.66685	Yes	817.1	126273656	55.2	94952
H11a 2	835.66675	Yes	297.5	47124472	6.2	95445
H11a 3	835.66600	Yes	254.5	31670468	24.3	95769
H12a 1	835.66714	Yes	344.8	56462560	12.6	95477
H12a 2	835.66714	Yes	342.6	55135736	11.2	94523
H12a 3	835.66705	Yes	396.8	65895404	16.4	95643
H13aii 1	835.66697	Yes	259.2	44430600	11.3	95803
H13aii 2	835.66691	Yes	142.7	23033540	5.9	96284
H13aii 3	835.66658	Yes	208.4	31506474	5.3	95178
H14a 1		No				
H14a 2		No				
H14a 3		No				
H14bi 1		No				
H14bi 2		No				
H14bi 3		No				
V1a 1		No				
V1a 2	835.6662	Yes	7.4	1596818	0.3	116427
V1a 3		No				
B1a 1	835.66608	Yes	13.5	2704777	0.5	100735
B1a 2	835.66547	Yes	7	1397958	0.5	105472
B1a 3	835.66686	Yes	4.5	939459	0.2	151921
DHB 1		No				
DHB 2		No				
DHB 3		No				
Soil 3a 1		No				
Soil 3a 2		No				
Soil 3a 3		No				
Soil 3b 1		No				
Soil 3b 2		No				
Soil 3b 3		No				
Solvent 1		No				
Solvent 2		No				
Solvent 3		No				

Table 71. Summary of signal at *m/z* 836

Calculated *m/z*	836.658					
Sample designation + MALDI replicate no.	Measured *m/z*	Present	S:N	Intensity	Rel. Int. %	Resolution
Y1a 1	836.65883	Yes	117.2	20470886	6.8	80241
Y1a 2	836.65835	Yes	107.8	17560274	6.5	87762
Y1a 3	836.65860	Yes	117.7	20577296	6.0	90041
Original Heslington		No				
H1a 1	836.65819	Yes	51.8	7739227	0.8	96226
H1a 2	836.65816	Yes	93.8	13246263	3.3	89378
H1a 3	836.65793	Yes	98.6	13311500	2.0	94718
H1b 1	836.65765	Yes	169.4	24661972	2.9	95203
H1b 2	836.65781	Yes	262.0	36523932	9.5	94440
H1b 3	836.65754	Yes	197.2	27276056	6.4	95756
H2a 1	836.65742	Yes	238.8	32156544	6.0	94912
H2a 2	836.65751	Yes	211.8	30778760	9.3	94706
H2a 3	836.65770	Yes	196.1	25933810	7.3	93868
H3a 1	836.65831	Yes	251.1	35855632	6.5	95868
H3a 2	836.65853	Yes	388.4	58273816	9.5	94983
H3a 3	836.65812	Yes	153.7	21059062	2.8	95264
H4a 1	836.65864	Yes	302.9	51719852	3.0	94059
H4a 2	836.65915	Yes	1239.2	245283968	28.0	93883
H4a 3	836.65873	Yes	551.6	100651888	12.1	92918
H5a 1	836.65759	Yes	288.7	37707780	19.8	95787
H5a 2	836.65773	Yes	353.3	49220212	16.2	95131
H5a 3	836.65762	Yes	233.4	34643400	4.0	94673
H6a 1	836.65846	Yes	213.1	30929132	4.2	90082
H6a 2	836.65845	Yes	136.1	19354982	2.6	88358
H6a 3	836.65833	Yes	130.9	18728980	2.0	92484
H7a 1	836.65827	Yes	213.4	32268320	7.9	93609
H7a 2	836.65834	Yes	193.2	30333858	4.8	95881
H7a 3	836.65818	Yes	318.3	47868100	7.1	94870
H8a 1	836.65844	Yes	430.5	66307916	11.4	94630
H8a 2	836.65872	Yes	313.4	46654640	10.8	92784
H8a 3	836.65821	Yes	304.1	42845520	8.3	93681
H9a 1	836.65848	Yes	183.4	27261892	3.4	92962
H9a 2	836.65848	Yes	226.2	33530986	3.9	94210
H9a 3	836.65809	Yes	114.1	16439404	3.6	93341
H10a 1	836.65833	Yes	817.8	122328568	20.5	95362
H10a 2	836.65779	Yes	383.9	50242784	25.7	94398
H10a 3	836.65832	Yes	852.5	125192024	34.0	95077
H11a 1	836.65932	Yes	293.0	45497636	19.9	78972
H11a 2	836.65920	Yes	116.6	18679456	2.4	81551
H11a 3	836.65840	Yes	117.7	14806367	11.4	86824
H12a 1	836.65950	Yes	261.7	42939216	9.6	91798
H12a 2	836.65949	Yes	240.7	38834268	7.9	89231
H12a 3	836.65952	Yes	216.0	36029580	9.0	89742
H13aii 1	836.65936	Yes	187.0	32154044	8.1	92284
H13aii 2	836.65928	Yes	146.6	23652990	6.1	90948
H13aii 3	836.65894	Yes	153.5	23292632	4.0	92381
H14a 1		No				
H14a 2		No				
H14a 3		No				
H14bi 1		No				
H14bi 2	836.65896	Yes	7.0	1392079	0.2	107317
H14bi 3		No				
V1a 1	836.65857	Yes	103.8	17821124	0.8	95778
V1a 2	836.65859	Yes	99.7	17069834	2.7	95318
V1a 3	836.65844	Yes	85.1	13864774	3.0	94546
B1a 1	836.65921	Yes	237.6	41409604	8.1	94559
B1a 2	836.65845	Yes	224.3	34072992	11.1	95409
B1a 3	836.65794	Yes	293.2	40186720	9.4	95655
DHB 1		No				
DHB 2		No				
DHB 3		No				
Soil 3a 1		No				
Soil 3a 2		No				
Soil 3a 3		No				
Soil 3b 1		No				
Soil 3b 2		No				
Soil 3b 3		No				
Solvent 1		No				
Solvent 2		No				
Solvent 3		No				

Table 72. Summary of signal at *m/z* 848

Calculated *m/z*	848.561					
Sample designation + MALDI replicate no.	Measured *m/z*	Present	S:N	Intensity	Rel. Int. %	Resolution
Y1a 1		No				
Y1a 2		No				
Y1a 3		No				
Original Heslington		No				
H1a 1		No				
H1a 2		No				
H1a 3		No				
H1b 1	848.56153	Yes	12.5	2127682	0.2	114526
H1b 2		No				
H1b 3	848.56203	Yes	7.4	1342976	0.3	122571
H2a 1		No				
H2a 2		No				
H2a 3		No				
H3a 1		No				
H3a 2		No				
H3a 3		No				
H4a 1	848.56159	Yes	37.4	6686596	0.4	86851
H4a 2	848.56257	Yes	26.2	5577573	0.6	96742
H4a 3	848.56212	Yes	35.5	6861711	0.8	93090
H5a 1		No				
H5a 2		No				
H5a 3		No				
H6a 1	848.56178	Yes	62.6	9337389	1.3	92689
H6a 2	848.56181	Yes	69.6	10074768	1.4	96217
H6a 3	848.56178	Yes	61.8	9021509	1.0	97548
H7a 1	848.56176	Yes	266.1	40420960	9.9	92848
H7a 2	848.56181	Yes	186.7	29318610	4.6	92849
H7a 3	848.56165	Yes	65.4	10140202	1.5	94435
H8a 1		No				
H8a 2	848.56077	Yes	8.3	1569875	0.4	94667
H8a 3		No				
H9a 1	848.56214	Yes	23.3	3768247	0.5	86884
H9a 2	848.56145	Yes	6.4	1279130	0.1	84856
H9a 3	848.56278	Yes	13.7	2274075	0.5	103732
H10a 1		No				
H10a 2		No				
H10a 3		No				
H11a 1	848.56266	Yes	19.1	3302526	1.4	91912
H11a 2	848.56178	Yes	8.3	1666498	0.2	103672
H11a 3		No				
H12a 1		No				
H12a 2		No				
H12a 3		No				
H13aii 1	848.56260	Yes	10.8	2195567	0.6	99240
H13aii 2	848.56364	Yes	8.3	1668702	0.4	68688
H13aii 3		No				
H14a 1		No				
H14a 2		No				
H14a 3		No				
H14bi 1		No				
H14bi 2		No				
H14bi 3		No				
V1a 1		No				
V1a 2		No				
V1a 3	848.56199	Yes	5.4	1206237	0.3	120506
B1a 1		No				
B1a 2	848.56157	Yes	6.0	1259117	0.4	88599
B1a 3		No				
DHB 1		No				
DHB 2		No				
DHB 3		No				
Soil 3a 1		No				
Soil 3a 2	848.56503	Possibly	20.0	5253643	0.5	72980
Soil 3a 3	848.56553	Possibly	21.0	5061953	1.1	72358
Soil 3b 1	848.56956	Possibly	11.6	3178572	0.4	64612
Soil 3b 2	848.56288	Possibly	10.9	2870315	0.2	60640
Soil 3b 3	848.56561	Possibly	14.6	4115814	0.8	87883
Solvent 1	848.56606	Possibly	24.6	5707658	0.2	49750
Solvent 2		No				
Solvent 3		No				

Table 73. Summary of signal at *m/z* 850

Calculated *m/z*	850.673					
Sample designation + MALDI replicate no.	Measured *m/z*	Present	S:N	Intensity	Rel. Int. %	Resolution
Y1a 1	850.67409	Yes	329.9	56908884	18.9	91243
Y1a 2	850.67371	Yes	316.9	50851312	18.7	91822
Y1a 3	850.67393	Yes	361.5	62394216	18.1	91846
Original Heslington		No				
H1a 1	850.67371	Yes	145.0	20949284	2.1	94182
H1a 2	850.67350	Yes	287.3	39728664	10.0	92913
H1a 3	850.67344	Yes	329.0	43707860	6.6	93433
H1b 1	850.67319	Yes	523.1	75562120	8.8	93427
H1b 2	850.67334	Yes	803.5	111472224	29.0	92877
H1b 3	850.67297	Yes	600.9	82540904	19.5	93883
H2a 1	850.67285	Yes	793.9	106139416	19.7	93563
H2a 2	850.67301	Yes	719.8	103002288	31.1	93419
H2a 3	850.67325	Yes	593.6	78217464	22.0	93365
H3a 1	850.67377	Yes	721.8	102309128	18.6	93542
H3a 2	850.67400	Yes	1160.5	174155216	28.5	93217
H3a 3	850.67356	Yes	429.0	58373728	7.7	93995
H4a 1	850.67400	Yes	1010.8	171511712	10.0	93217
H4a 2	850.67439	Yes	4109.5	816641728	93.4	93348
H4a 3	850.67408	Yes	1872.9	342682112	41.3	93161
H5a 1	850.67306	Yes	848.0	111252360	58.5	93425
H5a 2	850.67329	Yes	984.7	138028112	45.4	93844
H5a 3	850.67306	Yes	611.2	90793576	10.4	93498
H6a 1	850.67382	Yes	666.6	96225648	13.0	92942
H6a 2	850.67383	Yes	450.1	63376912	8.6	93422
H6a 3	850.67376	Yes	405.4	57322184	6.1	92732
H7a 1	850.67370	Yes	635.7	96096720	23.5	92987
H7a 2	850.67377	Yes	652.5	101591608	16.0	93638
H7a 3	850.67361	Yes	1058.0	158982672	23.5	93714
H8a 1	850.67390	Yes	1121.6	172735088	29.7	93373
H8a 2	850.67414	Yes	882.0	131380536	30.5	92272
H8a 3	850.67366	Yes	817.4	115042408	22.3	92459
H9a 1	850.67389	Yes	463.9	68430864	8.5	92169
H9a 2	850.67392	Yes	604.3	88986736	10.3	92907
H9a 3	850.67339	Yes	285.3	40949284	9.0	92901
H10a 1	850.67377	Yes	2421.3	365529600	61.1	93276
H10a 2	850.67336	Yes	1103.9	144765680	74.2	92597
H10a 3	850.67376	Yes	2502.8	368020000	100.0	93293
H11a 1	850.67467	Yes	776.3	120246872	52.5	91506
H11a 2	850.67461	Yes	318.5	50772452	6.6	92137
H11a 3	850.67382	Yes	317.6	39671292	30.5	92354
H12a 1	850.67495	Yes	611.9	98919760	22.0	91493
H12a 2	850.67494	Yes	567.8	90346480	18.4	91302
H12a 3	850.67490	Yes	521.7	85691704	21.3	91329
H13aii 1	850.67478	Yes	456.9	77738328	19.7	92800
H13aii 2	850.67467	Yes	360.6	57654172	14.8	91398
H13aii 3	850.67441	Yes	394.8	59414368	10.1	92974
H14a 1		No				
H14a 2	850.67470	Yes	8.2	1620527	0.2	109886
H14a 3		No				
H14bi 1	850.67557	Yes	7.1	1485480	0.2	99948
H14bi 2	850.67585	Yes	5.3	1139259	0.2	129778
H14bi 3		No				
V1a 1	850.67413	Yes	288.8	48936688	2.2	93941
V1a 2	850.67408	Yes	297.2	50219460	8.0	93576
V1a 3	850.67396	Yes	251.4	40182744	8.6	93872
B1a 1	850.67459	Yes	627.3	109082720	21.3	93423
B1a 2	850.67386	Yes	630.3	95825648	31.3	92724
B1a 3	850.67341	Yes	792.3	108749840	25.5	93839
DHB 1		No				
DHB 2		No				
DHB 3		No				
Soil 3a 1	850.67695	Possibly	5.5	1693337	0.2	95990
Soil 3a 2		No				
Soil 3a 3		No				
Soil 3b 1		No				
Soil 3b 2	850.67781	Possibly	5.6	1678905	0.1	106383
Soil 3b 3		No				
Solvent 1	850.67676	Possibly	7.2	1962182	0.1	57442
Solvent 2	850.67852	Possibly	4.0	1244486	0.2	92277
Solvent 3	850.67695	Possibly	5.5	1693337	0.2	95990

Table 74. Summary of signal at *m/z* 852

Calculated *m/z*	852.631					
Sample designation + MALDI replicate no.	Measured *m/z*	Present	S:N	Intensity	Rel. Int. %	Resolution
Y1a 1	852.63243	Yes	226.2	39137804	13.0	81863
Y1a 2	852.63216	Yes	202.6	32629614	12.0	79792
Y1a 3	852.63232	Yes	218.7	37904140	11.0	81383
Original Heslington		No				
H1a 1		No				
H1a 2	852.63204	Yes	26.9	4013304	1.0	84220
H1a 3	852.63176	Yes	25.7	3708269	0.6	104318
H1b 1	852.63152	Yes	108.2	15904056	1.9	92435
H1b 2	852.63138	Yes	65.1	9328204	2.4	90604
H1b 3	852.63133	Yes	88.3	12405865	2.9	90752
H2a 1	852.63134	Yes	50.3	7023293	1.3	95473
H2a 2	852.63177	Yes	30.2	4640963	1.4	75920
H2a 3	852.63173	Yes	66.7	9068568	2.6	93401
H3a 1	852.63199	Yes	99.0	14316330	2.6	93474
H3a 2	852.63232	Yes	259.9	39274788	6.4	93054
H3a 3	852.63187	Yes	161.3	22152042	2.9	93272
H4a 1	852.63237	Yes	337.3	57473308	3.4	92169
H4a 2		No				
H4a 3	852.63243	Yes	214.1	39506408	4.8	86500
H5a 1	852.63134	Yes	458.3	60274400	31.7	93276
H5a 2	852.63162	Yes	515.7	72440240	23.8	93147
H5a 3	852.63141	Yes	445.2	66235356	7.6	92763
H6a 1	852.63222	Yes	212.5	30904736	4.2	82953
H6a 2	852.63223	Yes	192.1	27237376	3.7	82052
H6a 3	852.63211	Yes	185.9	26462390	2.8	82070
H7a 1	852.63200	Yes	237.0	36044064	8.8	92613
H7a 2	852.63206	Yes	175.0	27506568	4.3	92982
H7a 3	852.63202	Yes	108.9	16670544	2.5	95618
H8a 1	852.63225	Yes	203.8	31668226	5.4	93261
H8a 2	852.63243	Yes	110.4	16747439	3.9	91734
H8a 3	852.63208	Yes	170.5	24253032	4.7	92021
H9a 1	852.63231	Yes	272.2	40300344	5.0	89705
H9a 2	852.63229	Yes	140.8	20991626	2.4	91098
H9a 3	852.63175	Yes	189.1	27245454	6.0	90431
H10a 1	852.63207	Yes	117.7	18086572	3.0	92901
H10a 2	852.63171	Yes	69.4	9398925	4.8	93511
H10a 3	852.63215	Yes	82.4	12445331	3.4	93639
H11a 1	852.63301	Yes	134.8	21171094	9.3	88924
H11a 2	852.63298	Yes	68.8	11237416	1.5	87724
H11a 3	852.63211	Yes	41.6	5461554	4.2	79527
H12a 1	852.63334	Yes	94.5	15579422	3.5	80434
H12a 2	852.63327	Yes	64.0	10486964	2.1	81388
H12a 3	852.63322	Yes	86.0	14431590	3.6	82188
H13aii 1	852.63318	Yes	315.3	53765284	13.6	77768
H13aii 2	852.63313	Yes	228.2	36616448	9.4	80041
H13aii 3	852.63275	Yes	212.8	32187310	5.5	80035
H14a 1		No				
H14a 2	852.63091	Yes	9.9	1879773	0.3	94843
H14a 3		No				
H14bi 1	852.63369	Yes	9.9	1935512	0.2	94637
H14bi 2	852.63237	Yes	13.1	2317039	0.4	100037
H14bi 3		No				
V1a 1	852.63244	Yes	197.7	33609852	1.5	92930
V1a 2	852.63244	Yes	240.7	40742748	6.5	92718
V1a 3	852.63228	Yes	165.2	26527772	5.7	93679
B1a 1		No				
B1a 2		No				
B1a 3	852.63173	Yes	479.7	65974600	15.4	93391
DHB 1		No				
DHB 2		No				
DHB 3		No				
Soil 3a 1		No				
Soil 3a 2		No				
Soil 3a 3		No				
Soil 3b 1		No				
Soil 3b 2		No				
Soil 3b 3		No				
Solvent 1		No				
Solvent 2		No				
Solvent 3		No				

Table 75. Summary of signal at *m/z* 853

Calculated *m/z*	853.65577					
Sample designation + MALDI replicate no.	Measured *m/z*	Present	S:N	Intensity	Rel. Int. %	Resolution
Y1a 1	853.65577	Yes	1055.2	181226224	60.3	90679
Y1a 2	853.65542	Yes	877.9	140216368	51.5	90831
Y1a 3	853.65567	Yes	1058.9	182047712	52.8	90998
Original Heslington	853.65632	Yes	12.5	1895970	1.5	59989
H1a 1	853.65591	Yes	21.4	3372314	0.3	100473
H1a 2	853.65491	Yes	59.6	8506539	2.1	90124
H1a 3	853.65507	Yes	41	5729343	0.9	92342
H1b 1	853.65492	Yes	70.9	10538196	1.2	93001
H1b 2	853.65452	Yes	53.8	7776198	2	96173
H1b 3	853.65469	Yes	67.6	9580399	2.3	90215
H2a 1	853.65452	Yes	90.3	12353556	2.3	93107
H2a 2	853.65449	Yes	47.5	7110992	2.1	95280
H2a 3	853.65474	Yes	61.9	8437551	2.4	91751
H3a 1	853.65527	Yes	15.7	2551265	0.5	90087
H3a 2	853.65606	Yes	38	6029401	1	95084
H3a 3	853.65494	Yes	27.1	3994806	0.5	97786
H4a 1	853.65577	Yes	273.3	46642656	2.7	90597
H4a 2	853.65629	Yes	295.0	58974368	6.7	90845
H4a 3	853.65589	Yes	438.4	80489712	9.7	91399
H5a 1	853.65478	Yes	326.1	42979728	22.6	92882
H5a 2	853.65500	Yes	387.4	54496360	17.9	92308
H5a 3	853.65467	Yes	193.8	29025950	3.3	92351
H6a 1	853.65550	Yes	294.7	42731324	5.8	88156
H6a 2	853.65544	Yes	282.2	39862140	5.4	87874
H6a 3	853.65536	Yes	254.7	36134964	3.8	85533
H7a 1	853.65517	Yes	59.6	9315660	2.3	91113
H7a 2	853.65538	Yes	54.4	8787891	1.4	92535
H7a 3	853.65604	Yes	19.2	3226777	0.5	99379
H8a 1	853.65552	Yes	99.6	15652687	2.7	91134
H8a 2	853.65592	Yes	53.8	8337139	1.9	92959
H8a 3	853.65533	Yes	84.7	12212203	2.4	92014
H9a 1	853.65561	Yes	177.5	26398160	3.3	89425
H9a 2	853.65573	Yes	95.5	14355231	1.7	92282
H9a 3	853.65512	Yes	152.5	22043978	4.9	91584
H10a 1	853.65535	Yes	10.6	1931577	0.3	99380
H10a 2	853.65558	Yes	9.4	1549076	0.8	105170
H10a 3	853.65461	Yes	10.6	1892346	0.5	93914
H11a 1	853.65625	Yes	356.7	55435324	24.2	87222
H11a 2	853.65636	Yes	212.5	33995216	4.4	88190
H11a 3	853.65541	Yes	82.1	10476626	8.1	89635
H12a 1	853.65666	Yes	138.2	22614922	5.0	90355
H12a 2	853.65667	Yes	102.9	16654875	3.4	88843
H12a 3	853.65662	Yes	163	27025154	6.7	87519
H13aii 1	853.65647	Yes	378.4	64440656	16.3	87161
H13aii 2	853.6563	Yes	214	34350776	8.8	86381
H13aii 3	853.65599	Yes	289.5	43657052	7.4	88703
H14a 1		No				
H14a 2		No				
H14a 3		No				
H14bi 1		No				
H14bi 2		No				
H14bi 3		No				
V1a 1	853.65589	Yes	84.1	14507082	0.7	93728
V1a 2	853.65589	Yes	106	18140208	2.9	92265
V1a 3	853.65562	Yes	67.3	11014724	2.3	93516
B1a 1	853.65620	Yes	119.5	21079274	4.1	91690
B1a 2	853.65546	Yes	127	19590120	6.4	92147
B1a 3	853.65507	Yes	106.5	14902762	3.5	94325
DHB 1		No				
DHB 2		No				
DHB 3		No				
Soil 3a 1		No				
Soil 3a 2		No				
Soil 3a 3		No				
Soil 3b 1		No				
Soil 3b 2		No				
Soil 3b 3	853.65614	Yes	4.5	1620096	0.3	131725
Solvent 1		No				
Solvent 2		No				
Solvent 3		No				

Table 76. Summary of signal at *m/z* 857

Calculated *m/z*	857.26					
Sample designation + MALDI replicate no.	Measured *m/z*	Present	S:N	Intensity	Rel. Int. %	Resolution
Y1a 1		No				
Y1a 2		No				
Y1a 3		No				
Original Heslington		No				
H1a 1		No				
H1a 2		No				
H1a 3		No				
H1b 1		No				
H1b 2		No				
H1b 3		No				
H2a 1		No				
H2a 2		No				
H2a 3		No				
H3a 1		No				
H3a 2		No				
H3a 3		No				
H4a 1		No				
H4a 2		No				
H4a 3		No				
H5a 1		No				
H5a 2		No				
H5a 3		No				
H6a 1	857.25952	Yes	8.7	1588095	0.2	103572
H6a 2		No				
H6a 3		No				
H7a 1		No				
H7a 2		No				
H7a 3		No				
H8a 1		No				
H8a 2	857.26098	Yes	180.5	27152672	6.3	91721
H8a 3		No				
H9a 1		No				
H9a 2		No				
H9a 3		No				
H10a 1	857.26041	Yes	1104.8	166969232	27.9	93191
H10a 2	857.26226	Yes	6.3	1146524	0.6	71115
H10a 3		No				
H11a 1		No				
H11a 2		No				
H11a 3		No				
H12a 1		No				
H12a 2		No				
H12a 3		No				
H13aii 1	857.26145	Yes	4.2	1077569	0.3	96064
H13aii 2		No				
H13aii 3	857.26118	Yes	8	1542696	0.3	112078
H14a 1		No				
H14a 2		No				
H14a 3		No				
H14bi 1	857.26191	Yes	6	1320513	0.1	111900
H14bi 2		No				
H14bi 3		No				
V1a 1		No				
V1a 2		No				
V1a 3		No				
B1a 1		No				
B1a 2		No				
B1a 3		No				
DHB 1		No				
DHB 2		No				
DHB 3		No				
Soil 3a 1		No				
Soil 3a 2		No				
Soil 3a 3		No				
Soil 3b 1		No				
Soil 3b 2		No				
Soil 3b 3		No				
Solvent 1		No				
Solvent 2		No				
Solvent 3		No				

Table 77. Summary of signal at *m/z* 866

Calculated *m/z*	866.64642					
Sample designation + MALDI replicate no.	Error [ppm]	Present	S:N	Intensity	Rel. Int. %	Resolution
Y1a 1	-0.59	Yes	583.2	100280728	33.4	88374
Y1a 2	-0.09	Yes	511.9	81783160	30.0	88842
Y1a 3	-0.47	Yes	566.6	97536528	28.3	88627
Original Heslington		No				
H1a 1	0.02	Yes	28.7	4384112	0.4	96808
H1a 2	0.26	Yes	71.0	10032262	2.5	91321
H1a 3	0.33	Yes	81.3	11061937	1.7	91052
H1b 1	0.62	Yes	307.5	44625348	5.2	91727
H1b 2	0.37	Yes	156.4	21990544	5.7	91161
H1b 3	0.73	Yes	244.3	33783672	8.0	90875
H2a 1	1.07	Yes	171.2	23143036	4.3	91534
H2a 2	0.66	Yes	86.5	12568269	3.8	90960
H2a 3	0.50	Yes	170.6	22811172	6.4	92278
H3a 1	-0.13	Yes	264.5	37639228	6.8	91756
H3a 2	-0.44	Yes	661.8	99897528	16.3	90960
H3a 3	0.16	Yes	427.3	58304740	7.7	90975
H4a 1	-0.51	Yes	940.3	159298368	9.3	91381
H4a 2	-1.22	Yes	464.4	93125200	10.6	90636
H4a 3	-0.68	Yes	642.2	118401352	14.3	90953
H5a 1	0.87	Yes	1294.9	171511376	90.1	91666
H5a 2	0.53	Yes	1467.3	207730496	68.3	91706
H5a 3	0.71	Yes	1116.8	166784544	19.2	91477
H6a 1	-0.24	Yes	597.5	86483664	11.7	91196
H6a 2	-0.15	Yes	576.3	81225624	11.1	90818
H6a 3	-0.07	Yes	538.9	76103256	8.1	90871
H7a 1	-0.12	Yes	676.1	102886432	25.1	90979
H7a 2	-0.11	Yes	533.8	83174488	13.1	92153
H7a 3	0.09	Yes	338.0	51245596	7.6	91906
H8a 1	-0.36	Yes	518.8	80355000	13.8	91445
H8a 2	-0.73	Yes	298.8	44980476	10.4	90149
H8a 3	-0.04	Yes	387.2	54882408	10.6	90787
H9a 1	-0.35	Yes	600.5	88468776	11.0	89997
H9a 2	-0.29	Yes	310.2	45820756	5.3	90662
H9a 3	0.28	Yes	405.0	58445188	12.9	90076
H10a 1	-0.12	Yes	296.4	45565756	7.6	91113
H10a 2	0.67	Yes	196.0	26134532	13.4	90618
H10a 3	-0.10	Yes	226.6	33736220	9.2	91863
H11a 1	-1.16	Yes	331.1	51589644	22.5	88237
H11a 2	-1.21	Yes	170.2	27489014	3.6	90048
H11a 3	-0.10	Yes	104.5	13339066	10.3	89990
H12a 1	-1.63	Yes	198.3	31962536	7.1	88802
H12a 2	-1.50	Yes	136.8	21836590	4.4	88311
H12a 3	-1.55	Yes	204.0	33378428	8.3	88212
H13aii 1	-1.39	Yes	716.4	121156480	30.7	89937
H13aii 2	-1.24	Yes	534.2	85189768	21.9	89198
H13aii 3	-0.85	Yes	525.4	78993328	13.4	89116
H14a 1		No				
H14a 2	-0.52	Yes	22.8	3779781	0.6	94433
H14a 3	-1.28	Yes	23.9	4547973	0.2	87076
H14bi 1	-1.71	Yes	13.9	2567017	0.3	97363
H14bi 2	-0.79	Yes	22.8	3779781	0.6	94433
H14bi 3		No				
V1a 1	-0.67	Yes	503.9	85048648	3.9	91526
V1a 2	-0.69	Yes	645.6	108747888	17.3	91132
V1a 3	-0.41	Yes	441.5	70172664	15.0	91906
B1a 1	-1.26	Yes	1220.0	212526496	41.4	91464
B1a 2	-0.29	Yes	1158.8	177176896	57.8	91022
B1a 3	0.31	Yes	1238.5	171004384	40.0	92158
DHB 1		No				
DHB 2		No				
DHB 3		No				
Soil 3a 1	-2.19	Possibly	6.5	1924502	0.2	79439
Soil 3a 2		No				
Soil 3a 3		No				
Soil 3b 1		No				
Soil 3b 2		No				
Soil 3b 3		No				
Solvent 1		No				
Solvent 2		No				
Solvent 3		No				

Table 78. Summary of signal at *m/z* 968

Calculated *m/z*	968.585					
Sample designation + MALDI replicate no.	Measured *m/z*	Present	S:N	Intensity	Rel. Int. %	Resolution
Y1a 1	968.58618	Yes	441.3	71453576	23.8	81560
Y1a 2	968.58588	Yes	384.9	58805740	21.6	81927
Y1a 3	968.58612	Yes	482.0	77728504	22.6	82025
Original Heslington		No				
H1a 1	968.58473	Yes	9.9	1703817	0.2	80506
H1a 2	968.58562	Yes	34.9	5049937	1.3	83704
H1a 3	968.58557	Yes	31.6	4523876	0.7	83541
H1b 1	968.58517	Yes	92.6	13356062	1.6	82096
H1b 2	968.58536	Yes	108.7	15131043	3.9	80795
H1b 3	968.58502	Yes	93.0	12953893	3.1	83703
H2a 1	968.58477	Yes	129.3	17614082	3.3	82909
H2a 2	968.58507	Yes	142.1	20040200	6.0	82166
H2a 3	968.58547	Yes	150.0	20438892	5.8	81579
H3a 1	968.58601	Yes	129.9	18403682	3.3	82040
H3a 2	968.58638	Yes	394.3	58729404	9.6	81975
H3a 3	968.58577	Yes	151.9	20979482	2.8	82467
H4a 1	968.58643	Yes	35.0	5956002	0.3	83175
H4a 2	968.58669	Yes	205.6	38007372	4.3	81964
H4a 3	968.58630	Yes	194.9	33613028	4.1	81582
H5a 1	968.58524	Yes	392.0	52544504	27.6	82018
H5a 2	968.58550	Yes	451.6	63561436	20.9	81979
H5a 3	968.58510	Yes	177.0	26157540	3.0	82962
H6a 1	968.58610	Yes	331.2	47307864	6.4	82157
H6a 2	968.58602	Yes	256.1	35734616	4.9	81270
H6a 3	968.58603	Yes	187.5	26247116	2.8	83066
H7a 1	968.58583	Yes	315.4	46827556	11.4	82196
H7a 2	968.58586	Yes	281.9	42270504	6.7	82003
H7a 3	968.58588	Yes	191.3	28405462	4.2	82557
H8a 1	968.58617	Yes	447.5	66862784	11.5	81786
H8a 2	968.58641	Yes	242.7	36054052	8.4	80758
H8a 3	968.58592	Yes	299.3	41883624	8.1	82186
H9a 1	968.58618	Yes	216.7	31277282	3.9	81874
H9a 2	968.58632	Yes	173.9	25169072	2.9	83089
H9a 3	968.58570	Yes	175.9	25303602	5.6	81813
H10a 1	968.58596	Yes	199.3	29972804	5.0	82041
H10a 2	968.58557	Yes	103.0	13986070	7.2	82425
H10a 3	968.58609	Yes	144.9	21206696	5.8	81595
H11a 1	968.58697	Yes	219.2	32850686	14.4	81749
H11a 2	968.58690	Yes	95.7	14995575	2.0	82427
H11a 3	968.58593	Yes	53.7	7147024	5.5	85619
H12a 1	968.58708	Yes	81.6	12739157	2.8	81423
H12a 2	968.58738	Yes	67.9	10545885	2.1	86020
H12a 3	968.58738	Yes	77.2	12205683	3.0	84629
H13aii 1	968.58715	Yes	178.6	28746404	7.3	82798
H13aii 2	968.58703	Yes	100.3	15673367	4.0	83084
H13aii 3	968.58675	Yes	154.7	22850260	3.9	81805
H14a 1		No				
H14a 2		No				
H14a 3		No				
H14bi 1		No				
H14bi 2	968.58542	Yes	9.4	1751261	0.3	83588
H14bi 3		No				
V1a 1	968.58648	Yes	74.2	12448198	0.6	84182
V1a 2	968.58642	Yes	79.7	13326226	2.1	82164
V1a 3	968.58611	Yes	49.2	7989501	1.7	83591
B1a 1	968.58699	Yes	232.2	38803304	7.6	81474
B1a 2	968.58605	Yes	250.0	37837228	12.3	81651
B1a 3	968.58560	Yes	280.8	39308656	9.2	81816
DHB 1		No				
DHB 2		No				
DHB 3		No				
Soil 3a 1		No				
Soil 3a 2		No				
Soil 3a 3		No				
Soil 3b 1		No				
Soil 3b 2		No				
Soil 3b 3		No				
Solvent 1		No				
Solvent 2		No				
Solvent 3		No				

ABBREVIATIONS

AA	amino acid
ATP	adenosine triphosphate
BARC	Biological Anthropological Research Centre, Bradford
BP	before present (1 January 1950 = present)
CID	collision induced dissociation
CNS	central nervous system
CT	computed tomography
d.p.	decimal place(s)
Da	Dalton, unit of mass
dbes	double bond equivalents
DHB	2,5-dihydroxybenzoic acid
DNA	deoxyribonucleic acid
ESI	electrospray ionisation
FT	Fourier transform
GalC	galactocerebroside(s)
GC	gas chromatography
HPLC	high performance liquid chromatrography
ICR	ion cyclotron resonance
KMA	5-keto-D-mannuronic acid (or D-lyxo-5-hexosylopyranuronic acid)
LC	liquid chromatography
LDS	lithium dodecyl sulfate
MALDI	matrix assisted laser desorption/ionisation
mmu	millimass units
MRI	magnetic resonance imaging
MS	mass spectrometry
MS/MS	tandem mass spectrometry
m/z	mass to charge ratio
PAGE	polyacrylamide gel electrophoresis
PC	phosphatidylcholine(s)
PCSII	protein calibration standard II
PMF	peptide mass fingerprintingPMF
ppm	parts per million
QUAD	quadrupole (MS analyser)

RNA	ribonucleic acid
SDS	sodium dodecyl sulfate
sds	standard deviations
SEM	scanning electron microscopy
rf	radio frequency
SM	sphingomyelin(s)
S:N	signal to noise ratio
TEM	transmission electron microscopy
TLC	thin layer chromatography
TOF	time of flight (MS analyser)
UV	ultraviolet

REFERENCES

1. S. O'Connor, E. Ali, S. Al-Sabah, D. Anwar, E. Bergstroem, K. A. Brown, J. Buckberry, S. Buckley, M. Collins, J. Denton, K. M. Dorling, A. Dowle, P. Duffey, H. G. M. Edwards, E. C. Faria, P. Gardner, A. Gledhill, K. Heaton, C. Heron, R. Janaway, B. J. Keely, D. King, A. Masinton, K. Penkman, A. Petzold, M. D. Pickering, M. Rumsby, H. Schutkowski, K. A. Shackleton, J. Thomas, J. Thomas-Oates, M.-R. Usai, A. S. Wilson and T. O'Connor, *Journal of Archaeological Science*, 2011, **38**, 1641-1654.
2. A. J. Dunn and S. C. Bondy, *Functional Chemistry of the Brain*, Spectrum Publications, Inc., New York, 1974.
3. H. McIlwain and H. S. Bachelard, *Biochemistry and the Central Nervous System*, Churchill Livingstone, Edinburgh, 5th Edition edn., 1985.
4. H. McIlwain, *Biochemistry and the Central Nervous System*, J. & A. Churchill, Ltd., Great Britain, 2nd edn., 1959.
5. Y. A. Hannun and L. M. Obeid, *Nature Reviews Molecular Cell Biology*, 2008, **9**, 139-150.
6. M. C. Raff, R. Mirsky, K. L. Fields, R. P. Lisak, S. H. Dorfman, D. H. Silberberg, N. A. Gregson, S. Leibowitz and M. C. Kennedy, *Nature*, 1978, **274**, 813-816.
7. A. Bosio, E. Binczek and W. Stoffel, *Proceedings of the National Academy of Sciences of the United States of America*, 1996, **93**, 13280-13285.
8. R. W. Ledeen, *Journal of Supramolecular Structure*, 1978, **8**, 1-17.
9. A. Lajtha, *Handbook of Neurochemistry*, Plenum Press, New York, 1969.
10. M. A. Clark, M. B. Worrell and J. E. Pless, in *Forensic Taphonomy : the postmortem fate of human remains*, eds. W. D. Haglund and M. H. Sorg, CRC Press, Boca Raton, 1997, ch. 9, pp. 151-164.
11. H. Gill-King, in *Forensic Taphonomy : the postmortem fate of human remains*, eds. W. D. Haglund and M. H. Sorg, CRC Press, Boca Raton, 1997, ch. 6, pp. 93-108.
12. J. Hunter, C. A. Roberts, D. R. Brothwell and A. Martin, *Studies in crime: an introduction to forensic archaeology*, Batsford, London,, 1996.
13. A. C. Aufderheide, *International Journal of Paleopathology*, 2011, **1**, 75-80.
14. A. T. Chamberlain and M. Parker Pearson, *Earthly remains : the history and science of preserved human bodies*, British Museum, London, 2001.
15. A. C. Aufderheide, *The scientific study of mummies*, Cambridge University Press, Cambridge, 2003.
16. A. Boddington, A. N. Garland and R. C. Janaway, *Death, decay, and reconstruction : approaches to archaeology and forensic science*, Manchester University Press, Manchester, 1987.
17. A. A. Vass, *Forensic Science International*, 2011, **204**, 34-40.
18. S. Fiedler and M. Graw, *Naturwissenschaften*, 2003, **90**, 291-300.
19. B. Ioan, C. Manea cas. Amariei, B. Hanganu, L. Statescu, L. Solovastru and I. Manoilescu, *The chemistry decomposition in human corpses*, 2017.
20. S. Alvarez-Perez, J. L. Blanco, P. Alba and M. E. Garcia, *Revista Iberoamericana De Micologia*, 2011, **28**, 159-165.
21. R. C. Janaway, S. Percival and A. Wilson, *Decomposition of Human Remains*, 2009.
22. M. S. Micozzi, in *Forensic Taphonomy: the post-mortem fate of human remains*, eds. W. D. Haglund and M. H. Sorh, CRC Press, Boca Raton, 1997, ch. 11, pp. 171-180.
23. R. C. Murray and J. C. F. Tedrow, *Journal*, 1975
24. F. Backhed, R. E. Ley, J. L. Sonnenburg, D. A. Peterson and J. I. Gordon, *Science*, 2005, **307**, 1915-1920.

25. P. S. Sledzik and M. S. Micozzi, in *Forensic Taphonomy : the postmortem fate of human remains*, eds. W. D. Haglund and M. H. Sorg, CRC Press, Boca Raton, 1997, ch. 31, pp. 483-495.
26. E. M. J. Schotsmans, W. Van de Voorde, J. De Winne and A. S. Wilson, *Forensic Science International*, 2011, **206**, e43-e48.
27. S. Aturaliya and A. Lukasewycz, *Journal of Forensic Science*, 1999, **44**, 893–896.
28. A. Galloway, W. H. Birkby, A. M. Jones, T. E. Henry and B. O. Parks, *Journal of Forensic Sciences*, 1989, **34**, 607–616.
29. E. Tapp, *Paleopathology newsletter*, 1985, 10-13.
30. L. M. McKinley, *The Journal of Pathology*, 1977, **122**, 27-28.
31. F. Kauffmann-Doig, *Politica Internacional*, 1996, **46**, 113-143.
32. H. Nushida, J. Adachi, A. Takeuchi, M. Asano and Y. Ueno, *Forensic Science International*, 2008, **175**, 160-165.
33. M. S. Micozzi, *Journal of Forensic Sciences*, 1986, **31**, 953-961.
34. R. Amy, R. Bhatnagar, E. Damkjar and O. Beattie, *Canadian Medical Association Journal*, 1986, **135**, 115-117.
35. D. N. H. Notman, L. Anderson, O. B. Beattie and R. Amy, *American Journal of Roentgenology*, 1987, **149**, 347-350.
36. W. A. Kowal, P. M. Krahn and O. B. Beattie, *International Journal of Environmental Analytical Chemistry*, 1989, **35**, 119-126.
37. W. Kowal, O. B. Beattie and P. M. Krahn, *Nature*, 1990, **343**, 319-320.
38. W. Kowal, O. B. Beattie, H. Baadsgaard and P. M. Krahn, *Journal of Archaeological Science*, 1991, **18**, 193-203.
39. D. Notman and O. Beattie, in *Human Mummies: Global Survey of Their Status and the Techniques of Conservation*, eds. K. Spindler, H. Wilfing, E. RastbichlerZissernig, D. zurNedden and H. Nothdurfter, 1996, vol. 3, pp. 93-106.
40. S. Mays and O. Beattie, *International Journal of Osteoarchaeology*, 2016, **26**, 778-786.
41. C. F. Merbs, *Arctic Anthropology*, 1995, **32**, 173-177.
42. J. P. H. Hansen and J. Nordqvist, *Human Mummies: Global Survey of Their Status and the Techniques of Conservation*, 1996, **3**, 107-121.
43. E. M. Kreps, E. V. Chirkovskaya, L. F. Pomazanskaya, N. F. Avrova, M. V. Levitina and M. A. Chebotareva, *Journal of Evolutionary Biochemistry and Physiology*, 1979, **15**, 194-202.
44. E. M. Kreps, N. F. Avrova, M. A. Chebotarëva, E. V. Chirkovskaya, M. V. Levitina and L. F. Pomazanskaya, *Comparative Biochemistry and Physiology Part B: Comparative Biochemistry*, 1981, **68**, 135-140.
45. J. Schobinger, *Natural History*, 1991, 62-69.
46. K. Makristathis, R. Mader, K. Varmuza, I. Simonitsch, J. Schwarzmeier, H. Seidler, W. Platzer, H. Unterndorfer and R. Scheithauer, in *Human Mummies: Global Survey of Their Status and the Techniques of Conservation*, eds. K. Spindler, H. Wilfing, E. RastbichlerZissernig, D. zurNedden and H. Nothdurfter, 1996, vol. 3, pp. 279-281.
47. M. W. Hess, G. Klima, K. Pfaller, K. H. Kunzel and O. Gaber, *American Journal of Physical Anthropology*, 1998, **106**, 521-532.
48. D. Zurnedden, K. Wicke, R. Knapp, H. Seidler, H. Wilfing, G. Weber, K. Spindler, W. A. Murphy, G. Hauser and W. Platzer, *Journal of Archaeological Science*, 1994, **21**, 809-818.
49. H. Seidler, W. Bernhard, M. Teschler-Nicola, W. Platzer, D. z. Nedden, R. Henn, A. Oberhauser and T. Sjøvold, *Science*, 1992, **258**, 455-457.
50. J. M. Pestka, F. Barvencik, F. T. Beil, R. P. Marshall, E. Jopp, A. F. Schilling, A. Bauerochse, M. Fansa, K. Pueschel and M. Amling, *Naturwissenschaften*, 2010, **97**, 393-402.

51. T. J. Painter, *Carbohydrate Polymers*, 1991, **15**, 123-142.
52. P. V. Glob, *The bog people : iron-age man preserved*, Faber, London, 1969.
53. J. B. Bourke, D. R. Brothwell, British Museum. and I. M. Stead, *Lindow Man : the body in the bog*, Published for the Trustees of the British Museum by British Museum Publications, London, 1986.
54. H. Rydin, J. K. Jeglum and A. Hooijer, *The Biology of Peatlands*, Oxford University Press, Oxford, 2006.
55. S. A. Waksman, *American Journal of Science*, 1930, **19**, 32-54.
56. M. A. Monetti and M. I. Scranton, *Biogeochemistry*, 1992, **17**, 23-47.
57. T. J. Painter, in *Bog bodies : new discoveries and new perspectives*, eds. R. C. Turner and R. G. Scaife, British Museum Press, London, 1995, ch. 10, pp. 88-99.
58. F. Czapek, *Naturwissenschaften*, 1913, **1**, 1105-1107.
59. H. Rudolph and B. Engmann, *Berichte Der Deutschen Botanischen Gesellschaft*, 1967, **80**, 114-&.
60. O. Smidsrod and T. J. Painter, *Carbohydrate Research*, 1984, **127**, 267-281.
61. K. Y. Børsheim, B. E. Christensen and T. J. Painter, *Innovative Food Science & Emerging Technologies*, 2001, **2**, 63-74.
62. T. J. Painter, *Carbohydrate Polymers*, 1998, **36**, 335-347.
63. T. Stalheim, S. Ballance, B. E. Christensen and P. E. Granum, *Journal of Applied Microbiology*, 2009, **106**, 967-976.
64. S. Ballance, K. Y. Borsheim, K. Inngjerdingen, B. S. Paulsen and B. E. Christensen, *Carbohydrate Polymers*, 2007, **67**, 104-115.
65. R. J. Schulting, in *In Proceedings of the First World Congress on Mummy Studies*, Archaeological and Ethnographical Museum of Tenerife, Santa Cruz, Tenerife, Canary Islands, 1995, vol. 2, pp. 771-780.
66. A. G. Morris, *South African Archaeological Bulletin*, 1981, 36-42.
67. D. H. Ubelaker and K. M. Zarenko, *Forensic Science International*, 2011, **208**, 167-172.
68. G. E. Cotton, A. C. Aufderheide and V. G. Goldschmidt, *Journal of Forensic Sciences*, 1987, **32**, 1125-1130.
69. T. L. Bereuter, E. Lorbeer, C. Reiter, H. Seidler and H. Unterdorfer, *Human Mummies: Global Survey of Their Status and the Techniques of Conservation*, 1996, **3**, 265-273.
70. T. Browne, *Hydriotaphia, Urn Burial, or, a Discourse of the Sepulchral Urns lately found in Norfolk*, London, http://penelope.uchicago.edu/hgc.html edn., 1658.
71. A. F. Fourcroy, *Annales de Chimie*, 1791, **8**, 17-73.
72. A. Fourcroy, *Memoires. Academie de Chirurgie*, 1789.
73. M. Thouret, *Histoire de la Société Royale de Médecine avec les Mémoires de Médecine et de Physique Médicale*, 1790, 238-271.
74. L. E. den Dooren de Jong, *Antonie Van Leeuwenhoek Journal of Microbiology and Serology*, 1961, **27**, 337-361.
75. R. F. Ruttan and M. J. Marshall, *Journal of Biological Chemistry*, 1917, **29**, 319-327.
76. J. B. Williams, C. Clarkson, C. Mant, A. Drinkwater and E. May, *Water Research*, 2012, **46**, 6319-6328.
77. C. H. Vane and J. K. Trick, *Forensic Science International*, 2005, **154**, 19-23.
78. T. Takatori, *Legal medicine (Tokyo, Japan)*, 2001, **3**, 193-204.
79. J. Adachi, Y. Ueno, A. Miwa, M. Asano, A. Nishimura and Y. Tatsuno, *Lipids*, 1997, **32**, 1155-1160.
80. M. Algarra, J. E. Rodriguez-Borges and J. C. G. Esteves da Silva, *Journal of Separation Science*, 2010, **33**, 143-154.
81. K. Saito, *Journal of Biochemistry*, 1966, **59**, 487-&.
82. S. L. Forbes, B. B. Dent and B. H. Stuart, *Forensic Science International*, 2005, **154**, 35-43.

83. S. L. Forbes, B. H. Stuart and B. B. Dent, *Forensic Science International*, 2005, **154**, 24-34.
84. S. L. Forbes, B. H. Stuart and B. B. Dent, *Forensic Science International*, 2005, **154**, 44-52.
85. D. Schoenen and H. Schoenen, *Forensic Science International*, 2013, **226**, 301.e301-301.e306.
86. S. Fiedler, F. Buegger, B. Klaubert, K. Zipp, R. Dohrmann, M. Witteyer, M. Zarei and M. Graw, *Journal of Archaeological Science*, 2009, **36**, 1328-1333.
87. B. P. Tissot and D. H. Welte, *Petroleum Formation and Occurrence*, Springer Verlag, Berlin, 2 edn., 1984.
88. B. Durand, *Kerogen : insoluble organic matter from sedimentary rocks*, Technip ; London : Distributed by Graham & Trotman, Paris, 1980.
89. N. Eklektos, M. R. Dayal and P. R. Manger, *Journal of Forensic Sciences*, 2006, **51**, 498-503.
90. C. Barras, *New Scientist*, 2013, **220**, 11-11.
91. G. Prats-Munoz, A. Malgosa, N. Armentano, I. Galtes, J. Esteban, J. A. Bombi, M. Tortosa, E. Fernandez, X. Jordana, A. Isidro, J. M. Fullola, M. Angels Petit, V. M. Guerrero, M. Calvo and P. L. Fernandez, *Pathobiology*, 2012, **79**, 239-246.
92. G. Prats-Munoz, I. Galtes, N. Armentano, S. Cases, P. L. Fernandez and A. Malgosa, *Journal of Archaeological Science*, 2013, **40**, 4701-4710.
93. W. Royal and E. Clark, *American Antiquity*, 1960, **26**, 285-287.
94. G. H. Doran, D. N. Dickel, W. E. Ballinger, O. F. Agee, P. J. Laipis and W. W. Hauswirth, *Nature*, 1986, **323**, 803-806.
95. S. Radanov, S. Stoev, M. Davidov, S. Nachev, N. Stanchev and E. Kirova, *International Journal of Legal Medicine*, 1992, **105**, 173-175.
96. C. Papageorgopoulou, K. Rentsch, M. Raghavan, M. I. Hofmann, G. Colacicco, V. Gallien, R. Bianucci and F. Ruehli, *Neuroimage*, 2010, **50**, 893-901.
97. J. Folch, I. Ascoli, M. Lees, J. A. Meath and F. N. Lebaron, *Journal of Biological Chemistry*, 1951, **191**, 833-841.
98. J. Folch, M. Lees and G. H. S. Stanley, *Journal of Biological Chemistry*, 1957, **226**, 497-509.
99. G. H. Doran and D. N. Dickel, *Purdy, B. a. (Ed.). Wet Site Archaeology; International Conference Held in Gainesville, Florida, USA, December 12-14, 1986. Xiii+338p. Telford Press: Caldwell New Jersey, USA. Illus. Maps*, 1988, 263-290.
100. W. W. Hauswirth, C. D. Dickel, G. H. Doran, P. J. Laipis and D. N. Dickel, *Ortner, D. J. and a. C. Aufderheide (Ed.). Human Paleopathology: Current Syntheses and Future Options; Meeting, Zagreb, Yugoslavia, July 24-31, 1988. Viii+311p. Smithsonian Institution Press: Washington, D.C., USA; London, England, Uk. Illus. Maps*, 1991, 60-72.
101. C. M. Stojanowski, R. M. Seidemann and G. H. Doran, *American Journal of Physical Anthropology*, 2002, **119**, 15-26.
102. N. Armentano Oller, X. Esteve Gracia, D. Nociarova and A. Malgosa Morera, *Quaternary International*, 2012, **275**, 112-119.
103. A. Makristathis, J. Schwarzmeier, R. M. Mader, K. Varmuza, I. Simonitsch, J. C. Chavez, W. Platzer, H. Unterdorfer, R. Scheithauer, A. Derevianko and H. Seidler, *Journal of Lipid Research*, 2002, **43**, 2056-2061.
104. K. Varmuza, A. Makristathis, J. Schwarzmeier, H. Seidler and R. M. Mader, *Mass Spectrometry Reviews*, 2005, **24**, 427-452.
105. M. J. Thali, B. Lux, S. Losch, F. W. Rosing, J. Hurlimann, P. Feer, R. Dirnhofer, U. Konigsdorfer and U. Zollinger, *Forensic Science International*, 2011, **211**, 34-40.
106. K. Hollemeyer, W. Altmeyer, E. Heinzle and C. Pitra, *Rapid Communications in Mass Spectrometry*, 2012, **26**, 1735-1745.

107. F. Maixner, T. Overath, D. Linke, M. Janko, G. Guerriero, B. H. J. van den Berg, B. Stade, P. Leidinger, C. Backes, M. Jaremek, B. Kneissl, B. Meder, A. Franke, E. Egarter-Vigl, E. Meese, A. Schwarz, A. Tholey, A. Zink and A. Keller, *Cellular and Molecular Life Sciences*, 2013, **70**, 3709-3722.
108. K. P. Oakley, *Man*, 1960, **60**, 90-91.
109. I. Tkocz, P. Bytzer and F. Bierring, *American Journal of Physical Anthropology*, 1979, **51**, 197-202.
110. J. J. Thomson, *Proceedings of the Royal Society of London. Series A*, 1913, **89**, 1-20.
111. A. O. Nier, *Physical Review*, 1939, **55**, 0150-0153.
112. R. Conrad, *Transactions of the Faraday Society*, 1934, **30**, 0215-0220.
113. W. E. Stephens, *Physical Review*, 1946, **69**, 691-691.
114. A. E. Cameron and D. F. Eggers, *Review of Scientific Instruments*, 1948, **19**, 605-607.
115. J. A. Hipple, H. Sommer and H. A. Thomas, *Physical Review*, 1949, **76**, 1877-1878.
116. W. Paul and H. Steinwedel, *Zeitschrift Fur Naturforschung Section a-a Journal of Physical Sciences*, 1953, **8**, 448-450.
117. W. Paul, H. P. Reinhard and U. Vonzahn, *Zeitschrift Fur Physik*, 1958, **152**, 143-182.
118. H. Dehmelt and N. Yu, *Proceedings of the National Academy of Sciences of the United States of America*, 1997, **94**, 10031-10033.
119. A. Makarov, *Analytical Chemistry*, 2000, **72**, 1156-1162.
120. A. J. Dempster, *Physical Review*, 1918, **11**, 316-325.
121. Matthias Mann, Ronald C. Hendrickson and A. Pandey, http://dx.doi.org/10.1146/annurev.biochem.70.1.437, 2003.
122. M. Karas, D. Bachmann, U. Bahr and F. Hillenkamp, *International Journal of Mass Spectrometry and Ion Processes*, 1987, **78**, 53-68.
123. M. B. Comisarow and A. G. Marshall, *Chemical Physics Letters*, 1974, **25**, 282-283.
124. A. G. Marshall, C. L. Hendrickson and G. S. Jackson, *Mass Spectrometry Reviews*, 1998, **17**, 1-35.
125. Bruker - solariX MRMS - routine IFS for unambiguous results, *https://www.bruker.com/products/mass-spectrometry-and-separations/mrms/solarix/overview.html*, (accessed September 2018).
126. A. Pandey and M. Mann, *Nature*, 2000, **405**, 837-846.
127. R. Aebersold and M. Mann, *Nature*, 2003, **422**, 198-207.
128. H. J. Issaq and T. D. Veenstra, *Biotechniques*, 2008, **44**, 697-+.
129. P. Roepstorff and J. Fohlman, *Biomedical Mass Spectrometry*, 1984, **11**, 601-601.
130. P. Roepstorff, *Biomedical Mass Spectrometry*, 1985, **12**, 631-631.
131. K. Biemann, *Biomedical and Environmental Mass Spectrometry*, 1988, **16**, 99-111.
132. K. Helsens, L. Martens, J. Vandekerckhove and K. Gevaert, *Proteomics*, 2007, **7**, 364-366.
133. D. Hussain, M. Najam-ul-Haq, F. Jabeen, M. N. Ashiq, M. Athar, M. Rainer, C. W. Huck and G. K. Bonn, *Analytica Chimica Acta*, 2013, **775**, 75-84.
134. Matrix Science, http://www.matrixscience.com, (accessed March 2018).
135. B. Antoni, M. Johnson and J. McConish, *The University of York, Heslington East, York, Assessment report 48.*, York Archaeological Trust for Excavation and Research Ltd, 2009.
136. I. Mason and J. McComish, *Campus 3Development, University of York, Zone E: Campus 3 Development, University of York, Zone E: Report on an Archaeological Desktop Study.* , York Archaeological Trust, (unpublished developer report), 2003.
137. A. D. H. Bartlett and M. J. Noel, *University of York Heslington East Development Archaeological Geophysical Survey Phases 1, 2 and 3*, GeoQuest Associates, 2004.
138. M. Collins, E. R. Waite and A. van Duin, *Predicting protein decomposition: The case of aspartic-acid racemization kinetics*, 1999.

139. M. L. Moro, M. J. Collins and E. Cappellini, *Biochemical Society Transactions*, 2010, **38**, 539-544.
140. D. H. Evans, *Project Design for the Magistrates Courts Site, Kingston Upon Hull*, Humberside Archaeology Unit, Beverley, 1994.
141. D. H. Evans, *The Post-excavation Assessment and Updated Project Design for The Hull Magistrates Courts Site*, Humber Archaeology Partnership, Hull, 1998.
142. R. Middleton , C. Wells and E. Huckerby, *The Wetlands of North Lancashire*, Lancaster Imprints, Lancaster, 1995.
143. J. Griffiths, *St. John the Evagelist Churchyeard, Church Street, Blackpool.*, Oxford Archaeological North, Oxford, 2010.
144. A. M. Alessi, S. M. Bird, J. P. Bennett, N. C. Oates, Y. Li, A. A. Dowle, I. Polikarpov, J. P. W. Young, S. J. McQueen-Mason and N. C. Bruce, *Scientific Reports*, 2017, **7**.
145. A. A. Dowle, J. Wilson and J. R. Thomas, *Journal of Proteome Research*, 2016, **15**, 3550-3562.
146. F. Sabbadin, G. Pesante, L. Elias, K. Besser, Y. Li, C. Steele-King, M. Stark, D. A. Rathbone, A. A. Dowle, R. Bates, J. R. Shipway, S. M. Cragg, N. C. Bruce and S. J. McQueen-Mason, *Biotechnology for Biofuels*, 2018, **11**.
147. F. Sabbadin, G. R. Hemsworth, L. Ciano, B. Henrissat, P. Dupree, T. Tryfona, R. D. S. Marques, S. T. Sweeney, K. Besser, L. Elias, G. Pesante, Y. Li, A. A. Dowle, R. Bates, L. D. Gomez, R. Simister, G. J. Davies, P. H. Walton, N. C. Bruce and S. J. McQueen-Mason, *Nature Communications*, 2018, **9**.
148. D. Fenyo and R. C. Beavis, *Analytical Chemistry*, 2003, **75**, 768-774.
149. E. N. Nikolaev, I. A. Boldin, R. Jertz and G. Baykut, *Journal of the American Society for Mass Spectrometry*, 2011, **22**, 1125-1133.
150. M. L. Easterling, T. H. Mize and I. J. Amster, *Analytical Chemistry*, 1999, **71**, 624-632.
151. M. Easterling, *Technical Note # TN-33: Top-Down Analysis Using the solariX-TD*, Bruker Daltonics, Billerica, MA, USA, 2009.
152. B. Fuchs and J. Schiller, *European Journal of Lipid Science and Technology*, 2009, **111**, 83-98.
153. J. B. Hu, Y. C. Chen and P. L. Urban, *Analytica Chimica Acta*, 2013, **766**, 77-82.
154. R. G. Bergman, *Nature*, 2007, **446**, 391-393.
155. G. R. Harvey, D. A. Boran, L. A. Chesal and J. M. Tokar, *Marine Chemistry*, 1983, **12**, 119-132.
156. C. Mencarelli and P. Martinez-Martinez, *Cellular and Molecular Life Sciences*, 2013, **70**, 181-203.
157. I. A. Breger, *Geochimica Et Cosmochimica Acta*, 1960, **19**, 297-308.
158. M. Siskin, S. G. Scouten, K. D. Rose, T. Aczel, S. G. Colgrove and R. E. Pabst Jr., in *Composition, Geochemistry and Conversion of Oil Shales*, ed. C. Snape, Kluwer Academic Publishers, Dordrecht, 1995, pp. 143-158.
159. M. Vandenbroucke and C. Largeau, *Organic Geochemistry*, 2007, **38**, 719-833.
160. M. Vandenbroucke, *Oil & Gas Science and Technology-Revue D Ifp Energies Nouvelles*, 2003, **58**, 243-269.
161. D. W. van Krevelen, *Coal: Typology – Chemistry – Physics – Constitution*, Elsevier Science, United Kingdom, 3 edn., 1981.
162. P. Farrimond, G. D. Love, A. N. Bishop, H. E. Innes, D. F. Watson and C. E. Snape, *Geochimica Et Cosmochimica Acta*, 2003, **67**, 1383-1394.
163. P. Farrimond, G. D. Love, A. N. Bishop, H. E. Innes, D. F. Watson and C. E. Snape, *Geochimica Et Cosmochimica Acta*, 2003, **67**, 1385.
164. A. G. Marshall and R. P. Rodgers, *Accounts of Chemical Research*, 2004, **37**, 53-59.
165. S. Kim, R. P. Rodgers and A. G. Marshall, *International Journal of Mass Spectrometry*, 2006, **251**, 260-265.

166. A. G. Marshall and R. P. Rodgers, *Proceedings of the National Academy of Sciences of the United States of America*, 2008, **105**, 18090-18095.
167. Y. Cho, A. Ahmed, A. Islam and S. Kim, *Mass Spectrometry Reviews*, 2015, **34**, 248-263.